THE USE OF CONTINUOUS WAVE ULTRASOUND TO DIAGNOSE STENOSES IN THE CAROTID ARTERIES

BY

WILLIAM FINLAYSON TAIT
MB ChB FRCS

Thesis submitted for the Degree of
Doctor of Medicine
of the University of Glasgow
based on research carried out in
the University Department of Surgery
University Hospital of South Manchester
Submitted December 1985

TABLE OF CONTENTS

LIST OF TABLES

LIST OF ILLUSTRATIONS

ACKNOWLEDGEMENTS

I would like to thank Mr D Charlesworth of the University Hospital of South Manchester who stimulated my interest in this research, for his help and criticism with the experiments and for allowing me to study his patients. His enthusiasm for research work in general I found most infectious!

My thanks are also due to Mr C J Underwood, my colleague in the vascular laboratory with whom I discussed many difficulties, Miss B Twisse who assisted me in the examination of patients and those other members of staff of the Research and Teaching Department of the above hospital who gave advice, repaired equipment and volunteered for my experiments. Mr B Faragher and Mr C Roberts gave valuable help with statistical analyses and the latter wrote the computer program used in Chapter 3. Mr G P Naylor (Department of Medical Physics, University Hospital of South Manchester) helped me with the relationship between the velocity profile and the ultrasound frequency/intensity spectrum and I am grateful to Dr J H Gerrard (Department of Aeronautical Engineering, University of Manchester) who discussed aspects of disturbances of flow with me.

Finally I would like to thank Miss A Hall for typing the manuscript.

SUMMARY

In this thesis the detection of atherosclerotic disease of the extracranial carotid arteries using continuous wave ultrasound is studied. The pathophysiology, natural history and treatment of carotid artery disease and its importance as a cause of stroke are described. Methods of investigation other than by ultrasound eg arteriograms, carotid phonoangiography, oculoplethysmography with their inability to identify mild degrees of stenosis and other drawbacks are discussed.

The carotid arteries of normal volunteers and patients with symptoms of carotid artery disease were examined with an instrument which uses continuous waves of ultrasound. Real time waveform analysis calculated the maximum systolic frequency, the degree of spectral broadening at peak systole and a resistance parameter from the Doppler spectra. It was found that the use of the maximum systolic frequency, the degree of spectral broadening and ultrasonic imaging (the formation of a map of the arteries using waveform analysis) could only accurately identify those carotid arteries with a stenosis causing a reduction in the luminal diameter of 50% or more when the results of ultrasound were compared with arteriograms or the findings at operation. Furthermore ultrasound could not accurately distinguish between arteries with a severe stenosis or those with an occlusion.

Factors affecting the values of the variables computed by the instrument were studied and it was found that the values could vary quite considerably. There were errors in their measurement which were small (but consistent) under certain circumstances but which could be considerable eg if the degree of spectral broadening was measured using the bidirectional facility of the instrument. Experiments found the resistance parameter to be of little value in the detection of carotid artery disease probably due to the way in which it was calculated. The level of instrument gain was also found to significantly affect the maximum systolic frequency and the degree of spectral broadening. The origin of these measurement errors is discussed.

Experiments (both in a hydraulic model and in vivo) are described which attempted to increase the diagnostic accuracy of ultrasound by

(i) the calculation of the maximum velocity of flow,

(ii) the calculation of a ratio from measurements of Doppler shifted frequencies both proximal and distal to a stenosis, and

(iii) the detection of disturbances of flow.

A new method of calculating the angle of insonation between an ultrasound beam and a vessel is described. It involves the rotation of the ultrasound probe around a known angle and 2 measurements of the maximum Doppler shifted frequencies. From this information the maximum velocity of flow was calculated.

It was found during these experiments that the maximum Doppler shifted frequency decreased when a certain critical angle of insonation was exceeded. A further study using a hydrophone found that this was due to reflection of the ultrasound beam from the surface of the vessel and the critical angle varied with the physical properties of the vessel eg it was higher in calcified arteries than in normal ones.

It was shown in a study using the model that a ratio of the maximum Doppler shifted frequency proximal to a stenosis to that distal to a stenosis could accurately assess the degree of stenosis even if the constriction was less than 50% of the diameter of the lumen. However when compared with arteriograms or the findings at operation neither the maximum velocity of flow nor the ratio described above could identify mild stenoses in patients ie those causing a reduction of luminal diameter of less than 50%. Reasons for this are discussed.

Studies in the model found that CW ultrasound could readily identify turbulent steady flow but it was not possible to show that turbulent oscillatory flow could be demonstrated using ultrasound. From these results the relationship of the velocity profile to the Doppler spectrum, of spectral broadening to turbulent flow, and the occurrence of disturbances of flow in normal arteries are discussed.

GENERAL INTRODUCTION

In this introduction the nature of extracranial carotid artery disease and its importance are described. Methods currently used in its detection and the aims and scope of this thesis are also introduced.

Atherosclerosis in the extracranial carotid arteries is one of the principle varieties of cerebrovascular disease and is important as a treatable cause of stroke. There are causes of carotid artery disease other than atherosclerosis eg trauma but atherosclerosis is by far the commonest. The cause of atherosclerosis is unknown but may result from haemodynamic stress.[1,2] Common complications of an atherosclerotic plaque in the carotid arteries are ulceration, stenosis and thrombosis. Aneurysm formation in this site is very rare.[3]

Blood reaches the brain from the aortic arch via the arterial routes illustrated in Figure 1. Inside the skull both vertebral arteries unite to form the basilar artery and an anastomotic circle (Circle of Willis) is formed from the latter artery and both internal carotid arteries. It is not uncommon for the origins of the great vessels to be different from those portrayed in Figure 1.

Disease anywhere along these pathways may interfere with the cerebral circulation and one of the features of atheroma is its patchy distribution thus multiple sites may co-exist. In a pathological study of the vertebral and carotid systems in unselected patients Schwartz and Mitchell found severe stenoses most commonly at both carotid bifurcations and both

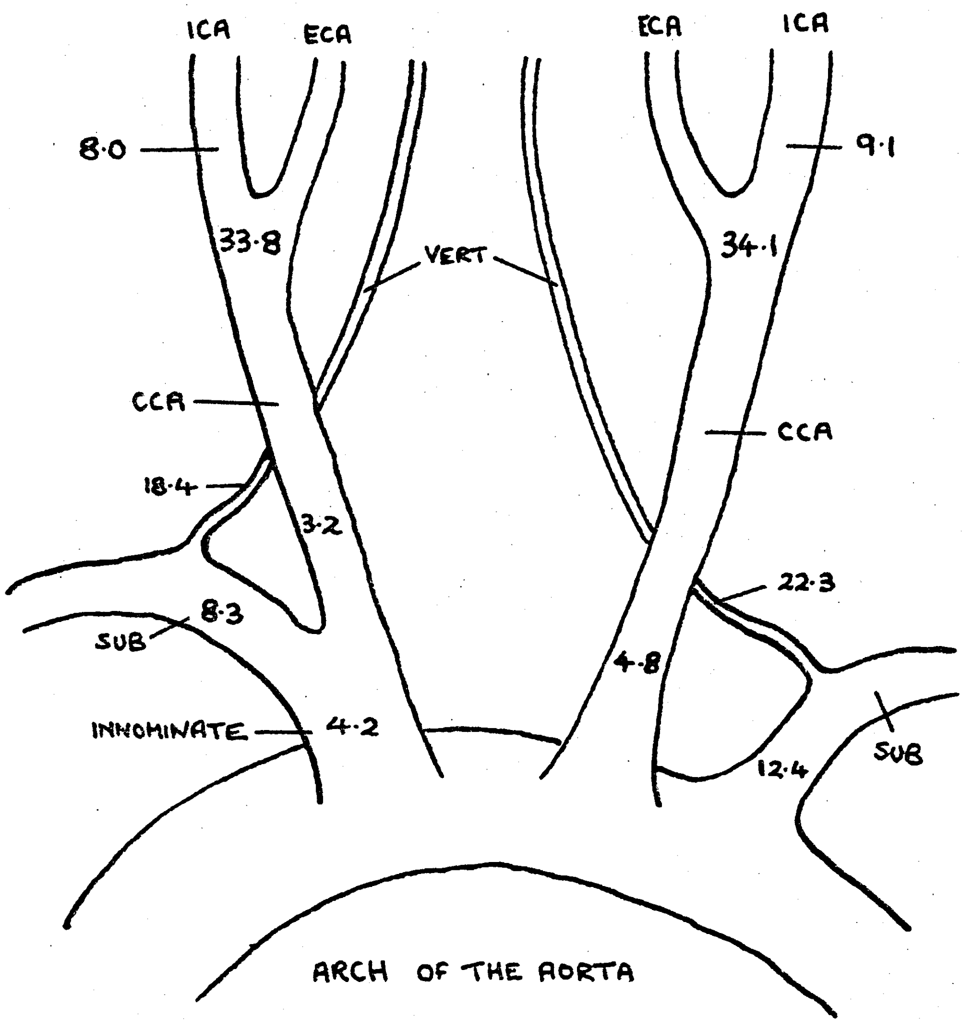

FIGURE 1

The frequency distribution of arterial stenoses in the arteries leading to the brain. The figures express the percentage of patients with a stenosis at that site. (After Hass et al[5])

CCA - common carotid artery
ICA - internal carotid artery
ECA - external carotid artery
SUB - subclavian artery
VERT - vertebral artery

vertebral arteries.[4] Severe stenoses were found at proximal sites in the innominate, both subclavian, both vertebral and the left common carotid arteries and at distal sites in both common carotid and the left vertebral arteries. An arteriographic study of patients with symptomatic cerebrovascular disease found a similar distribution of stenoses (see Figure 1) although in this particular study they were more common at the carotid bifurcation than in the vertebral arteries.[5] The commonest site for thrombosis is the internal carotid artery with the vertebral, common carotid and the left subclavian arteries less frequently affected.[5]

Stroke is likely to have been a cause of death since the days of the earliest civilisations as Soranus of Ephesus (AD 98-138) wrote about apoplexy followed by paralysis and Paul of Aegina, a Surgeon who practised in Alexandria in the 7th century described its treatment.[6] However it is only comparatively recently that atherosclerosis of the carotid arteries in the neck has been implicated in its aetiology. Atherosclerosis was described during the Renaissance by Gabrielle Fallopio (1523-62) and Andreas Vesalius (1514-64) his teacher described the brain and its blood vessels accurately, although he overlooked the circulosus arteriosus not described until 1664 by Thomas Willis.[7-9] The relationship between thrombosis of the intracranial vessels and stroke became established in the 19th century but although certain authors* referred to the importance of disease in the arteries of the neck in the aetiology of cerebral

*It is of interest that one of these authors, Sir William Gull BT, MD, FRCP, FRS (1816-1890) who reported the association between paralysis and occlusion of the innominate and left common carotid arteries was accused of being the infamous Jack the Ripper.[10,13] Gull, Physician to Prime Ministers and Royalty himself died of a stroke.

symptoms their views were largely disregarded.[10,11] The reluctance of pathologists to dissect the neck at post mortem meant that the extra-cranial carotid arteries were largely ignored in both clinical and neuro-pathological studies with the result that the nature of one third of all strokes was unresolved.[12] Thus Hicks concluded as recently as 1949 from the results of 155 autopsies on stroke victims whose carotid bifurcations were not examined "that intrinsic functional vascular disease of the brain (was) the major factor in the pathogenesis of infarction and haemorrhage because of the absence of thrombosis in the arteries of the brain" and 2 years later that "apoplexy (was) an ischaemic disease of the brain most often caused by cerebral vasospasm".[14,15] In the early 1950's Fisher studied the cervical portion of the carotid arteries in 432 consecutive routine autopsies and reported that 9.5% had occlusions or advanced disease of the carotid arteries in the neck.[12] This incidence was equal to that of cerebral haemorrhage and greater than that of intracranial cerebral thrombosis. His experience was to reduce the number of strokes whose cause was unknown to less than 5%.

Cerebrovascular disease is currently the 4th leading cause of death in England and Wales and Table 1 gives the mortality from diseases of the cardiovascular system for the years 1953, 1963 and 1973, a period which has seen the total number of deaths from all causes increase although due to an increase in population the death rate has declined.[16-18] The number of deaths from cerebrovascular disease has increased only in the case of women, a trend not seen in men despite an increase in deaths from ischaemic heart disease over the same period. In the case of

TABLE 1 Deaths from Cardiovascular Disease by Sex in England and Wales[16-18]

	1953 ♂	1953 ♀	1963 ♂	1963 ♀	1973 ♂	1973 ♀
IHD	68251	63185	83559	71256	87158	64735
CVD	28762	39307	32264	48076	31082	49501
C Haem	12831	18274	11754	17656	6229	9151
C Emb	12916	17025	15719	23139	10203	17027

IHD = Ischaemic Heart Disease
CVD = Cerebrovascular Disease
C Haem = Cerebral Haemorrhage
C Emb = Cerebral Embolism and Cerebral Thrombosis

cerebral haemorrhage the numbers of deaths have dropped for both sexes. In Scotland the trends are similar although the death rate from cerebrovascular disease is higher. It was 189 per 100,000 population in 1963 and 197 per 100,000 in 1973.[19,20] There is a regional variation in the mortality from strokes which is strikingly correlated with that from ischaemic heart disease. A study conducted on behalf of the Royal Geographical Society found that Glasgow and Manchester were at the centre of 2 of the areas with the highest mortality from stroke in the United Kingdom.[21] As a major cause of disability it represents a considerable burden for both the family of the victim and the health care resources of the nation quite apart from the effect on the patient. The cost in the United States of America was estimated to be $ 7 billion in 1976 and it is the third leading cause of disability in that country with a prevalence for acute stroke of 794 per 100,000 population.[22,23]

Carotid artery disease may cause cerebral ischaemia in several ways.

Critical Stenosis: A plaque may encroach upon the lumen of a vessel to produce a short, well localised stenosis or a longer length of irregular narrowing. As the cross sectional area of the lumen is reduced the mean velocity of flow needs to increase to maintain the same volume flow. Although a stenosis in its early stages will not reduce volume flow due to an increase in velocity, as the stenosis gets tighter a critical situation is reached whereby any further reduction in area causes a precipitous fall in both flow and pressure.

Crawford et al showed that a 50% reduction in the diameter of the lumen caused a measurable drop in blood pressure and was therefore of functional significance.[24] May et al showed that the critical stenosis could vary in different arteries and was dependant on the velocity in any particular artery.[25] A mean blood pressure of approximately 80 mm Hg is required to maintain cerebral perfusion and stenoses less severe than "critical" may become functionally significant should hypotension occur.[26]

In transient ischaemic attacks the symptoms are often identical in recurrent episodes suggesting the same area of cerebral ischaemia. If both intracranial and extracranial disease are present then the reproducibility of the symptoms may be explained by some factor upsetting the haemodynamic balance eg hypotension through the carotid stenosis causing cerebral ischaemia in that site rendered most deficient in blood supply by the intracranial disease.

Occlusion: A thrombotic occlusion of the internal carotid artery usually occurs from enlargement of mural thrombus or from stasis distal to a stenosis. This leads to a cessation of flow through that vessel but as the pathological process is usually slow it may be symptomless. The efficiency of the collateral circulation and the anatomy of the Circle of Willis will determine whether symptoms ensue.[27]

Embolisation: A plaque may ulcerate at any stage of the disease (before any significant stenosis is apparent). Elements from the blood may adhere to the ulcerated area and subsequently form emboli. Microemboli composed of blood platelets and fibrin may arrest in the small arteries of the brain or retina causing transient ischaemic attacks or larger emboli of atheromatous material or laminated thrombus may occlude larger cerebral vessels causing infarction.[28-30]

"Steal": Cerebral ischaemia may also result from disease of the subclavian artery proximal to the origin of the vertebral artery causing retrograde flow in the latter artery.[31,32]

Atherosclerotic plaques commonly remain unchanged in size for years although some increase in size.[33,34] Others are complicated by the addition of an overlying thrombosis. Not all plaques cause symptoms but tight stenoses and plaques complicated by local thrombosis are thought to place the patient at higher risk of stroke. Asymptomatic carotid artery disease is the expression used to describe patients who have atherosclerotic plaques at the carotid bifurcation but who have no symptoms. Little is known of the natural history of asymptomatic carotid artery disease, Colgan et al recently reported that of 309 patients with asymptomatic carotid stenoses followed up for 3 years there were no deaths from stroke and only 17 became symptomatic.[35,36] The risk associated with an asymptomatic carotid bruit ie a noise heard over the carotid arteries of patients who have no symptoms of cerebrovascular disorder is not defined particularly since some authors have found a high incidence of transient ischaemic attacks and stroke whilst others have reported them to be harmless.[37,38]

Symptomatic patients fair less well and patients who have suffered a recent stroke have a bad prognosis with a mortality ranging from 30-60% for hospitalized patients within 4 weeks of an acute stroke.[39] The mortality from recurrent stroke is 20-50% and in addition the late survival is much reduced, death from some cardiovascular cause occurring in 75% reflecting the widespread arteriopathy.[39] The incidence of further non fatal strokes in untreated patients is 15% but is much higher if the patient has had several previous strokes.[40] Patients with transient ischaemic attacks ie a transient disorder of cerebral function lasting for less than 24 hours have a definite risk of impending stroke. Toole et al reviewed 6 series and found that in 26 patients reveiwed for an average of 45 months, 24% had recurrent transient ischaemic attacks, 26% had a stroke and 21% died.[23] This compared with his own series where 15% had recurrent transient ischaemic attacks, 7% had a stroke, 20% died and 45% remained asymptomatic.[23]

If cerebral infarction has occurred an improvement in the circulation will not cause a return to normal and the treatment for a completed stroke is mainly rehabilitation. One of the factors highlighting the importance of carotid stenoses was the recognition that strokes could be prevented by treating carotid artery disease. The questions of which patients to treat and in what manner are not yet resolved. Treatment may be medical eg aspirin has been shown to reduce the incidence of transient ischaemic attacks but the beneficial effects of dipyrimadole or anticoagulants are much less clear.[41,42] The first operation on the carotid arteries in the neck in a patient who had transient ischaemic attacks was carried out 30 years ago and surgery is now common.[43] It involves either an endarterectomy of the carotid bifurcation or more rarely a reconstruction or extra anatomical bypass of an occluded carotid artery. Surgery for transient ischaemic attacks has been shown to reduce the incidence of both recurrent episodes and stroke when compared with non surgical treatment but whether survival is prolonged is debatable.[23,44,45]

As the pathophysiology of carotid stenoses is poorly understood the selection of other cases for surgery is unclear. Whether to operate and what are the risks associated with operation in patients with bilateral disease, asymptomatic stenoses per se or when other surgery is contemplated eg cardiac is not clear. The timing of surgery in relation to the presence of a stroke in evolution or the time which has elapsed after a completed stroke are also unresolved questions. Surgery is usually contra-indicated when occlusion is present as the majority of patients fail to benefit. The mortality is higher and poor results often obtained if more than one operative procedure is performed or multiple stenoses are present.[45] The risk of surgery is not inconsiderable although the quoted operative mortality is 1-3% and a perioperative neurological deficit is said to occur in 2.5-4.8%.[44-48]

The presence of carotid artery disease may be suspected from the clinical findings alone eg from the history or the detection of a bruit over the artery. It classically results in ipsilateral transient ocular blindness (amaurosis fugax), a stroke, or transient ischaemic attacks affecting the other side of the body.

The relationship between carotid artery disease and symptoms is complex and when disease is diffuse it may not be possible to determine the most important lesion. Disease may be symptomless and although as a group patients with severe stenoses are more likely to have symptoms than those with mild stenoses, in an individual patient it is not possible to predict the presence of a stenosis from the symptoms.[49,50] Again the detection of a carotid stenosis does not imply that any cerebral symptoms which are present result from the stenosis and the role of vertebrobasilar disease must also be considered.

The detection of a cervical bruit is common in patients over the age of 40, (approximately 10% of patients) and may, but by no means always, indicate an underlying carotid stenosis.[49,51,52] The bruit associated with a carotid stenosis may disappear when the stenosis exceeds 75% of the cross sectional area of the lumen of the artery.

The clinical findings for carotid artery disease are not specific and some form of investigation is required which can be used to confirm or refute the diagnosis.

Visualisation of cerebral vessels by contrast radiology was introduced by the Portugese Egas Moniz in 1927 and percutaneous carotid angiography in 1936 by Lomom and Myerson.[53,54] With the introduction of Seldinger's technique to perform arteriography, which he had been using in Sweden since 1952, arteriography flourished although it was accepted in the United States of America rather later than in Europe.[55] It is generally accepted as the gold standard for the assessment of carotid artery disease against which new methods are compared. Its drawbacks are that it is invasive, expensive, it usually requires some form of anaesthesia with in patient hospitalization and it carried a risk. The complications of the procedure include death due to aortic dissection, aneurysm rupture, cardiac complications and haemorrhage; transient or permanent neurological complications; those directly related to the puncture site eg haemorrhage, thrombosis, false aneurysm and arterio-venous fistula; and wire-catheter problems eg perforation, embolism and breakage.[56,57]

Because of these problems and doubts about its accuracy other methods were investigated. These methods include digital intravenous angiography, thermograpy, oculoplethysmography (OPG), carotid phonoangiography (CPA) and ultrasound.[58-85]

OPG is a method of detecting decreased flow in the internal carotid artery by recording the pulse waveforms from bilateral corneal suction cups simultaneously. The ocular pulsations result mainly from ophthalmic arterial flow (from the internal carotid artery) and in order to compare them with external carotid pulsations the test usually involves the application of photoplethysmography to both ears.[58,60]

CPA involves the spectral analysis of sound recordings from the heart and along the course of the carotid arteries.[61] Both techniques are often combined to assess the degree of carotid disease however they are unable to grade the degree of stenosis accurately if it is greater than 40-50% and have a high rate of false negative results (40%) for severe stenoses.[50,60,62-64] Using this technique one cannot reliably distinguish normal patients from those with mild disease. When compared with Doppler ultrasound, whether by a direct examination of the carotid bifurcation or by a peri orbital examination, CPA/OPG has been shown to be less accurate.[63,65] Malone et al who reported a diagnostic accuracy of 91.6% for OPG conceded that it is of minimal value in patients with symptomatic cerebrovascular disease.[60]

Doppler-shifted ultrasound has been used to test for disease of the carotid arteries either by a direct technique where the carotid bifurcation itself is insonated or an indirect technique where a more distal artery is examined.

INDIRECT TECHNIQUES

Pulse Wave Transit Time (TT): This test compares the time it takes a pulse wave to travel from the common carotid artery to the supra orbital artery with the time taken for a wave to travel from the common carotid artery to the superficial temporal artery. A stenosis of the internal carotid artery prolongs the TT from the common carotid artery to the supra orbital artery.[66]

Compression Tests: In these tests the direction of flow in the supra orbital artery (usually antegrade from the internal carotid artery) is determined when the ipsilateral superficial temporal or internal carotid arteries are compressed. In the temporal artery occlusion test a positive result ie an abnormal response is when the flow in the supra orbital artery diminishes, stops or reverse during compression.[67] In a positive test blood flow is retrograde from branches of the external carotid artery and the test is therefore only reliable when there is a critical stenosis in the internal carotid artery reducing mean pressure.[68]

A/B Ratio: The amplitudes of a primary peak A and a secondary peak B in the systolic part of a Doppler spectrum are measured and expressed as a ratio A/B. This ratio is reduced in the presence of disease in the internal carotid artery.[67,68]

The results of indirect tests whether used alone or in combination have been shown to be useful in the detection of severe stenoses.[63,65,67-69] They are of much less value in the detection of lesser grades of disease and are not conclusive in the diagnosis of occlusion of the internal carotid artery.[70]

DIRECT TECHNIQUES

There has been considerable recent interest in the spectral analysis of signals taken at and around the carotid bifurcation using both continuous wave (CW) and pulsed wave (PW) ultrasonic instruments.[63,65,69-83]

The usefulness of several variables computed from spectrum analysed signals, principal component factor analysis (a mathematical technique whereby a waveform under investigation is reconstructed to match a standard image), and ultrasonic arteriography (the construction of an image of the arteries using ultrasound) in the diagnosis of carotid artery disease are undergoing assessment.[65,67,70,71,73,76,77,80,85] Reported results of direct examinations are discussed in Chapter 1.

It is clear that there is a need for an accurate non-invasive test to detect carotid artery disease. Such a test should be able to distinguish reliably between normal and diseased carotid arteries and would be useful in increasing our knowledge of the natural history of the disease. If population subgroups which would benefit from treatment could be identified then the usefulness of the screening of asymptomatic patients could be established. Whether continuous wave ultrasound can meet these requirements is not yet known.

In this thesis the ability to detect carotid disease using continuous wave ultrasound has been investigated both in patients and in a laboratory model. In Chapter 1 the results of a direct examination of the carotid bifurcation using ultrasound were compared with both arteriograms and the findings at operation. In Chapter 2 factors affecting the accuracy of waveform analysis are described. Experiments are described in Chapters 3 and 4 which investigated the possibility of increasing the diagnostic accuracy of ultrasound. The methods included the calculation of the maximum velocity of flow from analysis of Doppler-shifted frequencies and the calculation of a ratio from measurements of maximum Doppler-shifted frequencies both proximal and distal to a stenosis. The detection of disturbances of flow was also investigated (described in Chapter 5). The ability to detect disturbances of flow non-invasively would increase our knowledge of the aetiology of atherosclerosis and stroke as well as being a useful test for the presence of disease.

C H A P T E R 1

AN EVALUATION OF 3 VARIABLES USED IN THE DETECTION OF CAROTID ARTERY DISEASE

INTRODUCTION

This Chapter introduces how ultrasound is used to measure blood velocity and describes 2 experiments: the first investigates the normal ranges of 3 variables, the maximum systolic frequency, a resistance parameter and the degree of spectal broadening computed from spectral analysis of ultrasound waveforms obtained from over the carotid arteries of asymptomatic volunteers; In the second, the results of a direct examination of the carotid bifurcation are analysed to ascertain its value in the detection of carotid artery disease.

THE DOPPLER EFFECT

For all kinds of waves the apparent frequency depends on the motion of the source and the observer and may depend on the motion of the medium. Christian J Doppler (1803-1853) gave his name to this phenomenon when he applied it (albeit incorrectly) in 1842 to explain the changing colour of stars.[86]

THE NATURE OF ULTRASOUND

Ultrasound is generated by transducers, which convert electrical energy into mechanical energy, and is propagated by vibration of the small elements of the medium through which it travels. Ultrasound is the name given to sound waves with frequencies beyond the range of human hearing ie greater than 20 KHz. In medical practice the frequencies of ultrasonic waves used in diagnosis range from 1-20 MHz.

ULTRASOUND AND THE MEASUREMENT OF BLOOD VELOCITY

Satomura first measured blood velocity by the application of Doppler's principle to ultrasound.[87] In vascular work a common arrangement is to have both ultrasound emitter and receiver elements (piezo-electric crystals) housed together in a small cylindrical probe. This probe is then used to insonate any artery under investigation (see Figure 2). The beam from the emitter is scattered by moving blood cells and its frequency is changed. The receiver detects the backscattered ultrasound which has undergone a frequency change - the Doppler-shift. This change in frequency is related to the velocity of the blood cells and the velocity can be measured from the relationship

$$V = \frac{\Delta F\ C}{2F\ \cos\theta} \qquad \text{Equation 1.1}$$

where V is the velocity of the blood, ΔF the Doppler-shifted frequency, F the frequency of the emitted ultrasound, C the velocity of ultrasound in tissue and θ the angle of inclination of the ultrasound beam to the direction of blood flow. Because blood cells travel at different velocities (which vary with time) a range of frequencies is received, known as the Doppler spectrum (see Figure 6). Attractive features of this method of investigation are that it can be performed non-invasively, it is painless and free from complications.

METHODS OF SIGNAL PROCESSING

The development of direction resolving circuitry made it possible to differentiate between targets moving away from and towards the probe.[88] This allowed the direction of arterial flow to be recognised and also

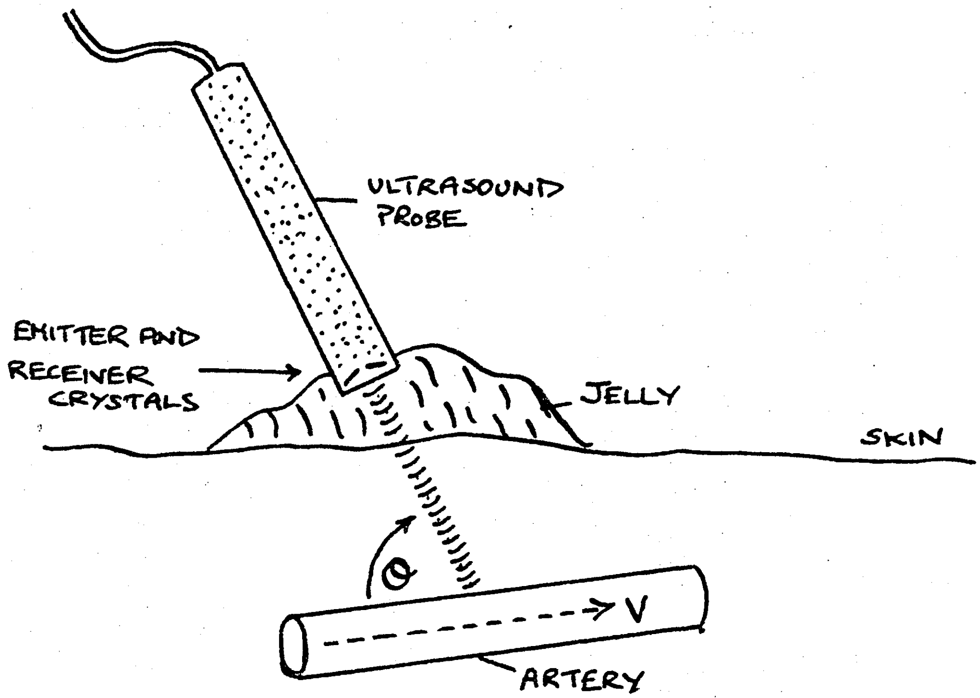

FIGURE 2

The insonation of an artery using a conventional CW probe. θ is the angle of insonation and V is the velocity of flow in the artery.

distinguished it from venous flow. Simply listening to the audio output of the instrument, one of the first methods of signal interpretation, is still of clinical use but some method of displaying the signals is required for more detailed examination.[89] This can be done using a zero-crossing frequency meter which allows the mean frequency of the Doppler spectrum to be displayed as a single line. Errors resulting from background noise, co-existing venous flow, errors in processing signals of low velocity, and in distinguishing reverse flow have given this method a poor reputation.[90,91] Spectral analysis is preferrable, this allows the display of all Doppler frequencies with time; some instruments also have the capability to display the amplitude of each frequency component. The sonograph was an early method of doing this, by recording 3 seconds of information on a magnetic disc and post processing it. Modern machines are able to record and display simultaneously in real time.

CONTINUOUS AND PULSED WAVE INSTRUMENTS

Instruments emitting continuous waves of ultrasound (CW instruments) have 2 crystals which emit and receive ultrasound continuously and employ a relatively broad beam width. They are more common and less expensive than pulsed wave instruments but have certain drawbacks. Among them: velocity information from the entire volume of tissue which is insonated is processed ie signals from more than one artery or vein will be processed if they are within the beam, also the angle between the ultrasound beam and the vessel under investigation can only be estimated making measurement of velocity grossly inaccurate.

Pulsed wave instruments (PW) emit and receive short bursts of ultrasound alternately and have a single crystal. The sample volume (the volume of tissue/fluid from which information is derived) is controlled by the duration and beam width of the ultrasound burst and an electronic range gate controls the depth to which the beam penetrates. Sample volumes as small as 1 mm^3 can be processed.[92] By combining the pulsed wave instrument with a conventional pulse echo ultrasound imaging system (eg the Duplex scanner) information from within the lumen of a particular artery can be obtained.[70,78,82] It is possible to use multiple range gates to construct the velocity profile across an artery and, using the imaging system, to determine the angle between the ultrasound beam and the vessel.[92,93] Measurement of the internal diameter of the vessel using the imaging system allows calculations of absolute volume flow to be made.

METHODS

THE INSTRUMENT

The ultrasonic instrument used in this study was a Vasoscan* (see Figure 3) a computerized vascular diagnostic and imaging system which uses continuous wave ultrasound. Figure 4 shows a diagram of the system's important features which include the map position arm (spatial sensing arm, see Figure 5), the bidirectional facility, the spectrum analyser, and the microcomputer allowing the retrieval and storage of data. The machine was equipped with 4 MHz and 8 MHz transducers. In addition to a visual display the operator could also monitor the signals using a stereo audio system and there was a colour printer for permanent recordings.

Spectral Analysis: The Doppler-shifted signals were processed and displayed in colour as a frequency versus time spectrum. Processing includes digitization of samples with subsequent Fourier analysis into 128 frequency components which are displayed as a vertical line of colour points. The position of a point on a line indicates its frequency and the colour its amplitude.

*Sonicaid Limited, Chichester, United Kingdom

FIGURE 3

Vasoscan

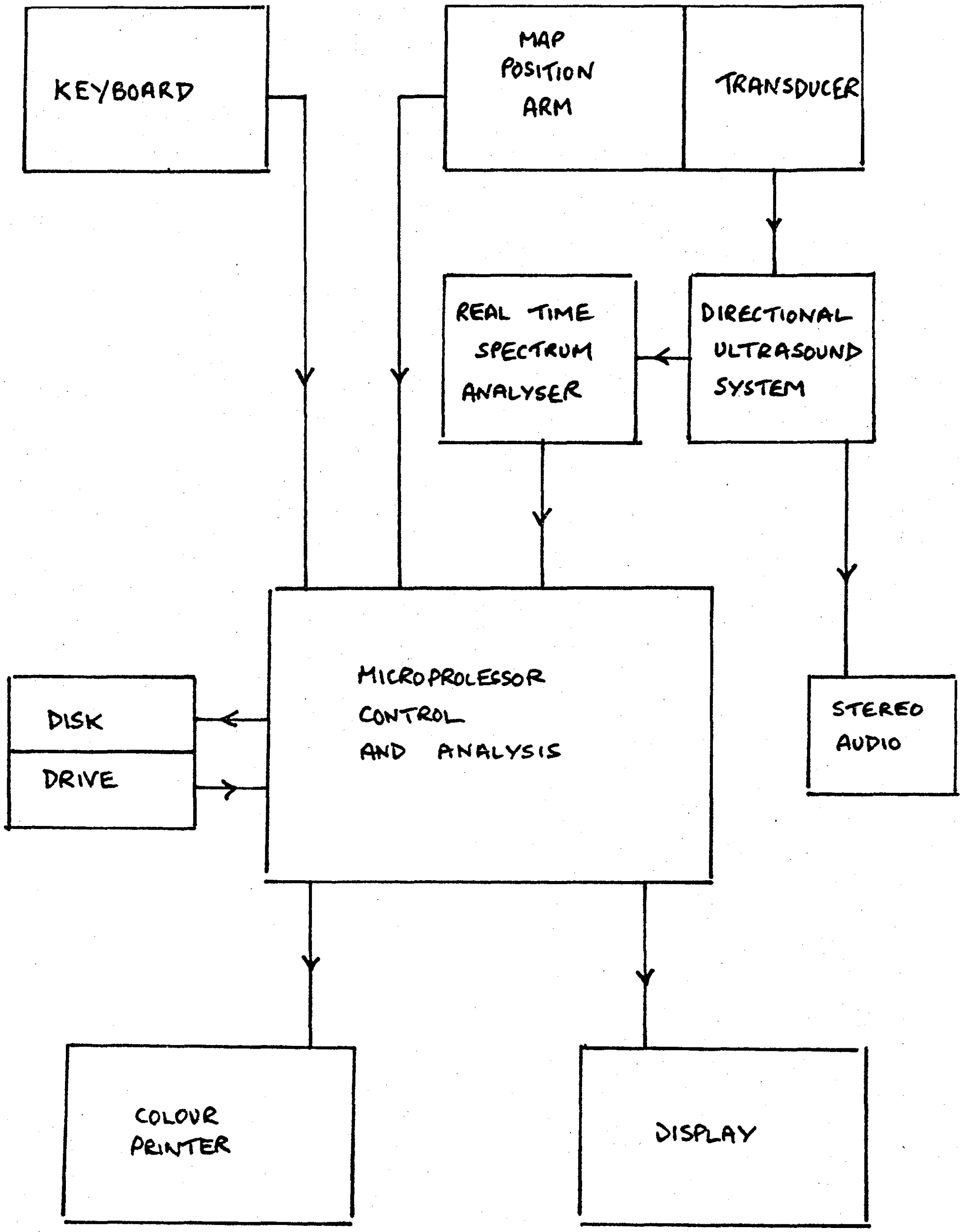

FIGURE 4

A block diagram of Vasoscan

FIGURE 5

The spatial sensing arm

The instrument automatically calculates several variables from the spectrum and displays them in a list on the screen. These variables include:

the maximum systolic frequency (max A, see Figure 6)

the maximum end diastolic frequency (max D, see Figure 6)

a resistance parameter (RP, calculated from equation 1.2)

$$RP = \frac{\text{max A} - \text{max D}}{\text{max A}} \qquad \text{Equation 1.2}$$

and the degree of spectral broadening (SB) determined over a 51.2 m sec interval at peak systole calculated from equation 1.3

$$SB = \frac{\text{F max} - \text{F mean}}{\text{F max}} \times 100\% \qquad \text{Equation 1.3}$$

where F max and F mean represent the maximum and mean frequencies at peak systole.

<u>The Flow Map:</u> The formation of an arterial image (flow map) involved moving the transducer (held in the spatial sensing arm) over the arteries and coloured dots were displayed on the screen at positions where blood flow was detected by ultrasound. The colour of the dot depended on the values of max A and SB calculated from the Doppler signals at that site and by slow movement of the probe a 2 dimensional image was constructed (see Figures 6 and 7).

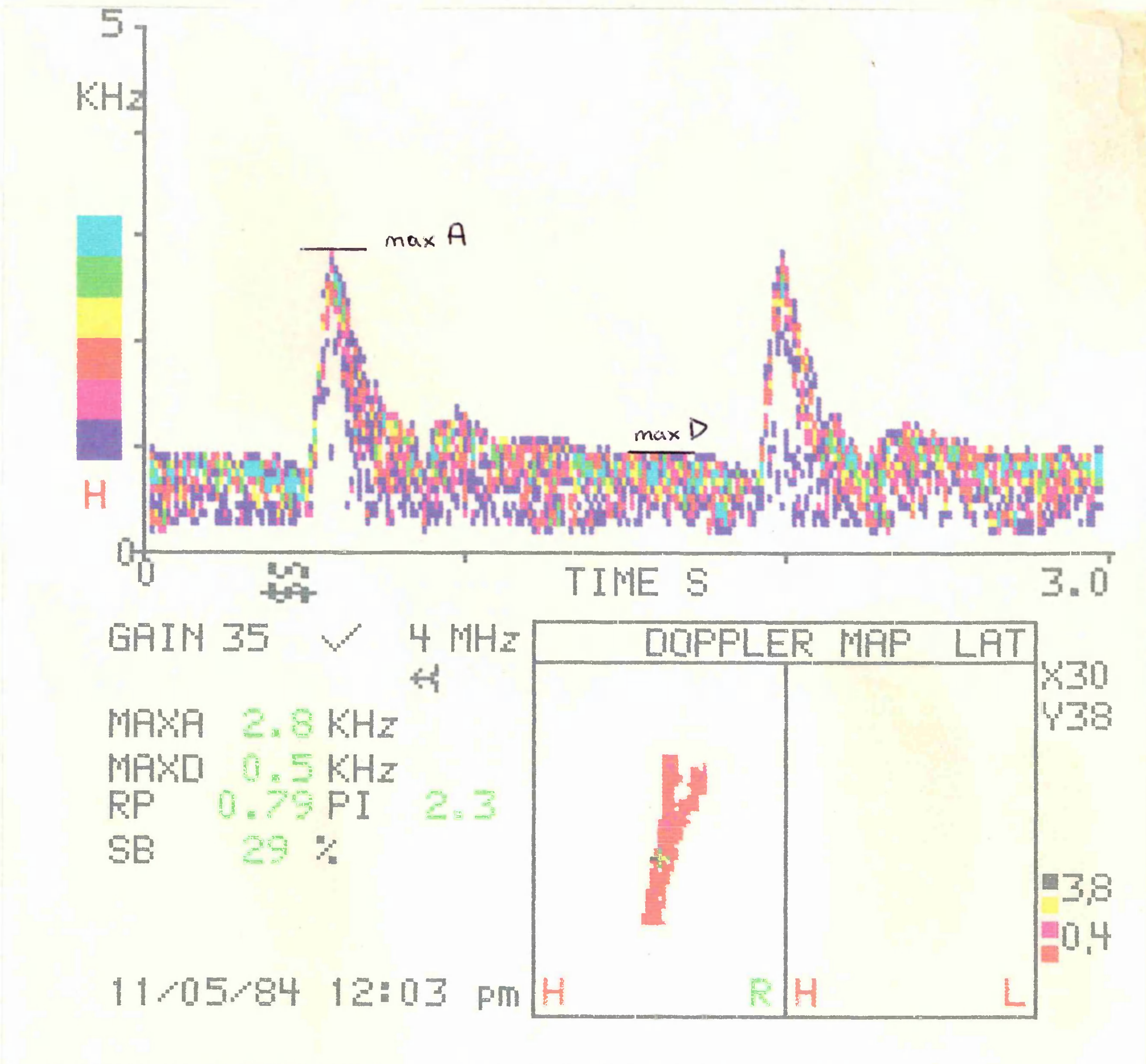

FIGURE 6

A Doppler spectrum and flow map. The typical appearance of spectra from the common carotid artery with a normal flow map recorded using the unidirectional facility. The cross on the map gives the position of the probe relative to the arteries. The colour of each dot of the spectrum represents the intensity of each frequency.

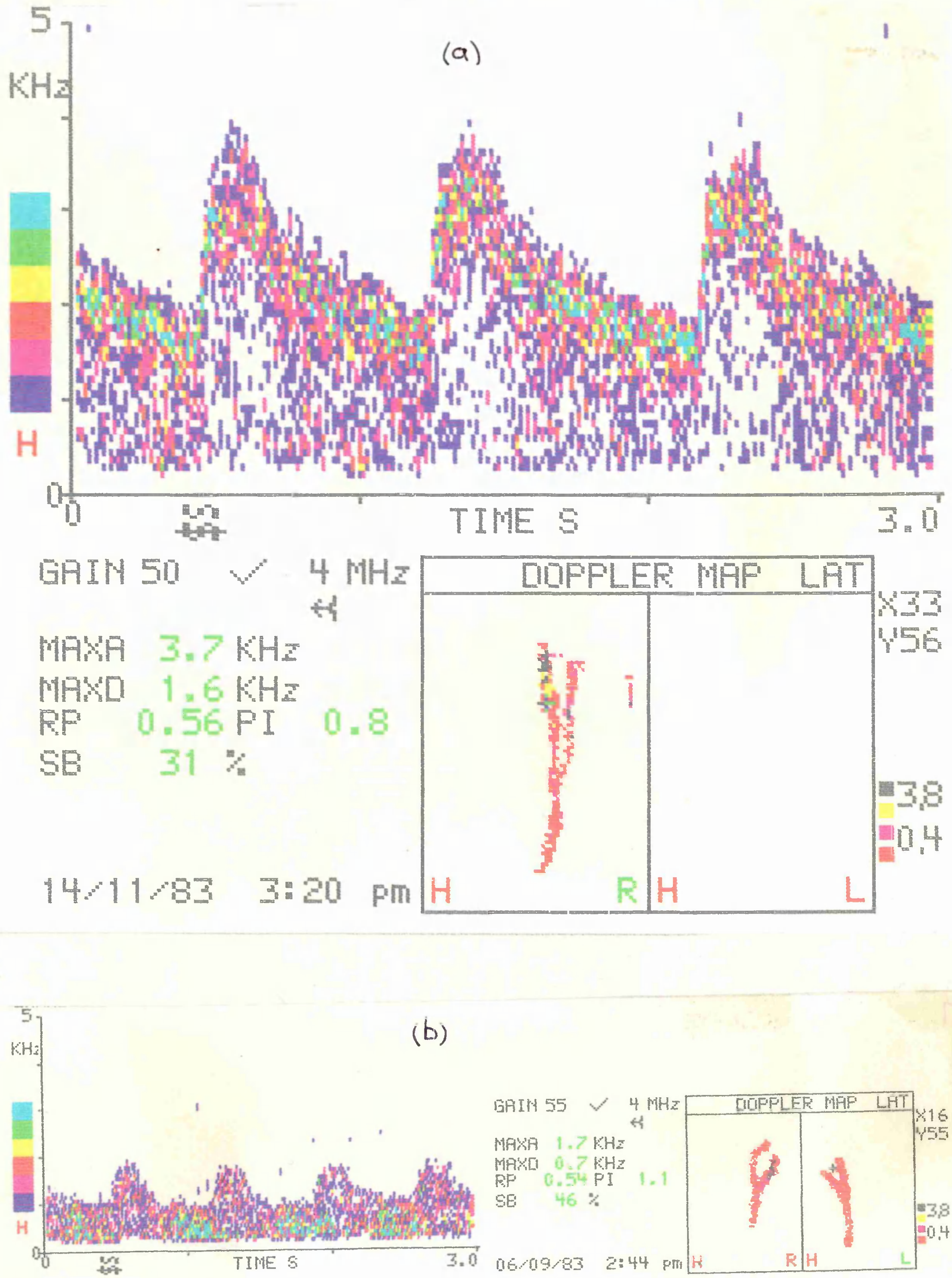

FIGURE 7

Abnormal flow maps. The upper map (a) of the right carotid arteries has black and yellow dots in the right internal carotid artery and the lower map (b) of the right carotid arteries has black dots in the right external carotid artery.

Display: The display included 3 seconds duration of spectrum analysed signals, flow maps of both carotid bifurcations and a list of the variables quoted above.

THE METHOD OF THE EXAMINATION OF PATIENTS

Each patient lay supine on a couch in a warm room with his/her head beneath the spatial sensing arm with the chin elevated and turned slightly away from the side under investigation. After a short period of rest the 4 MHz transducer, held in a position lateral to the patient's neck in a coronal plane, was used to insonate the carotid arteries (see Figure 8). When satisfactory signals were obtained from the arteries rotation of the probe was prevented by tightening a screw (which prevented the operator from changing the angle of insonation) and mapping was begun. During the procedure it was important to keep the ultrasound beam directed onto the artery under examination and to follow the course of the artery accurately. Extraneous noise could produce dots on the screen when the probe was not directed at an artery. The mapping colours were represented as follows:

Black/White :	max A $>$ 3.8 KHz and SB $>$ 45%
Yellow :	max A $>$ 3.8 KHz and SB $<$ 45%
Magenta :	0.4 KHz $<$ max A $<$ 3.8 KHz and SB $>$ 45%
Red :	0.4 KHz $<$ max A $<$ 3.8 KHz and SB $<$ 45%

The position of the probe during mapping was indicated by a white cross (the cursor) on the flow map. This enabled the operator to identify the sampling site at any given moment.

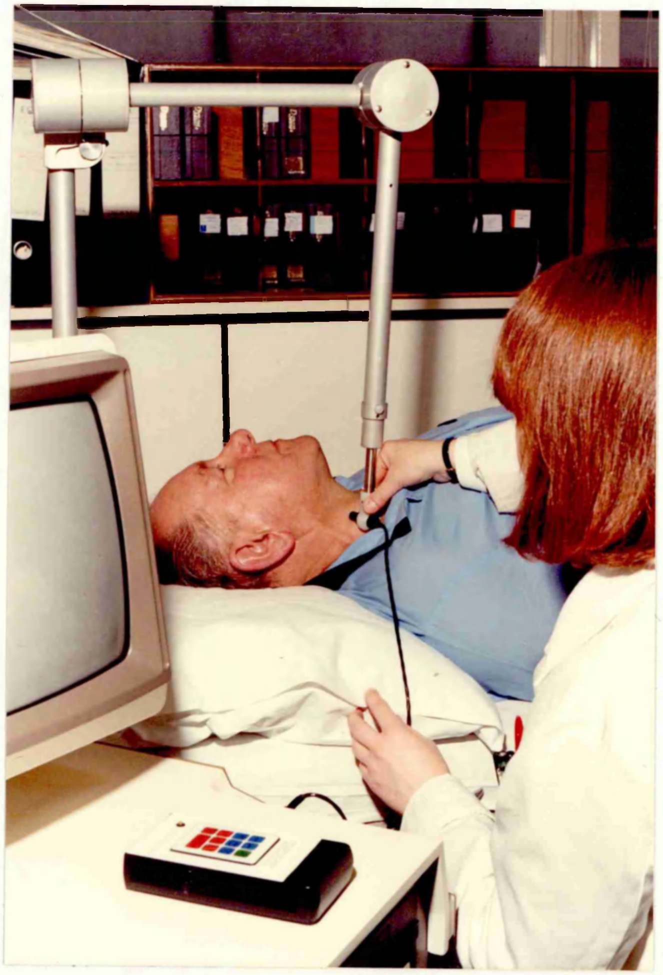

FIGURE 8

The method of examining the carotid arteries of the right side of the neck.

Examinations were performed either by myself or a technician, using an optimum level of instrument gain. The time necessary to examine both right and left carotid arteries in a patient was approximately 20-30 minutes.

METHOD OF SELECTING SAMPLE SITES

Using the flow map and cursor we made the following definitions. When the cursor was measured to be beyond 1 cm of the carotid bifurcation then that site was classed as either proximal common carotid artery, distal internal carotid artery or distal external carotid artery. When the cursor was within 0.5-1 cm of the bifurcation then the site was classed as distal common carotid artery, proximal internal carotid artery or proximal external carotid artery. Signals were also recorded from as close to the bifurcation as possible, when they appeared to have the characteristics of spectra from the external carotid artery they were classified as bifurcation (BIF 1), and when the configuration of the spectra were typical of the internal carotid artery as bifurcation 2 (BIF 2).

The scale of the flow map displayed on the screen was found to be 1.25 : 1 from an experiment (see Appendix 1). The scale of the larger scale printed record was 1.67 : 1 and of the smaller scale printed record 3.33 : 1.

EXPERIMENTS

EXPERIMENT 1.1 The Normal Ranges of Max A, RP and SB in the Carotid Arteries of Asymptomatic Volunteers

Seventeen volunteers (mean age of 25 years) were examined using Vasoscan. Flow maps of both right (n = 17) and left (n = 14) carotid bifurcations were constructed and displays from the carotid arteries both proximal to and distal from the bifurcation (proximal common carotid artery, internal carotid artery and external carotid artery, distal common carotid artery, internal carotid artery and external carotid artery and bifurcation [BIF 1 and BIF 2]) were stored on computer floppy discs. Values for max A, RP and SB at each site in each volunteer were noted.

Means and standard deviations were calculated for all values of each variable at each site and then for all values in each artery. A threshold value equal to the mean plus 1.95 times one standard deviation was calculated. Assuming a Gaussian distribution then 95% of random observations would lie below the threshold value defined above.

EXPERIMENT 1.2 The Detection of Carotid Artery Disease Using Max A, RP and SB

In a prospective study the results of direct examinations of the carotid bifurcation in patients were compared both with the grading of disease from arteriograms and the findings at operation.

Methods

Study Groups: 57 patients (32 men and 25 women) with a mean age of 58 years were divided into 2 groups. Group one was comprised of all 57 patients. Of the possible 114 sides there were 7 exclusions: 5 because there were no angiograms (unilateral selective arteriograms) and 2 because of previous endarterectomies. The results of waveform analysis were compared with the grading of disease from arteriograms in 107 carotid arteries (see Figure 9).

Group 2 was comprised of 29 patients who had a surgical exploration of their carotid arteries. In 2 it was bilateral making a total of 31 sides. In this group the results of ultrasound were compared with the findings at operation.

The order of investigations was ultrasound followed by arteriograms followed by surgery if indicated.

Ultrasound: Signals were stored from the same sites as Experiment 1.1 with extra recordings from the site of stenoses if necessary. A pro-forma was completed for each side which included the displayed values for max A, RP and SB at each specific site and comments on the flow map. A flow map was judged abnormal if a cluster of white or yellow dots appeared in an artery or if no signals could be detected from an artery ie it was absent on the map. Neither a single yellow or white dot nor any number of magenta coloured dots were considered abnormal thus the degree of spectral broadening was not taken into account in judging a map normal or abnormal.

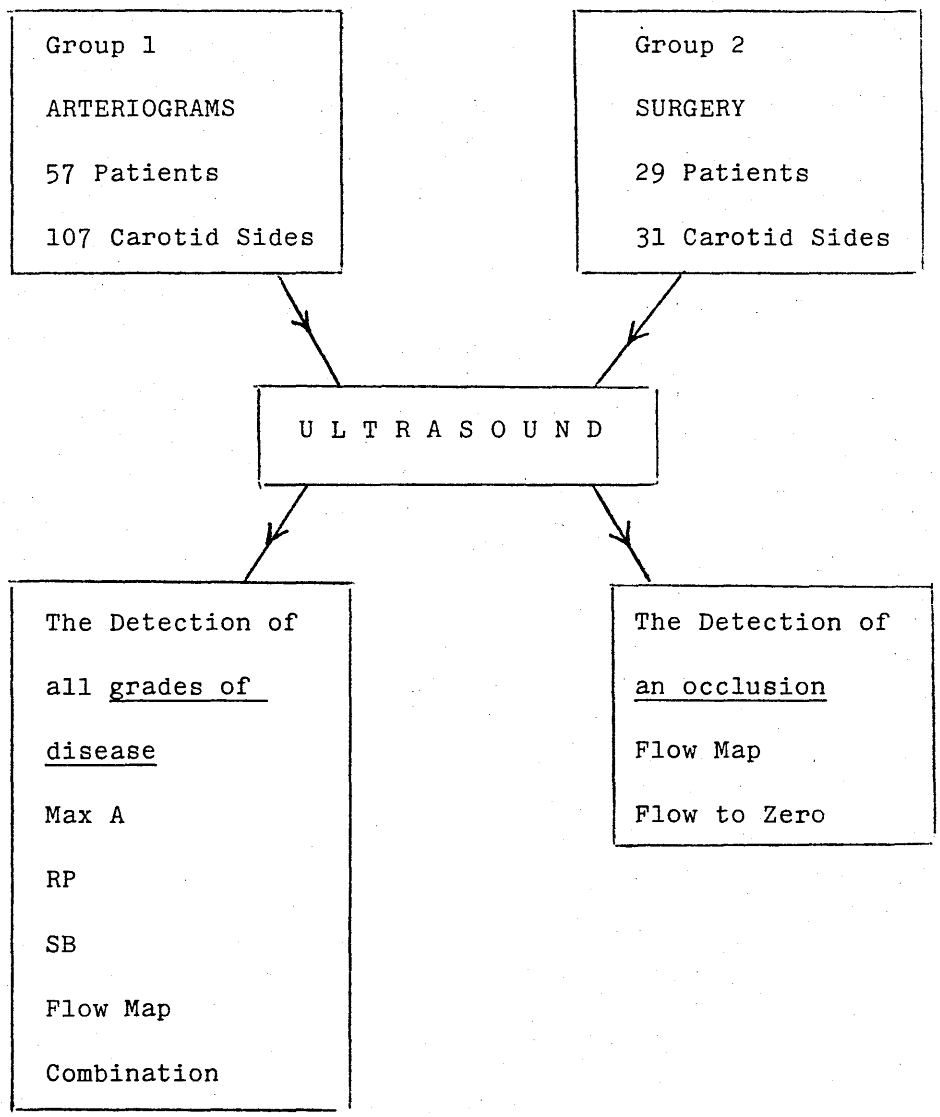

FIGURE 9

The 2 study groups in Experiment 1.2

Arteriograms: Biplanar views of the carotid arteries from the arch of the aorta to the base of the skull and the subclavian and vertebral arteries were obtained using a femoral, translumbar or axillary approach. Five patients referred from another hospital had had selective carotid punctures performed. Intracranial views were not routinely obtained.

The carotid arteries were graded by 2 surgeons as normal, showing minimal disease, a stenosis or an occlusion. Stenoses were further subdivided into those that were severe and those that were mild. A severe stenosis had a reduction in diameter of at least 50%. The presence of any atherosclerosis in the common carotid artery proximal to the bifurcation was also noted.

Surgery: At operation patients' carotid arteries were graded by one surgeon as minimal disease eg a small ridge or ulcer, mild or severe stenosis, or occlusion.

Analysis of Results

The Detection of Disease: Threshold values for max A of 3.5 and 3.8 KHz, for RP of 0.75 and 0.87, and for SB of 50% and 58% and the finding of an abnormal flow map were all tested for accuracy in Groups one and 2. A combination of max A (at a threshold value of 3.5 KHz), SB (at a threshold value of 58%) and the finding of an abnormal flow map was also tested along with the other variables. In the case of max A the highest value in any artery was used but if this was between 3.0 and 3.4 KHz the peak systolic frequency from the displayed spectra was measured by the operator (True max A) as this latter measurement was invariably higher (see Experiment 2.3). In the case of RP only those signals from the common carotid artery were used and for SB only those signals taken with the unidirectional facility (see Experiment 2.4) were used.

The Detection of an Occlusion: The absence of an artery on the flow map and the finding of flow to zero during late diastole in spectra from the common carotid artery or internal carotid artery were tested for accuracy in both groups.

Accuracy: The method of assessing the accuracy of each variable was by using decision matrices (see Appendix 2).

RESULTS

EXPERIMENT 1.1 The Normal Range of Max A, RP and SB in the Carotid Arteries of Asymptomatic Volunteers

Tables 2 and 3 give the means and standard deviations for max A, RP and SB at each site on different sides of the neck and Tables 4 and 5 give the means, standard deviations and threshold values for the same variable in each artery and at the bifurcation. Figure 10 and 11 give the mean values of max A, RP and SB at different sites in the carotid arteries of the volunteers.

EXPERIMENT 1.2 The Detection of Carotid Artery Disease Using Max A, RP and SB

The Detection of Disease

Table 6 gives the numbers of patients classified into different grades of disease on arteriograms and at operation. Tables 7-13 give the results of using ultrasound to test for carotid artery disease. Table 14 summarizes the results of comparing ultrasound with arteriograms.

(i) Specificity: The map had the highest specificity (92%) compared with the other variables and threshold values of 50% for SB and 0.75 for RP were clearly inadequate with specificities of 21% and 29% respectively.

(ii) Sensitivity: When comparing ultrasound with arteriograms the overall sensitivity of the variables ie for all grades of disease was low. It was only 41%-44% for max A, 34% for RP,

TABLE 2 Normal Values for Max A, RP and SB at Different Sites in the Right Carotid Arteries

Variable	Site	n	Mean	SD
Max A (right)	prox CCA	17	2.54 (KHz)	0.515 (KHz)
	dist CCA	17	2.49	0.543
	BIF 1	16	2.4	0.655
	BIF 2	16	2.11	0.562
	prox ICA	17	1.929	0.471
	dist ICA	16	2.013	0.415
	prox ECA	17	2.518	0.689
	dist ECA	17	2.39	0.654
RP (right)	prox CCA	17	0.786	0.05
	dist CCA	17	0.762	0.047
	BIF 1	16	0.77	0.074
	BIF 2	16	0.713	0.082
	prox ICA	17	0.699	0.064
	dist ICA	16	0.694	0.073
	prox ECA	17	0.825	0.059
	dist ECA	17	0.829	0.062
SB (right)	prox CCA	17	32.06 (%)	7.87 (%)
	dist CCA	17	27.94	6.68
	BIF 1	16	40.19	6.53
	BIF 2	15	43	5.54
	prox ICA	17	39.71	7.12
	dist ICA	16	42.75	6.56
	prox ECA	17	39.71	5.43
	dist ECA	17	41.65	6.43

SD - standard deviation
Prox - proximal
Dist - distal
CCA - common carotid artery
BIF - bifurcation
ICA - internal carotid artery
ECA - external carotid artery

The same abbreviations are used in subsequent tables

TABLE 3 Normal Values for Max A, RP and SB at Different Sites in the Left Carotid Arteries

Variable	Site	n	Mean (KHz)	SD (KHz)
Max A Left	prox CCA	14	2.585	0.677
	dist CCA	12	2.54	0.594
	BIF 1	10	2.13	0.495
	BIF 2	13	2.38	0.698
	prox ICA	14	1.89	0.462
	dist ICA	13	2.077	0.4
	prox ECA	14	2.5	0.655
	dist ECA	12	2.63	0.609

Variable	Site	n	Mean	SD
RP Left	prox CCA	14	0.761	0.066
	dist CCA	12	0.768	0.039
	BIF 1	10	0.758	0.076
	BIF 2	13	0.784	0.078
	prox ICA	14	0.676	0.079
	dist ICA	13	0.662	0.094
	prox ECA	14	0.822	0.044
	dist ECA	12	0.833	0.056

Variable	Site	n	Mean (%)	SD (%)
SB Left	prox CCA	14	32.5	6.17
	dist CCA	12	33.58	7.49
	BIF 1	10	42.2	7.18
	BIF 2	13	42.3	5.29
	prox ICA	14	42.93	6.37
	dist ICA	13	39	7.15
	prox ECA	14	43	6.78
	dist ECA	12	40	5.70

TABLE 4 Threshold Values for Max A, RP and SB in the Right Carotid Arteries

Variable	Site	n	Mean (KHz)	SD (KHz)	Threshold (KHz)
Max A Right	CCA	35	2.474	0.530	3.5
	BIF	32	2.25	0.612	3.4
	ICA	34	1.956	0.441	2.8
	ECA	37	2.476	0.695	3.8
Variable	**Site**	**n**	**Mean**	**SD**	**Threshold**
RP Right	CCA	35	0.772	0.051	0.87
	BIF	32	0.747	0.08	0.90
	ICA	34	0.694	0.068	0.83
	ECA	37	0.826	0.059	0.94
Variable	**Site**	**n**	**Mean (%)**	**SD (%)**	**Threshold (%)**
SB Right	CCA	35	29.8	7.47	44
	BIF	32	41.63	6.06	53
	ICA	34	40.09	9.33	58
	ECA	37	40.62	5.74	52

TABLE 5 Threshold Values for Max A, RP and SB in the Left Carotid Arteries

Variable	Site	n	Mean (KHz)	SD (KHz)	Threshold (KHz)
Max A Left	CCA	27	2.529	0.643	3.8
	BIF	23	2.274	0.619	3.5
	ICA	29	1.972	0.426	2.8
	ECA	26	2.612	0.591	3.8
Variable	**Site**	**n**	**Mean**	**SD**	**Threshold**
RP Left	CCA	27	0.763	0.053	0.87
	BIF	23	0.772	0.076	0.92
	ICA	29	0.664	0.085	0.83
	ECA	26	0.828	0.05	0.93
Variable	**Site**	**n**	**Mean (%)**	**SD (%)**	**Threshold (%)**
SB Left	CCA	27	33.29	6.74	46
	BIF	23	42.26	6.03	54
	ICA	29	40.69	6.92	54
	ECA	26	41.62	6.37	54

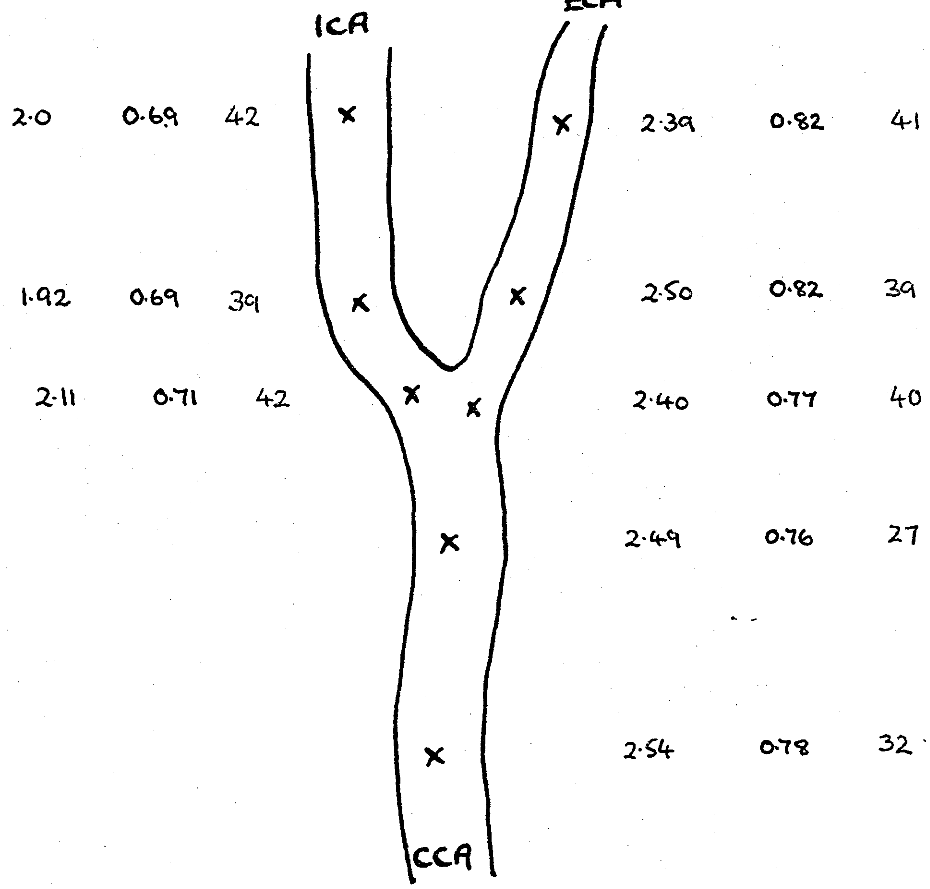

FIGURE 10

Experiment 1.1 Mean values of max A, RP and SB at different sites in the right carotid arteries.

Black - max A
Blue - RP
Red - SB

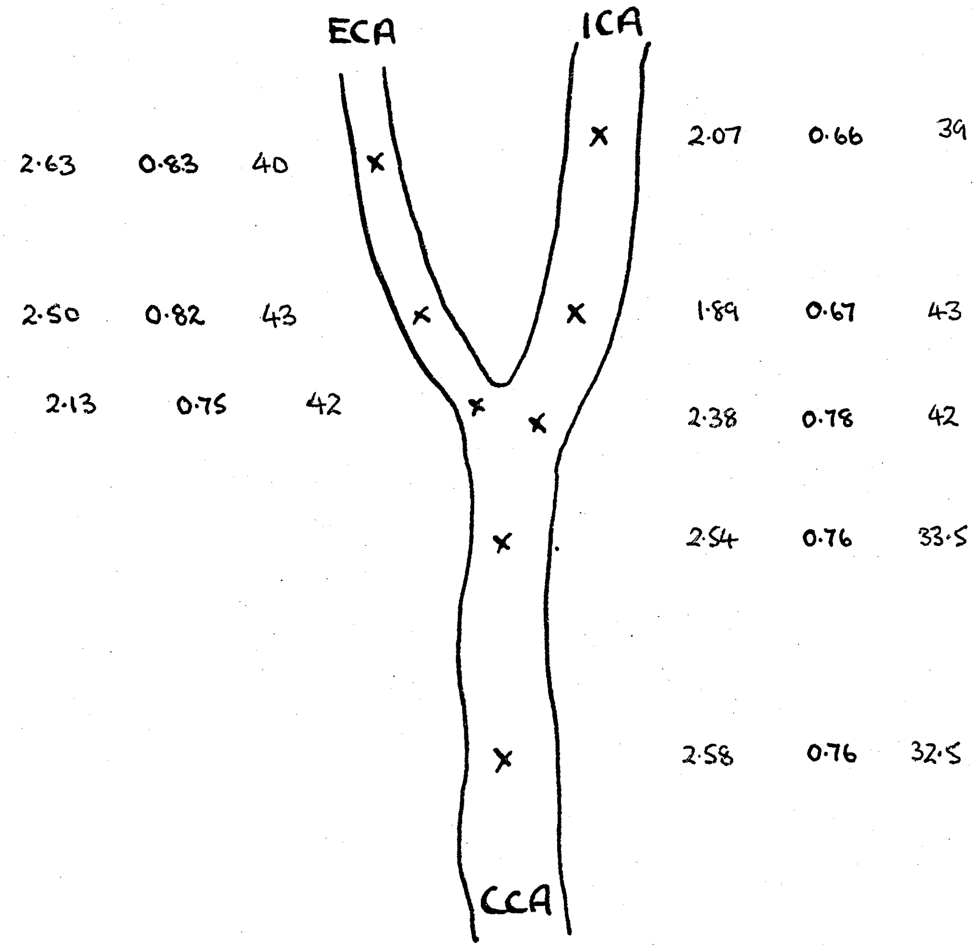

FIGURE 11

Experiment 1.1 Mean values of max A, RP and SB at different sites in the left carotid arteries.

Black - max A
Blue - RP
Red - SB

TABLE 6 The Grading of Carotid Bifurcations Using Arteriograms and the Findings at Operation

	Arteriograms	Surgery
Normal	48	0
Minimal Disease	15	3
Mild Stenosis ($<$50%)	19	14
Severe Stenosis ($>$50%)	18	11
Occlusion	7	3
Total	107	31

TABLE 7 A Comparison of Max A with Arteriograms

Variable	Max A		Max A	
Threshold	(3.5 KHz)		(3.8 KHz)	
	+	-	+	-
Normal	9	39	7	41
Minimal Disease	4	11	4	11
Mild Stenosis	7	12	7	12
Severe Stenosis	11	7	10	8
Occlusion	4	3	3	4
Specificity	39/48 (81%)		41/48 (85%)	
Overall Sensitivity	26/59 (44%)		24/59 (41%)	
Sensitivity for Severe Stenosis	11/18 (61%)		10/18 (56%)	

TABLE 8 A Comparison of RP with Arteriograms

	RP (CCA)		RP (CCA)	
Threshold	0.75		0.87	
	+	-	+	-
Normal	34	14	15	33
Minimal Disease	10	5	4	11
Mild Stenosis	17	2	7	12
Severe Stenosis	13	5	6	12
Occlusion	7	0	3	4
Specificity	14/48 (29%)		33/48 (69%)	
Overall Sensitivity	47/59 (80%)		20/59 (34%)	
Sensitivity for Severe Stenosis	13/18 (72%)		6/18 (33%)	

TABLE 9 A Comparison of SB with Arteriograms

Variable	SB		SB	
Threshold	50%		58%	
	+	−	+	−
Normal	19	5	5	19
Minimal Disease	4	2	2	4
Mild Stenosis	3	4	1	6
Severe Stenosis	7	2	4	5
Occlusion	2	2	2	2
Specificity	5/24 (21%)		19/24 (79%)	
Overall Sensitivity	16/26 (62%)		9/26 (35%)	
Sensitivity for Severe Stenosis	7/9 (78%)		4/9 (44%)	

TABLE 10 A Comparison of the Flow Map and the Combination with Arteriograms

Threshold	Flow Map		Combination (Map, Max A [3.5 KHz] and SB [58%]	
	+	-	+	-
Normal	4	44	11	37
Minimal Disease	4	11	7	8
Mild Stenosis	5	14	9	10
Severe Stenosis	9	9	17	1
Occlusion	5	2	7	0
Specificity	44/48 (92%)		37/48 (77%)	
Overall Sensitivity	23/59 (39%)		40/59 (68%)	
Sensitivity for Severe Stenosis	9/18 (50%)		17/18 (94%)	

TABLE 11 A Comparison of Max A and SB with the Findings at Operation

Variable	Max A		SB	
Threshold	3.5 KHz		58%	
	+	-	+	-
Minimal Disease	1	2	1	1
Mild Stenosis	5	9	3	4
Severe Stenosis	7	5	2	5
Occlusion	3	3	2	1
Overall Sensitivity	16/31 (52%)		8/19 (42%)	
Sensitivity for Severe Stenoses	7/12 (58%)		2/7 (29%)	

TABLE 12 A Comparison of the Flow Map and the Combination with the Findings at Operation

	Map		Combination (Flow Map, Max A [3.5 KHz] and SB [58%])	
	+	-	+	-
Minimal Disease	1	2	1	2
Mild Stenosis	4	10	8	6
Severe Stenosis	6	5	9	2
Occlusion	3	0	3	0
Overall Sensitivity	14/31 (45%)		21/31 (68%)	
Sensitivity for Severe Stenosis	6/11 (55%)		9/11 (82%)	

<u>TABLE 13</u> The Sensitivity of Ultrasound Compared with both Arteriograms and the Findings at Operation

		Max A	Flow Map	SB	Combination as before
Threshold		3.5		58%	
Overall	a) Arteriograms	44	39	35	68
	b) Surgery	52	45	42	68
All stenosing disease ie mild and severe stenoses combined	a) Arteriograms	49	38	31	70
	b) Surgery	46	40	36	68
Severe Stenoses	a) Arteriograms	61	50	44	94
	b) Surgery	58	55	29	82

TABLE 14 The Accuracy of Ultrasound Compared with Arteriograms (Expressed as %)

A Summary of Tables 7-10

Variable	RP	Max A	Flow Map	SB	Combination
Threshold	0.87	3.5 KHz		58%	
Specificity	69	81	92	79	77
Overall Sensitivity	34	44	39	35	68
Sensitivity for Severe Stenoses	33	61	50	44	94

35% for SB and 39% for the map. It was higher for the combination (68%) but only at the expense of a reduction in specificity. The sensitivity of the variables increased with increasing severity of disease such that for severe stenoses the combination achieved a sensitivity of 94%. The only exception to this was RP with a sensitivity for severe stenoses of only 33%.

Sensitivities were similar in the comparison of ultrasound with surgery (see Table 13).

The Detection of an Occlusion

(i) The Absence of an Artery on the Flow Map: This occurred in 4 of the 7 occlusions and 5 of the 18 severe stenoses demonstrated on arteriograms. Two of the latter 5 were subsequently found to have occlusions at operation.

(ii) The Detection of Diastolic Flow to Zero: This was found in 3 of the 7 occlusions and 6 of the 18 severe stenoses demonstrated on arteriograms (see Figure 12).

When ultrasound was compared with surgery the findings were similar eg in 5 of 11 severe stenoses found at operation an artery was absent on the map and diastolic flow to zero occurred in 4.

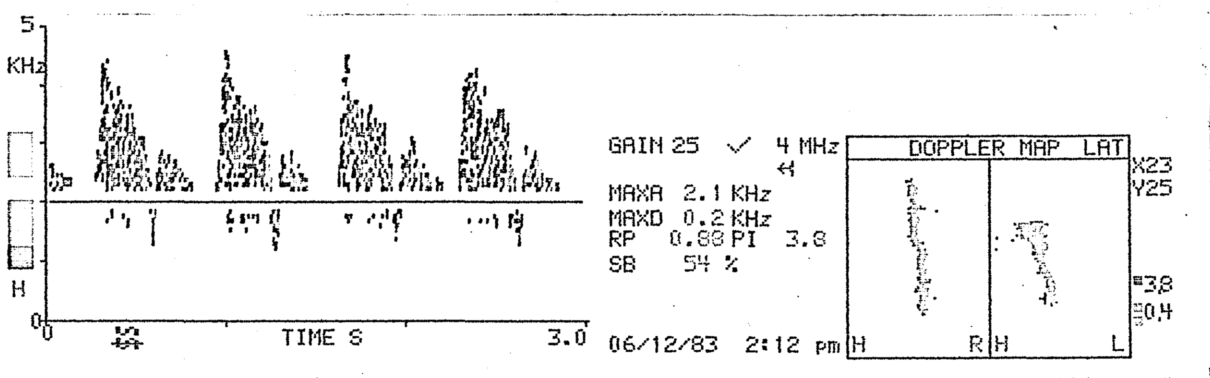

FIGURE 12

Flow to zero in diastole and reversal of flow in late systole in the left common carotid artery in a patient with an occlusion of the left internal carotid artery. The signal was recorded using the bidirectional facility.

DISCUSSION

Threshold values of 3.5-3.8 KHz for max A and 50% for SB have been used by others in the detection of carotid stenosis and the normal range for RP in the common carotid artery has been reported to be 0.55-0.75.[70,73,76,78,94] Pourcelot stressed the importance of symmetry.[94] In Experiment 1.1 a threshold value for max A of between 3.5-3.8 KHz depending on site was found and a value of 58% for SB, marginally higher than that quoted above. However the range of RP in our asymptomatic volunteers was considerably higher with a mean value in the common carotid artery of 0.76-0.77. A threshold of 0.87 was found to be necessary.

Obtaining the normal distribution of these variables from an age group so much younger than the age of symptomatic patients might have been a cause of error as one of the effects of age on arteries is to alter their compliance and possibly the intraluminal blood velocities and ultrasonic waveforms.[95] However as the prevalence of cerebrovascular disease in the community is high and may often be asymptomatic obtaining "normal" older patients is not straightforward.

The standard deviation of each variable at each site was high due to difficulties in ultrasound technique as well as population differences. Mapping difficulties included finding the exact location of the bifurcation which introduced an error in locating correctly the sites at which samples were taken and errors due to the simultaneous display of frequencies received from both the internal carotid artery and the external carotid artery in the region of the bifurcation. Signals that were not reproducible (ie when one waveform appeared different from the next) were not recorded. Variability was also caused by a variation in the angle of insonation. The operator was unable to change the angle of the probe during mapping therefore the angle which gave optimum signals in the common carotid artery could give low amplitude signals in the internal carotid artery.

The accuracy of arteriograms in assessing the degree of carotid stenosis is questionable and an error of as much as 20% for a stenosis of 50% has been shown.[96] Arteriograms remain the gold standard against which other methods of assessing carotid disease are usually judged. The grading of disease at operation has been performed by others and although in this study it was done from a visual assessment only, it nevertheless gave a more reliable grading than arteriograms.[97] Although this study was not primarily concerned with the accuracy of arteriograms 2 of the 3 patients with minimal disease (found at operation) had normal arteriograms, whilst 3 of the 25 stenoses and 2 of the 3 occlusions found at operation were incorrectly graded by arteriograms. However because of the similar sensitivities in Table 13 conclusions based on the results of comparing ultrasound with arteriograms would appear to be valid.

The reliability of the value for each variable computed by Vasoscan is investigated in Chapter 2 but it was important to take into account

True max A for values of max A between 3.0 and 3.4 KHz. Five of the 37 patients with stenoses demonstrated on arteriograms would have been incorrectly classified had the displayed value of max A alone been used.

Signals such as those in Figure 13 which exhibit high values of max A and SB were found in the arteries of several of the patients. Experiment 1.2 was an attempt to quantify how often they occurred and therefore how reliable their use is in the detection of disease. In Experiment 1.2 it was found that a combination of max A, SB and the flow map could detect severe stenoses with a sensitivity of 94%. It was of interest that the sensitivities of these variables individually were only 61%, 44% and 50% respectively but when combined so much higher. This was because in 4 of 7 carotid arteries with severe stenoses where max A did not exceed 3.5 KHz the flow map was abnormal due to the absence of an artery ie it suggested an occlusion.

The interpretation of some published reports is complicated by the use of different terms to express their results eg accuracy, positive predictive value, sensitivity and specificity and furthermore normal patients are often included in the same group as those with slight stenoses.[81] Reports of the sensitivity of the method in the detection of severe (ie $>$ 50%) stenoses range from the mediocre (63%) to excellent (96%).[63,65,69,72-74,98] For mild stenoses (ie $<$ 50%) sensitivities of less than 50% to 75% have been reported.[63,69,72,74]

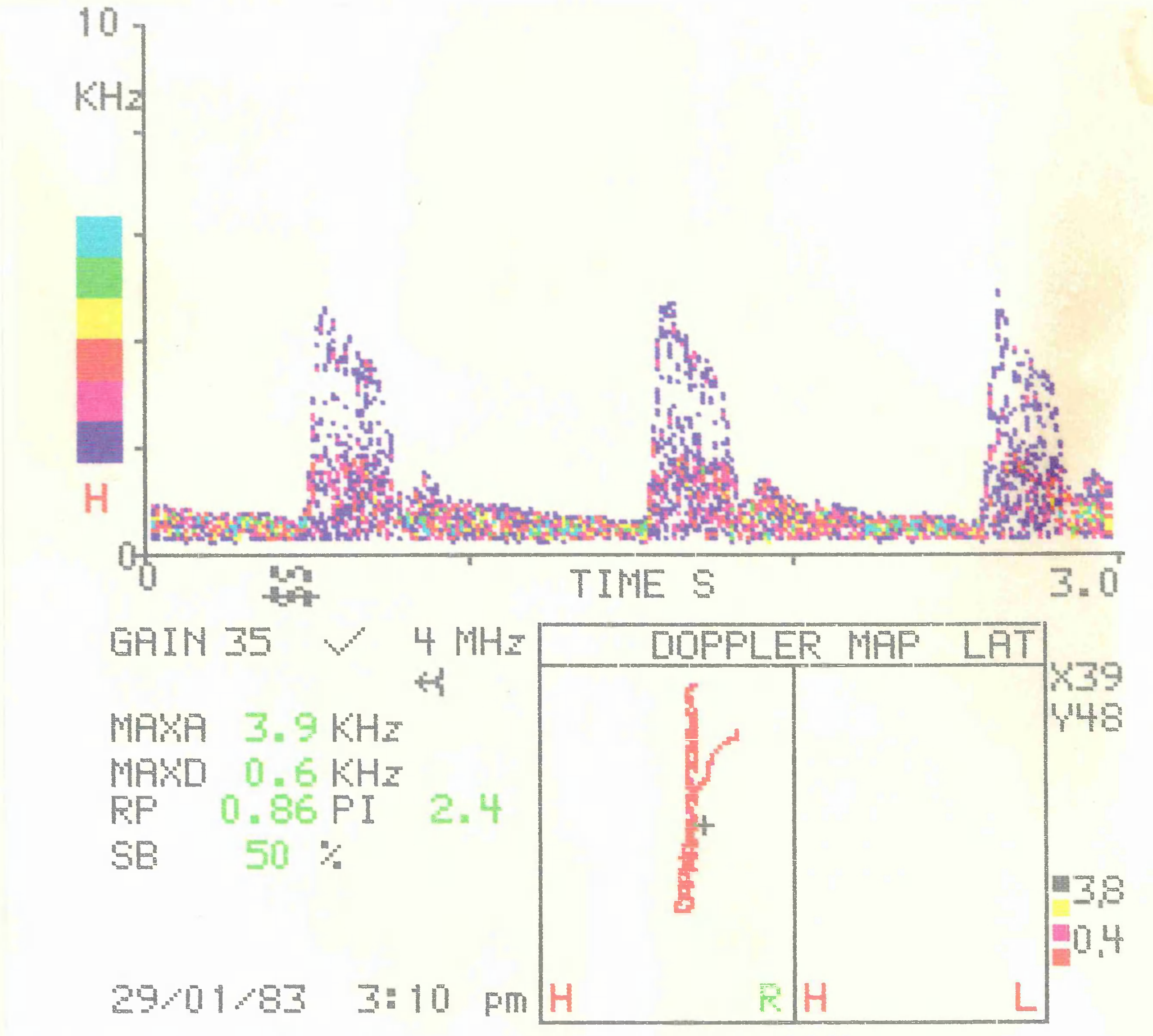

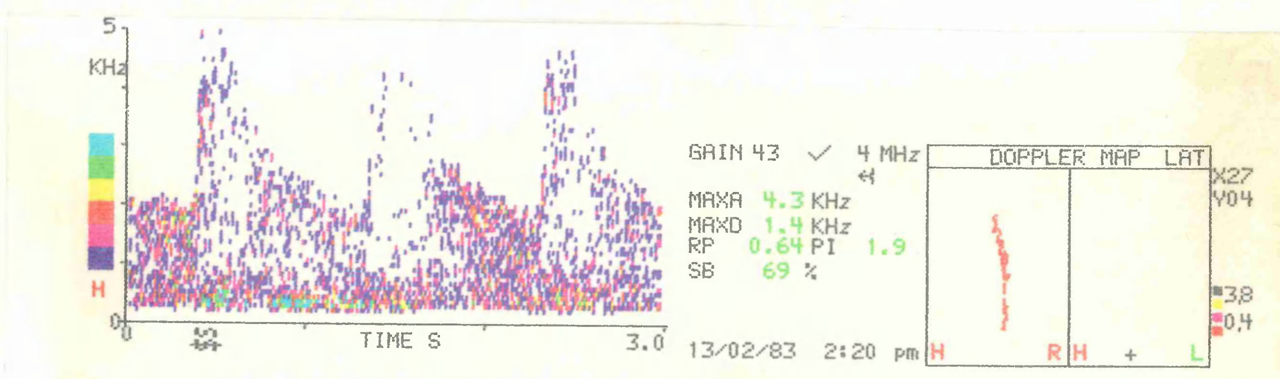

FIGURE 13

Doppler spectra recorded from carotid stenoses with high values of max A and SB.

In this study the sensitivity for the detection of grades of disease less than severe stenoses did not reach 50% for any variable and reported sensitivities of 80% for the detection of stenoses $>$ 10%; 91% for stenoses $>$ 25% and 94% for stenoses $>$ 35% are all much higher than we found for similar grades of stenosis in this study.[73,75,76] We have not been able to emulate Rutherford et al who claimed to be able to separate between normal, stenosed and occluded carotid arteries in 100% of cases using waveform analysis.[71]

The problem of not knowing the angle between the ultrasound beam and the artery is solved by the use of a Duplex scanner. PW instruments are reported to be more accurate in the diagnosis of grades of disease less than severe stenoses and may even detect early atherosclerotic plaques.[83,84,99] However there are some recent reports that CW examinations are as good or better than PW examinations in the detection of severe stenoses.[82,84]

Flow to zero in diastole has been reported to occur in patients with an occlusion or a stenosis of greater than 90% in the internal carotid artery.[79] It has also been reported in patients with aortic valve disease.[100] In Experiment 1.2 neither flow to zero in diastole nor the absence of an artery on the flow map were found to be specific to occlusion of the internal carotid artery. Although all occlusions gave abnormal results and none were categorised as normal it was not possible to reliably distinguish between severe stenoses and occlusions in that experiment. Ultrasound is therefore not 100% reliable in the detection of occlusions, a finding in agreement with others.[65]

C H A P T E R 2

FACTORS AFFECTING THE ACCURACY OF WAVEFORM ANALYSIS IN THE CAROTID ARTERIES

INTRODUCTION

In Experiment 1.2 the effect of disease on the value of several variables was studied but there appeared to be other factors which affected values of these variables. There appeared to be errors in the values computed from the Doppler spectra from the carotid arteries studied in Experiments 1.1 and 1.2 and furthermore these values seemed to vary considerably despite the sample volume being kept constant. It seemed likely that these errors were inherent in the apparatus, were because of variations in technique or were dependent upon the method of analysis.

In Experiment 2.1 the variability of max A, RP and SB at a constant site was studied and the effect of different levels of instrument gain on the values of the same variables was studied in Experiment 2.2. Measurement errors in both max A and max D were studied in Experiment 2.3 and a measurement error in the degree of spectral broadening due to scanning technique in Experiment 2.4.

METHODS

The carotid arteries were examined with Vasoscan using the same techniques described in Chapter 1.

THE AUTOMATIC GAIN CONTROL (AGC)

The AGC is a facility designed to keep the signal at a constant level of gain (which is adjustable). When tracking an artery during mapping it is easy for the probe to drift sideways thus decreasing the signal to noise ratio. The use of the AGC is an attempt by the instrument makers to correct this.

THE DIRECTIONAL FACILITY

Vasoscan gives a choice between a unidirectional display and a bidirectional display. With the unidirectional mode only those velocities moving in a single direction relative to the probe can be displayed (see Figure 6) but the use of the bidirectional facility allows the simultaneous display of velocities moving both away from and towards the probe. This is useful for example in demonstrating reverse flow (see Figure 12).

THE FREQUENCY CURSOR

This is a feature of the instrument which allows the operator to measure the frequency at any particular point on the Doppler spectra displayed on the screen. This was used to measure:

(i) The average maximum frequency at peak systole (True max A, see Figure 14)

(ii) The average maximum end diastolic frequency (True max D, see Figure 14).

(a)

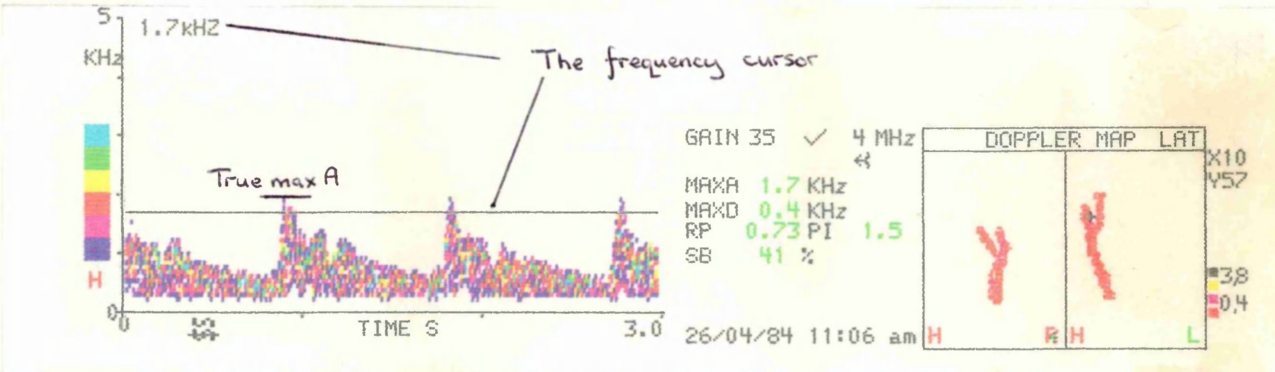

(b)

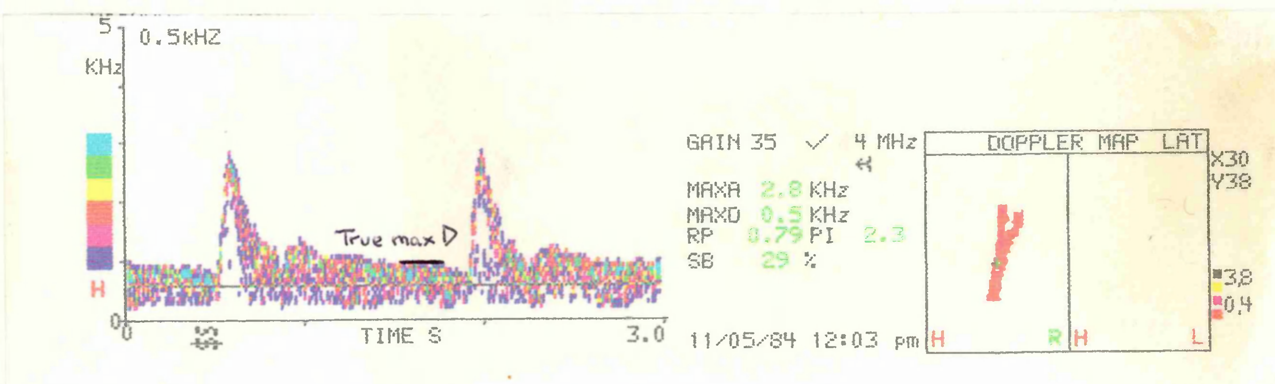

FIGURE 14

True max A and True max D. The operator can use a frequency cursor to determine any desired frequency. In the upper figure (a) the cursor demonstrates the displayed value of max A eg 1.7 KHz. In the lower figure (b) it demonstrates the display value of max D eg 0.5 KHz. The true values of these variables is clearly higher.

EXPERIMENTS

EXPERIMENT 2.1 The Variability of Max A, RP and SB at a Constant Site

Methods

Recordings were taken from several sites in the carotid arteries of 8 patients with symptoms of carotid artery disease during the course of an examination using Vasoscan. From any one site 5 to 7 consecutive values of max A, RP and SB displayed on the screen were recorded. The positions of the probe and patient were kept absolutely still between recordings. Two sweeps on the screen (6 seconds duration of signals) were allowed to pass between each recording. The position of the probe relative to the carotid arteries was given by x, y co-ordinates displayed adjacent to the flow map on the screen and these were checked to ensure they did not change. Five different sites were used (proximal and distal common carotid artery, proximal and distal internal carotid artery and external carotid artery) with a total of 31 recordings each comprised of 5 to 7 values of each variable.

Analysis of Results

(i) For each variable a series of consecutive values were obtained (ie 5 to 7 values recorded from one site). Then the mean, its standard deviation (SD) and the coefficient of variation (CV) were calculated. The coefficient of variation was calculated from Equation 2.1.

$$CV = \frac{SD}{mean} \times 100\% \qquad \text{Equation 2.1}$$

(ii) The overall variability of each variable was then assessed from the mean of all the coefficients of variation calculated in analysis (i).

(iii) The variability of each variable in each of the common, internal and external carotid arteries was assessed from the mean of all the coefficients of variation calculated at any site in that artery.

EXPERIMENT 2.2 The Effect of Instrument Gain on Max A, RP and SB

Methods

Thirty two pairs of signals were recorded from the carotid arteries of 5 patients using Vasoscan. The level of instrument gain was varied and was set at either 35, 60 or 80. Each pair of signals was recorded from the same site with a different level of gain for each signal. The position of the probe and the patient were kept constant as described in Experiment 2.1. From each signal displayed values of max A, RP and SB were noted and True max A was measured.

A comparison was made of the values of each variable at different levels of gain setting.

Analysis of Results

(i) Differences between the means of paired values of each variable at different levels of gain setting were calculated.

(ii) The significance of analysis (i) was tested using Student's t test on paired values.

EXPERIMENT 2.3 A Measurement Error in Both Max A and Max D

Methods

Certain signals from Experiment 1.1 and 1.2 were selected and they were divided into 2 groups. Group one was comprised of signals from both the right and left carotid arteries of 10 asymptomatic volunteers in Experiment 1.1. Group 2 was comprised of the first 25 signals from patients in Experiment 1.2 where max A was greater than 3.5 KHz (as max A was rarely greater than 3.5 KHz in Experiment 1.1). Displayed values of max A and max D were noted and True max A and True max D were measured on every signal. This resulted in 2 sets of paired values for each signal ie True max A and max A, and True max D and max D which were compared.

Analysis of Results

(i) Differences between the means of paired values of each variable in each artery were calculated in Group one.

(ii) Differences between the means of paired values of each variable were calculated in Group 2.

(iii) The significance of both anaylses (i) and (ii) was tested using Student's t test on paired values.

<u>EXPERIMENT 2.4</u> An Error in the Degree of Spectral Broadening due to Scanning Technique

<u>Methods</u>

Sixty signals were recorded from the internal carotid artery or common carotid artery of 13 patients with symptoms of carotid artery disease. The signals were paired and each pair was taken from the same site as described in Experiment 2.1 (see Figure 15). The first signal of each pair was taken using the unidirectional mode (Group one) and the second using the bidirectional mode (Group 2). Values of max A and SB were obtained for each signal and compared. The intention of also using values of max A had been to give another check that the sample sites had been kept constant.

<u>Analysis of Results</u>

(i) Difference between the means of paired values of both max A and SB were calculated in both Groups.

(ii) The significance of analysis (i) was tested using Student's t test on paired values.

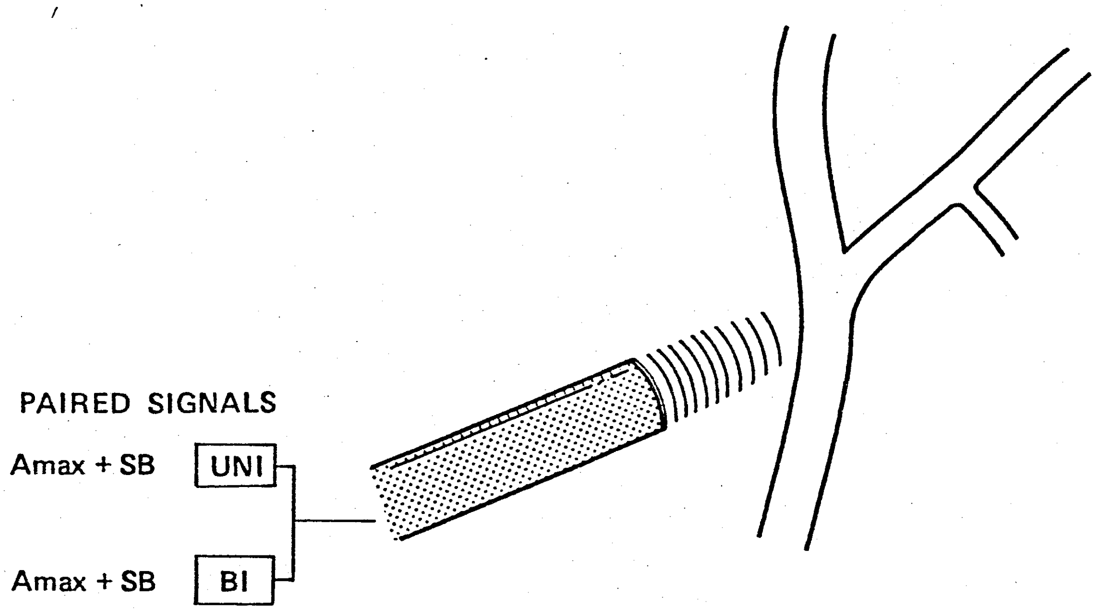

FIGURE 15

The 2 groups of signals used in Experiment 2.4

UNI - unidirectional facility
BI - bidirectional facility

RESULTS

EXPERIMENT 2.1 The Variability of Max A, RP and SB at a Constant Site

The results of analysis (i) are given in Tables 15-17 and of analyses (ii) and (iii) in Table 18. Whilst the coefficient of variation of each group of values was often high ie greater than 10% the overall mean coefficient of variation was 8% for max A and 6% for RP. For SB variability was greater with a mean coefficient of variation in each artery greater than or equal to 10%. 48% of the recordings had a mean coefficient of variation for SB greater than 10%.

EXPERIMENT 2.2 The Effect of Instrument Gain on Max A, RP and SB

The results of analysis (i) and (ii) are given in Table 19 which shows that there was a significant difference between values of both max A and SB at different levels of gain but not for RP or True max A. Thus the displayed values of both max A and SB increased significantly with an increase in gain. Table 20 emphasises the degree of difference. The figures in Table 20 are derived by subtracting the value of the variable in the first level of gain from the second eg G_{35} cf $G_{60} = G_{60} - G_{35}$.
The figures in the last column (4) were obtained by adding those in column one and 2 and gives another assessment of G_{35} cf G_{80}.

TABLE 15 The Variability of Max A at a Constant Site

Patient Code	Site	n	Range (KHz)	Mean (KHz)	SD (KHz)	CV (%)
1	prox CCA	7	1.1-1.2	1.129	0.049	4
	dist CCA	5	1.3-1.6	1.42	0.110	8
	ECA	3	1.3-1.7	1.467	0.208	14
	prox ICA	6	1.4-1.8	1.617	0.172	11
	dist ICA	5	1.6-2.0	1.84	0.152	8
2	prox CCA	7	2.0-2.5	2.186	0.157	7
	dist CCA	6	1.8-2.4	2.233	0.225	10
	prox ICA	6	1.7-1.9	1.833	0.082	4
	dist ICA	5	1.8-1.9	1.84	0.055	3
	ECA	6	1.2-2.1	1.783	0.319	18
3	prox CCA	6	1.0-1.4	1.267	0.137	11
	ECA	6	1.4-1.7	1.517	0.117	8
	prox ICA	7	1.9-2.3	2.171	0.150	7
	dist ICA	6	2.3-3.6	3.095	0.515	17
4	dist CCA	6	1.1-1.3	1.217	0.075	6
	ECA	6	1.9-2.1	2.05	0.084	4
	prox ICA	6	1.5-1.8	1.683	0.098	6
	dist ICA	6	1.9-2.0	2.0	0.089	4
5	prox CCA	6	1.3-1.6	1.467	0.121	8
	dist ICA	6	2.3-2.5	2.467	0.082	3
	ECA	6	1.8-2.1	2.017	0.117	6
6	dist CCA	6	2.0-2.2	2.05	0.084	4
	prox ICA	6	2.5-2.8	2.65	0.105	4
	ECA	6	2.0-2.1	2.05	0.055	3
	prox CCA	6	1.5-1.8	1.667	0.103	6
	prox ICA	6	2.6-2.8	2.65	0.084	3
	ECA	6	1.4-1.7	1.567	0.137	9
7	dist CCA	5	1.3-2.0	1.52	0.319	21
8	prox CCA	6	1.6-1.8	1.65	0.084	5
	prox ICA	6	1.9-2.2	2.083	0.117	6
	ECA	6	1.8-2.5	2.05	0.251	12

SD - standard deviation
CV - coefficient of variation

TABLE 16 The Variability of RP at a Constant Site

Patient Code	Site	n	Range (x 10^{-2})	Mean (x 10^{-2})	SD (x 10^{-2})	CV (%)
1	prox CCA	7	63-66	65.14	1.069	2
	dist CCA	5	72-80	75.4	2.996	4
	ECA	3	76-84	79	4.359	6
	prox ICA	6	56-63	59	3.098	5
	dist ICA	5	53-75	65.2	8.136	12
2	prox CCA	7	68-74	71.57	2.225	3
	dist CCA	6	75-81	76.83	2.317	3
	prox ICA	6	51-60	57.83	5.879	10
	dist ICA	5	58-75	64.6	7.603	12
	ECA	6	84-100	94.83	6.145	6
3	prox CCA	6	71-80	73.5	3.391	5
	ECA	6	70-75	71.83	1.722	2
	prox ICA	7	67-79	73.86	4.337	6
	dist ICA	6	74-82	78.5	3.082	4

<u>TABLE 16 (CONTD)</u> The Variability of RP at a Constant Site

Patient Code	Site	n	Range (x 10^{-2})	Mean (x 10^{-2})	SD (x 10^{-2})	CV (%)
4	dist CCA	6	66-73	68.67	2.503	4
	ECA	6	69-90	81.5	7.530	9
	prox ICA	6	43-75	57	10.334	18
	dist ICA	6	59-87	72.17	9.109	13
5	prox CCA	6	70-86	77.33	7.421	10
	dist ICA	6	65-70	68.17	2.483	4
	ECA	6	76-80	78	1.414	2
6	dist CCA	6	58-82	63.83	9.725	15
	prox ICA	6	45-50	47.67	1.751	4
	ECA	6	77-84	81.67	2.875	4
	prox CCA	6	61-73	66.5	3.987	6
	prox ICA	6	47-52	49	2.098	4
	ECA	6	95-100	97.3	2.160	2
7	dist CCA	5	67-83	75.2	7.362	10
8	prox CCA	6	72-78	75.33	2.658	4
	prox ICA	6	74-82	78	2.757	4
	ECA	6	85-89	88	1.549	2

TABLE 17 The Variability of SB at a Constant Site

Patient Code	Site	n	Range (%)	Mean (%)	SD (%)	CV (%)
1	prox CCA	7	40-53	48.43	4.860	10
	dist CCA	5	56-81	68.2	8.927	13
	ECA	3	47-64	53.33	9.292	17
	prox ICA	6	19-42	33.33	8.869	27
	dist ICA	5	24-35	29.4	5.320	18
2	prox CCA	7	44-62	52.71	6.157	12
	dist CCA	6	46-62	56	5.90	11
	prox ICA	6	52-65	58.67	4.633	8
	dist ICA	5	45-65	59.8	8.349	14
	ECA	6	34-56	49.17	8.281	17
3	prox CCA	6	45-49	47.17	1.329	3
	ECA	6	43-52	45.5	3.271	7
	prox ICA	7	44-92	71.86	19.351	27
	dist ICA	6	37-56	45	8.319	18
4	dist CCA	6	55-78	61.83	8.257	13
	ECA	6	79-83	80.67	1.862	2
	prox ICA	6	55-83	65.17	9.786	15
	dist ICA	6	50-62	58	4.561	8

<u>TABLE 17 CONTD</u> The Variability of SB at a Constant Site

Patient Code	Site	n	Range (%)	Mean (%)	SD (%)	CV (%)
5	prox CCA	6	39-52	49.17	13.06	27
	dist ICA	6	44-50	47	2.19	5
	ECA	6	35-53	43.5	7.714	18
6	dist CCA	6	36-45	41	4.382	11
	prox ICA	6	85-94	90	3.225	4
	ECA	6	36-48	43	4.517	10
	prox CCA	6	54-68	60.67	5.317	9
	prox ICA	6	54-59	56.33	2.251	4
	ECA	6	49-57	52	2.966	6
7	dist CCA	5	44-54	47.8	5.933	12
8	prox CCA	6	38-47	43.5	3.937	9
	prox ICA	6	47-52	49	2.098	4
	ECA	6	43-50	46.33	2.658	6

TABLE 18 Mean Coefficients of Variation for Max A, RP and SB in the Carotid Arteries

(Figures are in Percentages)

Artery	Max A	RP	SB
CCA	8	6	12
ICA	6	8	13
ECA	9	4	10
Overall mean	8	6	12

TABLE 19 The Effect of Instrument Gain on Waveform Analysis

Variable	n	Mean Value of variable at Level of Gain		Difference	p
		35	60		
Max A (KHz)	16	2.075	2.387	0.3125	0.0024*
RP	16	0.745	0.741	0.004	0.83
SB (%)	16	46.5	51.2	4.7	0.018*
True Max A (KHz)	16	2.437	2.6	1.662	0.114
		35	80		
Max A (KHz)	9	2.2	2.88	0.68	0.003*
RP	9	0.736	0.748	0.012	0.32
SB (%)	9	38.1	54.6	16.5	0.001*
True Max A (KHz)	9	2.61	2.77	0.167	0.108
		60	80		
Max A (KHz)	7	2.28	2.6	0.33	0.008*
RP	7	0.737	0.752	0.02	0.23
SB (%)	7	46.1	56.5	10.4	0.0075*
True Max A (KHz)	7	2.53	2.61	0.085	0.27

* Significant difference for $p < 0.05$

TABLE 20 The Effect of Instrument Gain on Max A and SB

Variable	1	2	3	4
	G35 cf G60	G60 cf G80	G35 cf G80	(1 + 2)
Max A (KHz)	0.3125	0.325	0.67	0.64
SB (%)	4.68	10.47	16.56	15.15

The figures represent the difference between the mean values of the variables at 2 levels of gain eg G35 cf G60 is equivalent to the mean value at a gain setting of 35 subtracted from that at the level of 60.

The figures in column 4 are obtained by adding the figures in the first 2 columns and are another estimate of G35 cf G80.

<u>EXPERIMENT 2.3</u> A Measurement Error in Both Max A and Max D

Tables 21 and 22 give the results of analyses (i) and (iii) for Group one and Table 23 the results of analyses (ii) and (iii) for Group 2. The values of True max A and True max D were always higher than their displayed values and Figure 14 shows examples. In Group one (ie signals where max A $<$3.5 KHz) there was a small but significant average difference of 0.2 KHz between values of True max A and max A and 0.3 KHz between values of True max D and max D.

The difference increased with increasing maximum frequency such that in Group 2 (ie signals where max A exceeded 3.5 KHz) the average difference was 0.49 and 0.4 KHz respectively.

<u>EXPERIMENT 2.4</u> An Error in the Degree of Spectral Broadening due to Scanning Technique

Table 24 gives the results of analyses (i) and (ii). There were significant differences between the means of the Groups for both max A and SB. In the case of max A the difference was small but in the case of SB it was considerably higher.

TABLE 21 A Measurement Error in Max A

Site	n	Mean Value Max A (KHz)	True Max A (KHz)	Difference (KHz)	p
Right CCA	20	2.47	2.63	0.16	$= 0.001$
Right ICA	20	2.12	2.31	0.19	$= 0.006$
Right ECA	20	2.55	2.79	0.24	< 0.001
Left CCA	19	2.55	2.77	0.22	< 0.001
Left ICA	21	2.11	2.31	0.20	< 0.001
Left ECA	19	2.64	2.86	0.22	< 0.001
Mean		2.41	2.61	0.20	

<u>TABLE 22</u> A Measurement Error in Max D

Site	n	Mean Value		Difference (KHz)	p
		Max D (KHz)	True Max D (KHz)		
Right CCA	20	0.45	0.76	0.31	<0.001
Right ICA	20	0.53	0.86	0.33	<0.001
Right ECA	20	0.31	0.58	0.27	<0.001
Left CCA	19	0.51	0.79	0.28	<0.001
Left ICA	21	0.63	0.91	0.28	<0.001
Left ECA	18	0.35	0.62	0.27	<0.001
Mean		0.46	0.75	0.29	

TABLE 23 The Measurement Error in High Frequency Values of Max A and Max D

n	Mean Value		Difference (KHz)	p
	Max A (KHz)	True Max A (KHz)		
25	4.11	4.60	0.49	<0.001
	Max D (KHz)	True Max D (KHz)		
25	0.74	1.14	0.40	<0.001

TABLE 24 An Error in SB - The Effect of the Directional Mode

Instrument Mode	Variable	n	Mean Value	Difference	p
Unidirectional	Max A	30	2.28 KHz	0.18 KHz	<0.001
Bidirectional	Max A	30	2.10 KHz		
Unidirectional	SB	30	36.80%	24.4%	<0.001
Bidirectional	SB	30	61.16%		

DISCUSSION

When assessing the reliability of a single displayed value of max A, RP or SB in the detection of carotid artery disease their variability and errors in their measurement need to be appraised.

A consideration of the errors involved in Experiments 1.1 and 1.2 needs to take into account the normal variation that occurs in arterial velocities at different arterial sites and in different patients. Physiological stimuli such as emotion or altering the percentage of inspired carbon dioxide affect blood flow and arterial velocity and there is a normal beat to beat variation in Doppler ultrasound signals.[101,102]

In Experiment 2.1 the variation in max A and SB was slightly higher than anticipated but to what extent this influenced the results of the clinical trial ie Experiment 1.2 is difficult to judge. Certainly it is important for the operator when performing a carotid examination to watch the values for max A and SB on the display in order that when the "freeze display" facility is used representative values of these variables are stored and not unduly low or high ones.

In Experiment 2.3 the difference between values of True max A and max A was virtually constant for values of max A less than 3.5 KHz at approximately 0.2 KHz. Similarly in the case of True max D and max D there was a constant difference although it was slightly higher.

The spectra were examined and the upper limits of the maximum frequency envelope were always of low amplitude, colour coded blue by the instrument. There were 2 possible reasons for the low values of max A and max D. This first was that the instrument was ignoring the low intensity frequencies in its calculations, the second : if a gap occurred in any displayed vertical line of points then any frequencies above the gap were ignored. Both would be valuable in excluding extraneous 'noise' from its calculations. In addition in the case of max D its value was equal to the maximum frequency when a pronounced 'dip' occurred at the end of diastole (see Figure 16). Such 'dips' are not uncommon and increasing the time averaging interval over which max D was calculated would have eliminated this problem.

In Experiment 2.2 a value of max A taken using a level of gain of 35 would have been increased on average by 15% had the level of gain been 60 and on average by 30% had the level been 80. The finding that values of max A tended to agree more closely with those of True max A with increasing level of gain supported the theory that the instrument was ignoring low intensity frequencies.

An unexpected finding was that the use of the bidirectional mode caused a small ($\sim$ 8%) but significant decrease in values of max A compared with the use of the unidirectional mode.

If the errors in max A and max D noted above are taken into account then the value for RP calculated by the instrument will be higher

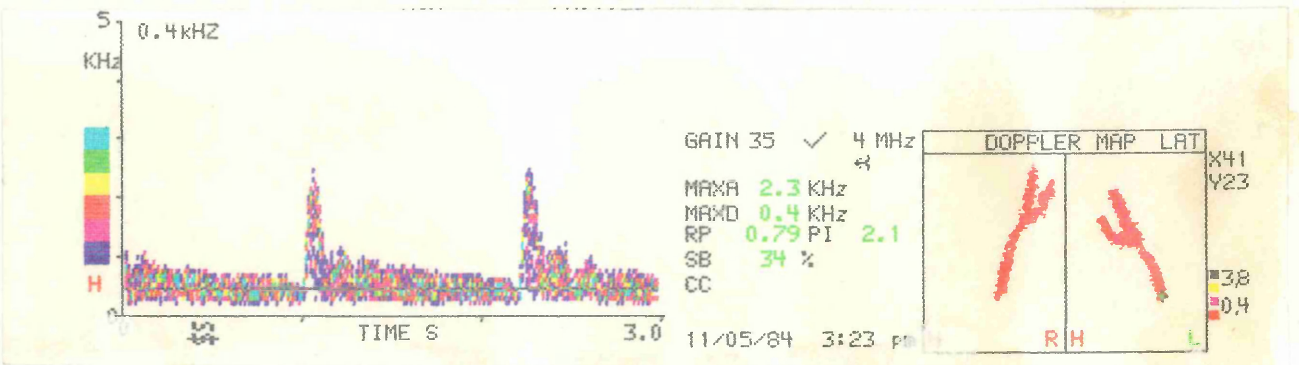

FIGURE 16

A time averaging error in calculating max D. This illustrates how the time averaging interval for calculating max D was too short. The value of max D was that of the pronounced 'dip' at the end of diastole.

than its true value. This can be deduced as follows:-

$$\text{If RP} = \frac{\text{max A} - \text{max D}}{\text{max A}} \qquad \text{Equation 2.1}$$

$$\text{then RP} = 1 - \frac{\text{max D}}{\text{max A}} \qquad \text{Equation 2.2}$$

$$\text{and True RP} = 1 - \frac{\text{True max D}}{\text{True max A}} \qquad \text{Equation 2.3}$$

It was found in Experiment 2.3 that the difference between paired values of True max D and max D was proportionally greater than the difference between True max A and max A in any one signal. Therefore in any signal the ratio max D/max A in Equation 2.2 will be less than the ratio True max D/True max A in Equation 2.3 making RP greater than True RP. This may account for the high values of RP found in the common carotid artery in Experiment 1.1.

There were 2 sources of error in the quantification of spectral broadening (SB) found from the experiments in this Chapter.

(i) The degree of SB increased as the level of gain increased. A reason for this might be that increasing the gain increases the intensities of the frequencies on both sides of the mean frequency at peak systole keeping it constant (see Figure 17). However as F max (max A) increases the ratio F mean/F max in Equation 1.3 diminishes thus increasing the percentage of SB.

(ii) In Experiment 2.4 the signals obtained using the bidirectional mode were examined. It was found that in 26/30 spectra appeared below the baseline either due to a mirror image of

$$SB = \frac{F_{max} - F_{mean}}{F_{max}} \times 100\%$$

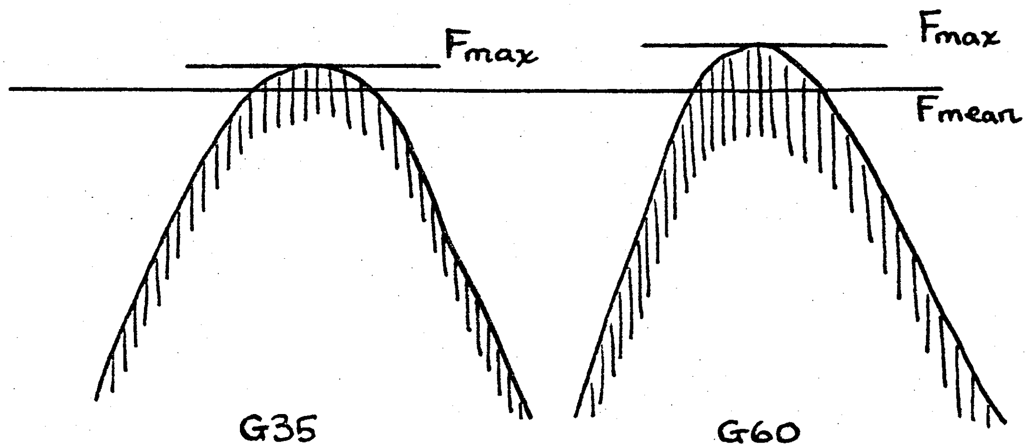

FIGURE 17

The effect of instrument gain on SB. G refers to the gain setting. Increasing the gain setting increases F max although F mean remains constant.

the arterial spectrum which may be caused by arterial wall calcification, or the presence of venous flow (see Figure 18).[103,104] In the 4 signals where no spectra appeared below the baseline there was no difference between the paired values of SB, (a mean difference of only 3.5%). It was in the 26 where spectra appeared below the baseline that the large discrepancies occurred, some values being doubled those obtained with the unidirectional mode when the bidirectional mode was used. The reason why values of SB were high using the bidirectional mode was because the instrument was taking into account the spectra below the baseline. This lowers the mean frequency at peak systole thereby increasing the value of SB (from Equation 1.3). If a threshold value of 58% for SB had been used to detect carotid artery disease then half the signals would have been given false positive answers with the bidirectional mode.

The spectrum may also be broadened artificially when using CW ultrasound because of its wide beam which detects low velocities near the arterial wall.[69] This may occur with the instrument in either mode.

The colours used to construct the flow map depend on the values of both max A and SB therefore any of the errors noted above will affect its construction and interpretation.

(a)

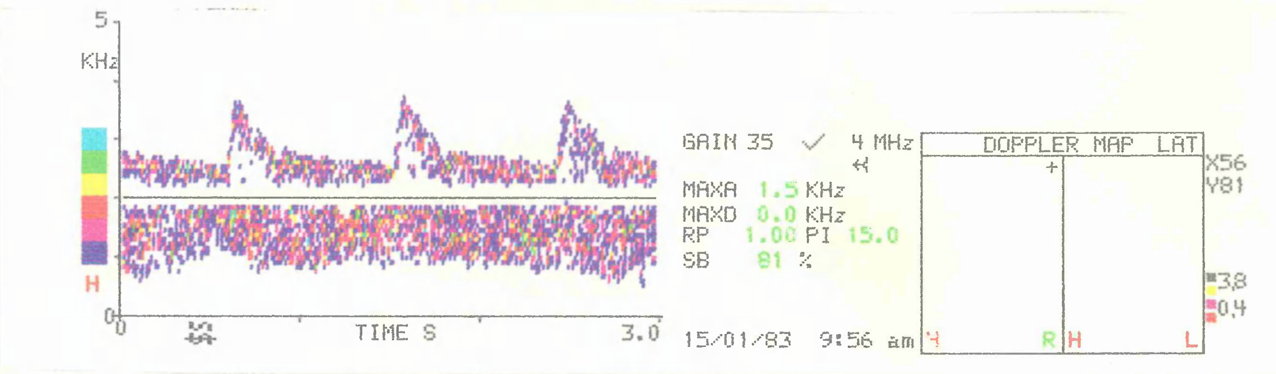

(b)

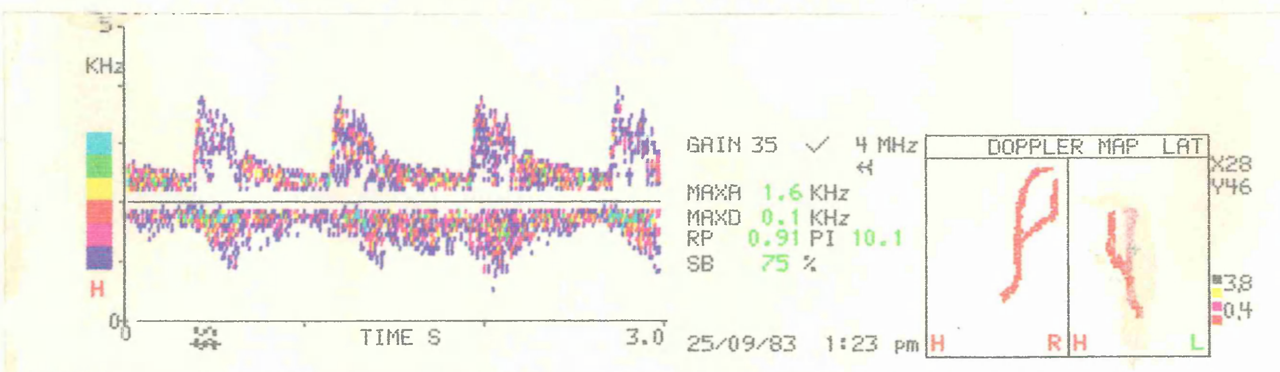

FIGURE 18

Errors in SB due to the display of the spectra below the baseline when using the bidirectional mode. The upper figure (a) has jugular venous signals and the lower figure (b) "mirror images" of the arterial flow.

In clinical practice it is essential that these errors are appreciated when considering values close to the threshold levels, particularly when the instrument is used in the bidirectional mode. Every effort should be made to maintain an optimum level of gain setting when insonating the different carotid arteries.

C H A P T E R 3

MAXIMUM VELOCITY MEASUREMENTS USING CW ULTRASOUND

INTRODUCTION

The Doppler formula (Equation 1.1) describes the relationships between the velocity of flow in the vessel under insonation and the observed Doppler shifted frequency (ΔF). The frequency of the backscattered ultrasound depends on the frequency of the incident beam (F), the speed of sound in the medium (C), (both of which are usually known), and the cosine of the angle between the beam and the vessel (θ). This angle is unknown when using systems other than those which incorporate pulsed wave ultrasound.

The normal range of max A in Experiment 1.1 took into account the variation in θ therefore a sufficiently high value of max A could with some certainty be attributed to the presence of disease. However as underestimation of max A in certain patients in Experiment 1.2 could have occurred because of high values of θ. This would result in an under diagnosis of carotid disease, as was the case in Experiment 1.2.

To allow more reliable comparisons between patients a method was devised to measure θ which enabled velocities to be calculated. The accuracy of this method of measuring θ was investigated in Experiment 3.4. The accuracy of maximum velocity (V max) calculations, using this method, in the detection of carotid disease was tested in Experiment 3.5 by comparison with arteriograms.

As the method was derived from the Doppler formula the relationship between maximum frequency (ΔF max) and θ was investigated in Experiments 3.1 and 3.3. An unexpected result from Experiment 3.1, a fall in ΔF max at low values of θ was studied in another experiment (Experiment 3.2). A laboratory model was used in Experiment 3.1 and 3.2 which was a convenient way of allowing multiple ultrasonic measurements to be taken from the same site at known angles of incidence. The velocity of flow can be kept constant in a model and with C and F also constant Equation 1.1 can be rearranged to give

$\Delta F = K \cos \theta$

If ΔF max is proportional to the maximum velocity then

$\Delta F\ max/\cos\theta = K$ Equation 3.1

There should therefore be a linear relationship between values of ΔF max and $\cos\theta$ for values of θ between 0^{o} and 90^{o}.

THEORY OF CALCULATING θ AND V MAX

If ΔF_y and ΔF_x represent the maximum frequencies of ultrasound spectra recorded from the same site at angles θ and $\theta + \omega$ respectively (see Figure 19) then at position x

$V\ max = (\Delta F_x\ C)/\ 2\ F \cos(\omega + \theta)$

and at position y

$V\ max = (\Delta F_y\ C)/(2\ F \cos\theta)$

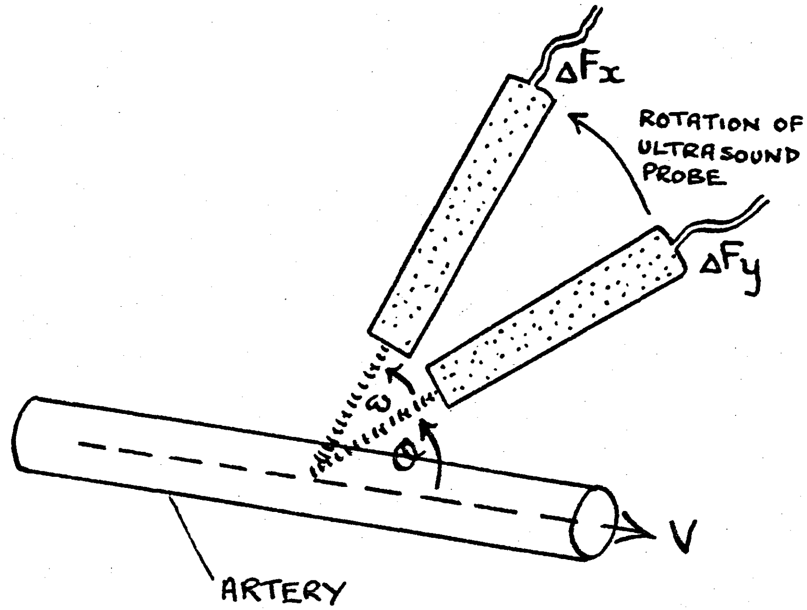

FIGURE 19

The method of calculating the angle of insonation and the maximum velocity of flow. ΔFy is the maximum Doppler shifted frequency with the probe making an angle θ with the artery. ΔFx is the maximum Doppler shifted frequency when the probe is rotated through angle ω. V is the velocity of flow in the artery.

If the signals are taken from the same site and V remains constant then

$\Delta F_x/\cos(\omega + \theta) = \Delta F_y/\cos\theta$

$\Longrightarrow \Delta F_x/\Delta F_y = \cos(\omega + \theta)/\cos\theta$

Let $R = \Delta F_x/\Delta F_y$

Then $R = (\cos\omega\cos\theta - \sin\omega\sin\theta)/\cos\theta$

$\Longrightarrow \cos\omega - R = (\sin\omega\sin\theta)/\cos\theta$

$\Longrightarrow \sin\theta/\cos\theta = (\cos\omega - R)/\sin\omega$

$\Longrightarrow \tan\theta = (\cos\omega - R)/\sin\omega$ Equation 3.2

Thus θ can be calculated from a ratio of 2 measurements of ΔF max and a value of ω determined by the operator.

In terms of vectors from Figure 19 V max can be expressed as

$V\ max = Ky/\cos\theta$ Equation 3.3

Where y is ΔF_y and K is a constant

V max may be calculated independently of θ from Equations 3.2 and 3.3 as follows

Let $\Delta F_x = x$ and $\Delta F_y = y$

Then $\tan\theta = \left\{\cos\omega - (x/y)\right\}/\sin\omega$

$\Longrightarrow \cos\theta = 1/\left([1 + \left\{\cos\omega - (x/y)\right\}^2]/\sin\omega\right)^{\frac{1}{2}}$

from a right angled triangle of sides one and $\left\{\cos\omega - (x/y)\right\}/\sin\omega$ and hypotenuse $\left(1^2 + [\left\{\cos\omega - (x/y)\right\}^2]/\sin\omega\right)^{\frac{1}{2}}$

$$\Longrightarrow \cos\theta = 1/[\{\sin^2\omega + \cos^2\omega - 2(x/y)\cos\omega + (x^2/y^2)\}/\sin^2 x]^{\frac{1}{2}}$$

$$\Longrightarrow \cos\theta = \sin\omega/\left\{\sin^2\omega + \cos^2\omega - 2(x/y)\cos\omega + (x^2/y^2)\right\}^{\frac{1}{2}}$$

$$\Longrightarrow \cos\theta = \sin\omega/\left\{1 - 2(x/y)\cos\omega + (x^2/y^2)\right\}^{\frac{1}{2}}$$

$$\Longrightarrow \cos\theta = y\sin\omega/\left\{x^2 - 2xy\cos\omega + y^2\right\}^{\frac{1}{2}} \qquad \text{Equation 3.4}$$

Substituting Equation 3.4 into 3.3 gives

$$V\ max = K(x^2 + y^2 - 2xy\cos\omega)^{\frac{1}{2}}/\sin\omega \qquad \text{Equation 3.5}$$

Finally to know V max we must calculate K

$$K = C/2F$$

Where F is equal to 4×10^3 KHz and C is the speed of sound in tissue equal to 1.54×10^5 cm/sec.[105] .

$$\Longrightarrow K = (1.54 \times 10^5)/(2 \times 4 \times 10^3)$$

$$\Longrightarrow K = 0.193 \times 10^2$$

$$\Longrightarrow K \doteq 20$$

METHODS

THE MODEL

The model (see Figure 20) consisted of the following apparatus although not all of it was used in each experiment.

(i) The Medium and Ultrasound Scatterer

Water was used as the medium with one of 3 additives to scatter the ultrasound:-

a) Bubbles of air (injected proximal to the test section through a No 25 gauge needle using a constant infusion pump)

b) An emulsion of milk in water (380 ml/l)

c) An emulsion of silicone liquid in water (0.5% silicone fluid MS 200/3 cs, Hopkin and Williams Ltd, Essex, England)

(ii) A Constant Head Tank (See Figure 46)

Steady flow was produced by gravity from the tank which was kept full by the roller pump. A constant overflow maintained a constant head of pressure. The rate of flow was controlled by an adjustable screw clamp at the distal end of the tubing.

(iii) A Reciprocating Piston and Scotch Yoke Assembly (See Figure 46)

Sinusoidal waves were superimposed on the steady flow by a piston which moved in simple harmonic motion through a

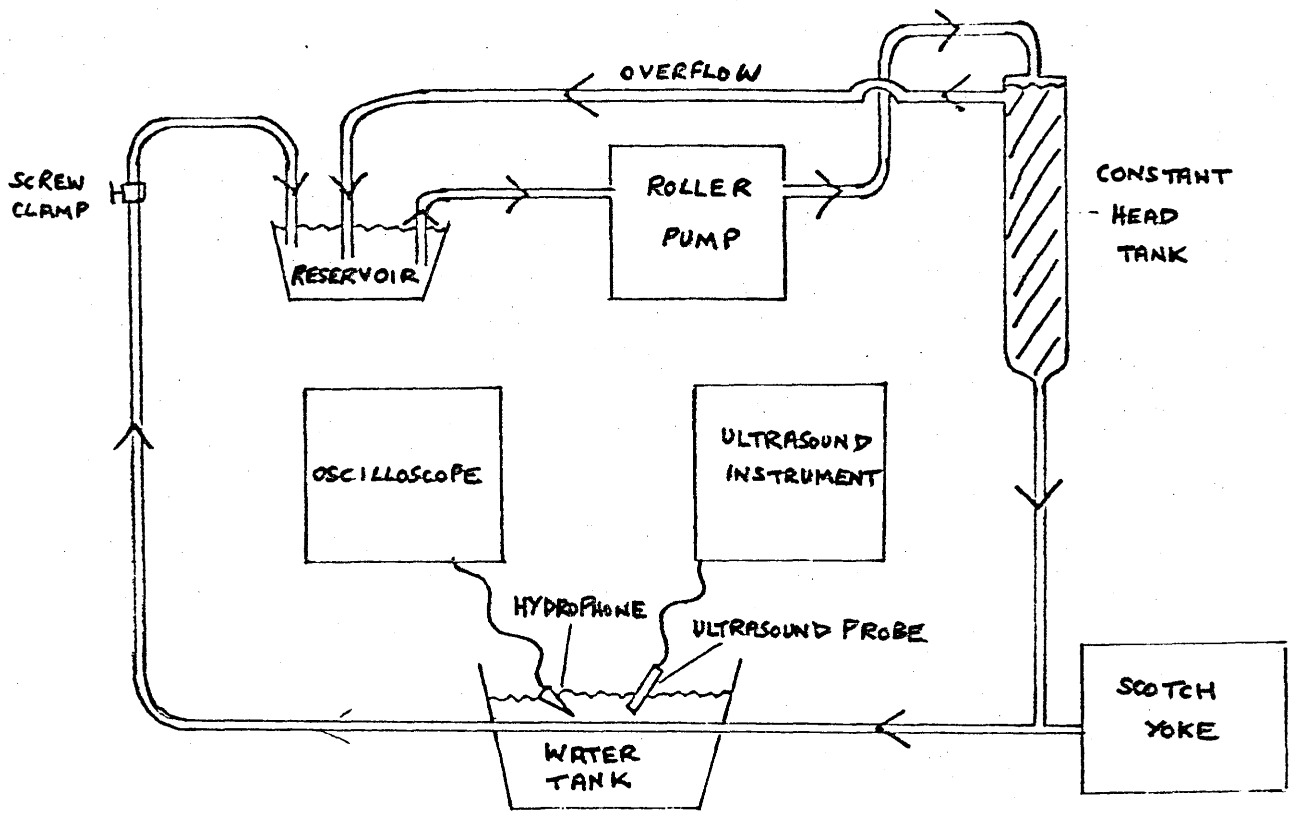

FIGURE 20

A diagram of the model used in Chapter 3

Scotch Yoke assembly. The amplitude of the oscillation could be varied by altering the length of stroke of the piston by adjusting the position of the spindle on the fly wheel of the Scotch Yoke. The frequency of oscillation could be varied from 8-240 cycles per minute.

(iv) <u>The Tubing</u>

A circuit of polyethylene tubing was used of internal diameter 0.6 cm and one of 2 different layouts were used for the test section:-

a) The tubing was supported on a foam rubber block and a generous quantity of aqueous jelly (Aquasonic) used as an accoustic coupler between the tubing and the ultrasound probe (see Figure 21)

b) The tubing was led through side holes in a water tank (see Figure 46)

The tubing on both sides of the test section was supported on foam rubber blocks.

(v) <u>A Reservoir</u>

Fluid was collected in a reservoir from the end of the tubing and recirculated by the roller pump.

(vi) <u>The Roller Pump (See Figure 47)</u>

A roller pump (H-R Flow Inducer, Watson-Marlow Ltd) was used to return the fluid to the constant head tank.

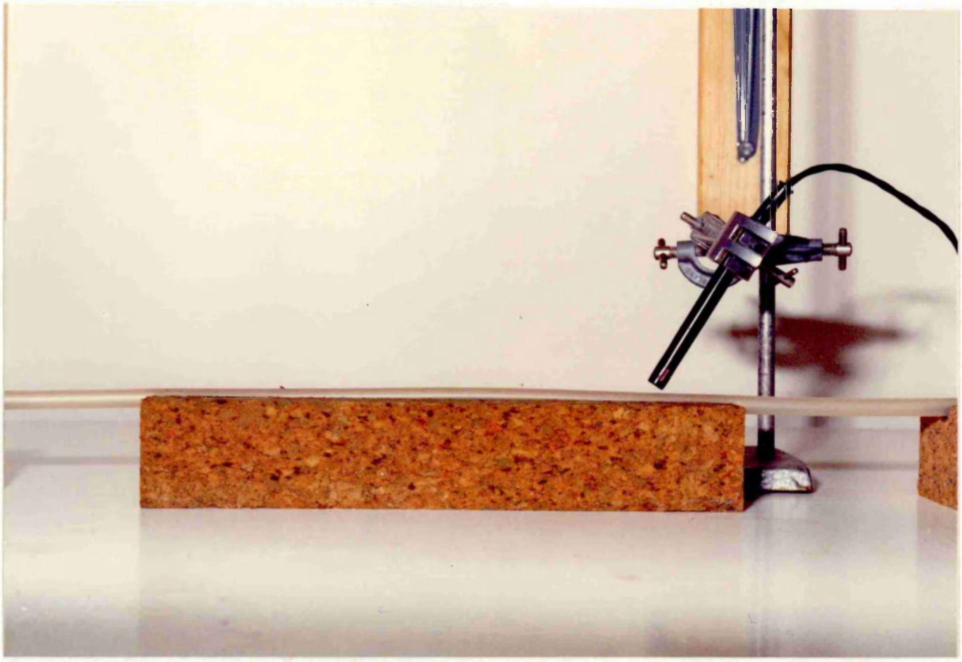

FIGURE 21

The test section : method (a). Aqueous jelly was used between the ultrasound probe and tubing.

(vii) The Ultrasonic Instruments

4 MHz probes of either a Vasoscan or a Sonicaid BV 380 blood velocimeter were used. Spectral analysis of the signals obtained using the latter instrument was performed by a Spectrascribe MK II Real Time Frequency Spectrum Analyser. The ultrasound probe was held in a clamp which allowed the angle of incidence to be varied. Angles were measured using a protractor.

(viii) A Hydrophone (See Figure 22)

A hydrophone was used to detect ultrasound reflected from the surface of the tubing. It could detect high frequency sound waves up to approximately 10 MHz.

(ix) An Oscilloscope (See Figure 22)

The hydrophone was connected to an oscilloscope (Tektronix) and the amplitude shift on the screen represented the amount of signal detected by the hydrophone.

METHOD OF EXAMINATION OF PATIENTS

The carotid arteries of patients were examined with CW ultrasound using the same methods described in Chapter 1 with some modification in technique described in Experiments 3.3 and 3.5.

DATA PROCESSING

A mini computer (Systime PDP 11/44 series 6400) was programmed to calculate and print out values of θ and V_{max} using Equations 3.2 and 3.5 for input data ΔF_x, ΔF_y and ω.

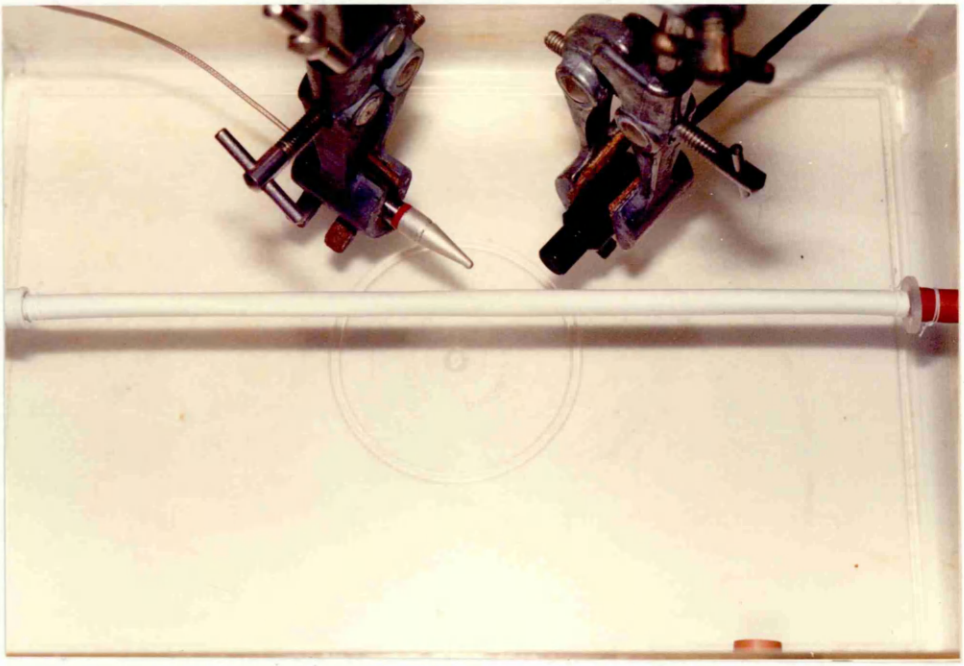

(a)

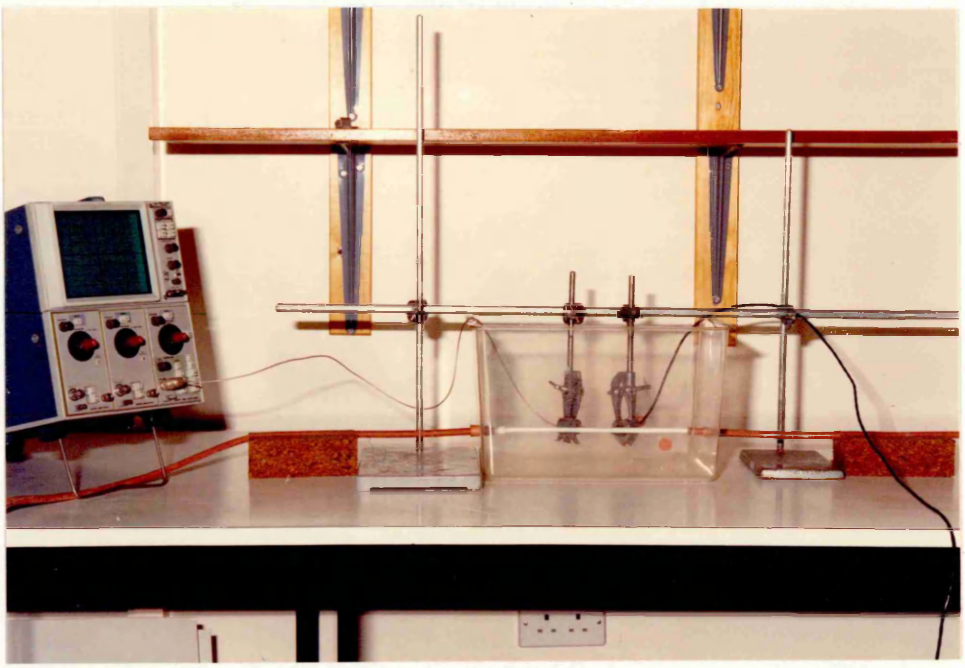

(b)

FIGURE 22

The arrangement of the hydrophone, ultrasound probe and tubing.
(a) plan view
(b) side view

EXPERIMENTS

EXPERIMENT 3.1

EXPERIMENT 3.1.1 The Relationship Between the Maximum Frequency and the Angle of Insonation

Methods

An emulsion of milk in water was circulated through the tubing under conditions of steady flow at a constant velocity using the roller pump, constant head tank and reservoir. The 4 MHz probe of the Sonicaid BV 380 blood velocimeter was used to record signals at multiple values of θ between 10° and 90° from the test section layout (a). The gain on the instrument was adjusted to give the best signal : noise ratio. Hard copy traces of each signal were obtained from the spectrascribe and the maximum frequency (ΔF max) was determined from the average of 20 measurements.

EXPERIMENT 3.1.2 The Relationship Between the Maximum Frequency and the Angle of Insonation - The Effect of Changing the Ultrasound Scatterer in the Medium

Methods

In this experiment the method was identical to Experiment 3.1.1 with the exception that the fluid was water with bubbles of air injected proximal to the test section.

EXPERIMENT 3.1.3 The Relationship Between the Maximum Frequency and the Angle of Insonation - The Effect of Changing the Coupling Between Probe and Vessel

Methods

In this experiment the method was the same as Experiment 3.1.1 with the exception that the water tank (test section layout (b)) was used to provide the most ideal coupling.

EXPERIMENT 3.1.4 The Relationship Between the Maximum Frequency and the Angle of Insonation - The Effect of Instrument Gain

Methods

In this experiment the method was identical to Experiment 3.1.1 with the exception that a high level of instrument gain was used.

EXPERIMENT 3.1.5 The Relationship Between the Maximum Frequency and the Angle of Insonation - The Effect of a Different Instrument

Methods

In this experiment the method was the same as Experiment 3.1.1 with the exception that Vasoscan was used as the ultrasound instrument. ΔF max was determined by measuring True max A (see Chapter 2).

EXPERIMENT 3.1.6 The Relationship Between the Maximum Frequency and the Angle of Insonation Under Conditions of Oscillatory Flow at Different Amplitude

Methods

In this experiment the method was similar to Experiment 3.1.5 with the introduction of the Scotch Yoke assembly to produce sinusoidal flow. Three amplitudes of oscillations were selected : the minimum and maximum amplitudes the Scotch Yoke could produce (the length of the piston stroke was set as approximately 3 and 12 cm respectively) and a third intermediate between these 2.

Analysis of Results - Experiments 3.1.1-3.1.6

For values of θ both greater than and less than a critical angle (defined on Page 132) the following 2 analyses were carried out:-

(i) The calculation of correlation coefficients (CC) for values of ($\cos\theta$, ΔF max)

(ii) The coefficients of variation (CV) were calculated from the means and standard deviations of the constant K derived from Equation 3.1.

EXPERIMENT 3.2 The Reflection of Ultrasound from the Surface of Arteries and Tubing

Introduction

From the results of Experiments 3.1.1-3.1.6 a hypothesis was made that for values of θ below a critical angle total reflection of the ultrasound beam occurred at the surface of the tubing and furthermore that the critical angle varies according to the physical properties of the tube.

Methods

The model used was similar to that in Experiment 3.1.6. An emulsion of silicone in water was circulated through plastic tubing at a constant velocity using the roller pump, constant head tank and reservoir. Sinusoidal flow was provided by the Scotch Yoke assembly and the 4 MHz probe of Vasoscan was used as the source of ultrasound. A hydrophone, connected to an oscilloscope, was used to measure the amount of ultrasound reflected from the surface of the tubing.

The materials to be tested were inserted into the test section in the circuit of tubing using connecting pieces which passed through side holes in the water tank. The materials tested were 30 cm long tubes of polytetrafluroethylene (PTFE) and polyurethane, (2 of the materials used in the fabrication of vascular grafts) silastic rubber, red rubber and both calcified and normal arteries. The calcified artery was an operative specimen of superficial femoral artery which was heavily calcified on all sides and the normal artery was a common iliac artery which felt soft and was macroscopically normal.

The hydrophone, tubing and ultrasound probe were arranged as follows under water (see Figure 22). Both the ultrasound probe and hydrophone were kept one cm distant from the tubing and as the ultrasound probe was rotated to change the angle of incidence (θ) from 10^{o} to 90^{o} the hydrophone was rotated to lie at a similar angle to the tubing but opposite in sign ie negative θ. The angles were measured accurately using a protractor. The orientation of the crystals of the ultrasound probe was kept constant, the emitter crystal being lateral to the receiver with respect to the tubing. The hydrophone was used to detect which crystal was the emitter and registered a maximum amplitude of 5.5 mV with the hydrophone one cm distant to the emitter crystal. The probe and hydrophone were attached to a single steel rod by 2 clamps which allowed lateral rotation of the instruments. The steel rod in turn traversed above the tank and was clamped to stands on both sides of the tank.

Measurements

For each position of the probe 2 hydrophonic recordings were measured because the ultrasound waves could reach the hydrophone directly or by reflection.

(i) The first measurement was taken with the probe and hydrophone orientated lateral to the tubing as described above :

the sum of both the reflected and direct ultrasound waves reaching the hydrophone.

(ii) The second measurement was taken immediately after the first when the stands on both sides of the tank were elevated enough to raise the level of the instruments above that of the tubing : in which case only direct ultrasound reached the hydrophone.

The amount of reflected ultrasound was calculated by subtracting the second measurement from the first. In addition the operator listened to the audio output which was simpler than making precise measurements of ΔF max. Precise measurements of ΔF max did not form an essential part of this experiment.

EXPERIMENT 3.3 To Quantify the Relationship Between the Maximum Systolic Frequency and the Angle of Insonation In Vivo

Methods

Signals were recorded from approximately the same site in the right common carotid artery of 4 patients and 2 volunteers using the 4 MHz probe of Vasoscan. A protractor was fixed to the spatial sensing arm and the angle of incidence of the beam of ultrasound varied in increments of 10^{o}. The displayed values for max A for each patient were plotted on a graph against the angle shown on the protractor (see Figure 35). To find θ, the angle between the ultrasound probe and the common carotid artery the lowest value of max A was presumed to have been recorded when θ equalled 90^{o}. As there was 10^{o} between the measurements other values of θ could then easily be found.

Although the patients would each have had a different velocity of flow in their common carotid arteries it was assumed that the velocity remained constant during the course of each experiment in a particular patient.

Analysis of Results

(i) The correlation coefficient was calculated for values of (ΔF max, $\cos\theta$) for both positive and negative values of between the critical angle and 80^{o}.

(ii) The mean slope was calculated for both positive and negative values of θ from those results of analysis (i) with a p value less than 0.05.

EXPERIMENT 3.4 The Accuracy of the Method in Measuring the Angle of Insonation

The method was tested for accuracy both in the model, from the results of Experiment 3.1.6, and in patients from Experiment 3.3. In these experiments values of ΔF max and θ were known therefore for any pair of values of ΔF max, ω could easily be determined.

Two values of ΔF max (ΔF_x and ΔF_y) and ω were used as input data and the value of θ calculated by the computer was compared with the known experimental value. This was repeated for all values of ΔF max with different values of ω from these experiments apart for any value of ΔF_x which was greater than ΔF_y.

EXPERIMENT 3.5 Measurements of Maximum Velocity in the Detection of Carotid Disease

22 patients with symptoms suggestive of carotid artery disease were examined using Vasoscan in the manner described in Chapter one. At the end of the examination the site in the common carotid artery or internal carotid artery at which the highest value of max A occurred was noted. Using the protractor fixed to the spatial sensing arm the transducer was rotated increasing the angle the ultrasound beam made with the carotid arteries by 10^{o}. The common carotid artery and internal carotid artery were re-examined at this new angle ($\theta + 10^{o}$) and a second recording made from the site giving the highest value of max A. The 2 sites ought theoretically to have been identical. There was evidence that this was the case because the position of the cursor on the flow map did not change much between recordings despite the fact that the flow map constructed at angle θ was invalidated by increasing the angle to $\theta + 10^{o}$. For each patient and on either side of the neck a pair of values of max A was obtained taken at angle θ and angle $\theta + 10^{o}$. One carotid artery was excluded because of a previous carotid endarterectomy. The 2 values of max A and the value of 10^{o} were used as input data for the computer and values for θ and V max were obtained from the computer print out. Data was also obtained on the carotid arteries from arteriograms

which were graded by 2 surgeons into the same categories as Chapter one.

Analysis of Results

(i) The higher of the pair of values of max A was compared with the values of V max obtained from the same site, using a decision matrix. A threshold value of 3.5 KHz for max A was used equivalent to a value for V max of 140 cm/sec.

(ii) The accuracies of both max A and V max in the detection of carotid disease using the threshold values quoted above were compared with the grading of disease by arteriograms.

RESULTS

EXPERIMENT 3.1 The Relationship Between the Maximum Frequency and the Angle of Insonation

EXPERIMENT 3.1.1 TO 3.1.6

The values of ΔF max for corresponding values of θ are shown in Tables 25-30 and in Figures 24 and 26-30. Figure 25 plots the values of ΔF max against those of cos θ for Experiment 3.1.1. Tables 31 and 32 give the results of analysis (i) and Tables 33 and 34 of analysis (ii). Figure 23 gives examples of the spectra-scribe traces from Experiment 3.1.1.

In Experiment 3.1.1 ΔF max increased as θ fell from 84° but once θ was less than 39° ΔF max started to fall. The critical angle was defined as that value of θ where ΔF max was found to be highest. Figure 25 demonstrates that there was a linear relationship between ΔF max and cos θ for values of θ between the critical angle and 84° with a correlation coefficient of 0.98 ($p = 0.0003$). There was also a linear relationship between them for values of θ between 19° and the critical angle but the correlation was negative.

Similar findings were obtained from Experiments 3.1.2-3.1.6 with the critical angle varying between 37° and 56°. In Experiment 3.1.4 (see Figure 28) it appeared from extrapolation that the value of ΔF max when θ was equal to 45° was inappropriately low therefore a critical angle of 40° was selected.

TABLE 25 Experiment 3.1.1 The Variation of the Maximum Frequency with the Angle of Insonation

θ (°)	ΔF max (Hz)
19	805
31	971
39	1067
46	1031
60	882
65	708
71	686
77	526
85	489

θ = angle of insonation
ΔF max = maximum frequency

TABLE 26 Experiment 3.1.2 The Variation of the Maximum Frequency with the Angle of Insonation

θ (°)	ΔF max (Hz)
20	3388
40	5279
46	5894
56	6332
64	5951
69	4795
75	4090
84	2581

TABLE 27 Experiment 3.1.3 The Variation of the Maximum Frequency with the Angle of Insonation

θ (°)	ΔF max (Hz)
22	1006
30	1151
34	1189
38	1675
40	1360
42	1319
44	1434
45	1413
46	1125
47	1282
48	1190
49	1099
50	1211
53	1040
54	1140
56	1148
58	1112
60	1034
62	823
64	770
65	974
70	651
74	480
79	460
83	985
90	784

TABLE 28 Experiment 3.1.4 The Variation of the Maximum Frequency with the Angle of Insonation

θ (°)	ΔF max (Hz)
20	775
30	931
35	1034
40	1086
45	982
50	1112
55	1066
60	758
65	633
70	741
75	551
80	581

TABLE 29 Experiment 3.1.5 The Variation of the Maximum Frequency with the Angle of Insonation

θ (°)	ΔF max (KHz)
5	0.5
13	0.7
16	0.7
23	0.6
26	0.9
34	0.4
37	0.8
39	0.6
44	0.8
48	1.0
52	0.8
57	0.4
58	0.4
61	0.6
66	0.5
67	0.7
71	0.6
74	0.5
82	0.4

<u>TABLE 30</u> Experiment 3.1.6 The Variation of the Maximum Frequency with the Angle of Insonation

Amplitude of Oscillation	Minimum		Intermediate		Maximum	
	θ (°)	ΔF max (KHz)	θ (°)	ΔF max (KHz)	θ (°)	ΔF max (KHz)
	8	0.9	25	0.4	37	2.2
	14	1.1	35	1.9	40	2.5
	19	1.0	37	2.1	45	2.3
	25	1.1	42	2.0	50	2.1
	35	1.6	50	1.7	55	2.0
	40	1.7	57	1.6	65	1.6
	45	1.7	65	1.1	70	1.2
	52	0.9	80	0.5	80	0.6
	60	1.0				
	68	1.1				
	75	0.8				
	80	0.4				

TABLE 31 The Relationship Between the Maximum Frequency and the Cosine of the Angle of Insonation for Values of θ Less than the Critical Angle

ΔF max : $\cos\theta$, $\theta < \theta$ crit

Experiment	θ(°)	n	CC	m	c	SE	p
3.1.1	19-39	3	- 0.99	- 1.565	2.293	0.016	0.081
3.1.2	20-56	4	- 0.967	- 7.92	11.081	0.334	0.030
3.1.3	22-38	4	- 0.88	- 4.36	4.969	0.136	0.116
3.1.4	20-40	4	- 0.99	- 1.846	2.521	0.021	0.0086
3.1.5	5-48	10	- 0.46	- 0.748	1.339	0.162	0.177
3.1.6 min osc	8-40	6	- 0.97	- 3.61	4.48	0.087	0.003
med osc	25-37	3	- 0.99	- 16.2	15.08	0.069	0.047

The correlation coefficient (CC) of a straight line of gradient (m) in joining values of ($\cos\theta$, ΔF max) cutting the y axis at point c.

SE - standard error of the mean
θcrit - the critical angle

TABLE 32 The Relationship Between the Maximum Frequency and the Cosine of the Angle of Insonation for Values of θ Greater than the Critical Angle

$\Delta F_{max} : \cos\theta, \ \theta > \theta_{crit}$

Experiment	θ(°)	n	CC	m	c	SE	p
3.1.1	39-84	7	0.98	0.917	0.373	0.042	0.0003
3.1.2	56-84	5	0.99	8.573	1.806	0.025	0.0016
3.1.3	40-79	21	0.95	1.675	0.119	0.088	0.000
3.1.4	40-80	9	0.90	1.005	0.345	0.099	0.0013
3.1.5	48-82	10	0.56	0.683	0.291	0.163	0.565
3.1.6 min osc	45-80	6	0.81	1.68	0.249	0.247	0.049
med osc	37-80	6	0.99	2.60	0.059	0.065	0.0005
max osc	40-80	7	0.99	3.11	0.146	0.079	0.0001

TABLE 33 The Variability of the Constant (K) for Values of θ Less than the Critical Angle

$K = \Delta F\ max/\cos\theta,\ \theta < \theta\ crit$

Experiment	θ (°)	n	Mean	SD	CV (%)
3.1.1	19-39	3	1.11	0.260	23
3.1.2	20-56	4	7.58	3.21	42
3.1.3	22-38	4	1.5	0.446	30
3.1.4	20-40	4	1.148	0.253	22
3.1.5	5-48	10	0.845	0.309	37
3.1.6 min osc	8-40	6	1.408	0.536	38
med osc	25-37	3	1.79	1.18	66

TABLE 34 The Variability of the Constant (K) for Values of θ Greater than the Critical Angle

$K = \Delta F \max/\cos\theta,\ \theta > \theta_{crit}$

Experiment	θ (^{o})	n	Mean	SB	CV (%)
3.1.1	39-77	7	1.66	0.480	29
3.1.2	56-74	4	13.55	1.88	14
3.1.3	38-77	23	1.94	0.195	10
3.1.4	40-75	8	1.716	0.313	18
3.1.5	48-74	9	1.358	0.423	31
3.1.6 min osc	45-80	6	2.36	0.605	26
med osc	37-80	6	2.73	0.144	5
max osc	40-80	7	3.43	0.194	6

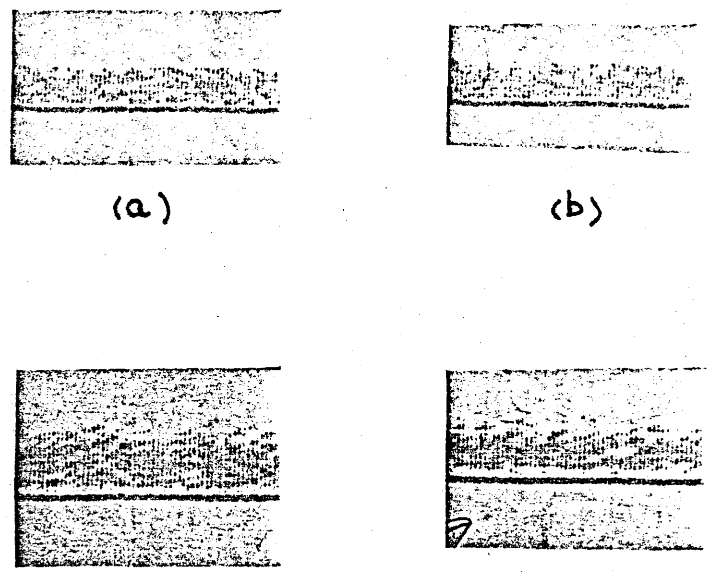

(a) (b)

(c) (d)

FIGURE 23

Spectrascribe traces from Experiment 3.1.1. Irregularities of the maximum frequency envelope made the results more variable.

(a) $\theta = 39^\circ$
(b) $\theta = 46^\circ$
(c) $\theta = 60^\circ$
(d) $\theta = 65^\circ$

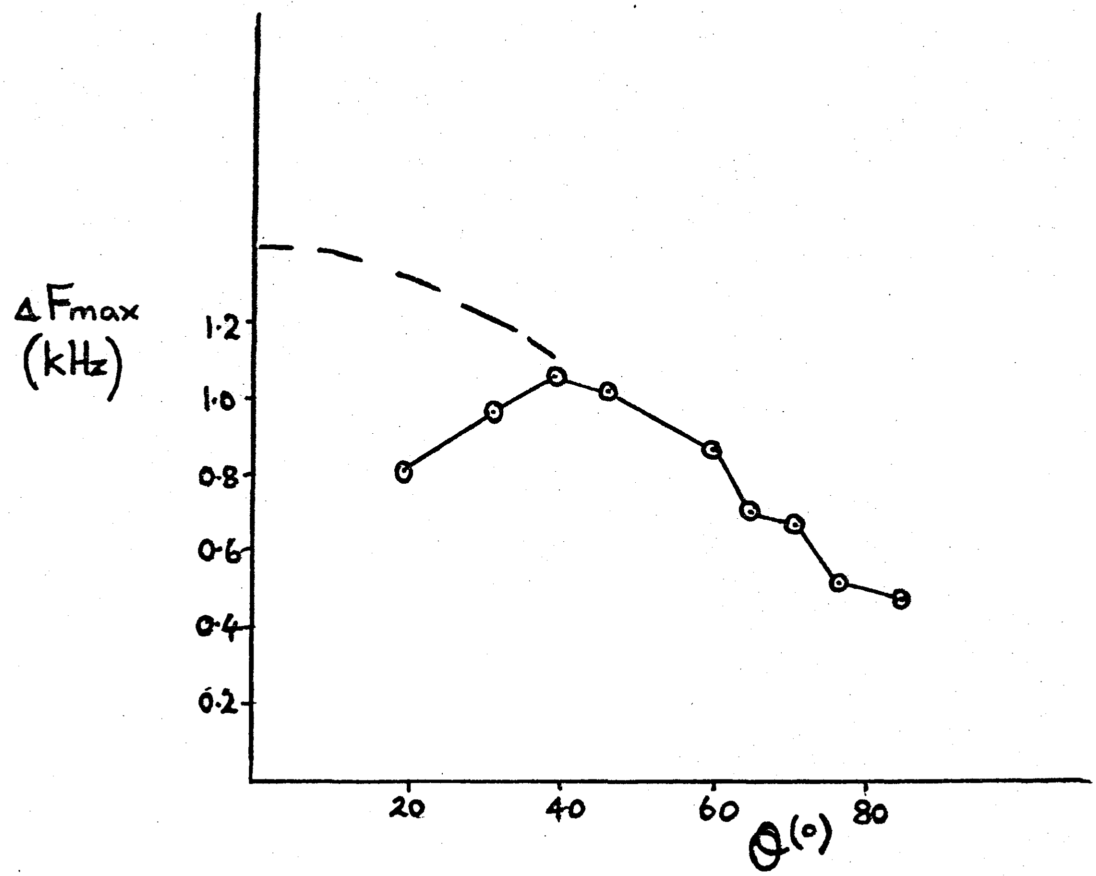

FIGURE 24

Experiment 3.1.1 The relationship between ΔF max and θ.
The interrupted line gives the expected result for values of $\theta < 40^{\circ}$ ie a cosine curve.

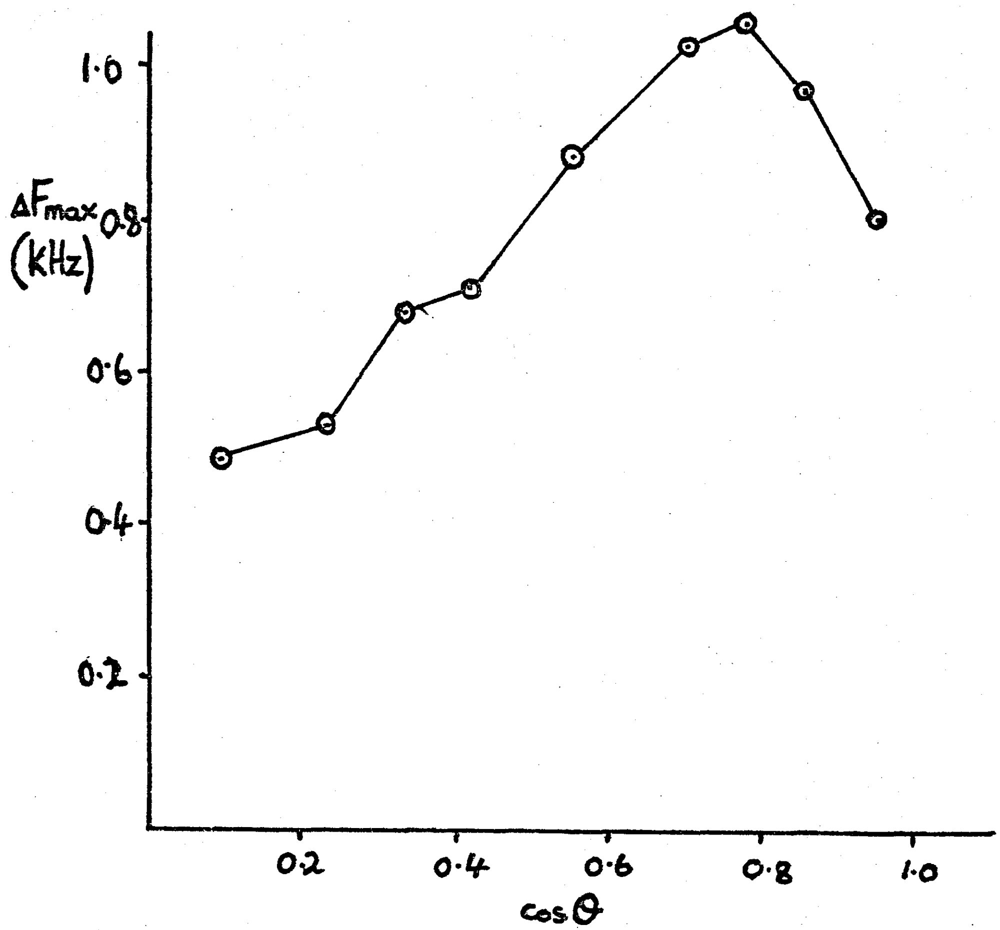

FIGURE 25

Experiment 3.1.1 The relationship between ΔF max and cos θ.

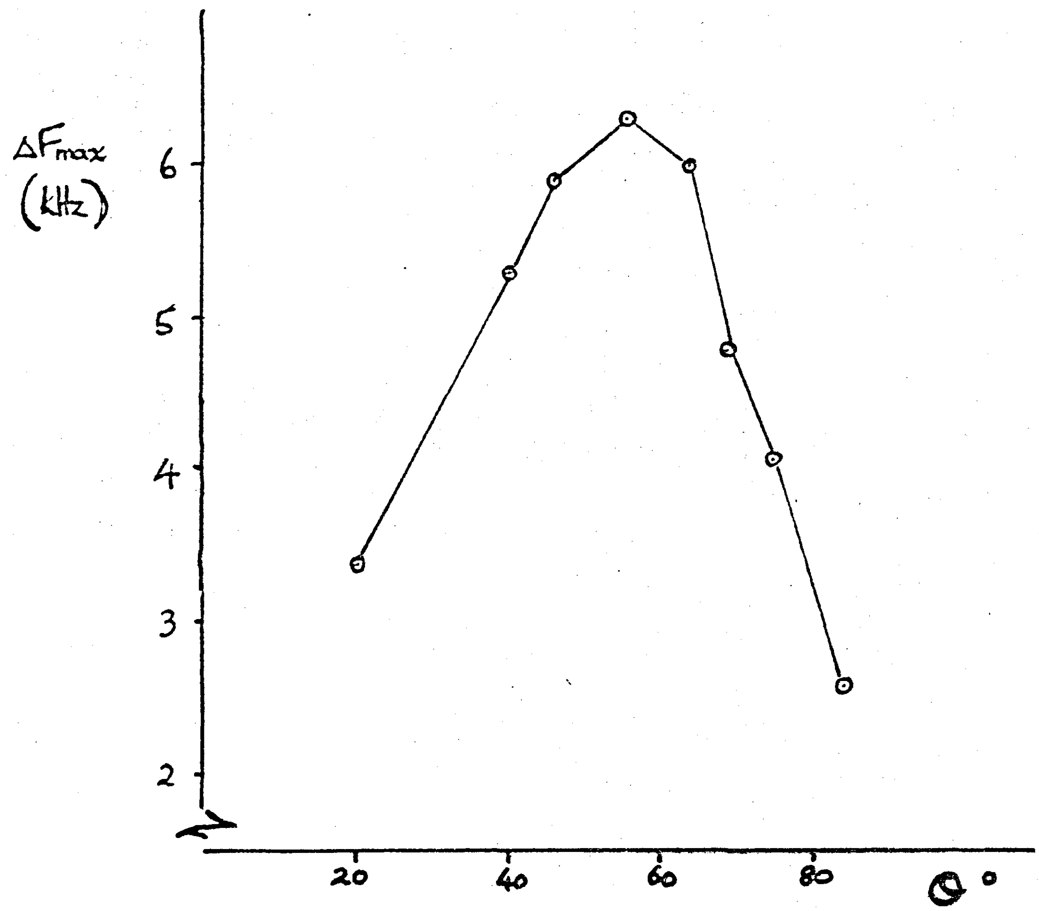

FIGURE 26

Experiment 3.1.2 The relationship between ΔF max and θ.

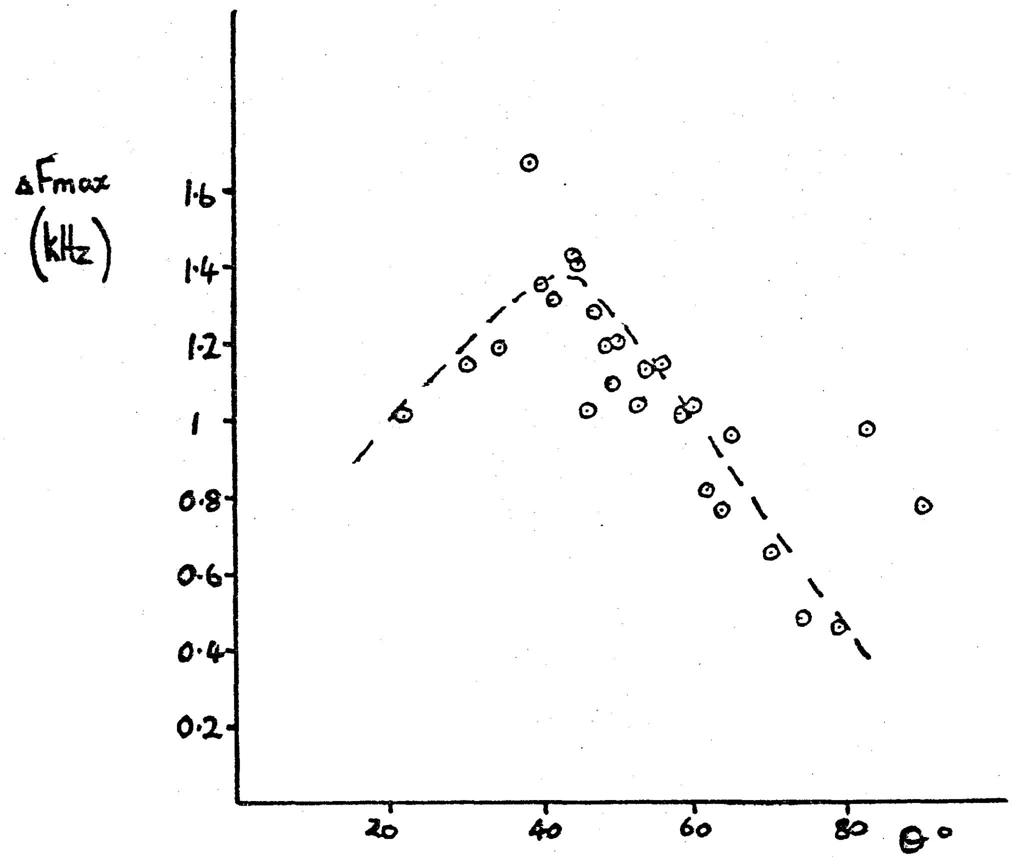

FIGURE 27

Experiment 3.1.3 The relationship between ΔF max and θ.

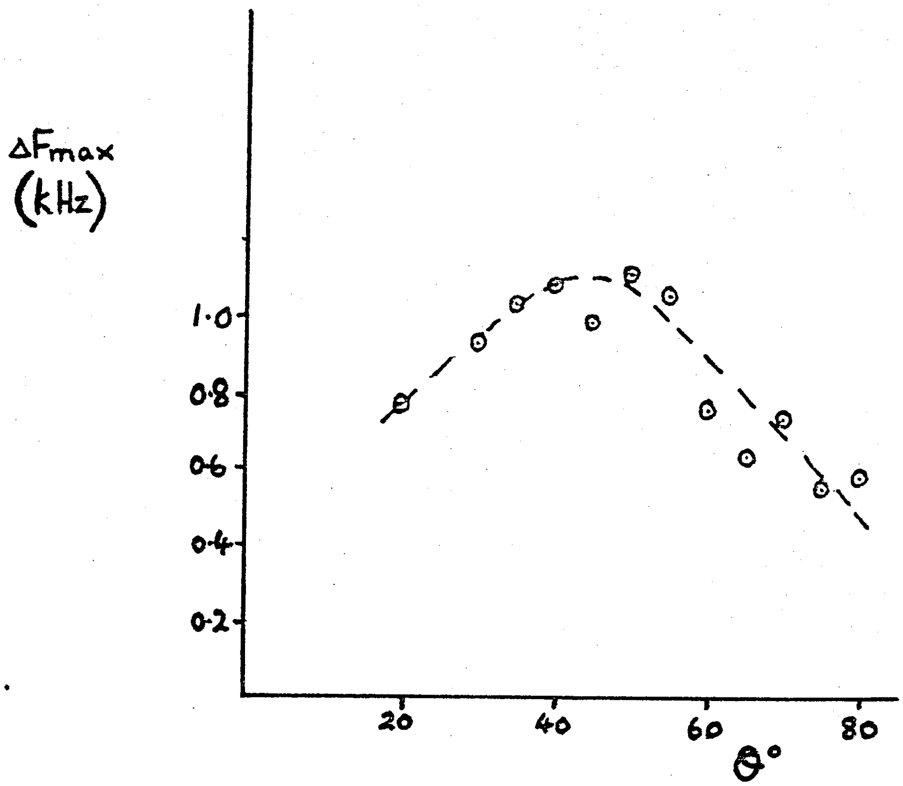

FIGURE 28

Experiment 3.1.4 The relationship between ΔF max and θ.

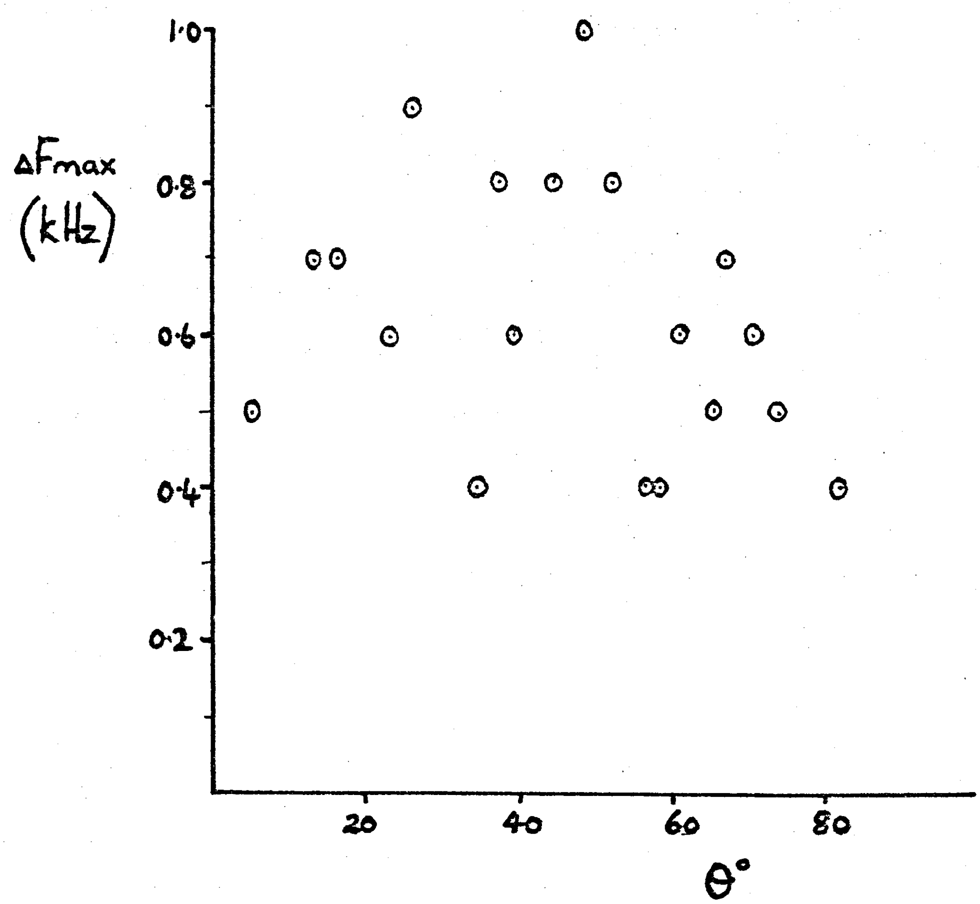

FIGURE 29

Experiment 3.1.5 The relationship between ΔF max and θ.

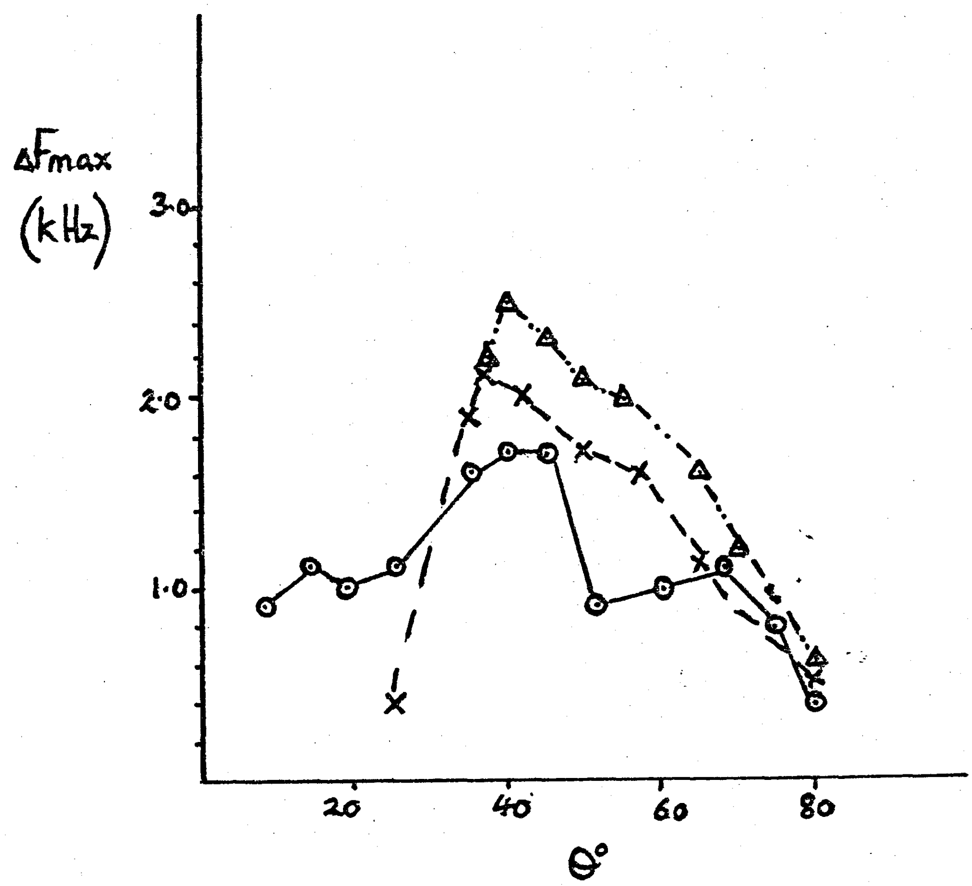

FIGURE 30

Experiment 3.1.6 The relationship between ΔF max and θ.

o———o = minimum amplitude of oscillation
x- - —x = intermediate amplitude of oscillation
Δ— ·· —Δ = maximum amplitude of oscillation

<u>EXPERIMENT 3.2</u> The Reflection of Ultrasound from the Surface of Arteries and Tubing

Tables 35-39 and Figures 31-34 give the amount of reflected ultrasound at different values of θ for the material tested.

In the cases of PTFE, polyurethane and calcified and normal arteries as θ fell from 90^{o} the signals recorded by the hydrophone were low until a critical angle was reached when a sharp increase was recorded. The increase reached approximately 5 mV which was almost the maximum emitted intensity of the ultrasound. In the cases of silastic and red rubber there was a more gradual increase in hydrophonic signal as θ fell from 90^{o}. The critical angle for each material was determined from the mean angle where the increase was noted for each experiment. The critical angles are displayed in Table 40. These critical angles, which were different for each material, corresponded with a fall in the audio output from the Vasoscan indicating a drop in ΔF max.

<u>EXPERIMENT 3.3</u> To Quantify the Relationship Between the Maximum Systolic Frequency and the Angle of Insonation In Vivo

Table 41 gives the results of max A for each value of θ for each patient and Figure 35 is a graph of the results for patient number one. It was found that max A rose as θ fell from 90^{o} until:-

(i) Max A fell at a critical angle (n = 5)

TABLE 35 The Reflection of Ultrasound from Silastic

	θ (^{o})	Hydrophonic Signal (mV) Measurement (i) (Total)	Measurement (ii) (Direct)	Amount of Reflected Ultrasound (mV)
Experiment (i)	20	2.8	0.4	2.4
	25	2.6	0.4	2.2
	35	1.8	0.2	1.6
	40	1.1	0.2	0.9
	45	1.1	0.4	0.7
	60	0.6	0.1	0.5
	75	0.6	0.16	0.44
Experiment (ii)	20	2.4	0.2	2.2
	30	2.2	0.4	1.8
	40	1.4	0.4	1.0
	50	1.6	0.4	1.2
	60	0.5	0.1	0.4
	70	0.7	0.2	0.5
	80	0.4	0.2	0.2
Experiment (iii)	20	2.4	0.2	2.2
	30	2.8	0.4	2.4
	40	1.6	0.3	1.3
	50	1.2	0.1	1.1
	60	1.3	0.4	0.9
	70	1.5	0.8	0.7
	75	0.8	0.4	0.4
	85	0.6	0.4	0.2

<u>TABLE 36</u> The Reflection of Ultrasound from PTFE

	θ (°)	Hydrophonic Signal (mV) Measurement (i) (Total)	Measurement (ii) (Direct)	Amount of Reflected Ultrasound (mV)
Experiment (i)	10	3.6	0.4	3.2
	20	3.2	0.4	2.8
	30	2.0	0.2	1.8
	40	1.6	0.4	1.2
	50	1.4	0.2	1.2
	60	1.6	0.4	1.2
	70	0.8	0.2	0.6
	80	1.2	0.4	0.8
	90	0.8	0	0.8
Experiment (ii)	20	5.0	0.4	4.6
	30	4.8	0.4	4.4
	40	5.0	0.2	4.8
	50	5.0	0.2	4.8
	60	0.8	0.2	0.6
	70	1.2	0.6	0.6
	80	1.0	0.2	0.8
	90	1.0	0.4	0.6

TABLE 36 (CONTD) The Reflection of Ultrasound from PTFE

	θ (°)	Hydrophonic Signal (mV) Measurement (i) (Total)	Hydrophonic Signal (mV) Measurement (ii) (Direct)	Amount of Reflected Ultrasound (mV)
Experiment (iii)	20	5.4	0.4	5.0
	30	5.4	0.4	5.0
	40	5.4	0.2	5.2
	50	5.0	0.2	4.8
	60	1.8	0.8	1.0
	70	1.0	0.4	0.6
	80	1.6	0.4	1.2
	90	0.8	0.6	0.2
Experiment (iv)	20	5.0	0.4	4.6
	30	3.6	0.4	3.2
	40	3.6	0.4	3.2
	50	5.0	0.4	4.6
	60	1.2	0.4	0.8
	70	1.6	0.4	1.2
	80	1.4	0.2	1.2

TABLE 37 The Reflection of Ultrasound from Polyurethane

	θ (°)	Hydrophonic Signal (mV) Measurement (i) (Total)	Measurement (ii) (Direct)	Amount of Reflected Ultrasound (mV)
Experiment (i)	20	5.2	0.2	5.0
	30	5.0	0	5.0
	40	3.8	0.6	3.2
	50	2.8	0.4	2.4
	60	2.1	0.1	2.0
	70	3.4	0.2	3.2
	80	2.4	0.4	2.0
Experiment (ii)	20	4.2	0.2	4.0
	30	4.8	0.2	4.6
	40	4.0	0.2	3.8
	50	4.0	0.2	3.8
	60	2.0	0.2	1.8
	70	2.2	0.2	2.0
	80	1.4	0.2	1.2

TABLE 38 The Reflection of Ultrasound from Red Rubber

	Θ (°)	Hydrophonic Signal (mV) Measurement (i) (Total)	Hydrophonic Signal (mV) Measurement (ii) (Direct)	Amount of Reflected Ultrasound (mV)
Experiment (i)	10	1.2	0.2	1.0
	20	1.0	0.2	0.8
	30	0.8	0.2	0.6
	40	0.4	0.2	0.2
	50	0.4	0.2	0.2
	60	0.4	0.2	0.2
	70	0.4	0.2	0.2
	80	0.2	0.2	0
Experiment (ii)	10	1.6	0.2	1.4
	20	1.4	0.2	1.2
	30	1.0	0.2	0.8
	40	1.0	0.2	0.8
	50	0.7	0.2	0.5
	60	0.7	0.2	0.5
	75	1.2	0.2	1.0

TABLE 39 The Reflection of Ultrasound from Calcified and Normal Arteries

	Θ (°)	Hydrophonic Signal (mV) Measurement (i) (Total)	Hydrophonic Signal (mV) Measurement (ii) (Direct)	Amount of Reflected Ultrasound (mV)
Calcified Artery				
	10	5.0	0.4	4.6
	20	5.0	0.2	4.8
	30	2.0	0.2	1.8
	40	2.0	0.2	1.8
	50	1.7	0.2	1.5
	60	2.2	0.2	2.0
	70	2.4	0.4	2.0
	80	1.6	0.2	1.4
Normal Artery				
	10	5.0	0.4	4.6
	20	0.4	0.2	0.2
	30	0.4	0.2	0.2
	40	0.4	0.2	0.2
	50	0.4	0.2	0.2
	60	0.8	0.4	0.4
	70	0.6	0.2	0.4
	80	0.4	0.2	0.2

TABLE 40 Values for the Critical Angle and the Speed of Sound in the Materials Tested in Experiment 3.2

Material	Experiment	Range θ (°)	θ Crit (°)	C (m/sec)
PTFE	(i)	40	51	2353
	(ii)-(iv)	50-60		
Polyurethane	(i)	30-60	50	2302
	(ii)	50-60		
Silastic	(i)	35-45		
	(ii)	30-40	37	1852
	(iii)	30-40		
Rubber	(i)	30-40	30	1709
	(ii)	20-30		
Calcified Artery	(i)	20-30	25	1634
Normal Artery	(i)	10-20	15	1532
Muscle				1590
Water				1480

Range θ refers to the angles over which the increase in the hydrophonic signal was detected. The speed of sound (C) was calculated from Equation 3.6 using θ crit. Values for muscle and water are after Wells.[105]

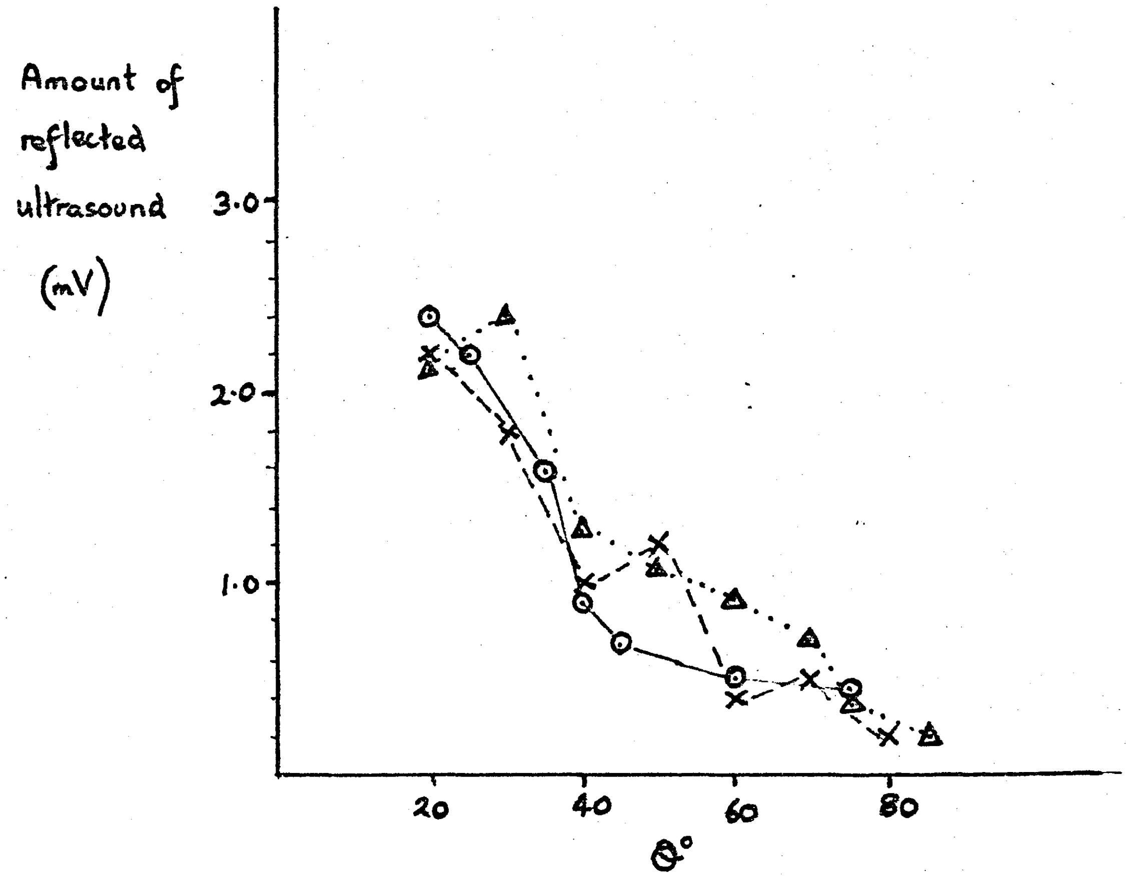

FIGURE 31

Experiment 3.2 The reflection of ultrasound from silastic tubing.

o —— o = Experiment (i)
x - - x = Experiment (ii)
Δ ... Δ = Experiment (iii)

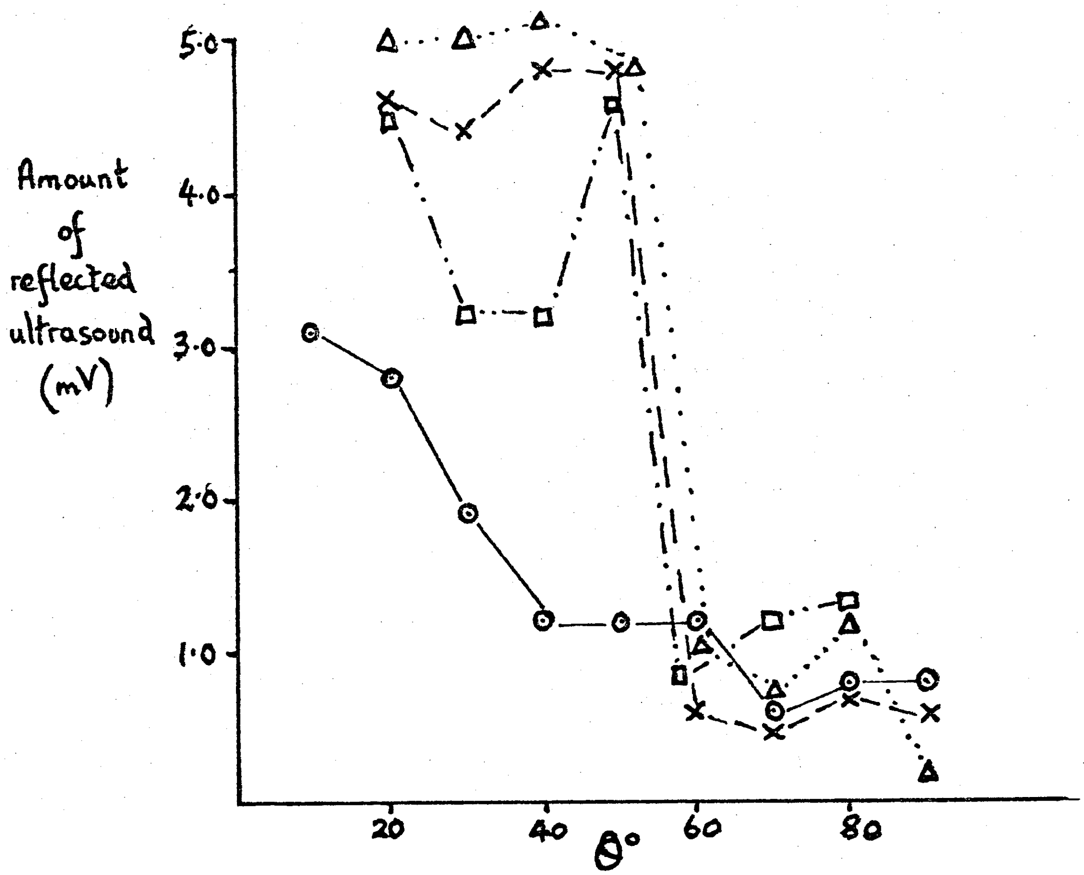

FIGURE 32

Experiment 3.2 The reflection of ultrasound from PTFE (Goretex)

o —— o = Experiment (i)
x --- x = Experiment (ii)
Δ . . . Δ = Experiment (iii)
□ -.- □ = Experiment (iv)

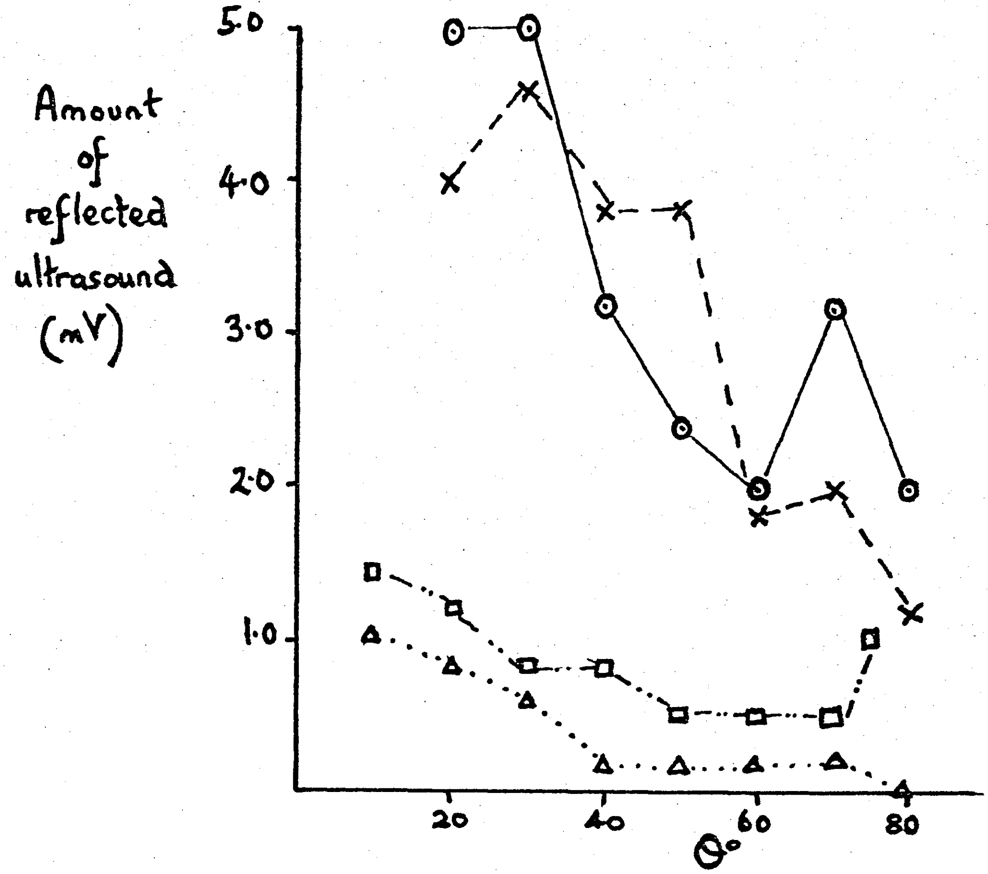

FIGURE 33

Experiment 3.2 The reflection of ultrasound from polyurethane and red rubber

o —— o = polyurethane Experiment (i)
x --- x = polyurethane Experiment (ii)
△ ... △ = red rubber Experiment (i)
□ -.- □ = red rubber Experiment (ii)

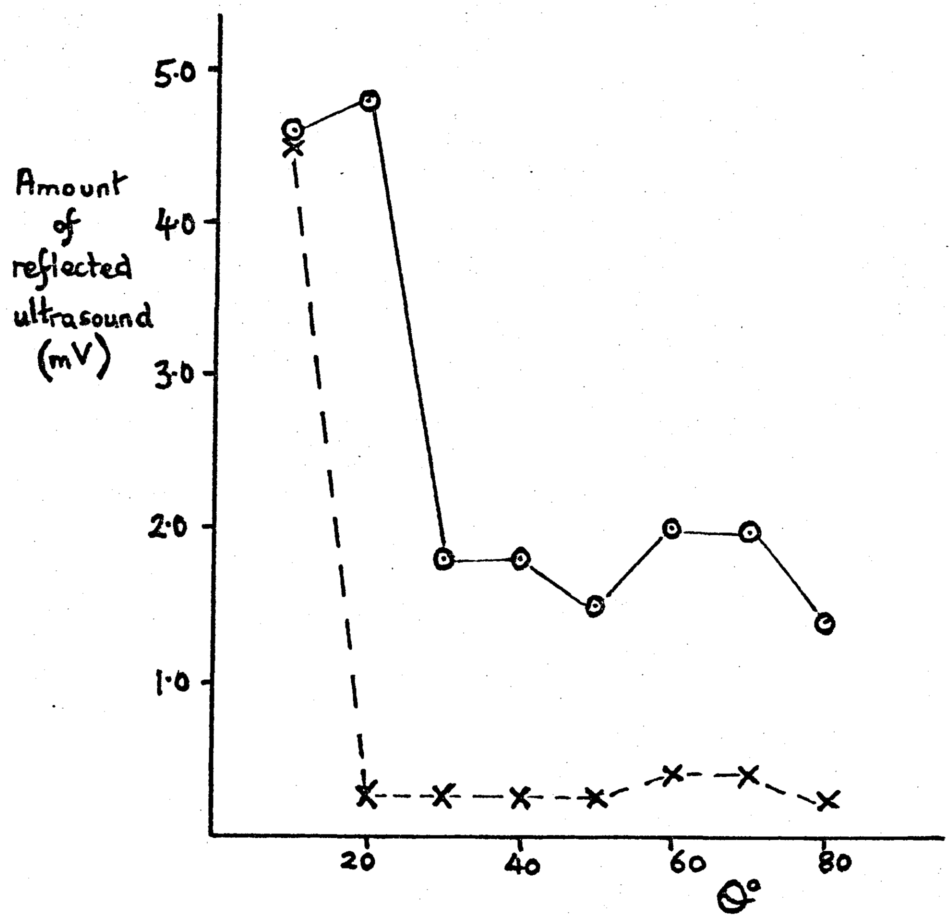

FIGURE 34

Experiment 3.2 The reflection of ultrasound from calcified and normal arteries

o —— o = calcified artery
x --- x = normal artery

or

(ii) No ultrasonic signal could be received ($n = 5$)

or

(iii) After a certain angle max A remain constant ie a plateau reponse and then no ultrasonic signal could be received ($n = 2$)

The critical angle was determined as the mean of all the responses and this was 32°. Table 42 gives the results of analysis (i). The mean gradients were:-

(a) θ positive:-

$$\cos\theta = 0.278 \text{ max A} - 0.057$$

$$\text{max A} = 3.6 \cos\theta + 0.21$$

(b) θ negative:-

$$\cos\theta = 0.436 \text{ max A} - 0.111$$

$$\text{max A} = 2.3 \cos\theta + 0.25$$

<u>EXPERIMENT 3.4</u> The Accuracy of the Method of Measuring the Angle of Insonation

In the case of the figures obtained from the model (Experiment 3.1.6) the method accurately calculated θ to within 10° in 21/24 (88%) (see Table 43) with little difference whether ω was between 5° and 23°.

TABLE 41 Experiment 3.3 - The Variation of Max A with the Angle of Insonation

θ (°)	max A Values (KHz) for Patient Number					
	1	2	3	4	5	6
- 30	-	1.1	2.3	1.7	3.9	3.6
- 40	1.5	1.3	1.5	1.4	3.8	3.8
- 50	1.6	1.1	1.4	1.2	3.0	3.5
- 60	1.3	0.8	1.8	0.8	2.5	2.9
- 70	1.1	0.7	1.4	0.7	2.0	2.0
- 80	0.9	0.5	1.0	-	2.2	1.0
90	0.6	1.0	0.5	-	0.8	-
80	0.7	0.6	1.0	-	1.3	1.7
70	0.8	0.9	1.5	1.0	2.3	2.4
60	1.1	1.4	2.1	1.4	3.1	3.1
50	1.5	1.5	2.5	1.5	3.6	3.3
40	1.7	1.9	2.8	2.8	3.6	3.9
30	2.3	2.2	2.8	2.3	3.6	4.6
20	2.1	2.4	-	-	-	-

TABLE 42 The Relationship Between Max A and the Cosine of the Angle of Insonation

cos θ : max A, $\theta_{crit} < \theta < 80^{\circ}$ ie θ is positive

Patient	n	CC	m	c	SE	p
1	6	.946	.353	+ .107	.086	= .006
2	7	.978	.342	- .007	.057	$<$ .001
3	6	.99	.322	- .204	.028	$<$ .0001
4	4	.955	.209	+ .172	.054	= .041
5	5	.99	.203	- .146	.017	= .003
6	6	.99	.243	- .262	.036	$<$ .001
mean			.278	- .057		

cos θ : max A, $\theta_{crit} > \theta > (-80^{\circ})$ ie θ is negative

Patient	n	CC	m	c	SE	p
1	5	.99	.518	- .199	.032	$<$ .001
2	5	.978	.569	- .062	.049	= .003
3	6	.889	.457	- .289	.119	= .018*
4	5	.996	.438	- .054	.018	$<$ .001
5	5	.82	.237	- .216	.133	= .086*
6	6	.978	.219	- .128	.054	= .002
mean			.436	- 0.111		

* Excluded from the mean

TABLE 43 The Accuracy of the Method of Determining the Angle of Insonation

W	θ correct to within 5^{o}	θ correct to within 10^{o}
$5-8^{o}$	4/8	6/8
10^{o}	1/3	3/3
$13-15^{o}$	5/8	7/8
$20-23^{o}$	3/5	5/5
Total	13/24	21/24

Figure 35

Experiment 3.3 The relationship between max A and θ. Patient number one.

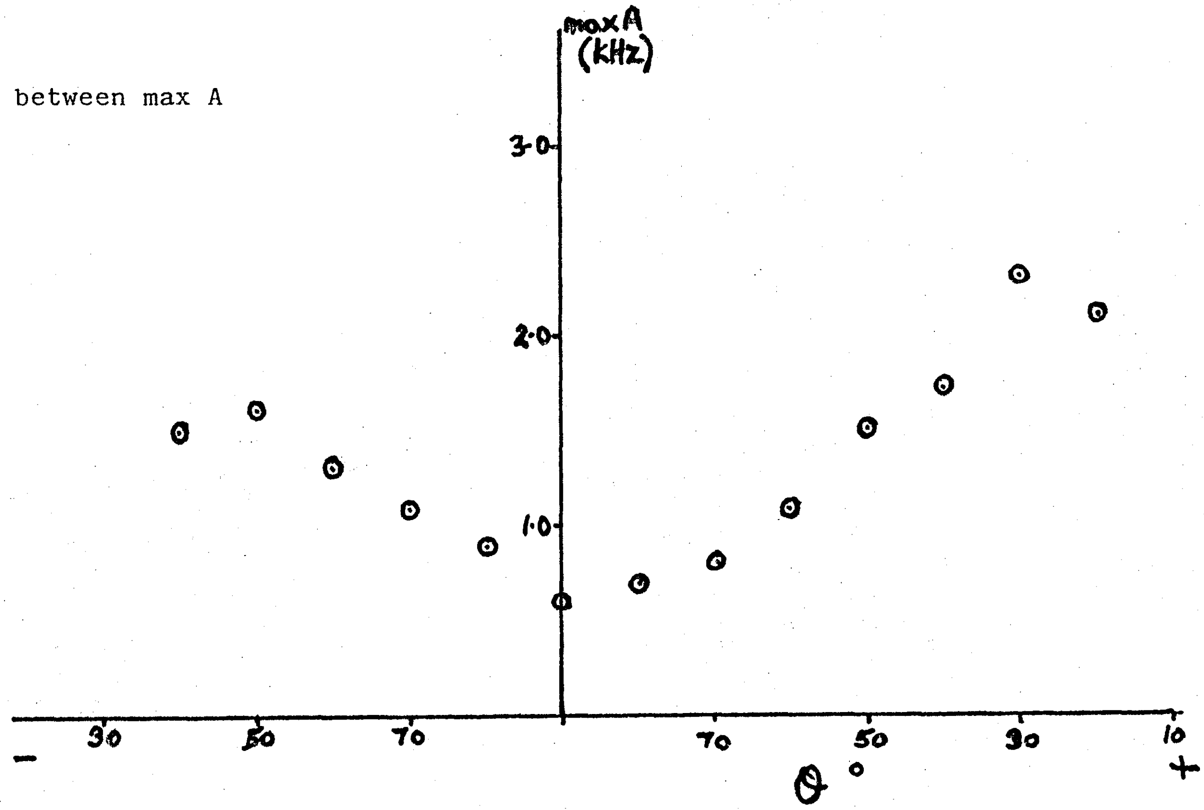

In Experiment 3.3 θ was correctly calculated by the method to within 15^{o} in 39/55 and if any value of θ less than 30^{o} was excluded the accuracy rose to 37/45 (82%).

EXPERIMENT 3.5 Measurements of Maximum Velocity in the Detection of Carotid Disease

Analysis (i) (See Table 44)

Eight values (ie 50%) of the positive answers for max A were falsely positive when compared with V max. Of those 8 values θ was found to be $\leqslant 30^{o}$ in 4; 43^{o} or 44^{o} in one and 55^{o} in 2. θ was less than 60^{o} in all 8. Only one value of max A gave a false negative answer and θ was found to have been 72^{o} ie $> 60^{o}$.

Analysis (ii) (See Table 45)

It was found that whilst the specificity of V max was superior to max A (100% cf 80%) the latter variable was more sensitive to all grades of disease as judged by arteriograms.

TABLE 44 A Comparison of Max A with Calculations of Maximum Velocity. Comparing Max A with V Max. Using a Decision Matrix and the Threshold Values shown in brackets

		Max A (3.5 KHz)	
		+	-
V Max (140 cm/sec)	+	8	1
	-	8	26

TABLE 45 A Comparison of both Max A and the Maximum Velocity with Arteriograms

Threshold	Max A 3.5 KHz		V max 140 cm/sec	
	+	-	+	-
Normal	2	8	0	10
Minimal Disease	2	10	1	11
Mild Stenosis	4	3	2	5
Severe Stenosis	5	4	3	6
Occlusion	3	2	3	2
Specificity	8/10 (80%)		10/10 (100%)	
Overall Sensitivity	14/33 (42%)		9/33 (27%)	
Sensitivity for Severe Stenoses	5/9 (56%)		3/9 (33%)	

DISCUSSION

Wells quotes an error of only 10% in measurements of velocity if θ is within 25^{o} of the true direction of motion however this is misleading as the operator usually endeavours to maintain an optimum angle of insonation of between 45^{o} and 60^{o}.[106] The errors in calculations of V max resulting from an error in measurement of of only 10^{o} are given in Table 46. For a value of θ of 50^{o} it is approximately 20% and for a value of θ of 60^{o} it is 33%. Figure 36 demonstrates the order of magnitude of the error that might result in an incorrect estimation of θ in patient number 5 from Experiment 3.3. There is therefore a need to determine θ accurately.

In Experiments 3.1.1-3.1.6 a linear relationship was demonstrated between values of ΔF max and cos θ consistent with the Doppler formula but only for values of θ between a critical angle and 80^{o}. When θ is 90^{o} ΔF max should theoretically be zero but some frequencies are always detected due to the arrangement of the crystals in the probe and the divergence of the ultrasound beam.[107]

In Experiment 3.1.1 the finding of a decrease in ΔF max for values of θ below the critical angle was unexpected, the interrupted line in Figure 24 shows the expected result ie a cosine curve. Below the critical angle a linear relationship was usually shown between ΔF max and cos θ so that an explanation based on physical theory was

TABLE 46 The Error in Velocity Measurements if the Angle of Insonation is Unknown

$\theta°$	R	ΔF max (KHz)	Error $\pm$ 10°
70	0.52	1.0	50%
60	0.69	1.5	33%
50	0.78	1.9	20%
40	0.84	2.3	15%
30	0.88	2.6	10%
20	0.92	2.8	5%
10	0.95	2.9	

Values of R calculated from Equation 3.2 for values of θ. When ΔF max is 1.0 KHz for θ equal to 70° corresponding values of ΔF max at the other angles are shown. If there was an error of only 10° in θ the percentage errors in measurements of maximum velocity are shown for the corresponding true values of θ. These percentage errors are constant regardless of the actual velocity in the vessel.

(a)

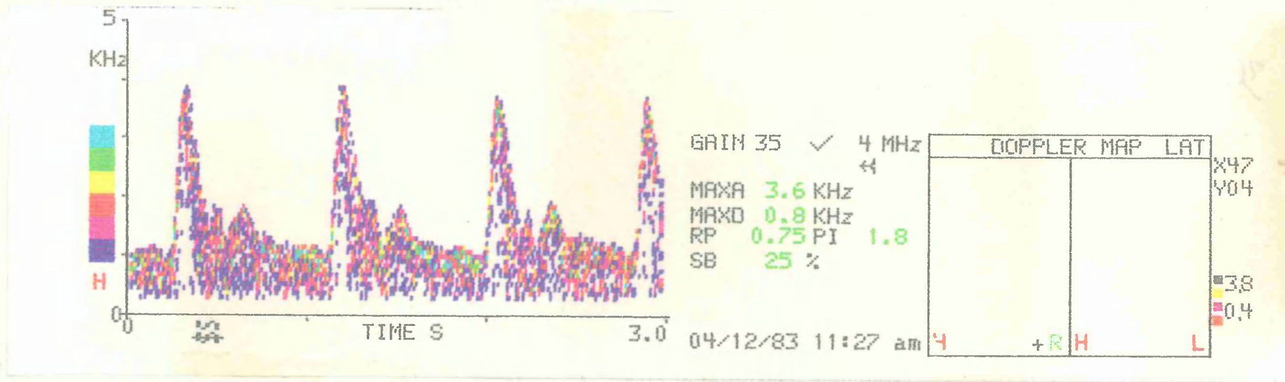

(b)

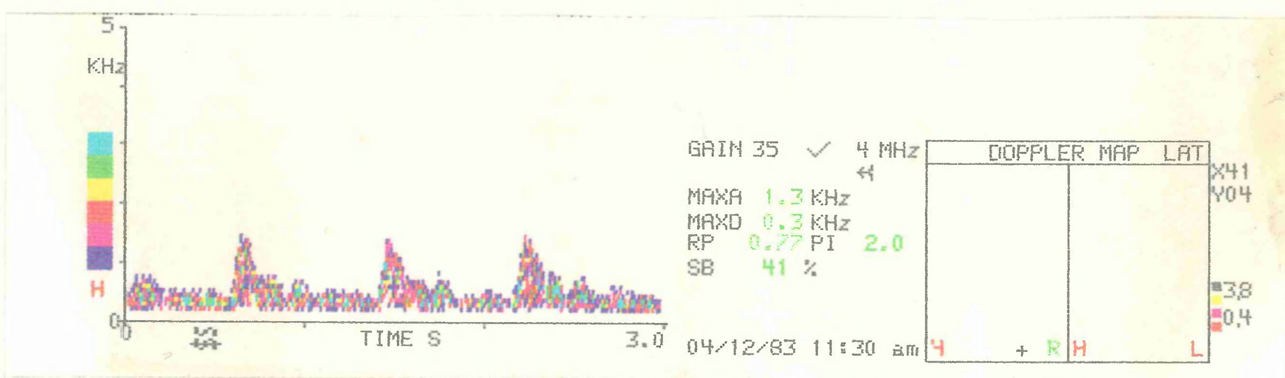

FIGURE 36

Experiment 3.3 The variation of max A with θ, patient number 5.

(a) max A = 3.6 KHz, θ = 40^{o}
(b) max A = 1.3 KHz, θ = 80^{o}

appropriate. The result was the same when the ultrasound scatterer was changed and when a water bath was used. This demonstrated that the effect was not due to a decrease in the received signal because of inadequate coupling at low values of θ. The signal to noise ratio was low at low values of θ and it was conceivable that increasing the level of instrument gain although increasing background noise might allow hitherto undetected signals to be recorded : this was not found to be the case. Shoor et al have published a graph with similar results and reported an optimum angle of insonation for each of 5 ultrasound probes tested in a similar experiment.[108] The optimum angles they report correspond to the critical angle found in this Experiment but changing the instrument did not affect the results in Experiment 3.1.5 and therefore the phenomenon was not primarily due to instrumentation. The phenomenon occurred under conditions of oscillatory flow and the decline in ΔF max below the critical angle became more marked with increasing amplitude of oscillation (Experiment 3.1.6) which might prevent its appreciation in vivo. The constant obtained from Equation 3.2 for values of θ greater than the critical angle was more variable than expected and this was due to disturbances of flow in the model making ΔF max measurements themselves more variable.

Total reflection of the ultrasound beam from the surface of different materials and arteries was found to occur at a critical angle which varied with the physical properties of the tube. This was the explanation of the fall in ΔF max in the previous experiments at low values of θ.

Snell's law applies to any wave traversing a boundary between 2 media and describes the relationship between the speeds of sound in the 2 media (C1 and C2) and the angles of incidence (i) and refraction (r) to the boundary, see Figure 37 and Equation 3.5.

$$\sin i/\sin r = C1/C2 \qquad \text{Equation 3.5}$$

When total reflection occurs angle r equals 90^{o}, sin r equals one therefore Equation 3.5 simplifies to:-

$$C2 = C1/\sin i \qquad \text{Equation 3.6}$$

The speed of sound (C) in each material tested in Experiment 3.2 was calculated from Equation 3.6 using the experimental values for their critical angles. Angle i was 90^{o} minus the critical angle. These values of C along with reported values for muscle and water are shown in Table 40.

As the speed of sound in a medium depends on the relationship between the Young's modulus of elasticity (Y) and the density (p) of the medium shown in Equation 3.7 the higher value for C in the calcified artery in Table 40 compared to that in the normal artery is what one would expect.

$$C = (Y/p)^{\frac{1}{2}} \qquad \text{Equation 3.7}$$

In Experiment 3.2 measurement of ultrasound intensities was the primary aim but there were some interesting observations

$$\frac{\sin i}{\sin r} = \frac{C_1}{C_2}$$

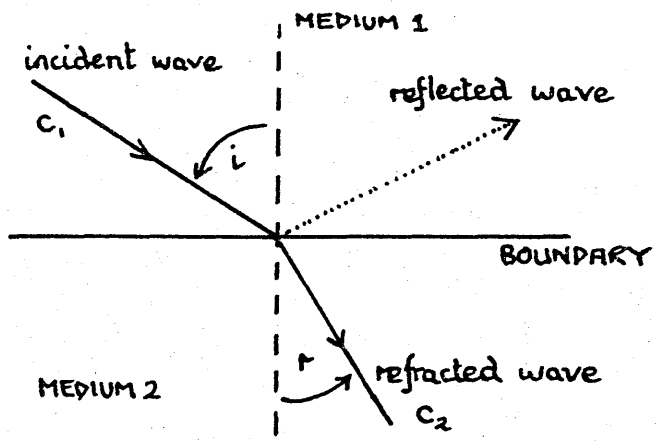

$$C_2 = \frac{C_1}{\sin i}$$

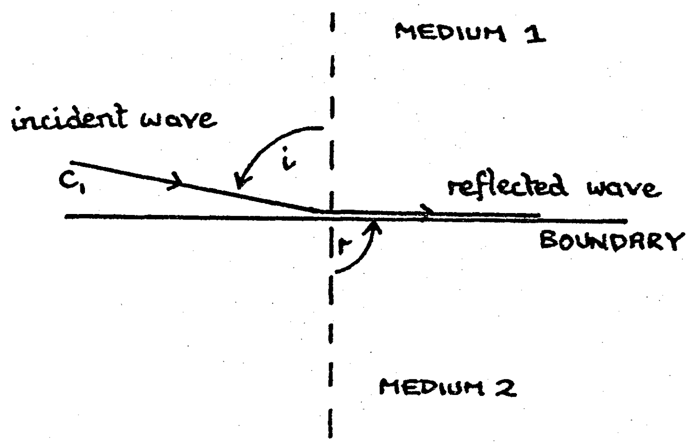

FIGURE 37

Snell's Law

to be made from the Doppler shifted frequencies. Total reflection implies that no ultrasound waves penetrate the lumen of the vessel yet some frequencies were detected for values of θ less than the critical angle. A possible explanation of this may be that as the emitted beam is divergent some waves enter at an angle greater than the critical angle. In the case of PTFE and polyurethane the critical angles were high. This is of importance in clinical work as vascular grafts are constructed from these materials, also even at high values of θ (ie greater than the critical angle) only a very low intensity signal was recorded. At low values of θ movement of the wall of the tube was detected rather than intraluminal velocities (see Figure 38).

The findings in Experiment 3.3 were similar to those in Experiments 3.1.1-3.1.6. A critical angle was identified although it was higher than expected. This may be because of total reflection of the ultrasound or because frequencies of low intensity were absorbed by the soft tissues overlying the arteries. In the clinical situation there are many tissue interfaces where reflection may take place, the most important being the skin : air interface. Difficulties encountered at the skin : air interface might have explained the high critical angle of 32° but in a separate experiment using the hydrophone no reflection was found from the skin provided a liberal quantity of water based jelly was applied between the probe and the skin. If air was present the ultrasound signal was greatly attenuated before it even reached the skin.

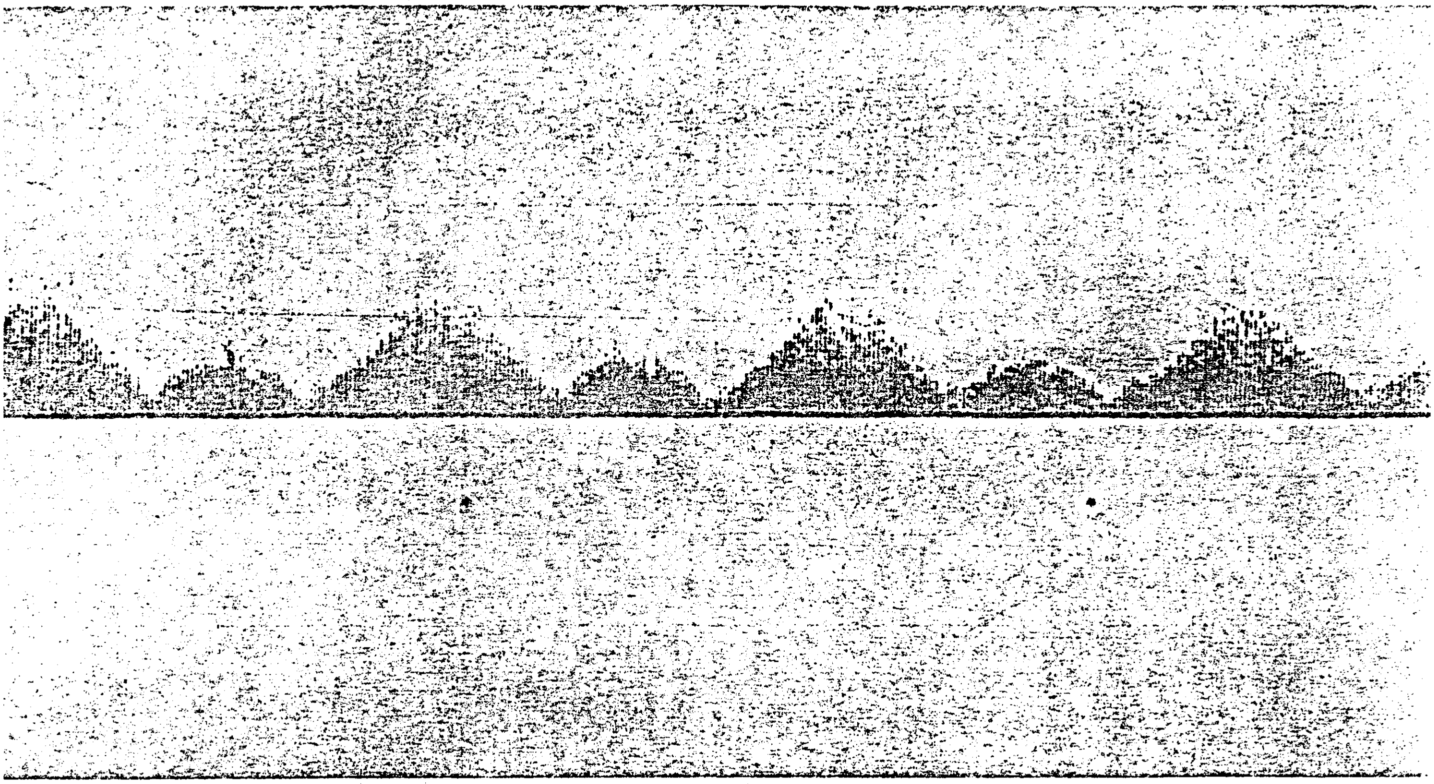

FIGURE 38

Wall movement of PTFE (Goretex)
This signal was recorded in Experiment 3.2 with an angle of insonation less than the critical angle and only water (ie it was free from any small particles which scattered ultrasound) in the tube.

The gradients of the straight lines and the critical angles ought to have been identical in any individual patient apart from opposite signs ie a positive gradient for positive values of θ and a negative gradient for negative values of θ. The reason the mean gradients differed was probably due to the fact that as the probe was rotated its position in relation to the artery was not truly lateral and rotation about a slightly oblique plane was taking place. This rotational error would affect the experimental results. Figure 39 demonstrates that if the x axis is moved by negative 10^{o} the gradients become more similar. There was therefore an error in calculating θ from the lowest max A in Experiment 3.3 which caused errors in both the critical angles and the gradients of the straight lines.

Several methods have been described to measure the angle of insonation using ultrasound.[109-112] Woodcock described the method used in Experiment 3.3 where the probe is orientated for the minimum signal which is assumed to be at right angles to the flow direction and Fahrbach used 2 beams at right angles to each other in a method similar to the one used in this chapter.[110,113] However we found errors in assuming that the minimum Doppler shift occurred when θ was equal to 90^{o} and the other methods involve the use of additional apparatus eg a second transducer or A scan probe. Such methods have not achieved any popularity.

FIGURE 39

Experiment 3.3 The relationship between max A and cos θ, patient number one. A possible error in assuming that the lowest value of max A occurs when θ is 90°. If the origin is moved by + 10° (+ cos θ ·174) the gradients (----) on either side of the y axis become more similar.

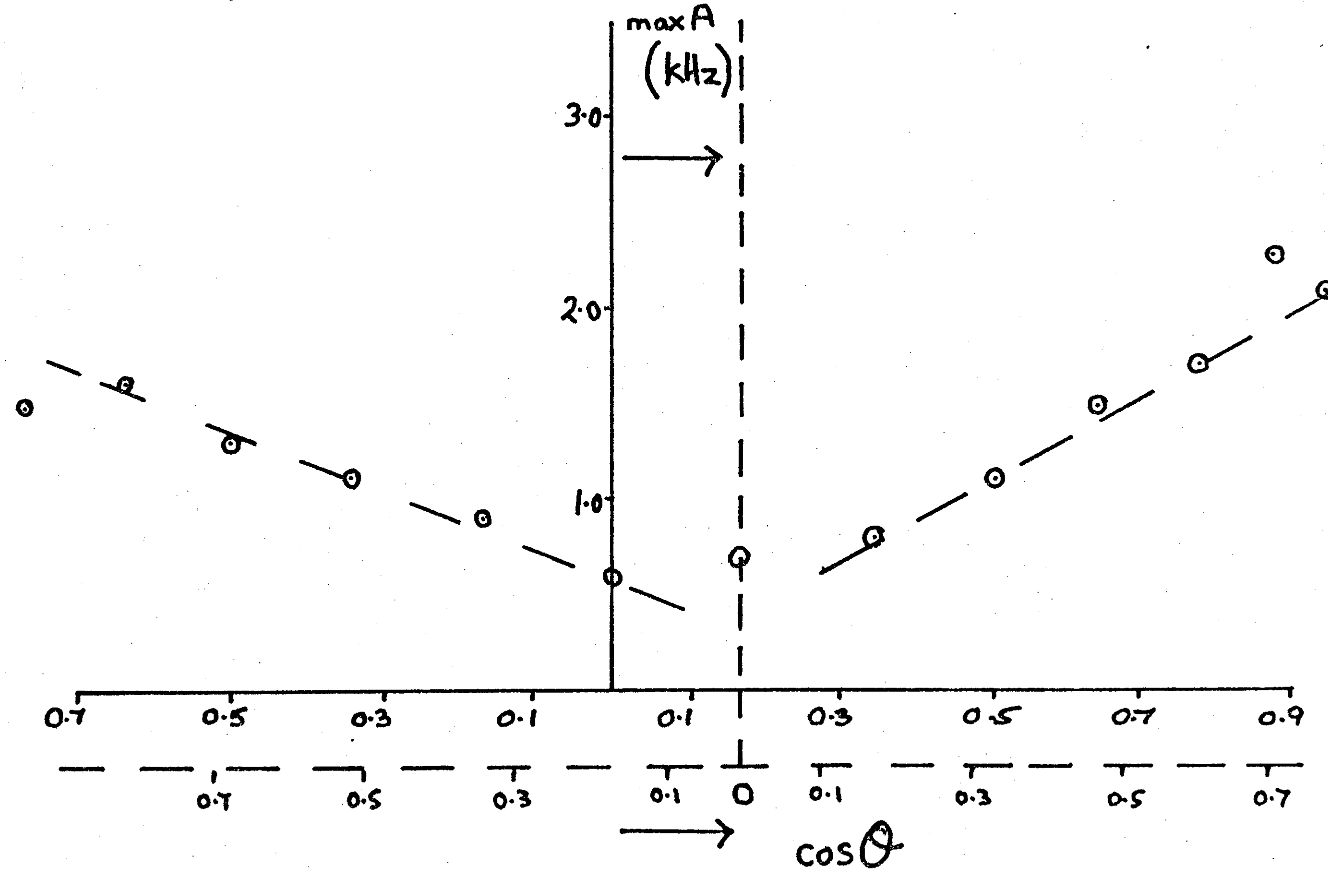

The method devised to measure the angle of insonation in this chapter is simple and easy to perform when the transducer is held in the spatial sensing arm of a Doppler imaging system. The only additional apparatus is a protractor.

The importance of Experiments 3.1-3.3 was in demonstrating that the method for measuring θ used in this chapter would only be accurate over a limited range of angles ie 30^{o}-80^{o}. This was why ω was chosen to be as low as practical (10^{o}) in Experiment 3.5. This allows θ to range as widely as possible ie between 30^{o} and 70^{o}. The use of ω equal to 10^{o} was found to be of acceptable accuracy in measuring θ.

The purpose of comparing max A with V max (analysis (i) Experiment 3.5) was to determine the number of values of max A $\geqslant$ 3.5 KHz taken with a value of θ less than 60^{o} (the optimum angle) and the number of values of max A $<$ 3.5 KHz taken with a value of θ greater than 60^{o}. As expected θ varied widely and all those values of max A $\geqslant$ 3.5 KHz where V max was less than 140 cm/sec were taken at low values of θ and the single value of max A $<$ 3.5 KHz where V max was greater than 140 cm/sec was taken at a high value of θ.

Whilst it was gratifying to find the specificity of V max so high (100%) for the detection of carotid disease it was unexpected that it was less sensitive than max A when compared with arteriograms. In order to account for this either the grading of disease by arteriograms was incorrect (which was possible although it seems unlikely that the presence of disease was overestimated), the method of measuring V max was inaccurate (experimental evidence suggested it was not) or the range of velocities in the normal carotid artery was too great to allow any distinction to be made between "normals" and patients with narrowed arteries.

It was noted in course of examining asymptomatic volunteers (Experiment 1.1) that max A did increase significantly. This was presumably due to a degree of vasospasm caused by apprehension. Atherosclerotic arteries do not react to sympathetic activity in the same way which would tend to create an overlap in the ranges of V max obtained from normal and diseased arteries.

The highest value of V max recorded in Experiment 3.5 was 300 cm /sec which was the highest found by Blackshear et al who measured V max using a Duplex scanner.[114] The same authors reported a range for V max of between 93.5 cm /sec and 304.6 cm /sec in the internal carotid artery for patients with severe carotid stenoses and Breslau found V max to range from 39 cm /sec to 325 cm /sec for patients with various degrees of stenosis.[102,114] These low measurements of V max obtained in patients with carotid stenoses is in agreement with our findings but lowering the threshold value of V max did not increase its diagnostic yield.

C H A P T E R 4

MAXIMUM FREQUENCY RATIOS AND THE DETECTION OF CAROTID ARTERY DISEASE

INTRODUCTION

In Chapter one it was shown that waveform analysis of CW ultrasound spectra from carotid arteries was only accurate in the detection of severe stenoses ie those causing a reduction in the lumen of an artery by 50% of the diameter or more. In this Chapter the possibility of increasing the diagnostic yield for lesser grades of disease was explored using a ratio of 2 measurements of max A ie one proximal to a stenosis and another distal. There was both theoretical and experimental evidence that this might be possible.[114,115]

The following experiments are described in this Chapter:-

(i) The variation of ΔF max when both the point of insonation relative to a stenosis and the size of the stenosis are varied in a model (Experiment 4.1)

(ii) The variation of max A at different sites in the carotid arteries of asymptomatic volunteers and patients (Experiment 4.2)

(iii) The accuracy of an index (FI) compared with max A alone in the detection of carotid artery disease (Experiment 4.3). The index (FI) was the ratio of max A in the internal carotid artery to that in the common carotid artery.

In a study on the mechanics of a critical stenosis in a blood vessel Berguer and Hwang put forward a theoretical solution for the relationships between the velocity of flow at a point proximal to a stenosis (V_I), the velocity at the stenosis (V_S) and the ratio of the cross sectional area at the stenosis to that at the point of measurement proximal to the stenosis.

$$V_S/V_I = 1/(r_s/r_I)^2 \qquad \text{Equation 4.1}$$

where r_I and r_s represent the radii of the prestenotic section and the stenosis respectively.[114]

This Equation can be rearranged to give:-

$$r_s/r_I = (V_I/V_S)^{\frac{1}{2}} \qquad \text{Equation 4.2}$$

The term r_s/r_I can be considered to express the degree of stenosis and the term $(V_I/V_S)^{\frac{1}{2}}$ is the equivalent of the square root of the inverse of the index FI quoted above. However as Equation 4.1 is based on the mean velocity of flow ($\bar{V}$) extrapolating the relationship to the situation in the carotid arteries is not straightforward where max A is proportional to the maximum velocity.

Using a Duplex scanner it has been reported that a ratio of the peak systolic velocity in the internal carotid artery to that in the common carotid artery was an accurate indicator of the degree of carotid stenosis.[115]

METHODS

The Model

A model using the same apparatus described in Chapter 3 was used with the introduction of stenoses in the test section and the use of Dextran 40 as the medium.

The Stenoses

Five stainless steel cylinders one cm long and of diameter 0.7 cm each had a smooth hole drilled through their centres. The diameters of the holes were 2, 3, 4, 5 and 6 mm respectively.

To introduce a stenosis the tubing was divided in the test section and its ends butted against the end of one of the cylinders to produce smooth joints (see Figure 40). A short 3 cm long plastic sleeve sprayed with an acrylic resin was placed over the top of the cylinder and both ends of the tubing to hold them firmly in place. No constriction of the tubing was caused by the outer sleeve.

The Medium

Dextran 40 has a higher viscosity than water (4.8 cp at 23° C at a shear rate of 128/sec measured using the method described by Humphreys) and its use along with the mean velocity of flow and frequency rate of the Scotch Yoke used in Experiment 4.1 allowed values for the Strouhal number (0.024), the Reynolds number (127, calculated using $\bar{V}$) and α (1.2) in the model to

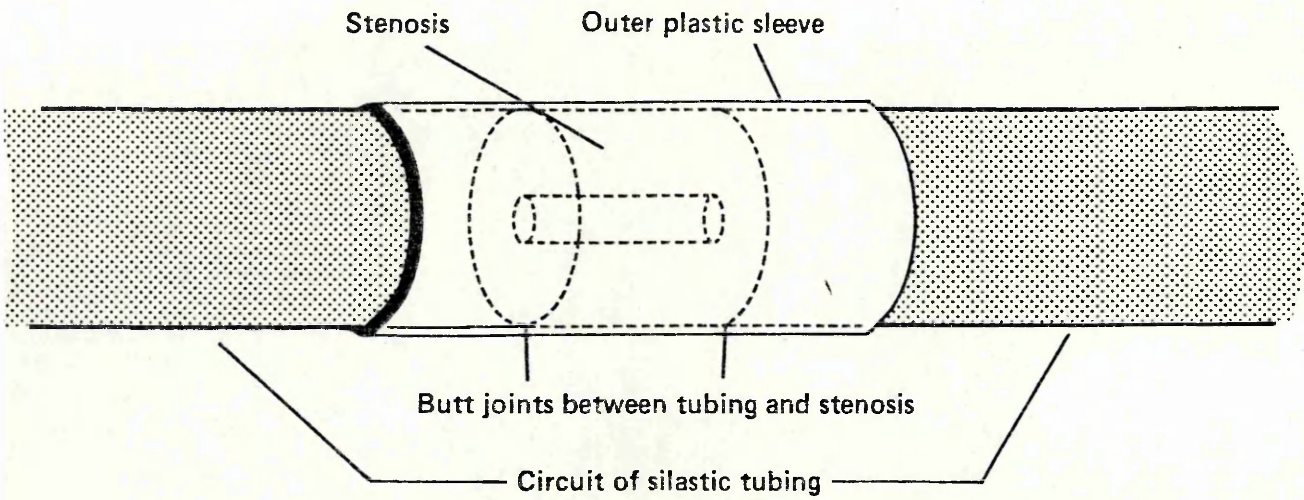

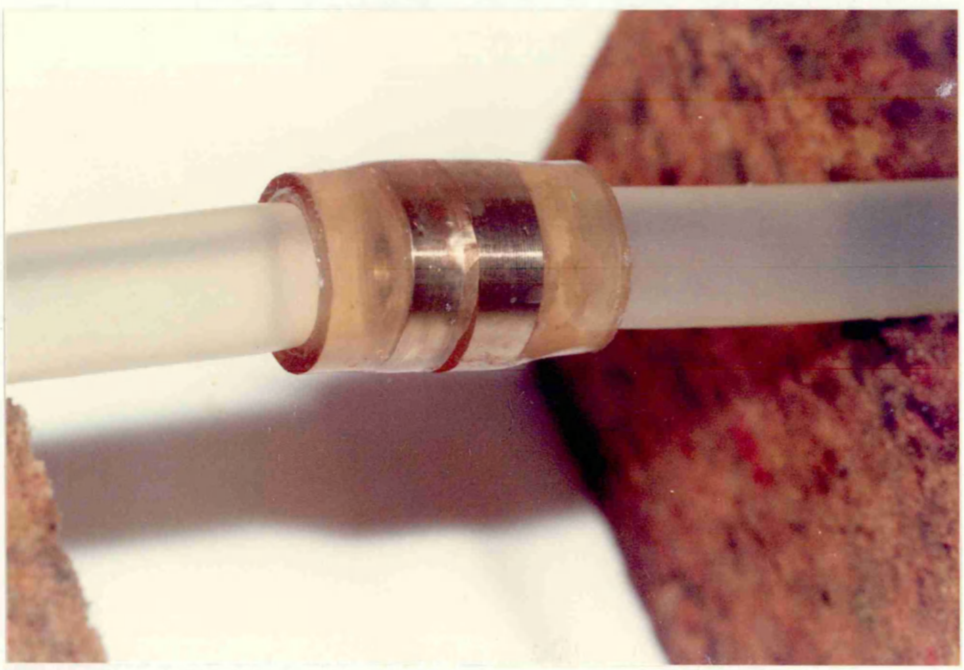

FIGURE 40

A stenosis introduced into the test section approximate those calculated for the internal carotid artery in vivo (see Page 227).[116]

EXPERIMENTS

EXPERIMENT 4.1 Measurements of Maximum Frequency when both the Point of Insonation Relative to a Stenosis and the Size of the Stenosis are Varied in a Model

Methods

An emulsion of silicone liquid in Dextran 40 was circulated through each of the 5 stenoses in turn at a mean velocity of 9 cm/sec (volume flow = 180 ml/min) with a frequency rate of the Scotch Yoke of 40 cycles/min (0.67 Hz). Measurements of ΔF max were taken using the 8 MHz probe of Vasoscan (with an angle of insonation of 60^{o}) from the following sites:-

a) Proximal to the stenosis

(i) 10 cm

(ii) 5 cm

(iii) within 1 cm

b) Distal to the stenosis

(i) 12 cm

(ii) 5 cm

(iii) within 1 cm

The degree of stenosis was calculated from:-

(i) r_S/r_I

(ii) $\left\{(ID_I - ID_S)/ID_I\right\} \times 100\%$

where ID refers to the internal diameter.

The following ratios were calculated:-

a) The highest ΔF max distal to a stenosis : the ΔF max 10 cm proximal to a stenosis ie $\Delta F\ max_S/\Delta F\ max_I$

b) The highest ΔF max distal to a stenosis : the ΔF max from within one cm of the proximal face of the stenosis ie $\Delta F\ max_S/\Delta F\ max_{PRE}$

c) The square root of the inverse of ratio a) ie $(\Delta F\ max_I/\Delta F\ max_S)^{\frac{1}{2}}$

d) The square root of the inverse of ratio b) ie $(\Delta F\ max_{PRE}/\Delta F\ max_S)^{\frac{1}{2}}$

e) The square root of the ratio of the mean velocity proximal to the stenosis to that within the stenosis, (from theory, Equation 4.2) ie $(\bar{V}_I/\bar{V}_S)^{\frac{1}{2}}$

f) The inverse of the above ratio squared ie $\bar{V}_S/\bar{V}_I$

<u>Analysis of Results</u>

(i) The ratios r_S/r_I, $(\Delta F\ max_I/\Delta F\ max_S)^{\frac{1}{2}}$, $(\Delta F\ max_{PRE}/\Delta F\ max_S)^{\frac{1}{2}}$ and $(\bar{V}_I/\bar{V}_S)^{\frac{1}{2}}$ were compared with each other.

(ii) The ratios $\left\{(ID_I - ID_S)/ID_I\right\} \times 100\%$, $\Delta F\ max_S/\Delta F\ max_I$, $\Delta F\ max_S/\Delta F\ max_{PRE}$ and $\bar{V}_S/\bar{V}_I$ were compared with each other

The reason for duplicating the ratios was to have one set in the form of Equation 4.2 derived from Berguer and Hwang's theory and another set in the form normally used in clinical work on the carotid arteries.

EXPERIMENT 4.2 The Variation of Max A at Different Sites in the Carotid Arteries of Asymptomatic Volunteers and Patients

Methods

The results of the carotid ultrasound examinations of the following groups of patients were selected from Experiments 1.1 and 1.2 for further study.

Group 1 - Young Normals

This Group was comprised of all the asymptomatic volunteers studied in Experiment 1.1 (n = 17) of mean age 25 years.

Group 2 - Old Normals

This Group was comprised of those patients in Experiment 1.2 (n = 7) who had bilateral normal arteriograms and ultrasound examinations. Their mean age was 55 years.

Group 3 - Mild Stenosis

This Group was comprised of those patients (n = 14) in Experiment 1.2 who had a mild stenosis found at operation.

Group 4 - Severe Stenosis

This Group was comprised of those patients (n = 9) in Experiment 1.2 who had a severe stenosis found at operation.

Group 5 - All Stenoses

This Group comprised both Groups 3 and 4 together (n = 23).

Group 6 - Stenosis : Exclusion

This Group comprised all those patients in both Groups 3 and 4 in whom the values of max A did not exceed 3.5 KHz in any site (n = 7).

The arterial sites from which data was analysed were proximal and distal internal, common and external carotid arteries and the bifurcation (BIF) for each patient in each Group. (BIF included data from sites BIF 1 and BIF 2 in Experiment 1.1). The reason for selecting Group 6 was to analyse data on patients who would otherwise have been classified as false negative ie normal on the basis of the measurement of max A.

Analysis of Results

(i) The mean value of max A at each site in the carotid arteries was determined in each Group.

(ii) An average index was determined for each site by dividing the mean value of max A for that site by the mean for the proximal common carotid artery.

(iii) Differences between the mean values of max A in the proximal common carotid artery in different Groups were tested using Student's t test on unpaired values.

EXPERIMENT 4.3 The Accuracy of a Ratio of 2 Measurements of Max A Compared with a Single Measurement of Max A in the Detection of Carotid Artery Disease

Methods

FI (the ratio of the highest value for max A in the common carotid artery or internal carotid artery to that in the proximal common carotid artery was determined in each of the 57 patients examined using ultrasound in Experiment 1.2.

In this Experiment the patients were divided into another 2 Groups:-

Group one was comprised of all 57 patients (n = 100 carotid arteries, those with occlusions were excluded), and Group 2 was comprised of those carotid arteries which had values of max A less than 3.5 KHz (n = 69) ie those arteries not already diagnosed as having disease on a single measurement of max A.

Analysis of Results

The accuracy of FI in the detection of carotid artery disease was tested using decision matrices (see Appendix 2). Threshold values of FI of 1.6, 2.0 and 2.3 in Group one and 1.3, 1.6, 2.0 and 2.3 in Group 2 were compared with the grading of disease as shown on arteriograms. Finally a combination of both max A and FI at 2 different threshold values of each was tested.

RESULTS

EXPERIMENT 4.1 Measurements of Maximum Frequency when both the Point of Insonation Relative to a Stenosis and the Size of the Stenosis are Varied in a Model

Table 47 gives the ΔF max measurements at each site for each stenosis and Table 48/Figure 41 and Table 49/Figure 42 give the results of analysis (i) and (ii) respectively. Figures 43 and 44 give examples of ultrasound spectra at the 2 mm stenosis.

Proximal to a stenosis of any degree ΔF max fell and distal to a stenosis ΔF max rose, the rise in ΔF max was directly proportional to the severity of the stenosis.

Analysis (i), (see Figure 41) confirmed that there was a linear relationship between both $(\Delta F\ max_I/\Delta F\ max_S)^{\frac{1}{2}}$ and $(\Delta F\ max_{PRE}/\Delta F\ max_S)^{\frac{1}{2}}$ and the degree of stenosis therefore the maximum velocity as measured by ultrasound was behaving in the same way as the mean velocity described by Berguer and Hwang.[114] The correlation coefficient of a straight line of gradient 0.90 joining values of $(\Delta F\ max_I/\Delta F\ max_S)^{\frac{1}{2}}$ and r_S/r_I was 0.995. The correlation co-efficient of a straight line of gradient 0.75 joining values of $(\Delta F\ max_{PRE}/\Delta F\ max_S)^{\frac{1}{2}}$ and r_S/r_I was 0.99. Thus the percentage reduction in diameter at a stenosis was inversely related to the square root of $\Delta F\ max_S/\Delta F\ max_I$ or $\Delta F\ max_S/\Delta F\ max_{PRE}$.

TABLE 47 The Variation of Maximum Frequency with the Degree of Stenosis and the Point of Insonation Relative to the Stenosis

Point of Insonation (cm)	Size of Stenosis (mm)				
	2	3	4	5	6
Proximal to Stenosis					
10	1.5	1.7	1.7	1.8	1.7
5	1.7	2.0	-	2.1	1.8
$<$ 1	1.3	1.4	1.3	1.4	1.3
Distal to Stenosis					
$<$ 1	7.2	5.0	3.6	2.4	1.7
5	4.8	-	-	1.9	-
12	1.7	2.0	2.3	-	-

ΔF max measurements at each stenosis in KHz

TABLE 48 The Relationship Between the Degree of Stenosis and the Frequency Ratios in Experiment 4.1, Analysis (i)

Size of Stenosis (mm)	r_s/r_I	$(\Delta F\ max_I/\Delta F\ max_s)^{\frac{1}{2}}$	$(\Delta F\ max_{PRE}/\Delta F\ max_s)^{\frac{1}{2}}$	$(\bar{V}_I/\bar{V}_s)^{\frac{1}{2}}$
2	.31	.46	.42	.31
3	.46	.58	.53	.46
4	.62	.69	.60	.61
5	.77	.88	.78	.77
6	.92	1.0	.87	.92

<u>TABLE 49</u> The Relationship Between the Degree of Stenosis and the Frequency Ratios in Experiment 4.1, Analysis (ii)

Size of Stenosis (mm)	$(ID_I - ID_S/ID_I) \times 100\%$	$\Delta F\ max_S/\Delta F\ max_I$	$\Delta F\ max_S/\Delta F\ max_{PRE}$	$\bar{V}_S/\bar{V}_I$
2	69	4.8	5.5	10.7
3	54	2.9	3.6	4.7
4	38	2.1	2.8	2.6
5	23	1.3	1.6	1.7
6	8	1	1.3	1.2

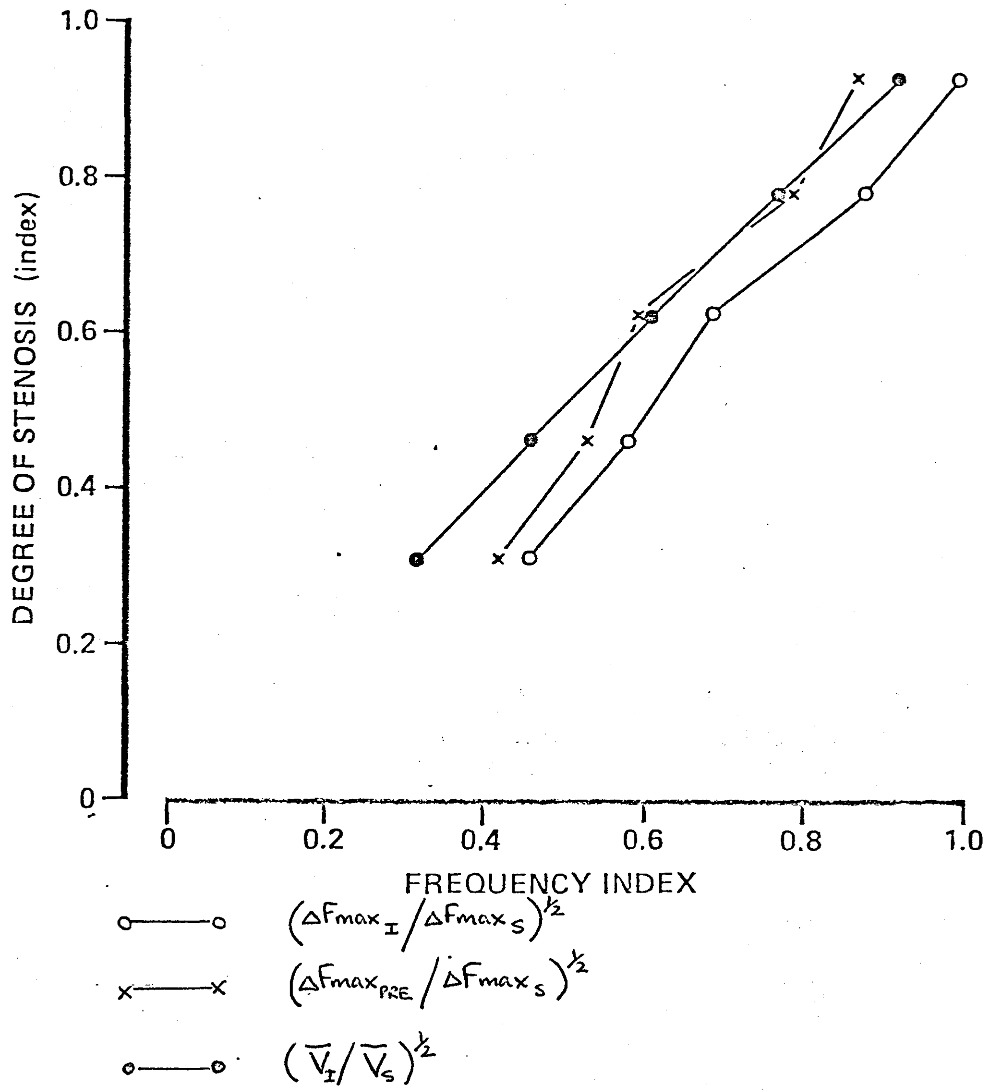

FIGURE 41

Experiment 4.1 The relationship between the degree of stenosis and the frequency ratios, analysis (i).

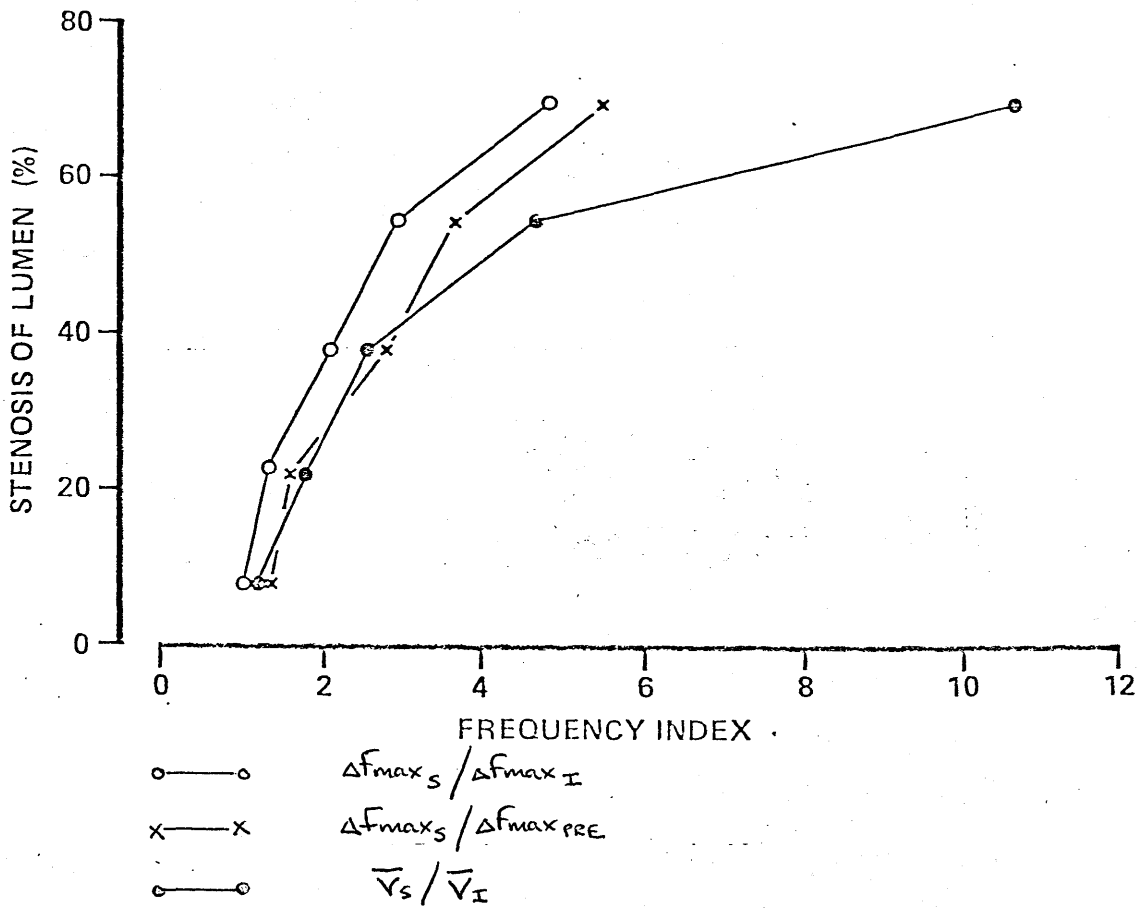

FIGURE 42

Experiment 4.1 The relationship between the degree of stenosis and the frequency ratios, analysis (ii).

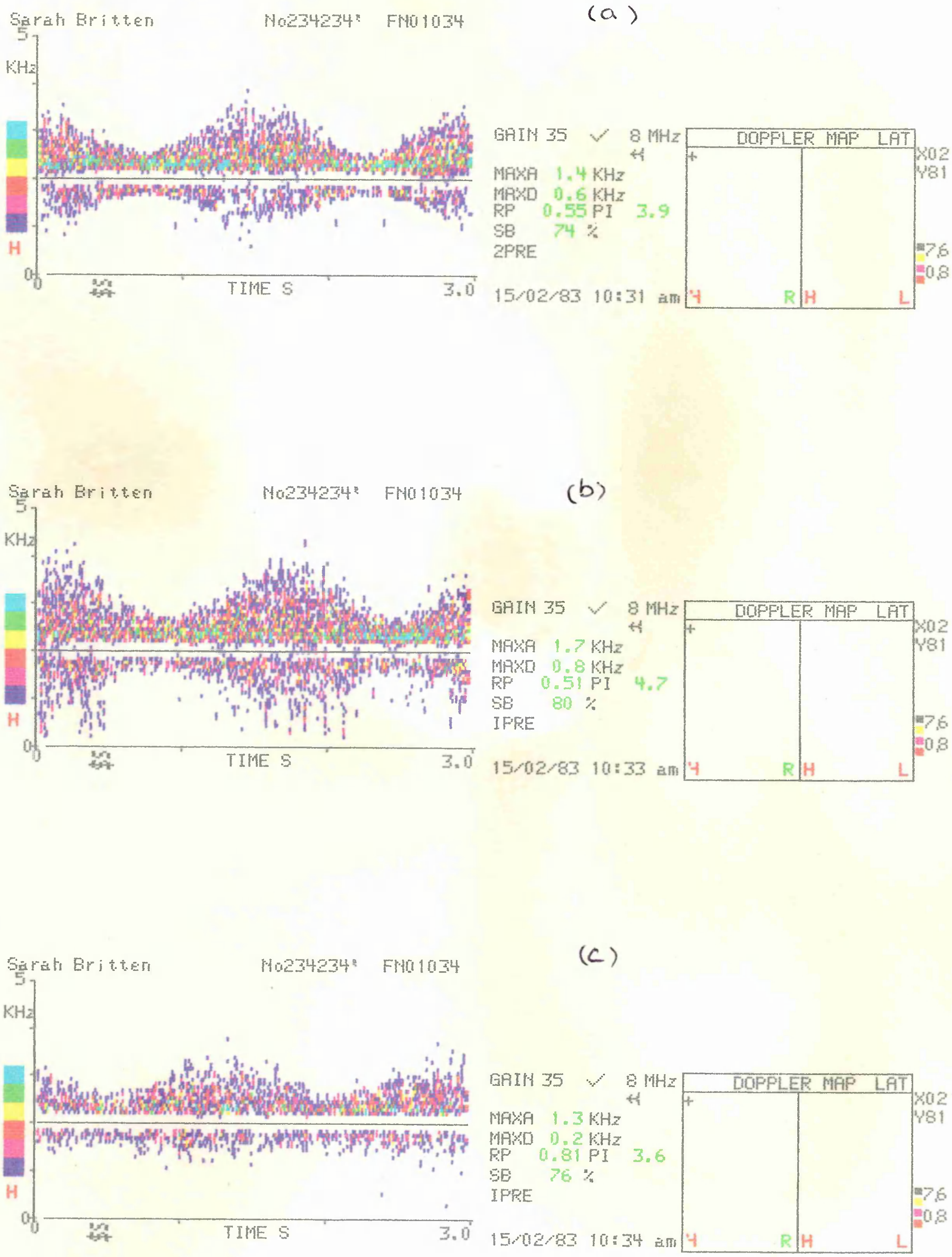

FIGURE 43

Ultrasound spectra proximal to the 2 mm stenosis.
(a) 10 cm (b) 5 cm (c) within one cm

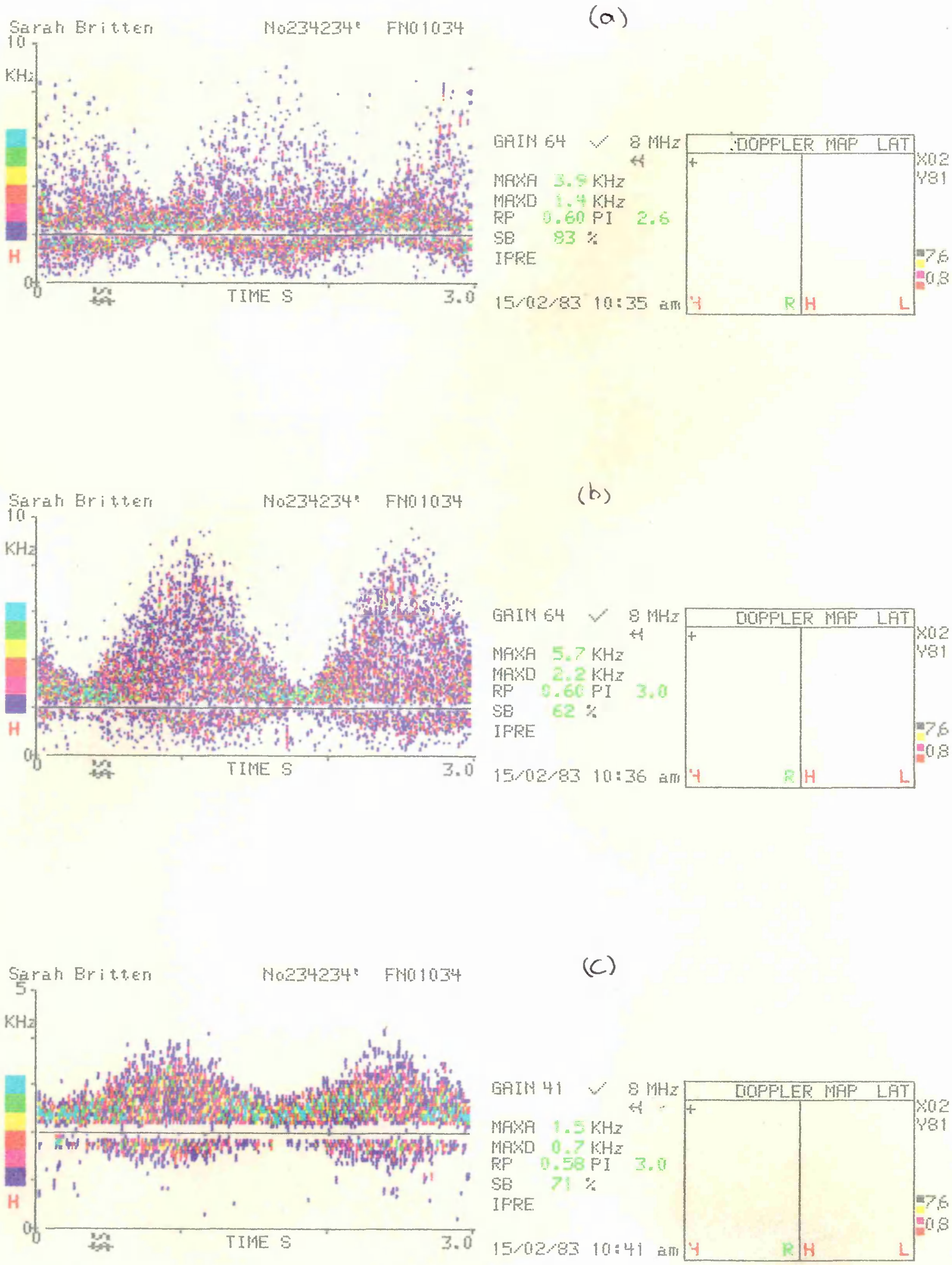

FIGURE 44

Ultrasound spectra distal to the 2 mm stenosis.
(a) within one cm (b) 5 cm (c) 12 cm

EXPERIMENT 4.2 The Variation of Max A at Different Sites in the Carotid Arteries of Asymptomatic Volunteers and Patients

The results of analysis (i) are summarised in Table 50 and of analysis (ii) in Table 51.

Mean Value of Max A:- there was a statistically significant drop in the mean value of max A in the proximal common carotid artery in Group 2 compared with Group one (p = 0.0003) ie older compared with younger normals. There was no difference however in values at this site between patients with stenoses and older normals.

Average Index:- the average index in the internal carotid artery in Group one was only 0.8 however in Group 2 (older normals) it rose to $\leqslant$ 1.3. In the other Groups with stenoses it was always $\geqslant$ 1.3 but except in the case of severe stenosis (Group 4) there was no statistical difference between older normals and the Groups with stenoses.

EXPERIMENT 4.3 The Accuracy of a Ratio of 2 Measurements of Max A Compared with a Single Measurement of Max A in the Detection of Carotid Artery Disease

Tables 52 and 53 give the accuracy of the FI compared with arteriograms for Groups one and 2 and Table 54 the accuracy of the combination.

TABLE 50 The Variation of Max A at Different Sites in the Carotid Arteries

(Figures are Mean Values in KHz)

	Group					
Site	1	2	3	4	5	6
prox CCA	2.5	1.7	1.8	1.3	1.6	1.5
dist CCA	2.5	1.7	2.0	1.4	1.7	1.5
BIF	2.3	1.6	2.7	3.2	2.9	2.4
prox ICA	1.9	1.8	2.3	2.4	2.3	2.0
dist ICA	2.0	1.9	2.3	2.2	2.3	2.2
prox ECA	2.5	2.2	2.5	2.8	2.6	2.4
dist ECA	2.4	2.0	2.5	2.4	2.5	2.4

TABLE 51 The Variation of the Average Index at Different Sites in the Carotid Arteries

(Average Index = Mean Max A at each Site ÷ Mean Max A at Prox CCA)

	Group					
Site	1	2	3	4	5	6
prox CCA	1	1	1	1	1	1
dist CCA	1	1	1.11	1.07	1.06	1
BIF	0.92	0.94	1.5	2.5	1.8	1.6
prox ICA	0.76	1.06	1.3	1.8	1.4	1.3
dist ICA	0.8	1.12	1.3	1.7	1.4	1.5
prox ECA	1	1.29	1.4	2.2	1.6	1.6
dist ECA	0.96	1.18	1.4	1.8	1.6	1.6

TABLE 52 A Comparison of the Index FI with Arteriograms in Group one, Experiment 4.3

	FI					
Threshold	1.6		2.0		2.3	
	+	-	+	-	+	-
Grading on Arteriograms						
Normal 48	20	28	8	40	3	45
Minimal Disease 15	4	11	1	14	1	14
Mild Stenosis 19	7 (37%)	12	5 (26%)	14	4 (21%)	15
Severe Stenosis 18	12 (67%)	6	10 (56%)	8	8 (44%)	10
Specificity	28/48 (58%)		40/48 (83%)		45/48 (94%)	
Overall Sensitivity	23/52 (44%)		16/52 (31%)		13/52 (25%)	

TABLE 53 A Comparison of the Index FI with Arteriograms in Group 2, Experiment 4.3

	Threshold Value of FI 1.3		1.6	
	+	−	+	−
Grading on Arteriograms				
Normal 39	19	20	15	24
Minimal Disease 11	7	4	3	8
Mild Stenosis 12	9	3	4 (33%)	8
Severe Stenosis 7	5	2	5 (71%)	2
Specificity	20/39 (51%)		24/39 (62%)	
Overall Sensitivity	21/30 (70%)		12/30 (40%)	

	Threshold Value of FI 2.0		2.3	
	+	−	+	−
Grading on Arteriograms				
Normal 39	5	34	1	38
Minimal Disease 11	0	11	0	11
Mild Stenosis 12	2 (17%)	10	1 (8%)	11
Severe Stenosis 7	4 (57%)	3	4 (57%)	3
Specificity	34/39 (87%)		38/39 (97%)	
Overall Sensitivity	6/30 (20%)		5/30 (17%)	

<u>TABLE 54</u> A Comparison of a Combination of Max A and FI with Arteriograms

(Threshold Values of Variables in brackets)

	Max A (3.5) FI (2.0)		Max A (3.5) FI (2.3)	
	+	–	+	–
Grading on Arteriograms				
Normal 48	14	34	10	38
Minimal Disease 15	4	11	4	11
Mild Stenosis 19	9 (47%)	10	8 (42%)	11
Severe Stenosis 18	15 (83%)	3	15 (83%)	3
Specificity	34/38 (71%)		38/48 (79%)	
Overall Sensitivity	28/52 (54%)		27/52 (52%)	

In Group one the overall sensitivity (ie the incidence of true positive results for all grades of disease) of FI was low and when its specificity was high eg 94% the sensitivity for severe stenoses was only 44%. The sensitivity of FI increased with increasing severity of disease.

In Group 2 ie those patients in whom a stenosis was not detected using max A the use of FI increased the diagnostic yield but only for those patients with severe stenoses. It was not helpful in detecting patients with less severe grades of disease. Using a combination of max A at a threshold of 3.5 KHz and FI at a threshold of 2.3 gave a specificity of 79% and a sensitivity for severe stenoses of 83% (see Table 54).

DISCUSSION

It is known that max A increases with increasing degree of stenosis in the carotid arteries and that the peak systolic velocity in the common carotid artery is lower in diseased arteries than in the arteries of individuals below the age of 35 years.[76,115] It seemed likely that a ratio of 2 measurements of max A would be more effective in the detection of carotid stenoses than a single measurement alone.

The results of Experiment 4.1 were important in demonstrating that ΔF max fell immediately proximal to a stenosis (possibly due to reflection of flow waves from the face of the stenosis). However the decrease in ΔF max was not related to the severity of the stenosis although only one mean velocity of flow was tested. The behaviour of the maximum velocity at each of the stenoses was also found to follow closely that of the mean velocity (at least until the diameter of the lumen was reduced by 50%) such that the relationship derived from Berguer and Hwang's formula (Equation 4.2) was correct ie the degree of stenosis was related to a ratio of 2 measurements of maximum frequency.

In the carotid arteries it has been shown that once a stenosis becomes critical ie with a reduction in diameter of the vessel of approximately 50% (equivalent to a reduction in the cross sectional area of the lumen of 75%) the volume flow is reduced hence although the mean velocity of flow increases it does not do so to the extent required in Equation 4.1.[24,25] In Experiment 4.1 it was found that this affected the maximum velocity of flow (see Figure 42). The ratios $\Delta F\ max_S/\Delta F\ max_I$ and $\Delta F\ max_S/\Delta F\ max_{PRE}$ failed to keep their relationship with the theoretical ratio $\bar{V}_S/\bar{V}_I$ once the percentage stenosis (diameter) had exceeded approximately 50%. However for stenoses greater than 50% the first 2 ratios tended to follow the last ratio in such a way that there was justification in believing that the index might be successful in the indentification of disease. The reason for calculating both $\Delta F\ max_S/\Delta F\ max_I$ and $\Delta F\ max_S/\Delta F\ max_{PRE}$ was that using CW systems the operator is uncertain as to the precise point of insonation in relation to the stenosis. As can be seen from Figures 41 and 42 it did not make much difference.

Before proceeding to the identification of atherosclerotic stenosis in patients using FI it was necessary to determine the behaviour of the index in groups of patients in whom the severity of disease was known. Experiment 4.2 confirmed that max A does fall in the common carotid artery proximal to a severe stenosis but it also fell in the group of older patients with no evidence of carotid disease. In Experiment 4.2 while it was found that the average index in the internal carotid artery was always less than or equal to 0.8 in young normals, (which was the identical threshold value reported by Blackshear et al) it was much higher in older normals such that there was little difference between this latter group and those with stenoses other than severe.[115]

From the results of Experiment 4.2 it could have been predicted that FI would only be successful in accurately identifying patients with severe stenosis and this was found to be the case in Experiment 4.3. FI at a threshold of 2.0 was of similar accuracy as max A at a threshold of 3.5 KHz (results of Experiment 1.2) and whilst some patients were identified using FI that were not detected using max A alone, the combination of using FI and max A was not quite as accurate as the combination of max A, SB and the flow map used in Experiment 1.2.

The reasons for this failure were two fold. Firstly there was the unexpected finding that values of max A tended to fall in the common carotid artery with increasing age irrespective of the presence of arteriosclerosis obvious on arteriograms. And secondly there were variations in the angle of insonation which resulted in a greater variability of max A making reliable comparisons difficult.

The reason why FI was successful in the indentification of severe stenoses can be seen from Figure 42 : for stenoses greater than 50% a small increase in stenosis caused a large increase in FI but for stenoses less than 50% a similar change in stenosis caused a much smaller change in the index.

C H A P T E R 5

THE DETECTION OF DISTURBANCES OF FLOW USING CW ULTRASOUND

INTRODUCTION

In this Chapter experiments investigating the use of CW ultrasound to detect disturbances of flow both in a laboratory model and in arteries are described. A model was used because the model could be insonated at a particular site under known conditions of flow and furthermore these conditions could be made similar (although not identical) to those in the carotid arteries. In the model disturbances were created by destabilizing flow in the section from which ultrasound signals were recorded.

Spectral analysis of ultrasound signals (eg Figure 6) shows the intensity of each frequency as a coloured dot. In Figure 6 frequency is proportional to velocity and the intensity of each frequency is proportional to the amount of red cells travelling at that velocity. In disturbances of flow the intensity/frequency pattern may be disorganised and experiments were designed to see whether variations in the intensity/frequency pattern could be correlated with known disturbances of flow.

Whilst it was relatively straight forward to create and demonstrate (by an independent method) disturbances of steady flow in Experiment 5.1, it was more difficult to do so for oscillatory flow. Hence in Experiments 5.2.1 to 5.2.4 the effects on the maximum velocity of flow and ultrasound spectra due to altering the stability of oscillatory flow were investigated. Disturbances of oscillatory flow were created by:-

(i) Increasing the frequency of oscillation (f), Experiment 5.2.1

(ii) Increasing the mean velocity of flow ($\bar{V}$), Experiment 5.2.2

(iii) Increasing the internal diameter of the vessel (ID), Experiment 5.2.3

and by

(iv) Inserting stenoses of different degrees in the test section, Experiment 5.2.4

Finally in Experiment 5.3 ultrasound signals from both normal and diseased arteries were examined for disturbances of flow.

DEFINITIONS OF FLOWS AND STABILITY

Laminar Flow

Laminar flow is where flow at one point correlates with that at every other point and sliding of fluid layers over one another occurs with no mixing other than molecular ie it is streamline.[117,118]

Turbulent Flow

Turbulence is when completely random motion of the individual fluid elements occurs.[117] It should be self-preserving and propagated distally ie not diminish with time.

A Vortex

A vortex (symonymous with 'eddy') is a fluid structure that possesses circular or swirling motion and is commonly seen distal to an obstruction.[119] Attinger et al consider that vortices that are shed regularly and predictably eg from stenoses, are a variety of laminar flow.[117] Their presence in the following experiments is considered to be an indication of a flow disturbance.

Stability of Flow and Disturbances

A stable flow is one which when disturbed will not undergo transition to a turbulent flow. Transition is the process a laminar flow undergoes to become turbulent thus transition is an entity and not a descriptive term in this context.[118,120] A disturbed flow is the transient response of a laminar flow to a source of instability which causes the flow to deviate from its streamline motion. It is not turbulent unless the disturbances are self perpetuating.[118] Instability of a flow refers to the initiation of the growth of disturbances which result when a destabilizing force overbalances a stabilizing one.[120] In oscillatory flow, flow is unstable if the disturbance undergoes a net growth in each period, stable if it decays continuously, and transiently stable if it grows for part of the cycle before decay.[120]

THE RELATIONSHIP BETWEEN THE VELOCITY PROFILE AND THE CHARACTER OF A FLOW

In steady laminar flow the velocity profile across the lumen of a vessel should be a parabola (see Figure 67) and in turbulent steady flow the front of the profile becomes flatter as in Figure 68. The shape of the velocity profile is affected by the formation of a boundary layer at the vessel wall, the entrance length (see Page 223), and the geometry of the vessel.[121] With a fully developed parabolic flow profile the ratio of the maximum to the mean velocity is 2 and with the flat profile seen in turbulent flow it decreases to almost one.[122]

A technique which demonstrated the velocity profile might enable the identification of flow disturbances. It was considered that CW ultrasound with its ability to demonstrate all the intraluminal velocities (because of its beamwidth) might achieve this.

METHODS

THE MODEL

The model (see Figures 45 and 46) consisted of a constant head tank, reservoir, Scotch Yoke assembly, roller pump and water tank described in Chapter 3 and graded stenoses were introduced in the manner described in Chapter 4. There were some additional features:-

The Medium and the Ultrasonic Scatterer

The medium used was water and the ultrasonic scatterer was one of the following:-

(i) Fixed red cells prepared by the method described in Appendix 3 and injected proximal to the test section by a constant infusion pump.

(ii) An emulsion of milk in water (40%).

(iii) An emulsion of silicone liquid in water (0.5% silicone fluid MS200/3 cs).

The viscosities of the different emulsions used in this thesis were determined using the method of Humphreys and are shown in Table 55.[116] Problems encountered with their use are described in Appendix 3.

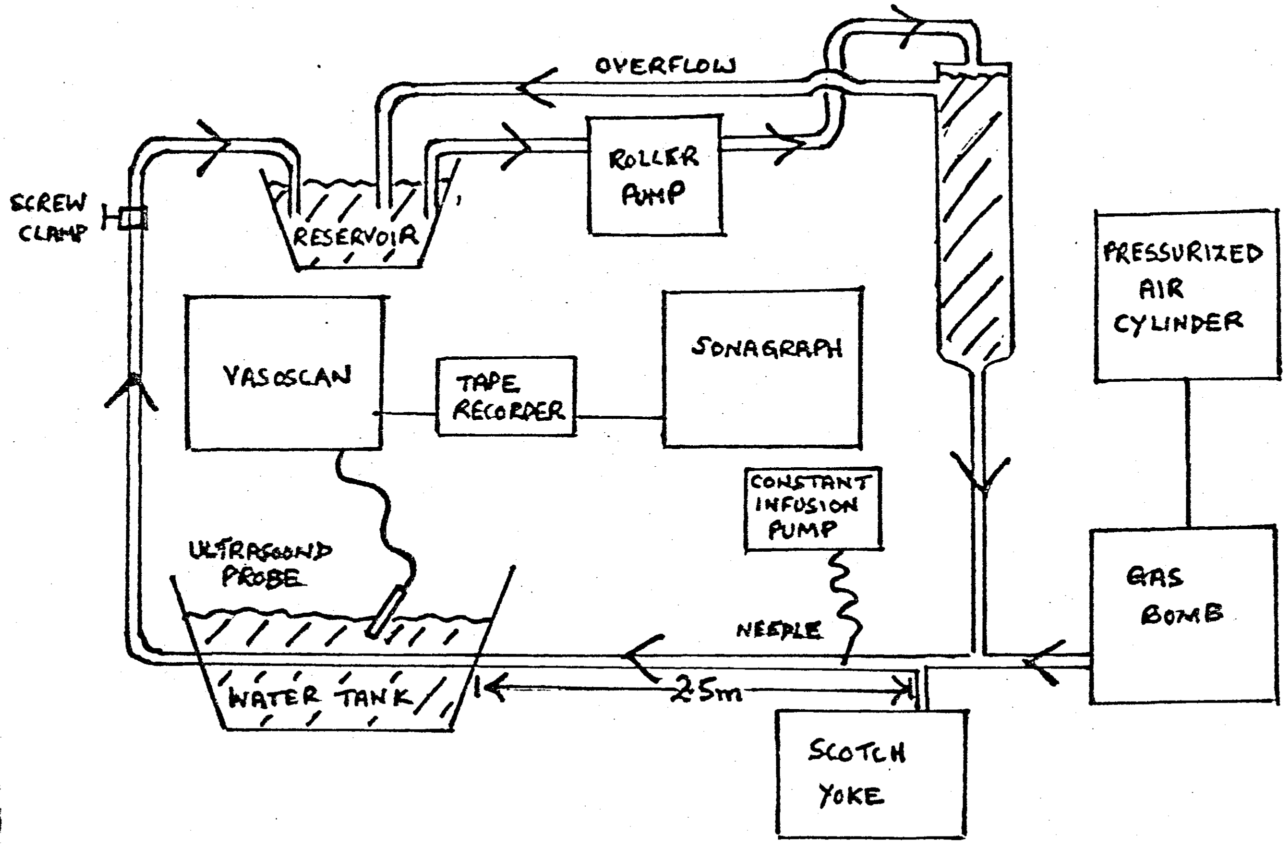

FIGURE 45

A diagram of the model used in Chapter 5

FIGURE 46

The apparatus used in the model

TABLE 55 Some Physical Properties of the Different Media Used in the Model

Mediums	Density (g/ml at 23^{o} C)	Viscosity (cp at 23^{o} C and D = 128/sec)	Kinematic Viscosity (stokes x 10^{-2})
Water	1.0	1.0	1.009
Emulsion of Milk in Water	1.00655	1.09	1.1
Emulsion of Silicone in Water	0.997115	1.0	1.0029
Emulsion of Silicone in Dextran 40	1.044629	4.8	4.5949

The Dye

A concentration of Biebrich scarlet of 10 g/l in water (injected proximal to the test section through a 25 gauge needle using the constant infusion pump) was used to demonstrate the character of the flow in the test section. Problems encountered in its usage are discussed in Appendix 4.

The Gas Bomb (see Figure 47)

To obtain velocities of flow higher than those obtainable using the roller pump and constant head tank, a gas bomb filled with the medium and connected to a cylinder containing air under pressure was introduced into the circuit. Pressures of between one and 5 atmospheres were used and when the gas bomb was in use the roller pump and constant head tank were excluded from the circuit.

The Tubing

The tubing used in all the experiments in this Chapter save Experiment 5.4 was made of silastic and it had an internal diameter of 0.65 cm. In Experiment 5.4 polyethylene tubing of internal diameter 1.5 cm was used in order to obtain values of α greater than 10. Using a medium of silicone in water in the silastic tubing to obtain a value of α greater than 10 would have required a frequency of oscillation greater than 568 cycles/min which was beyond the capability of the Scotch Yoke. (The use of Dextran 40 would have aggravated the problem ie f = 2611 cycles/min for α = 10).

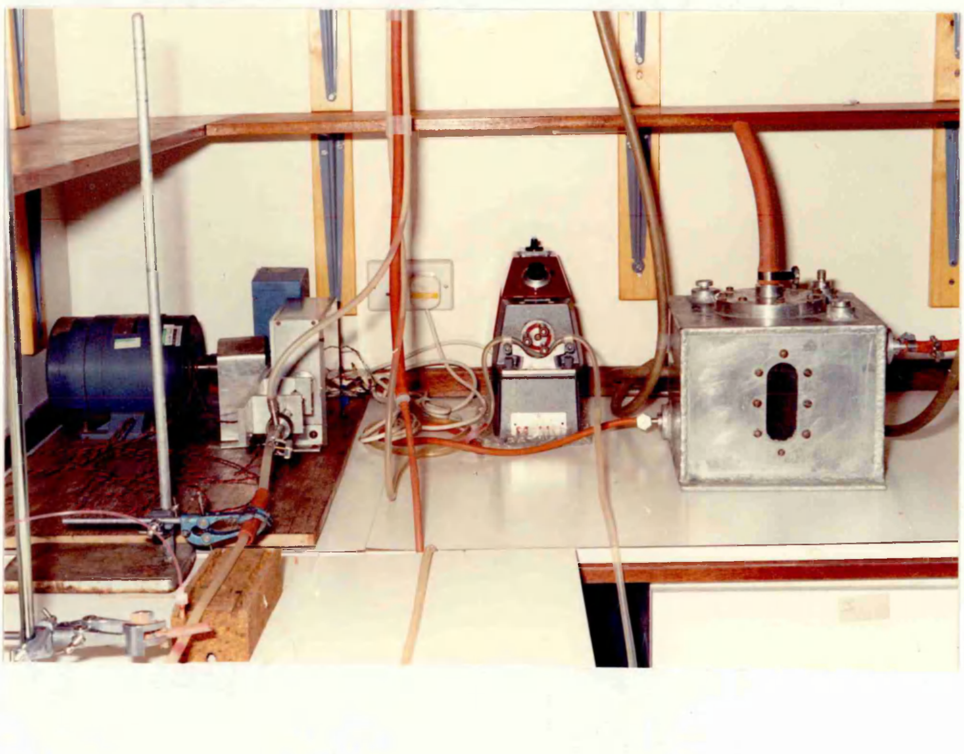

FIGURE 47

The gas bomb, constant head tank, roller pump and Scotch Yoke assembly.

Silastic tubing is elastic and the Young's modulus of the tubing used in this experiment was 20.94×10^5 Nm^{-2} which is of the same order as the value for the carotid artery (7.5×10^5 Nm^{-2}).[123] The tubing was divided into an entrance length, a test section and an exit length. The entrance length is the distance required for a fully developed parabolic flow profile to become established and is given by:-

$$(0.2 \times ID^2 \times V\ max)/(4 \times \nu)$$

where ν is the kinematic viscosity of the medium and ID is the internal diameter of the vessel.[124] It was calculated that an entrance length of 2.5 m was necessary.

The test section ran through the water tank and the tubing was either continuous or divided in the test section to include a stenosis. A total length of 6 m of tubing was used with an exit length of 3.5 m.

The Ultrasound Instruments

The ultrasound was emitted from either the 4 or 8 MHz probe of Vasoscan held in a clamp at an angle of 45° to the test section of tubing. The use of the 8 MHz probe allowed double the amplitude of display compared with the 4 MHz probe. The intensities of the emitted ultrasound beam at different distances from both the 4 MHz and 8 MHz transducers were determined and it was found that the beam was able to sample the whole lumen of the tubing of internal diameter 0.65 cm . The received signals were analysed both by Vasoscan and a sonagraph (Sona-graph, Kay Instrument, USA). The sonagraph (see Figure 48) is a spectrum analyser with the facility of 2 varieties of display.

(i) A #1 display is a 3 dimensional overall picture of the signal with frequency, intensity and time all displayed simultaneously as with a Vasoscan display (see Figure 65)

(ii) A #2 display permits the individual intensity of each frequency component to be displayed at any preselected point in time on a #1 display (see Figure 66).

<u>A Tape Recorder</u>

Doppler shifted ultrasound signals were recorded by means of a cable connecting an output terminal on the rear of the Vasoscan with the input terminal of a stereo cassette recorder (Sony). The connection permitted the recording of velocities moving away from the ultrasound probe only and those signals were subsequently re recorded from the tape recorder onto the Sonagraph.

MATCHING THE MODEL WITH THE CAROTID ARTERIES

To obtain a haemodynamic similarity values for the Reynolds and Strouhal numbers and α in the model were matched with those calculated for the carotid arteries.

FIGURE 48

The Sonagraph

Reynolds number (Re) is a dimensionless quantity calculated from Equation 5.1 and the critical Reynolds number (Re crit) specifies the conditions under which it is impossible to introduce turbulence in a flow channel. It is calculated from the following equation:-

$$Re = (\bar{V}.ID)/\nu \qquad \text{Equation 5.1}$$

where ν is the kinematic viscosity.

The Strouhal number (Str), another dimensionless number, takes into account the period of oscillatory flow and it determines the time available for vortex formation to occur. It is calculated from the following equation:-

$$Str = (f \cdot R)/\bar{V} \qquad \text{Equation 5.2}$$

where R is the internal radius of the vessel and f is the frequency of oscillation.

α, a third dimensionless number derived by Womersley characterizes kinematic similarities of oscillatory flows and takes into account both of the previous 2 numbers.[125] It is calculated from Equation 5.3:-

$$\alpha = R(f/\nu)^{\frac{1}{2}} \qquad \text{Equation 5.3}$$

Another variable of interest is λ which represents the ratio of the unsteady and steady velocity components of flow and is important in the distribution flow into branches.[126,127] Most importantly it takes into account the acceleration and deceleration of the flow when the frequency of oscillation is known. Simply matching values of $\overline{Re}$ and α in the model with those of the carotid arteries does not take into account flow acceleration or deceleration although the use of $\widehat{Re}$ and α will to some extent compensate ($\overline{Re}$ refers to the Reynolds number calculated using $\bar{V}$ and $\widehat{Re}$ that calculated using V max).

Values for Re, Str and α were calculated in the common, internal and external carotid arteries (see Table 56). In the case of Re, values were calculated using both $\bar{V}$ and V max at peak systole. The mean velocity of flow was calculated from:-

$$\bar{V} = Q/A$$

where Q is the volume flow (200 ml/min in the carotid arteries) and A is the area derived from reported values of the internal diameter of each artery (see Table 56).[128,129] Values of V max used to calculate $\widehat{Re}$ were 127 cm/sec in the common carotid artery and 77 cm/sec in the internal carotid artery.[102] The kinematic viscosity (ν) is calculated from:-

$$\nu = \eta/\rho$$

where ρ refers to the density of blood (1.05 - 1.055 g/ml) and η its viscosity.[122] Two values for ν were used because the viscosity of blood varies with the shear rate. Humphreys measured the asymptotic viscosity in our laboratory and found it to be 3.6 cp

TABLE 56 Values for the Reynolds and Strouhal Numbers and α Calculated for the Carotid Arteries

	CCA	ICA	ECA
ID (cm)	0.8	0.57	0.55
Area (cm^2)	0.503	0.255	0.238
$\bar{V}$ (cm/sec)	6.63	13.07	14
$\bar{Re}$ (calculated using $\bar{V}$ and ν = 3.4 cs)	156	219	226
$\bar{Re}$ (calculated using $\bar{V}$ and ν = 11.7 cs)	45	64	66
$\widehat{Re}$ (calculated using V max and ν = 3.4 cs)	2988	1291	-
$\widehat{Re}$ (calculated using V max and ν = 11.7 cs)	150	117	-
Str (calculated using $\bar{V}$ and f = 72 cycles/min)	0.072	0.026	0.024
Str (calculated using $\bar{V}$ and f = 120 cycles/min)	0.121	0.044	0.039
α (calculated using ν = 3.4 cs and f = 72 cycles/min)	2.38	1.69	1.63

cs = stokes x 10^{-2}

for a shear rate greater than 100/sec when blood behaves as a Newtonian fluid.[116] Strandness reported a value of 12.3 cp for a mean shear rate of 5.8/sec.[123] Values for η of 3.6 and 12.3 cp gave values for ν of 3.4×10^{-2} stokes and 11.7×10^{-2} stokes respectively.

Table 57 shows the velocities of different mediums in the test circuit of the silastic tubing necessary to approximate the haemodynamic conditions in the carotid arteries. In the case of V max, the volume flow (Q) is not able to be directly calculated therefore ΔF max is shown with the corresponding value of V max in brackets. With regard to the Strouhal number, values of frequency are shown and using those values of frequency and $\bar{V}$ resulted in a match for α.

METHOD OF EXAMINATION OF PATIENTS

The arteries of patients were examined using the 4 MHz probe of Vasoscan in the case of the carotid, femoral and subclavian arteries and the 8 MHz probe in the case of the radial and tibial arteries. Signals were recorded onto the Sonagraph via the tape recorder in the same manner as the model experiments.

METHODS OF SIGNAL RECORDING AND ANALYSIS

(a) <u>Vasoscan</u>:- This instrument has been described in Chapter 1.

(b) <u>Sonagraph</u>:- A signal was recorded from the stereo cassette

TABLE 57 Matching Values of the Reynolds and Strouhal Numbers and α in the Model with those in the Carotid Arteries

	Media		
	Milk in Water	Silicone in Water	Silicone in Dextran 40
Values in the Carotid Arteries	Figures give $\bar{V}$ in cm/sec with Q (ml/min) in brackets		
$\overline{Re} = 40$	0.67 (13)	0.62 (12)	2.82 (56)
$\overline{Re} = 230$	3.89 (77)	3.54 (71)	16.2 (323)
	Approximate figures for ΔF max are given (KHz) at $\theta = 45^{o}$ with corresponding values of V max (cm/sec) in brackets		
$\widehat{Re} = 1300$	2.0 (22)	1.8 (20)	11.5 (92)
$\widehat{Re} = 3000$	4.6 (51)	4.2 (46)	26.5 (212)
	Figures are for f (cycles/min) for a particular $\bar{V}$ (cm/sec) in brackets		
Str = 0.024	17 (3.89)	16 (3.54)	$\left\{\begin{array}{l}72\ (16.2)\\40\ (9.0)\end{array}\right.$
Str = 0.121	45 (2.0)	45 (2.0)	67 (3.0)
α	Using any of the above pairs will match α		

recorder onto the drum of the sonagraph setting the record level to plus 2 or 3 on the VU meter for signal peaks. A frequency scale marked in intervals of 0.5 KHz was recorded onto the end of the signal. To reproduce a #1 display the reproduce level was set at minus 2 or 3 on the VU meter and 3 seconds of information were recorded by a stylus marking a sheet of paper attached to the drum. To reproduce a #2 display involved the use of micrometer plate on the top of the drum. This was divided into 40 holes each 40 msec apart and each hole had 5 divisions thus sections at 8 msec intervals could be obtained. To obtain a #2 display a special pin was inserted into a hole with the micrometer plate positioned as desired and when the drum rotated a switch was activated causing the stylus to mark the paper.

For each ultrasound spectrum in Experiments 5.1 to 5.3 there were 3 varieties of display:-

(i) A Vasoscan display

(ii) A Sonagraph #1 display

(iii) Sonagraph #2 displays

The overall character of each display was examined eg the presence of a spectral window in oscillatory flow or irregularities of the maximum frequency envelope of the Vasoscan or Sonagraph #1 displays. For steady flow #2 displays were recorded at 8 msec intervals and for oscillatory flow at between 8 and 40 msec intervals through the acceleration, peak and deceleration phases of systole and at 120 msec intervals in diastole (if applicable). In Experiment 5.1 #2 displays were examined using a technique described in that experiment.

EXPERIMENTS

EXPERIMENT 5.1 The Characterization of Disturbances of Steady Flow in a Model Using CW Ultrasound

Methods

Two methods were used to create the necessary instability of flow.

Method I:- The critical Reynolds number was found to be approximately 1700 in the model by steadily increasing the mean velocity in the test section (see Appendix 5). Ultrasound signals were recorded for values of Re up to 215 under conditions of laminar flow, Re between 585 and 845 a period during which disturbances of flow were visualised using dye, and Re between 2210-3575 for conditions of turbulence.

Method II:- 2 mm and 5 mm stenoses were introduced in turn into the test section and ultrasound signals were recorded from sites both proximal and distal to the stenosis. Flow proximal to each stenosis was laminar with Reynolds numbers of 228 and 260 for each stenosis respectively.

Disturbances of flow were demonstrated independently for both methods using dye.

The Analysis of Certain #2 Displays

Certain Sonagraph #2 displays obtained by Method I were photographed and enlarged by a factor of 3. The displays photographed were 6 #2 displays for each of 2 signals taken from laminar flow and 6 #2 displays from a single signal from turbulent flow. The 6 displays were recorded each 8 m sec apart. The photographs were pinned to a board and divided into 0.17 KHz frequency bands. The area of the intensity of each frequency band was measured using a planimeter (Numonics).

(a) For each signal the coefficient of variation (CV) of the area of each frequency band of the 6 #2 displays was calculated from the mean and its standard deviation. This gave the variation of the intensity of each frequency band with time.

(b) For each signal the coefficient of variation of the areas of all the frequency bands for each of the 6 sections was calculated. This gave the variation of the intensities of the frequency bands within a single spectral section.

For analyses (a) and (b) Student's t test was performed on unpaired values of the mean coefficients of variation of both a laminar and a turbulent signal.

<u>EXPERIMENT 5.2</u> The Ability of CW Ultrasound to Detect Changes in the Character of Oscillatory Flow in a Model

<u>EXPERIMENT 5.2.1</u> The Effect of an Increase in the Frequency of Oscillation

Methods

In this experiment the frequency of oscillation was increased from 18 to 160 cycles/min* whilst the mean velocity of flow was kept constant at 6 cm/sec ($\overline{Re}$ was 392). Ultrasound signals were recorded from the test section at each frequency. ΔF max (steady) ie the maximum frequency of the steady component of flow alone, was 1.0 KHs. Values of ΔF max (osc), ie the maximum frequency detected when oscillations were superimposed on the steady flow, for each frequency were measured and values of α, λ and Re were calculated. λ was calculated from Equation 5.4:-

$$\lambda = [\Delta F \text{ max (osc)} / \Delta F \text{ max (steady)}] - 1 \qquad \text{Equation 5.4}$$

Values of frequency were compared with those of ΔF max (osc) and λ, and the ultrasound signals were examined.

EXPERIMENT 5.2.2 The Effect of an Increase in the Mean Velocity of Flow

In this experiment the mean velocity of flow in the test section was increased from 1.4 cm/sec to 72 cm/sec in increments and values of ΔF max were measured from ultrasound signals for each value of $\bar{V}$ under conditions of both steady and oscillatory flow. The experiment was performed at 2 frequencies of oscillation, 67 and 72 cycles/min. Values of α, λ and Re were calculated and $\bar{V}$ was compared with ΔF max (steady) and ΔF max (osc). Finally the

*Values for frequency are given in cycles/min rather than Hz to facilitate a comparison with heart rate.

ultrasound signals were examined.

EXPERIMENT 5.2.3 The Effect of an Increase in the Diameter of the Vessel

Methods

In this experiment the silastic tubing was substituted for polyethylene tubing of 1.5 cm internal diameter in order to obtain values of α greater than 10. Signals were recorded when the ultrasound probe was positioned frist over the centre of the tube and then over the side of the tube as the beam did not include velocity information from the whole lumen. However in each position the signal included information from both walls and the centre of part of the lumen. The mean velocity was 1.22 cm/sec ($\overline{Re}$ = 92) and ultrasound signals were examined for f = 110 cycles/min, α = 10.16; f = 168 cycles/min, α = 12.6; and f = 307 cycles/min, α = 17. For each signal Str was greater than one and λ very much greater than one.

EXPERIMENT 5.2.4. The Effect of Introducing a Stenosis

Methods

In this experiment 2 mm and 5 mm stenoses were introduced in turn into the test section and ultrasound signals were recorded from sites both proximal and distal to the stenosis. The flow conditions proximal to the stenosis approximated those in the carotid arteries : $\bar{V}$ was 2 cm/sec, Str was 0.121 for f = 45 cycles/min, α was 2.8,

$\overline{Re}$ was 118 (proximal to either stenosis) and $\widehat{Re}$ was estimated to be 1105 immediately distal to the 5 mm stenosis and 2730 immediately distal to the 2 mm stenosis.

<u>EXPERIMENT 5.3</u> The Detection of Disturbances of Flow in Arteries Using CW Ultrasound

<u>Methods</u>

Ultrasound signals were recorded from:-

(i) The internal, external and common carotid, subclavian, femoral, radial and tibial arteries of 3 asymptomatic volunteers all aged 20 years

(ii) The internal and common carotid arteries of 2 patients with a stenosis demonstrated on arteriograms at the carotid bifurcation.

RESULTS

EXPERIMENT 5.1 The Characterization of Disturbances of Steady Flow in a Model Using CW Ultrasound

Method I:- The maximum frequency envelope of the Vasoscan and #1 displays were regular for conditions of laminar flow eg Figures 49 and 50. Irregularities appeared when flow was disturbed (demonstrated by dye) and became more distinct once turbulence ensued eg Figures 49 and 51. With regard to the #2 displays the results of analysis (a) are given in Tables 58 to 60. The mean coefficient of variation for turbulent flow was found to be 10.8 compared with 4.4-5.2 for laminar flow ie it was twice as variable. A p value of 0.0275 (significant) was obtained for Student's t test between signal 2 (laminar) and signal 3 (turbulent). The results of analysis (b) are given in Table 61. Again the coefficient of variation for laminar flow was 5.2 whereas for turbulent flow it was 24 ($p < 0.001$). The character of the #2 spectra was quite different depending on the type of flow : it was virtually flat for laminar flow (see Figure 50) whereas turbulent #2 spectra had a 'waisted' appearance (see Figure 52).

Method II:- Irregularities appeared in the maximum frequency envelope immediately proximal and distal to a stenosis. Where vortices were demonstrated by dye eg distal to a stenosis retrograde flow was clearly seen on ultrasound spectra (see Figure 53).

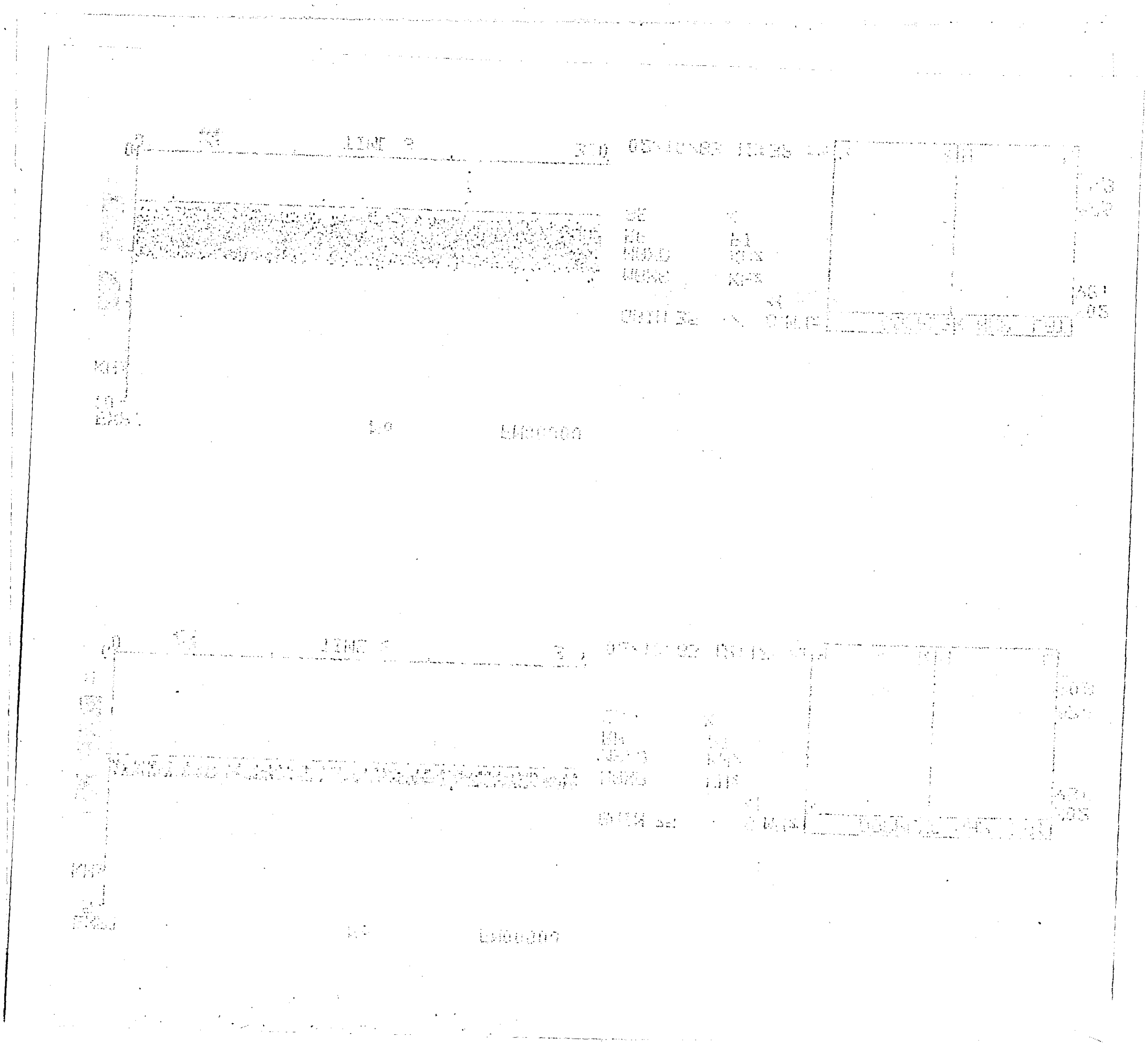

FIGURE 49

Vasoscan displays - Experiment 5.2.1, Method I
(a) laminar flow
(b) disturbed flow
(c) and (d) turbulent flow

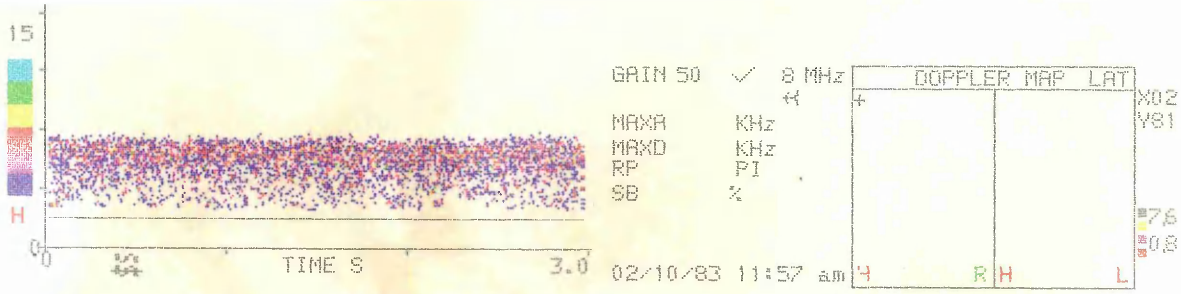

15
H
0
0
TIME S
3.0
GAIN 50
8 MHz
MAXA KHz
MAXD KHz
RP PI
SB %
DOPPLER MAP LAT
X02
Y81
7.6
0.8
02/10/83 11:57 am
H R H L

(d)

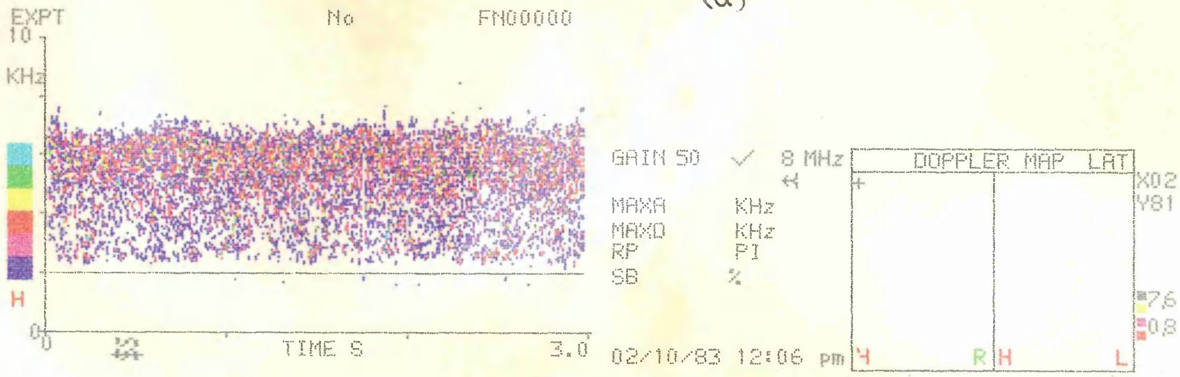

EXPT
No
FN00000
10
KHz
H
0
0
TIME S
3.0
GAIN 50
8 MHz
MAXA KHz
MAXD KHz
RP PI
SB %
DOPPLER MAP LAT
X02
Y81
7.6
0.8
02/10/83 12:06 pm
H R H L

(a)

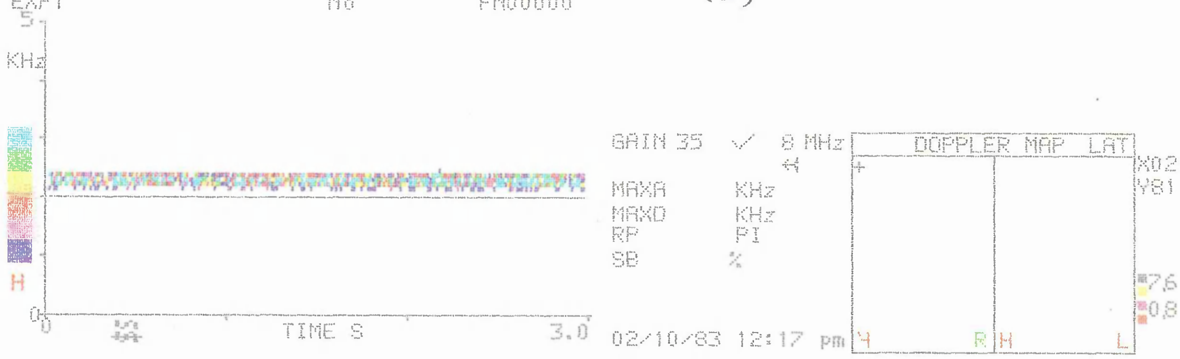

EXPT
No
FN00000
5
KHz
H
0
0
TIME S
3.0
GAIN 35
8 MHz
MAXA KHz
MAXD KHz
RP PI
SB %
DOPPLER MAP LAT
X02
Y81
7.6
0.8
02/10/83 12:17 pm
H R H L

(b)

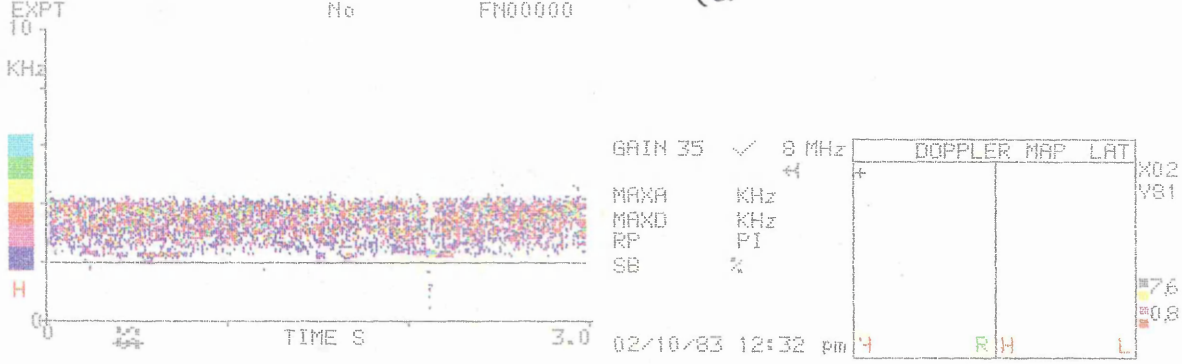

EXPT
No
FN00000
10
KHz
H
0
0
TIME S
3.0
GAIN 35
8 MHz
MAXA KHz
MAXD KHz
RP PI
SB %
DOPPLER MAP LAT
X02
Y81
7.6
0.8
02/10/83 12:32 pm
H R H L

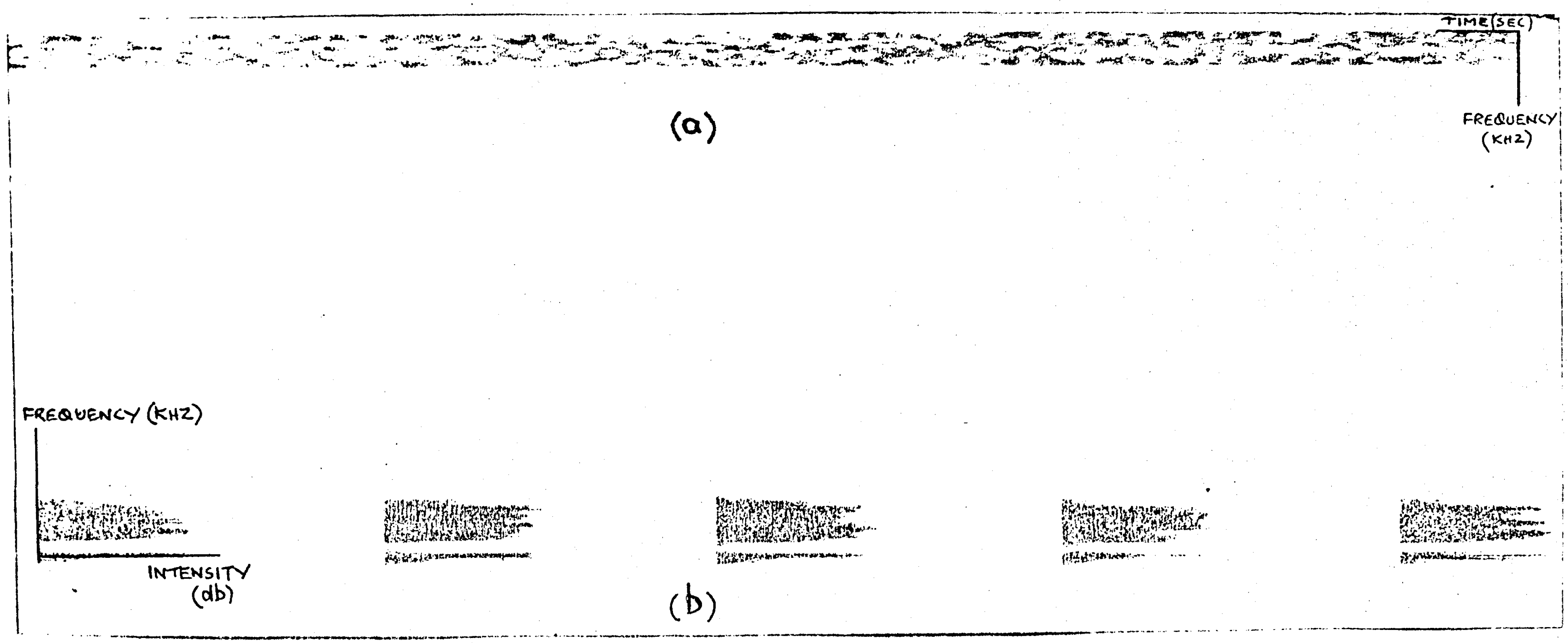

FIGURE 50

Sonagraph displays of steady, laminar flow

(a) #1 display (NB upside down)
(b) #2 displays
Note the relatively flat #2 spectrum

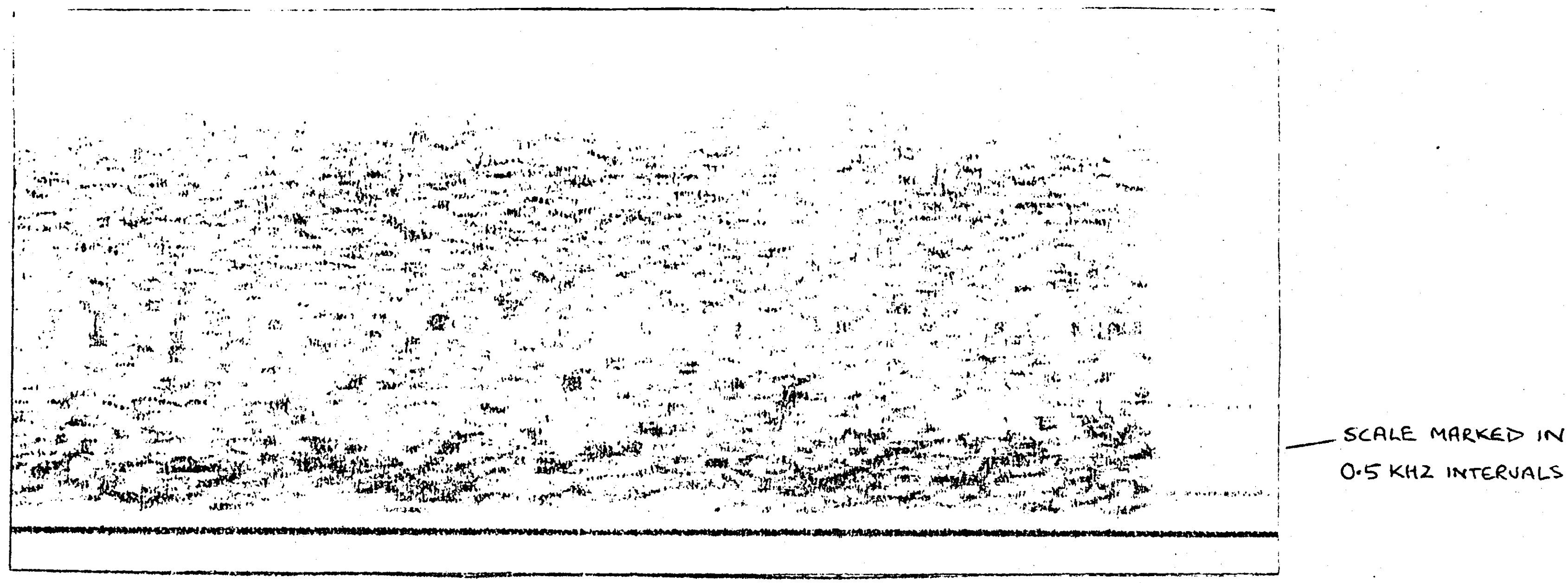

FIGURE 51

Sonagraph #1 display of steady, turbulent flow

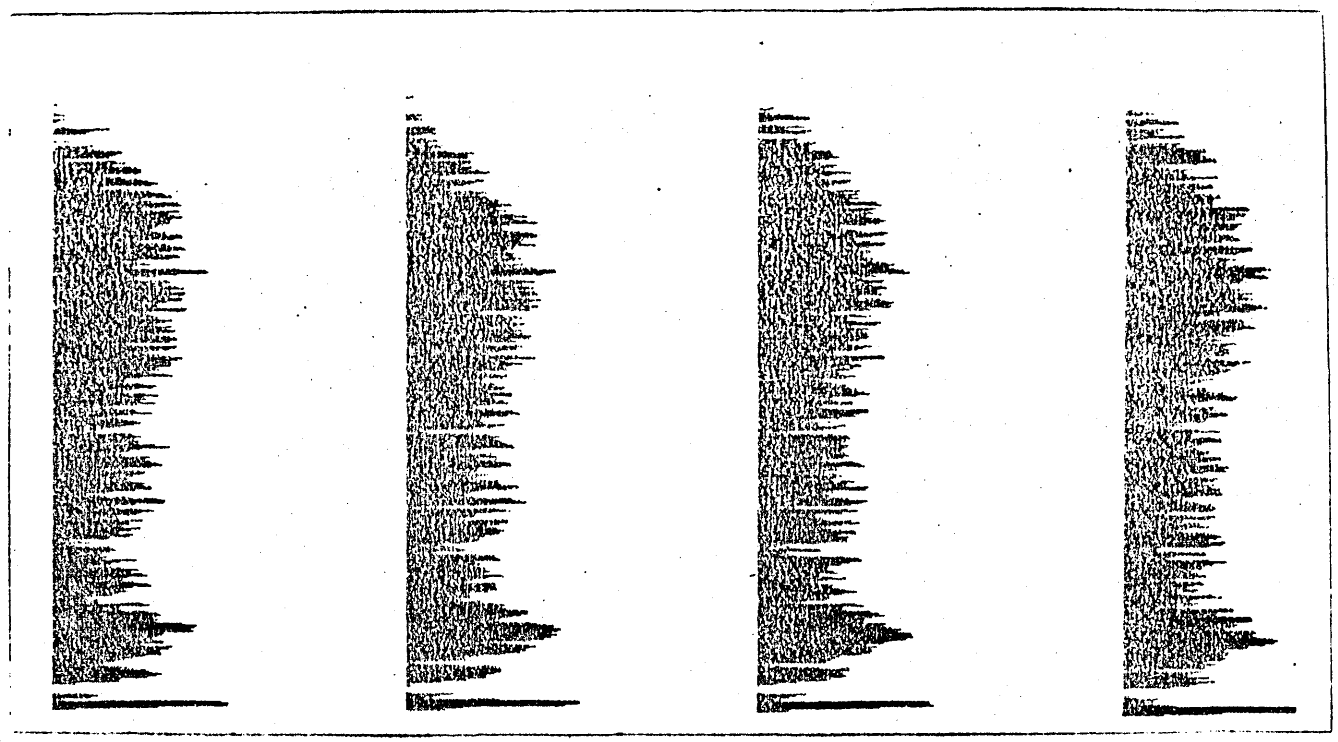

FIGURE 52

Sonagraph #2 displays of steady, turbulent flow. Note the high intensities of the higher and lower frequencies. The high intensities of the lower frequencies was attributed to wall movement. Each section is 8 msec apart.

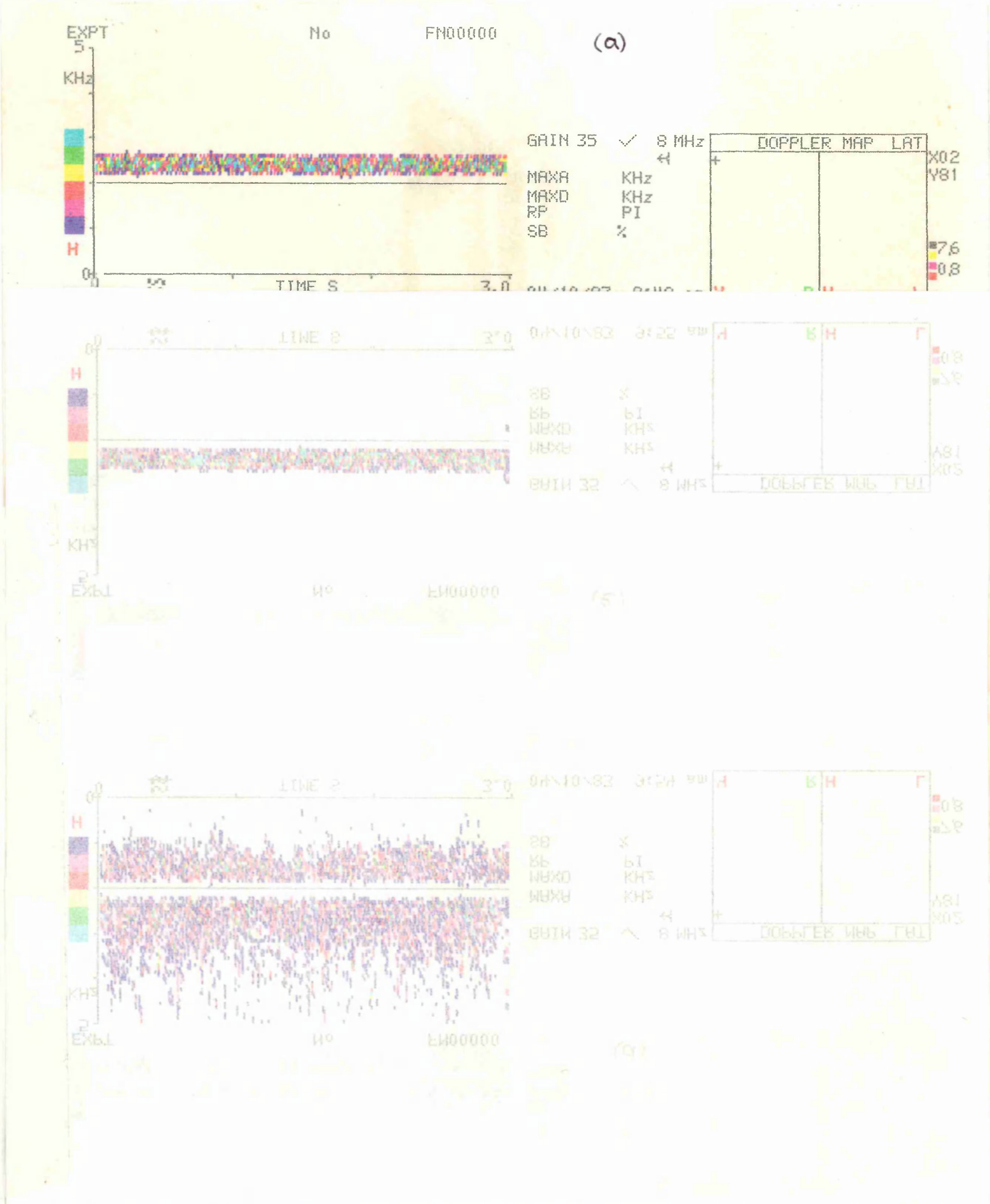

FIGURE 53

Vasoscan displays - Experiment 5.2.1, steady flow through a 2 mm stenosis.

(a) 6 cm proximal to stenosis
(b) < 1 cm proximal to stenosis
(c) < 1 cm distal to stenosis
(d) 2 cm distal to stenosis
(e) 6 cm distal to stenosis

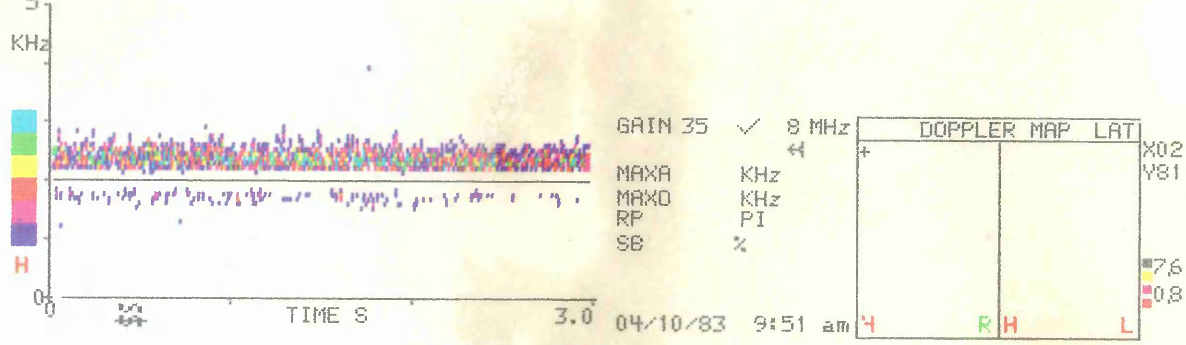
KHz
H
TIME S
3.0
GAIN 35
8 MHz
MAXA KHz
MAXD KHz
RP PI
SB %
DOPPLER MAP LAT
X02
Y81
7.6
0.8
04/10/83 9:51 am
R H L

(c)

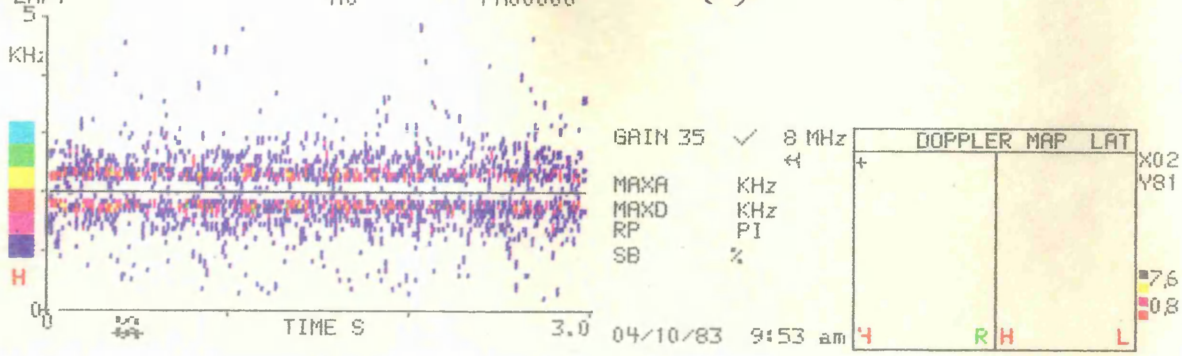
EXPT
No
FN00000
5
KHz
H
TIME S
3.0
GAIN 35
8 MHz
MAXA KHz
MAXD KHz
RP PI
SB %
DOPPLER MAP LAT
X02
Y81
7.6
0.8
04/10/83 9:53 am
R H L

(d)

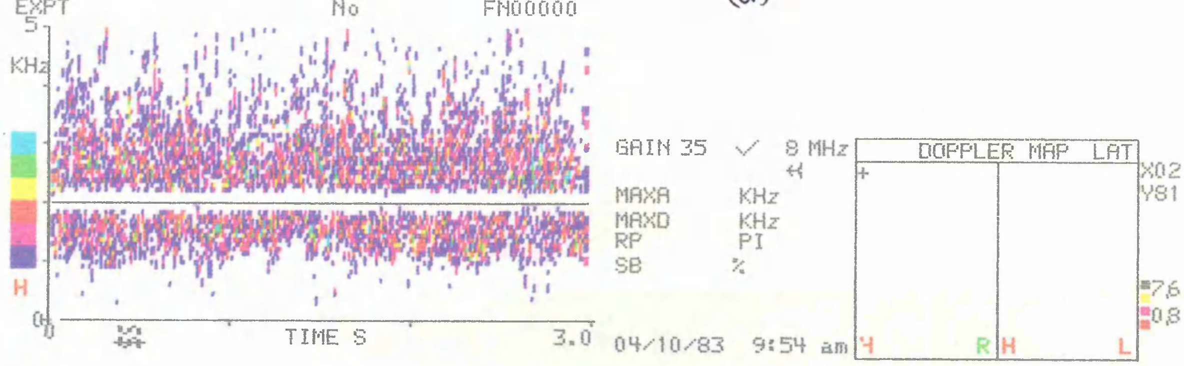
EXPT
No
FN00000
5
KHz
H
TIME S
3.0
GAIN 35
8 MHz
MAXA KHz
MAXD KHz
RP PI
SB %
DOPPLER MAP LAT
X02
Y81
7.6
0.8
04/10/83 9:54 am
R H L

(e)

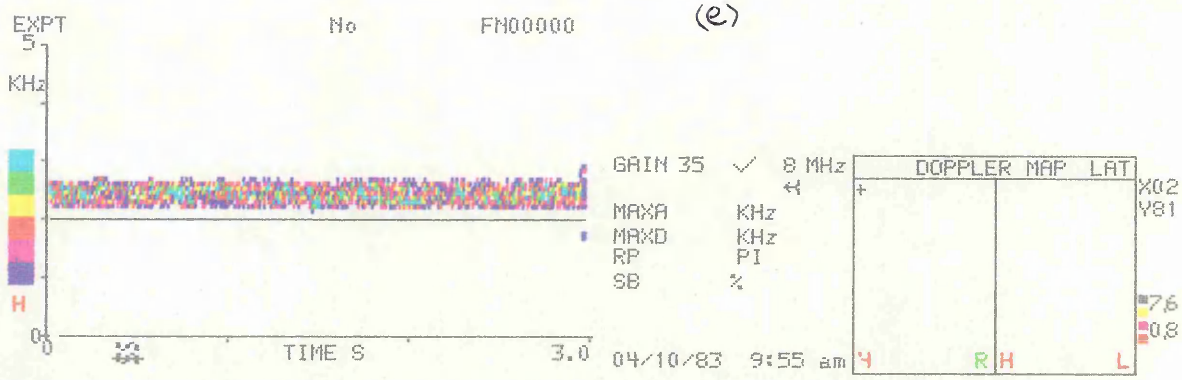
EXPT
No
FN00000
5
KHz
H
TIME S
3.0
GAIN 35
8 MHz
MAXA KHz
MAXD KHz
RP PI
SB %
DOPPLER MAP LAT
X02
Y81
7.6
0.8
04/10/83 9:55 am
R H L

TABLE 58 The Variation of Intensity with Time in Signals of Laminar Flow

	Frequency Band No	Area (mm^2) Cut No 1	2	3	4	5	6	Mean (mm^2)	SD (mm^2)	CV (%)
Signal 2 Laminar										
	8	-	-	-	8	-	-	-	-	-
	7	134	152	104	123	76	99	115	27.2	23.7
	6	349	379	336	352	345	347	351	14.6	4.2
	5	352	355	346	336	340	335	344	8.37	2.4
	4	339	369	333	326	314	296	330	24.65	7.5
	3	366	388	358	356	365	381	369	12.8	3.5
	2	225	257	266	231	198	215	232	25.6	11
	1	-	-	-	-	-	-	-	-	-
								Ave (bands 3-6)		4.4
Signal 1 Laminar										
	4	322	240	198	233	239	150	230	56.7	25
	3	495	529	511	476	457	481	492	25.8	5.2
	2	268	368	363	367	946	444	376	65.6	17.4
	1	-	-	-	-	-	-	-	-	-

TABLE 59 The Variation of Intensity with Time in a Signal of Turbulent Flow

Signal 3 (Turbulent)

Frequency Band No	Area (mm^2) #2 Cut No 1	2	3	4	5	6	Mean (mm^2)	SD (mm^2)	CV (%)
41	-	-	3	43	16	26			
40	31	33	20	45	32	44	34.17	9.28	27
39	123	74	69	132	143	146	115	34.33	30
38	145	122	126	167	133	146	140	16.49	11.8
37	215	182	125	180	147	156	168	31.56	19
36	216	198	132	191	181	189	185	28.30	15.3
35	258	250	226	258	239	237	245	12.83	5.2
34	266	257	257	259	245	236	253	10.86	4.3
33	243	254	293	255	219	234	250	25.12	10
32	269	279	258	264	234	231	255	19.46	7.6
31	251	250	253	291	271	265	264	15.89	6
30	253	254	285	260	280	253	264	14.52	5.5
29	263	291	282	272	284	277	278	9.83	3.5
28	261	248	280	258	257	262	261	10.55	4
27	207	241	243	236	261	279	245	24.31	9.9
26	221	264	257	248	225	223	240	18.99	7.9

TABLE 59 (CONTD) The Variation of Intensity with Time in a Signal of Turbulent Flow

Signal 3 (Turbulent)

Frequency Band No	Area (mm^2) #2 Cut No 1	2	3	4	5	6	Mean (mm^2)	SD (mm^2)	CV (%)
25	229	265	249	237	245	235	243	12.8	5.3
24	222	245	255	201	214	231	228	19.94	8.8
23	233	212	192	188	169	170	194	24.84	12.8
22	210	189	218	205	204	184	202	12.85	6.4
21	168	179	209	214	213	187	195	19.65	10
20	165	161	200	166	159	170	170	15.12	8.9
19	161	160	160	166	174	206	171	17.89	10.5
18	196	186	197	197	191	166	189	11.99	6.3
17	188	200	191	182	204	141	184	22.7	12
16	156	178	201	212	208	188	191	21.13	11
15	139	184	198	207	190	169	181	24.34	13.4
14	184	174	192	176	159	173	176	11.15	6.3
13	145	152	190	188	164	172	169	18.44	10.9
12	114	115	175	172	185	172	156	32.12	21
11	163	121	139	144	124	187	146	25.03	17

TABLE 59 (CONTD) The Variation of Intensity with Time in a Signal of Turbulent Flow

	Frequency Band No	Area (mm^2) #2 Cut No 1	2	3	4	5	6	Mean (mm^2)	SD (mm^2)	CV (%)
Signal 3 (Turbulent)										
	10	191	157	180	178	167	173	174	11.66	6.7
	9	179	185	194	138	162	122	163	28.3	17
	8	150	128	162	173	160	195	161	22.4	14
	7	154	210	244	256	253	242	227	39.11	17
	6	237	289	302	281	260	242	269	26.3	9.8
	5	197	256	299	321	315	313	284	48.5	17
	4	189	233	232	232	233	236	226	18.1	8
	3	142	186	173	163	168	172	168	15	8.9
	2	61	129	94	82	101	126	98.8	26	26
	1	-	-	-	-	-	-	-		

TABLE 60 The Variation of Intensity with Time in Signals of Laminar and Turbulent Flow - The Mean Coefficients of Variation

Signal	Frequency Bands	n of bands	Range of CV (%)	Mean CV (%)
1 (LAM)	3	1	5.2	5.2
2 (LAM)	3-6	4	2.4-7.5	4.4
3 (TURB)	3-39	37	3.5-30	10.8
3 (TURB)	8-38	31	3.5-21	10.0

TABLE 61 The Variation of the Intensities of the Frequency Bands within each Spectral Section

Signal 2 (LAM)
Data from frequency bands 3-6 included (n = 4)

#2 Display (Section No)	The Mean Intensity (Expressed as mm^2)	SD (mm^2)	CV (%)
6	340	35.1	10.3
5	341	20.99	6.2
4	343	13.98	4.1
3	343	11.3	3.3
2	373	14.15	3.8
1	352	11.15	3.2
		Mean	5.2

Signal 3 (TURB)
Data from frequency bands 3-39 included (n = 37)

#2 Display (Section No)	The Mean Intensity (Expressed as mm^2)	SD (mm^2)	CV (%)
6	205	45.1	22
5	206	47.5	23
4	213	47	22
3	212	55.2	26
2	203	54.2	27
1	197	44.5	23
		Mean	24

Reverse flow of lesser degree was also seen immediately proximal to a stenosis at a site where dye was seen to travel back from the front of a stenosis. Whilst a flat #2 spectrum was seen in the laminar flow proximal to a stenosis the character of the #2 spectra sampled from the turbulence distal to a 2 mm stenosis did not have the 'waisted' appearance seen in Method I. Disturbances of flow were represented on #2 displays by high frequencies of low intensity. Flow through the 5 mm stenosis was streamline (when dye was injected) but both a small disturbance of the maximum frequency envelope and retrograde flow were seen on signals recorded immediately proximal to the stenosis.

EXPERIMENT 5.2 The Ability of CW Ultrasound to Detect Changes in the Character of Oscillatory Flow in a Model

EXPERIMENT 5.2.1 The Effect of an Increase in the Frequency of Oscillation

Although $\overline{Re}$ was 392, values of $\widehat{Re}$ of up to 9000 were obtained. These values of Re were greater than those at which the onset of turbulence could be predicted.

ΔF max (osc) increased with frequency (see Table 62) but there was no evidence of any change in their relationship at high values of frequency nor between frequency and λ when λ changed from values less than one to values higher than one (see Figure 54).

TABLE 62 Experiment 5.2.1 The Effect of an Increase in the Frequency of Oscillation

Frequency (cycles/min)	ΔF max (osc) (KHz)	λ	α	$\hat{Re}$
18	1.0	0	1.8	715
24	1.2	0.2	2.1	850
28	1.4	0.4	2.2	992
34	1.4	0.4	2.4	992
67	4.0	3	3.4	2834
79	4.2	3.2	3.7	2976
114	5.6	4.6	4.5	3968
140	8.5	7.5	5.0	6022
160	12.6	11.6	5.3	8927

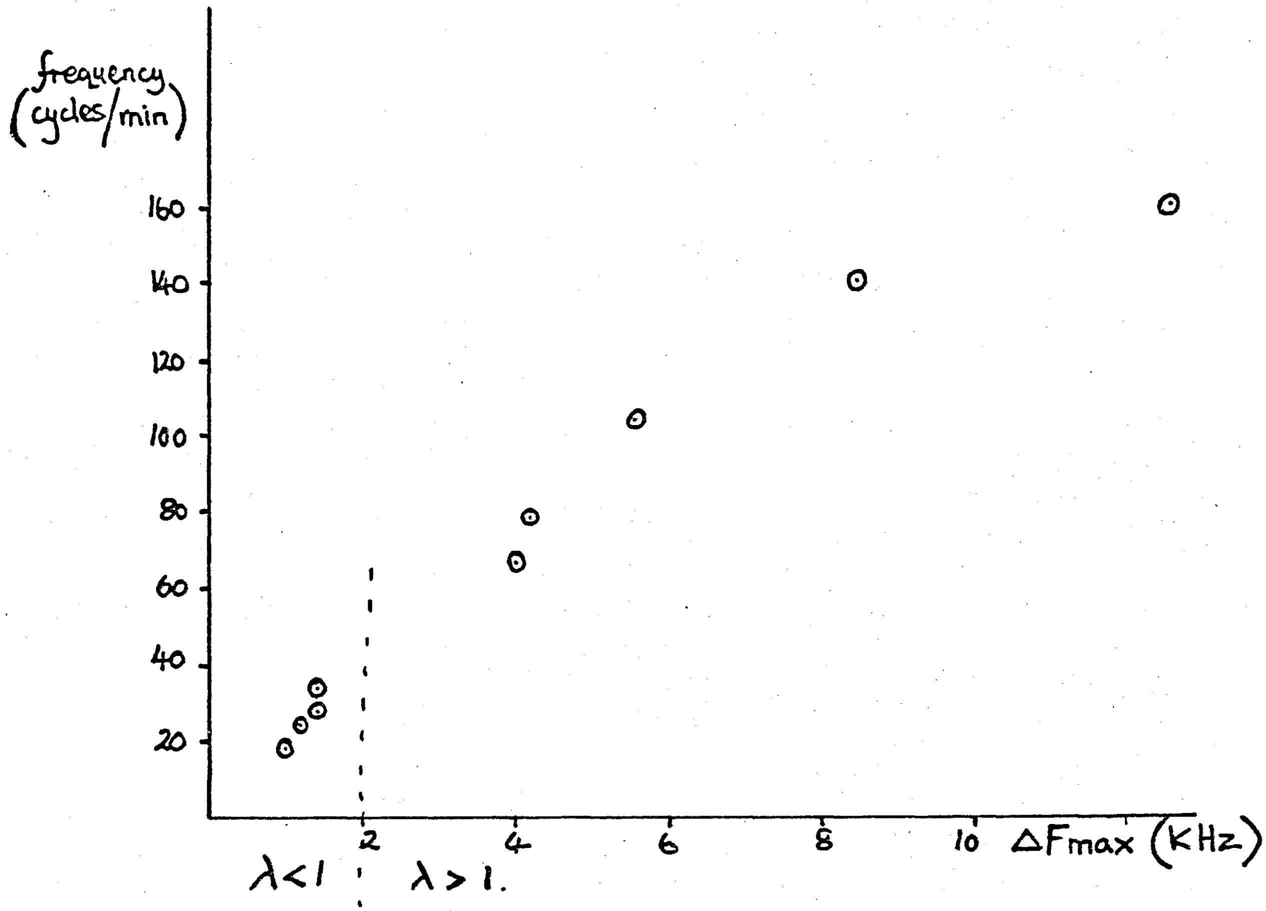

FIGURE 54

The relatioship between ΔF max and frequency - Experiment 5.2.1

A spectral window was present and there was no evidence of any irregularity in the maximum frequency envelope of the Vasoscan displays for any value of frequency (see Figure 55). However the Sonagraph #1 displays exhibited irregularities both in acceleration and deceleration at high values of frequency (see Figure 56). In the case of #2 displays 'waisted' spectra were seen from the earliest phase of acceleration and continued to peak "systole" or early deceleration for all values of frequency (see Figure 57).

EXPERIMENT 5.2.2 The Effect of an Increase in the Mean Velocity of Flow

Table 63 gives the values of ΔF max (osc), ΔF max (steady), $\overline{Re}$, $\widehat{Re}$, α and λ for both values of frequency. Figures 58 and 59 plot the values of $\bar{V}$ against those of ΔF max (steady) and ΔF max (osc). Values of both $\overline{Re}$ and $\widehat{Re}$ greater than those at which the onset of turbulence could be predicted were obtained.

When the steady component of flow was in the laminar range λ was always greater than one and when the steady component of flow entered the turbulent range λ was less than one. As $\bar{V}$ increased ΔF max (osc) increased virtually step by step with ΔF max (steady).

As in Experiment 5.2.1 a spectral window was present and there were no irregularities of the maximum frequency envelope of any of the Vasoscan displays (see Figure 60).

(a)

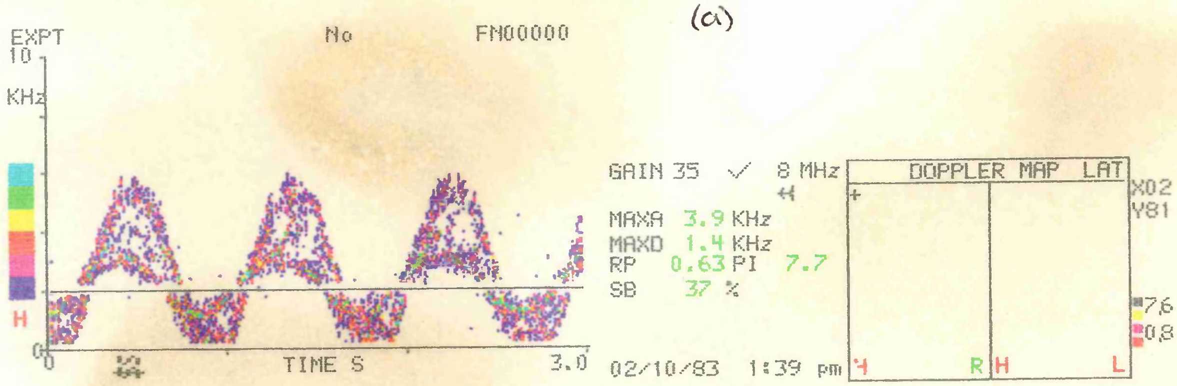
EXPT
No
FN00000
10
KHz
H
0
0
TIME S
3.0
GAIN 35
8 MHz
MAXA 3.9 KHz
MAXD 1.4 KHz
RP 0.63 PI 7.7
SB 37 %
02/10/83 1:39 pm
DOPPLER MAP LAT
X02
Y81
7.6
0.8
R
H
L

(b)

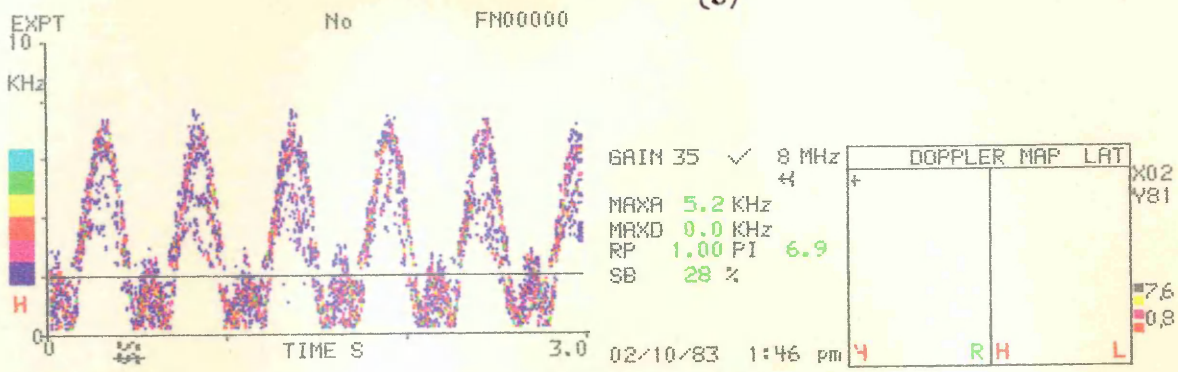
EXPT
No
FN00000
10
KHz
H
0
0
TIME S
3.0
GAIN 35
8 MHz
MAXA 5.2 KHz
MAXD 0.0 KHz
RP 1.00 PI 6.9
SB 28 %
02/10/83 1:46 pm
DOPPLER MAP LAT
X02
Y81
7.6
0.8
R
H
L

(c)

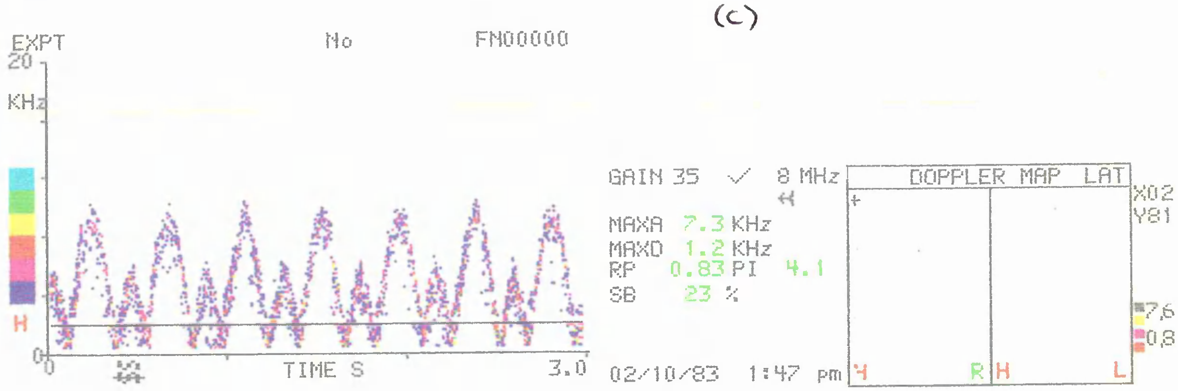
EXPT
No
FN00000
20
KHz
H
0
0
TIME S
3.0
GAIN 35
8 MHz
MAXA 7.3 KHz
MAXD 1.2 KHz
RP 0.83 PI 4.1
SB 23 %
02/10/83 1:47 pm
DOPPLER MAP LAT
X02
Y81
7.6
0.8
R
H
L

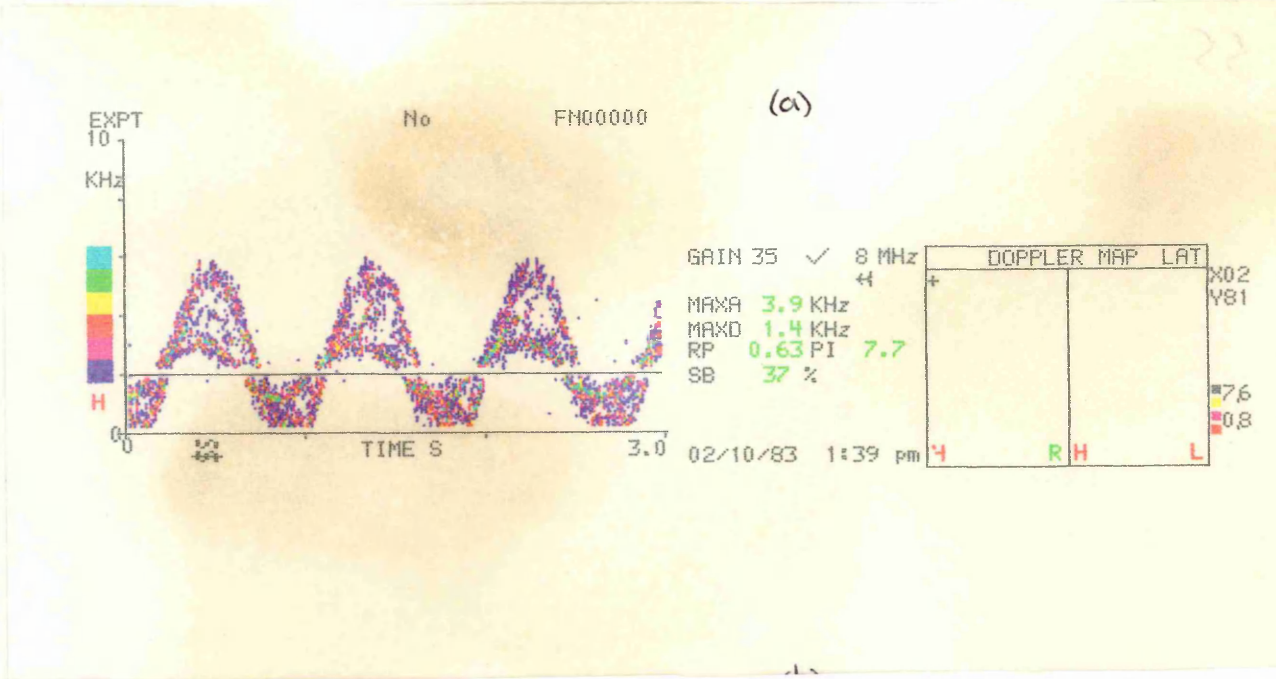

FIGURE 55

Vasoscan displays - Experiment 5.2.1

(a) $\widehat{Re}$ = 2834

(b) $\widehat{Re}$ = 3968

(c) $\widehat{Re}$ = 6022

NB The biphasic waveform on these and other displays is referred to in the discussion

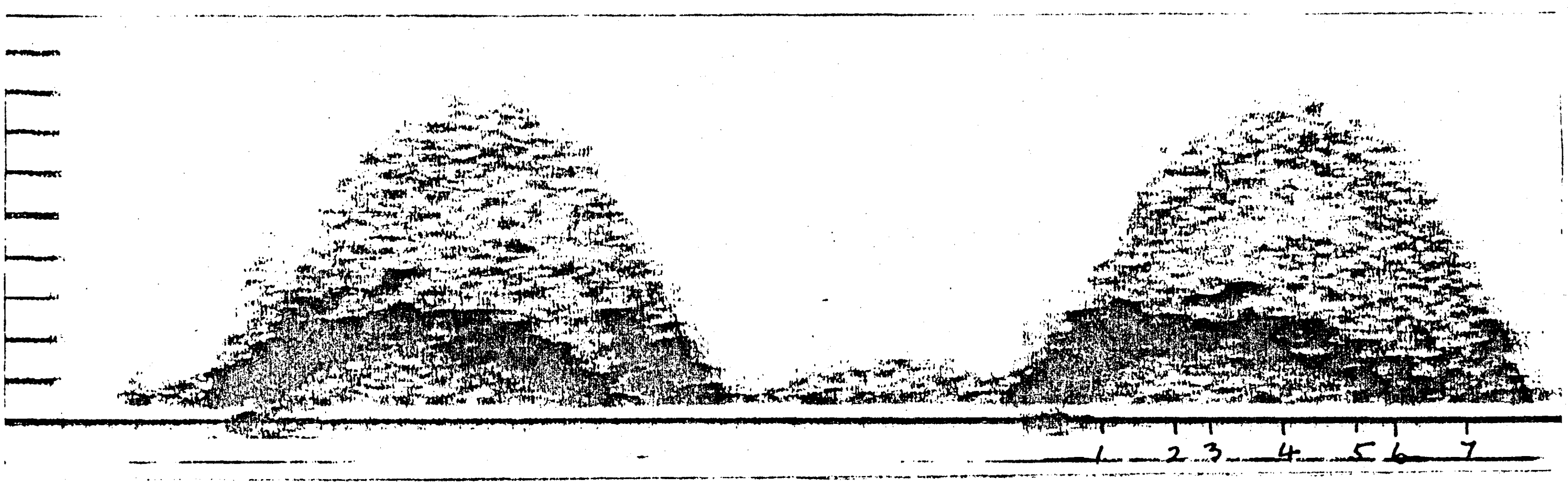

FIGURE 56

Sonagraph #1 display - Experiment 5.2.1

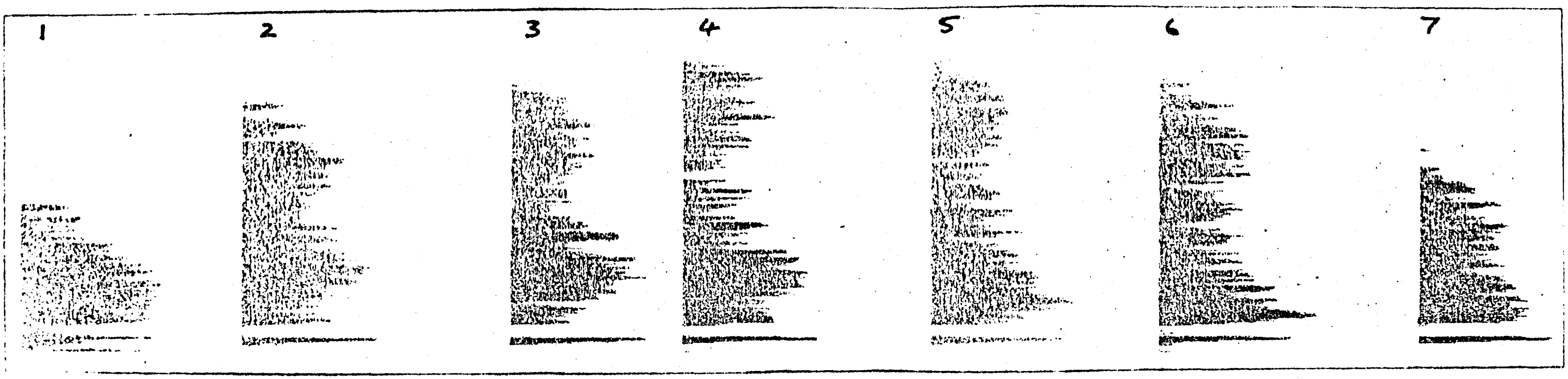

FIGURE 57

Sonagraph #2 displays - Experiment 5.2.1
The sections are recorded from the #1 display in Figure 56. There are 16 msec between sections one and 2, 3 and 4, and 6 and 7; and 8 msec between sections 2 and 3, and 5 and 6.

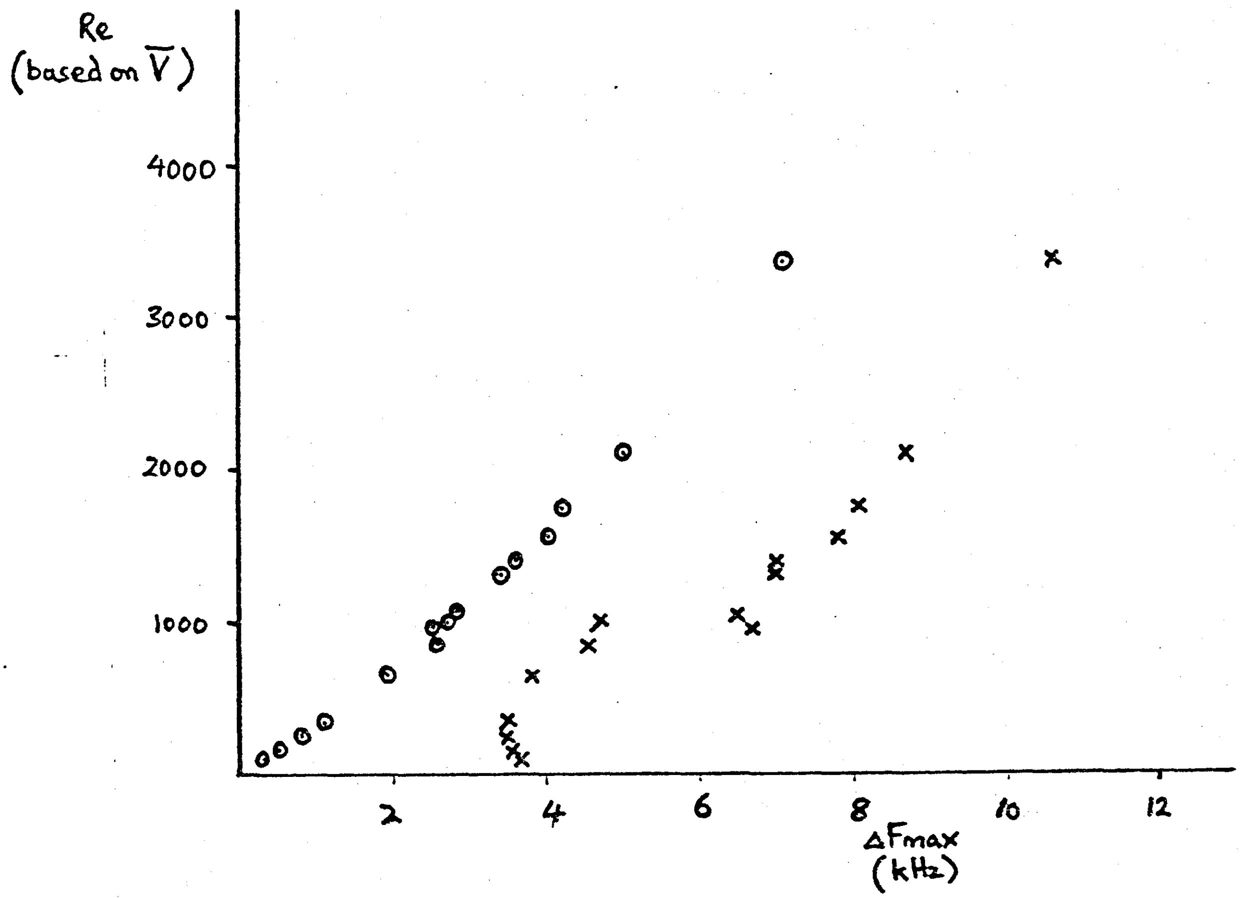

FIGURE 58

The relationship between $\bar{V}$, ΔF max (osc) and ΔF max (steady) for f = 72 cycles/min - Experiment 5.2.2

⊙ ⊙ = ΔF max (steady)
x x = ΔF max (osc)

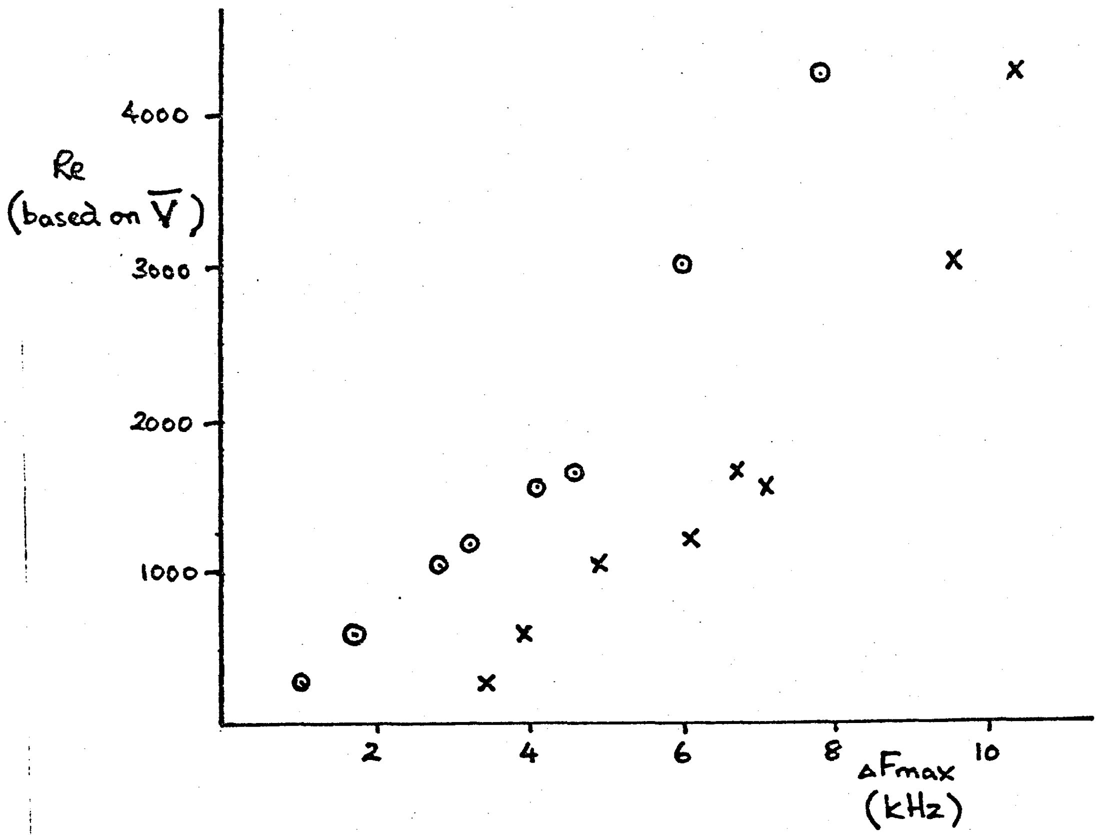

FIGURE 59

The relationship between $\bar{V}$, $\triangle$F max (osc) and $\triangle$F max (steady) for f = 67 cycles/min - Experiment 5.2.2

o o = $\triangle$F max (steady)
x x = $\triangle$F max (osc)

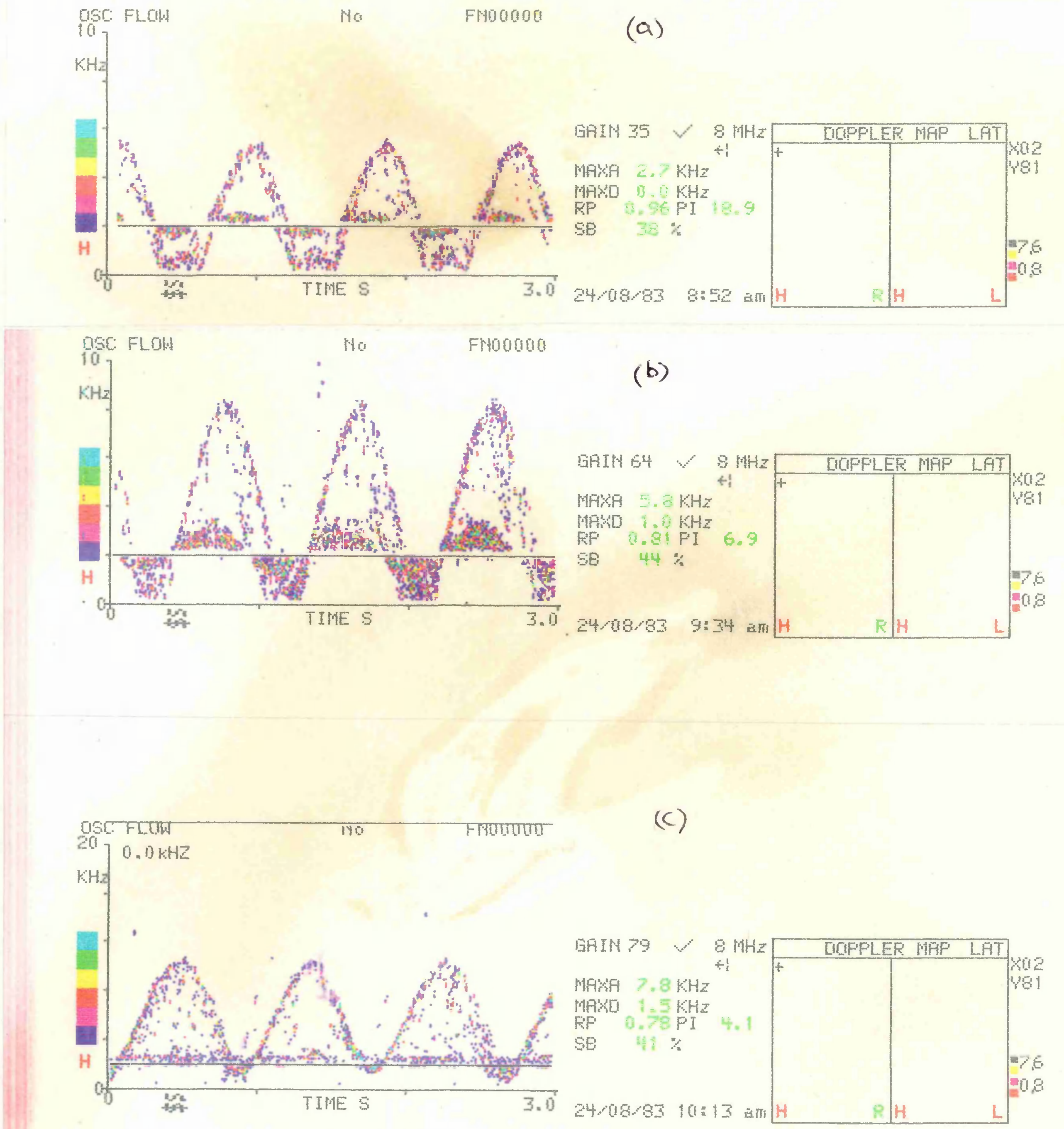

FIGURE 60

Vasoscan displays - Experiment 5.2.2

(a) $\widehat{Re}$ = 2315

(b) $\widehat{Re}$ = 4180

(c) $\widehat{Re}$ = 5595

TABLE 63 Experiment 5.2.2 The Effect of an Increase in the Mean Velocity of Flow

Experiment (i) f = 72 cycles/min, α = 3.27

$\bar{V}$ (cm/sec)	$\overline{Re}$	ΔF max (steady) (KHz)	$\widehat{Re}$	ΔF max (osc) (KHz)	λ	Str
0			3344	5.2		
1.4	83	0.3	2379	3.7	11	0.257
2.5	148	0.5	2315	3.6	6	0.144
4.8	284	0.8	2251	3.5	3.4	0.075
6.4	378	1.1	2251	3.5	2.2	0.056
11.2	662	1.9	2444	3.8	1.0	0.032
15	887	2.6	2958	4.6	0.8	0.024
16	946	2.5	4309	6.7	1.7	0.022
16.6	981	2.7	3023	4.7	0.7	0.022
18	1064	2.8	4180	6.5	1.3	0.020
22	1300	3.4	4502	7.0	1.1	0.016
24	1418	3.6	4502	7.0	0.9	0.015
26	1537	4.0	5016	7.8	1.0	0.014
30	1773	4.2	5209	8.1	0.9	0.012
36	2128	5.0	5595	8.7	0.7	0.010
57	3369	7.1	6817	10.6	0.5	0.006

Experiment (ii) f = 67 cycles/min, α = 3.39

$\bar{V}$ (cm/sec)	$\overline{Re}$	ΔF max (steady) (KHz)	$\widehat{Re}$	ΔF max (osc) (KHz)	λ	Str
4.6	272	1.0	2187	3.4	2.4	0.085
9.8	580	1.7	2508	3.9	1.3	0.039
17.5	1034	2.8	2891	4.9	0.8	0.022
20	1182	3.2	3923	6.1	0.9	0.020
26.4	1560	4.1	4566	7.1	0.7	0.015
28	1654	4.6	4309	6.7	0.5	0.014
51	3014	6.0	5664	9.6	0.6	0.008
72	4255	7.8	6136	10.4	0.3	0.005

EXPERIMENT 5.2.3 The Effect of an Increase in the Diameter of the Vessel

The Vasoscan displays did not show any irregularity of the maximum frequency envelope and a clear window remained present (see Figure 61). High frequency "spikes" did appear at various times in the cycle of #1 displays which may have been artefactual. The #2 displays did not have any characteristic appearance eg 'waisting'.

EXPERIMENT 5.2.4 The Effect of Introducing a Stenosis

In the case of the 5 mm stenosis the Vasoscan displays showed a loss of part of the window although there were no irregularities of the maximum frequency envelope. A double wave was apparent : a wave of low amplitude appearing in the acceleration phase of the main flow wave.

In the case of the 2 mm stenosis the same double wave was seen and the relationship between them was changed immediately proximal to the stenosis (see Figure 62). Like the 5 mm stenosis the window was partly lost in the Vasoscan displays 6 cm proximal to the stenosis and at the stenosis it disappeared completely. Marked irregularity of the maximum frequency envelope and retrograde flow were seen immediately proximal and distal to the stenosis before a return to previous appearances 6 cm distal to the stenosis.

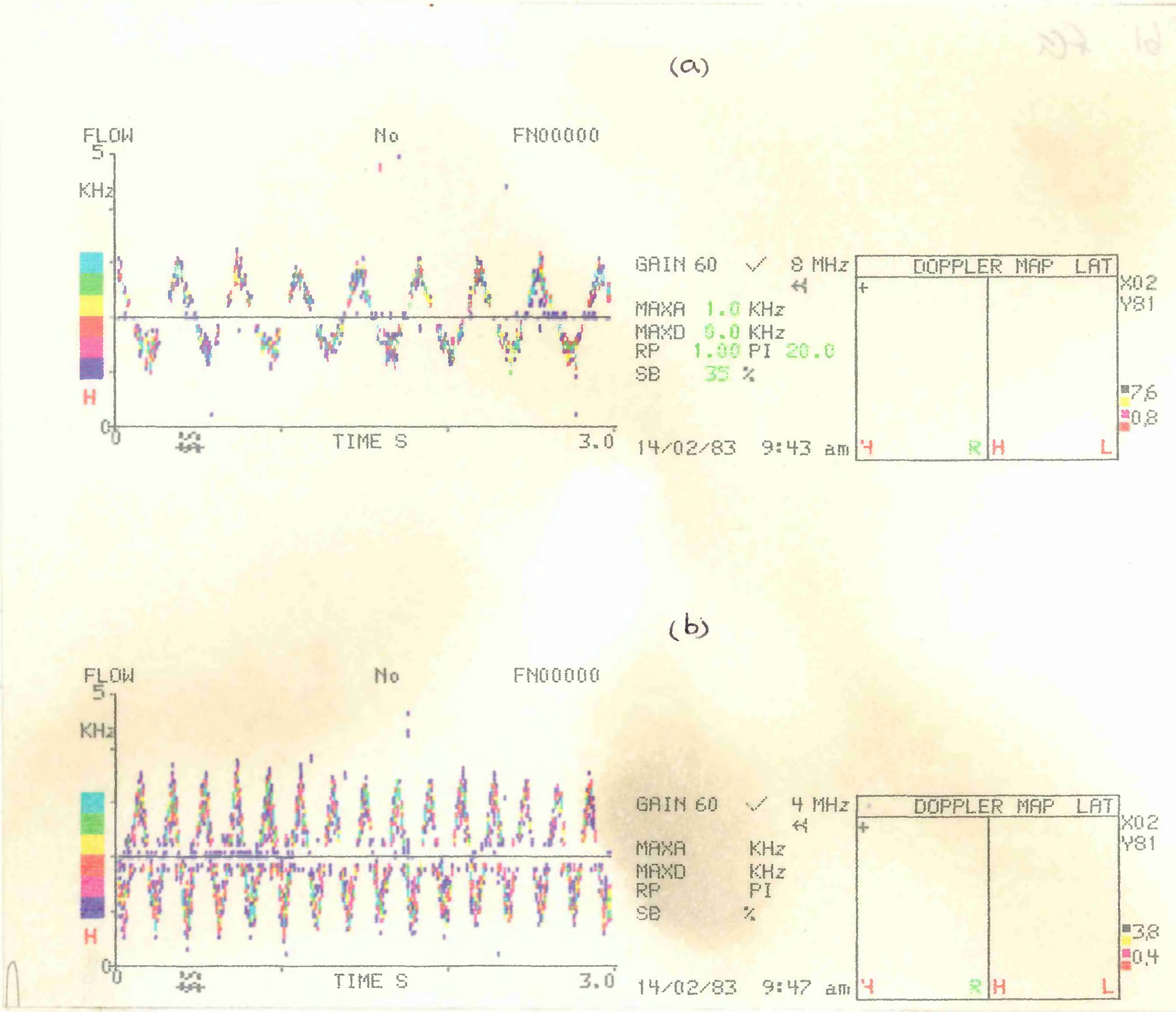

FIGURE 61

Vasoscan displays - Experiment 5.2.3

(a) α = 12.55

(b) α = 16.97

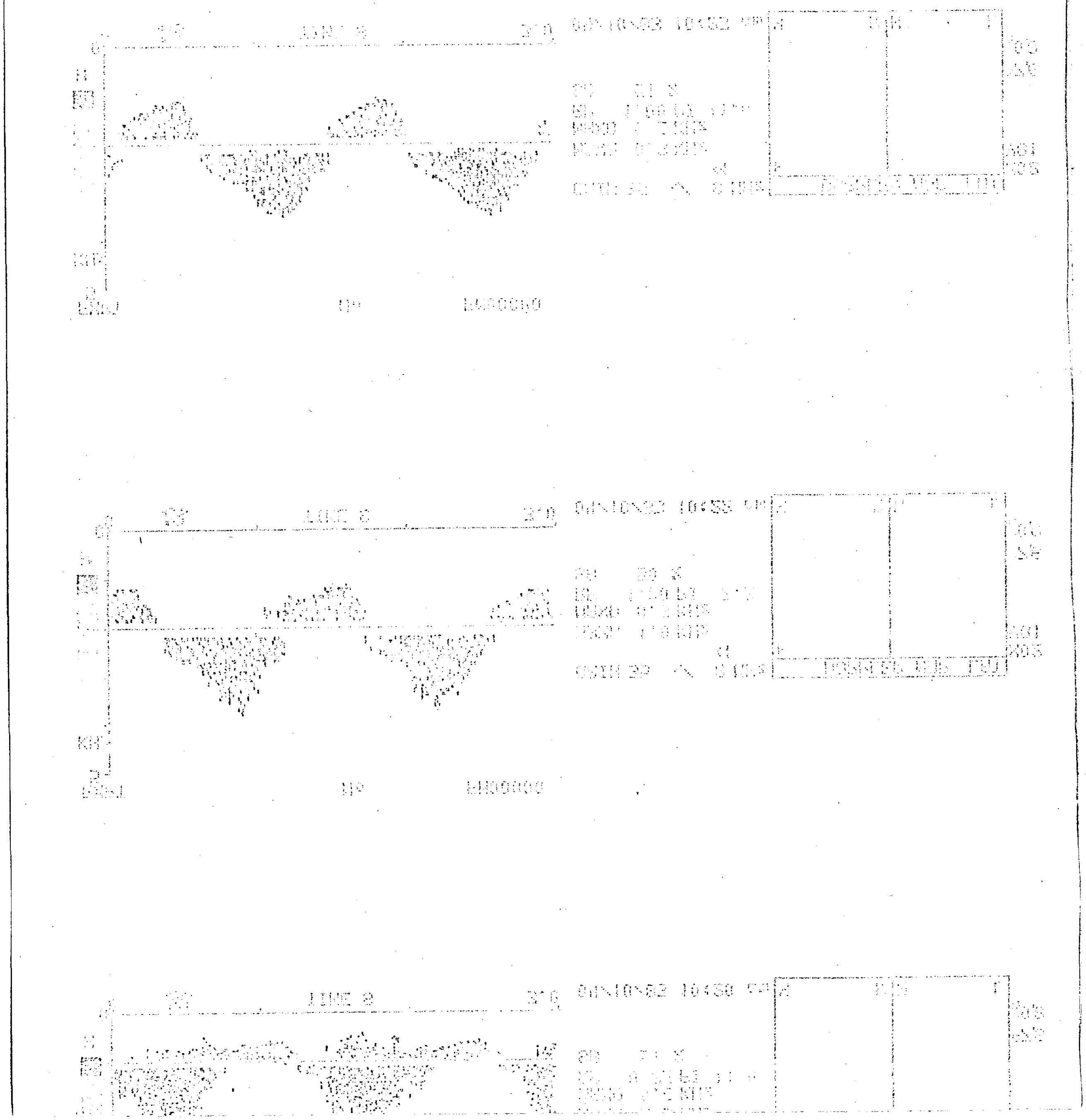

FIGURE 62

Vasoscan displays - Experiment 5.2.4, Oscillatory flow through a 2 mm stenosis

(a) 6 cm proximal to stenosis
(b) < 1 cm proximal to stenosis
(c) < 1 cm distal to stenosis
(d) 4 cm distal to stenosis
(e) 6 cm distal to stenosis

(b)

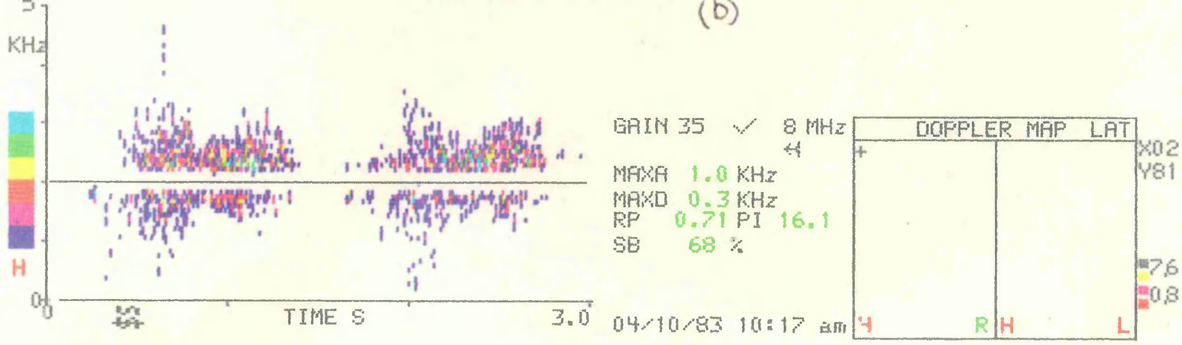
5
KHz
H
0
0
TIME S
3.0
GAIN 35
8 MHz
MAXA 1.0 KHz
MAXD 0.3 KHz
RP 0.71 PI 16.1
SB 68 %
04/10/83 10:17 am
DOPPLER MAP LAT
X02
Y81
7.6
0.8
R
H
L

(c)

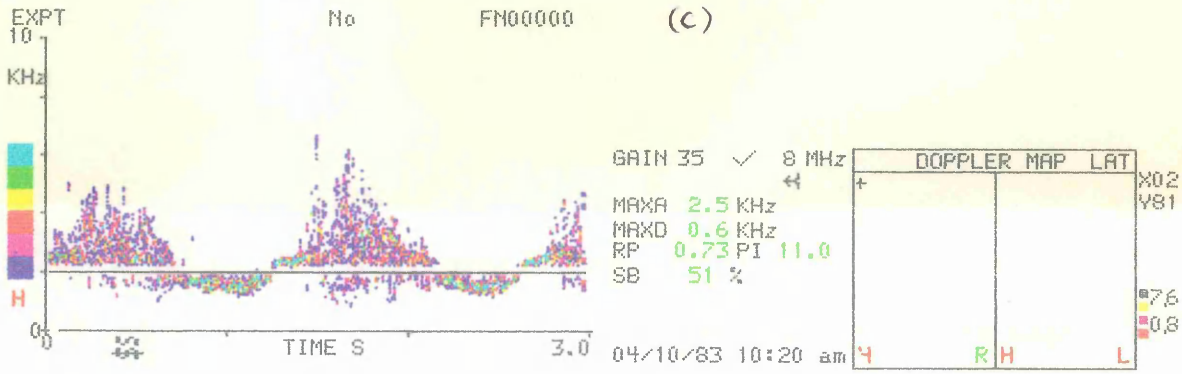
EXPT
No
FN00000
10
KHz
H
0
0
TIME S
3.0
GAIN 35
8 MHz
MAXA 2.5 KHz
MAXD 0.6 KHz
RP 0.73 PI 11.0
SB 51 %
04/10/83 10:20 am
DOPPLER MAP LAT
X02
Y81
7.6
0.8
R
H
L

(d)

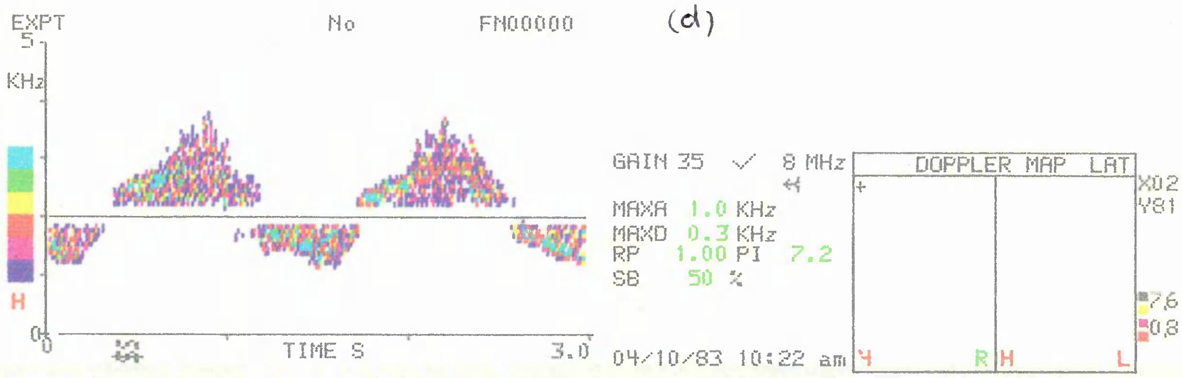
EXPT
No
FN00000
5
KHz
H
0
0
TIME S
3.0
GAIN 35
8 MHz
MAXA 1.0 KHz
MAXD 0.3 KHz
RP 1.00 PI 7.2
SB 50 %
04/10/83 10:22 am
DOPPLER MAP LAT
X02
Y81
7.6
0.8
R
H
L

(e)

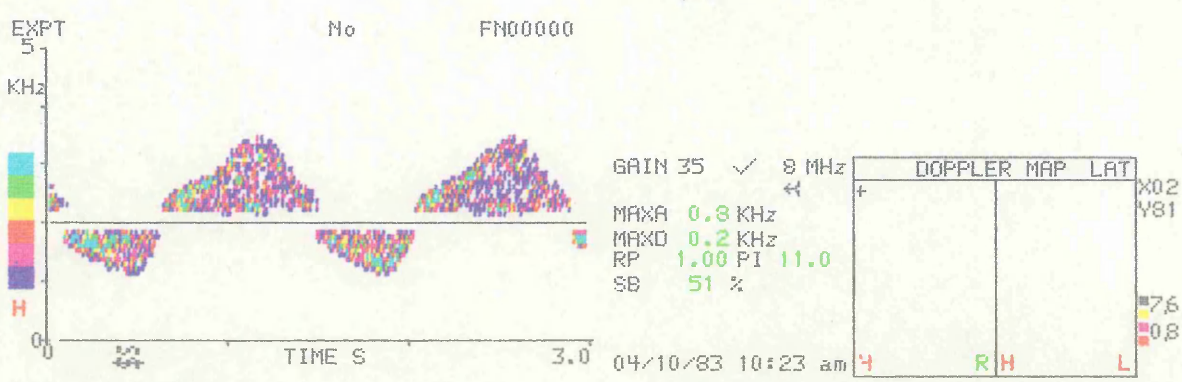
EXPT
No
FN00000
5
KHz
H
0
0
TIME S
3.0
GAIN 35
8 MHz
MAXA 0.8 KHz
MAXD 0.2 KHz
RP 1.00 PI 11.0
SB 51 %
04/10/83 10:23 am
DOPPLER MAP LAT
X02
Y81
7.6
0.8
R
H
L

The ≠2 displays demonstrated high frequency, low intensity disturbances but no characteristic pattern was seen.

EXPERIMENT 5.3 The Detection of Disturbances of Flow in Arteries Using CW Ultrasound

Normal Arteries:- The maximum frequency envelope of the Vasoscan displays was smooth in signals from all arteries and in most of the signals from the internal carotid artery, external carotid artery or common carotid artery a clear window was present in systole (of duration 30-80 msec, see Figure 63). In the carotid arteries in systole where no spectral window was present the ≠2 spectra were flat but where a window was present the spectra were 'waisted' eg Figure 63. In diastole eg in the internal carotid artery the ≠2 spectra were virtually always flat. In the limb arteries where no window was present the ≠2 displays of the tibial and radial waveforms had no characteristic pattern. In the subclavian and femoral arteries where the amplitude of the waveforms was higher than those of the tibial and radial arteries the ≠2 spectra tended to be flat in the acceleration, peak and deceleration phases of systole (see Figure 64).

Diseased Arteries:- Examination of the Vasoscan and Sonagraph ≠1 displays demonstrated that the peak frequency rose, the window present during systole disappeared and the maximum frequency envelope was often irregular (see Figure 65). In the case of the

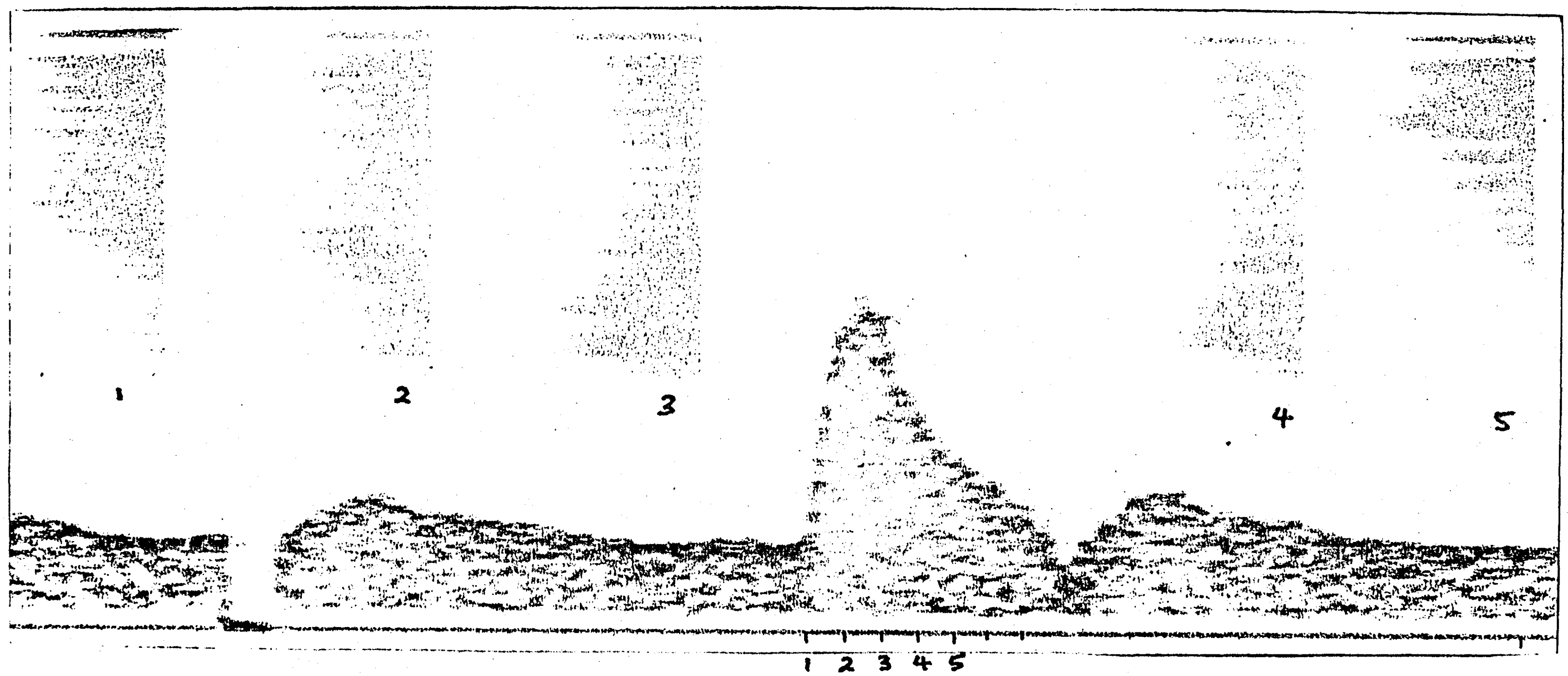

FIGURE 63

Sonagraph #1 and #2 displays - normal common carotid artery. The #2 displays have been recorded at the times numbered on the #1 display.

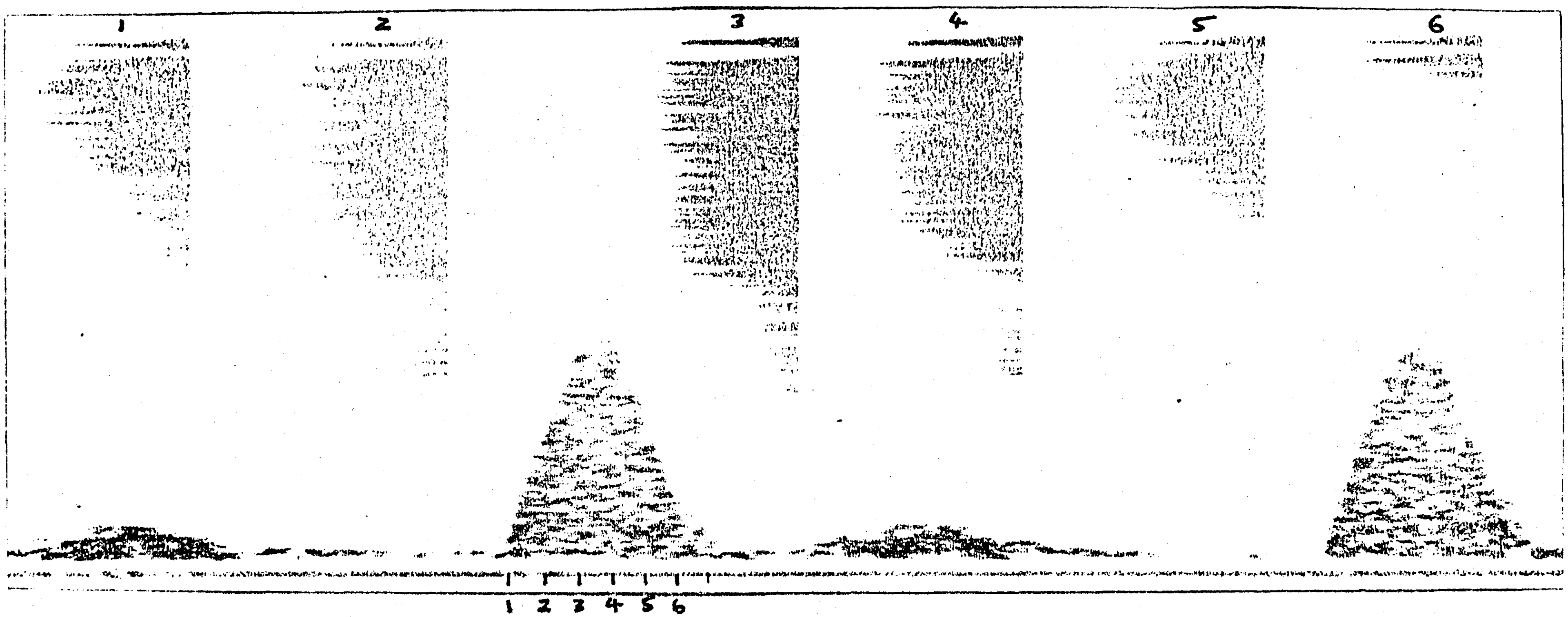

FIGURE 64

Sonagraph #1 and #2 displays - normal femoral artery

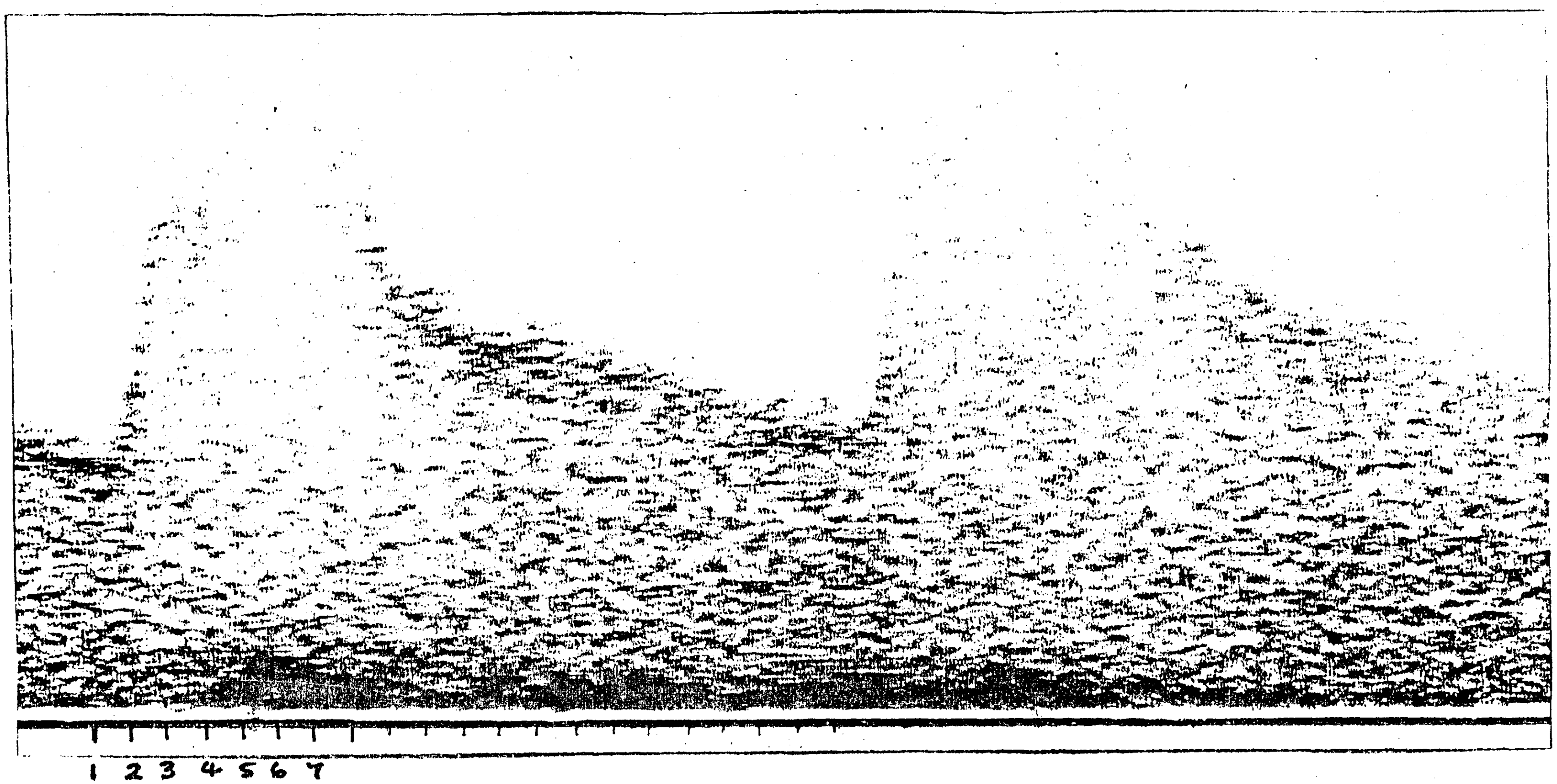

FIGURE 65

Sonagraph #1 display distal to internal carotid stenosis

#2 displays the amplitude of each frequency was much reduced but there was no characteristic pattern (see Figure 66).

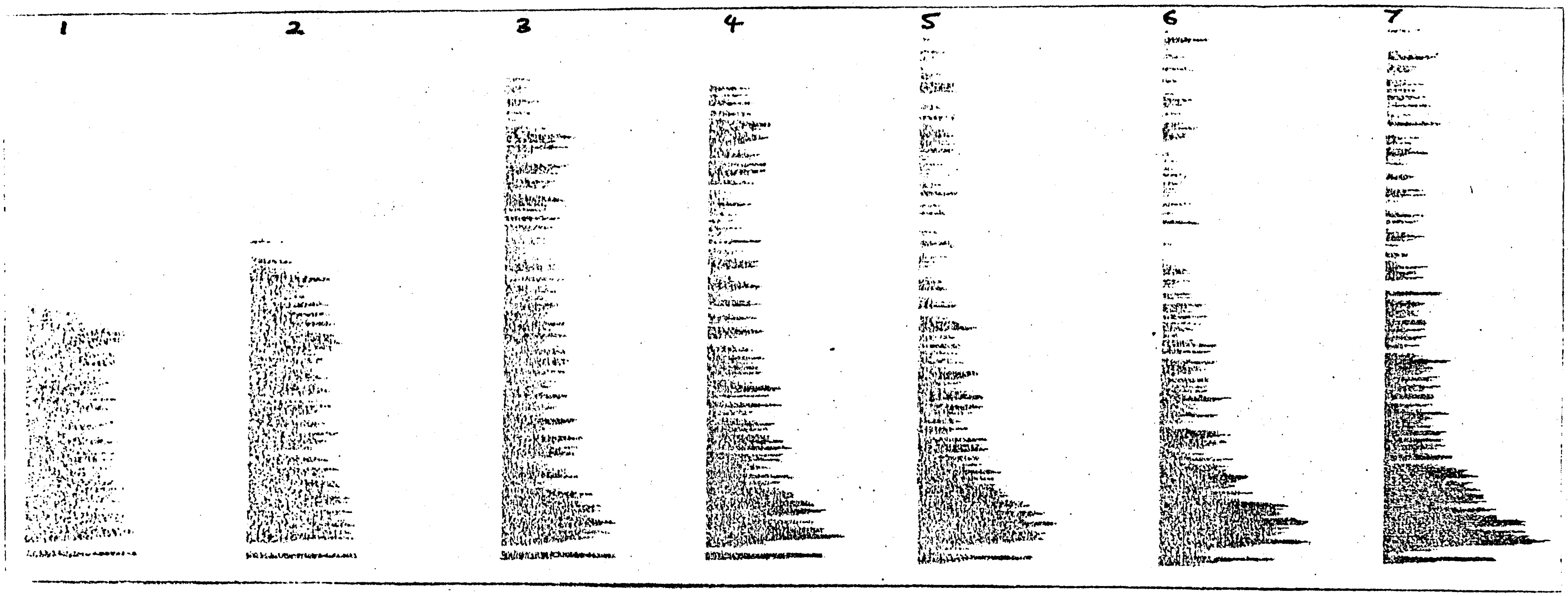

FIGURE 66

Sonagraph #2 displays distal to internal carotid stenosis. The #2 displays have been recorded at 8 msec intervals from the #1 display in Figure 65.

DISCUSSION

The application of the definitions quoted on Page 214 for laminar and turbulent flows to the human circulation is not straight forward. Reversal of flow occurs normally in many arteries with breakdown of the streamline pattern.[118] The common usage of the term turbulence to describe disturbed flows at a stenosis is outwith its definition as although these disturbances are propagated downstream they do not undergo a net growth with each cardiac cycle nor are they self perpetuating.[130] The distinction between these different types of flow is of some importance because in turbulence both pressure and velocity show a random variation with time resulting in energy dissipation from losses due to heat, friction, momentum and pressure.[126]

Flow disturbances have been demonstrated in models using birefringence techniques to demonstrate the flow patterns; dye; and hot film constant temperature or laser Doppler anamometers to demonstrate centre line velocities, turbulence spectra, the variability of velocity waveforms or the velocity spectra.[117,118,126,130-137] The use of both PW and CW ultrasound to demonstrate flow disturbances is attractive because it is non invasive and does not involve the introduction of a needle or other device into the lumen of a vessel which may be a source of disturbance to flow.[138,139]

The relationship between the velocity profile and the frequency/intensity ultrasound spectrum can be deduced from theory. For a parabolic velocity profile eg Figure 67 (a) to give a flat frequency/intensity spectrum eg Figure 67 (b) it has to be proven that the annuli in Figure 67 (c) are equal in area. The definition of parabolic flow (see Figure 67 [a]) is:-

$V_r = V\,max\,(1 - [r^2/a^2])$ Equation 5.5

Where r is the radius of any annulus and a is the radius of the vessel.

Small step changes in velocity are related to changes of radius by the differentiation of Equation 5.5:-

$dV_r = -\,2\,V\,max\,(r/a^2)\,dr$

The area of each annulus (A) in Figure 67 (c) is:-

$A = 2\,r\,dr$

$A = (\pi\,dV_r\,a^2)/(-\,V\,max)$

But πa^2 (area of vessel lumen) and V max are constant $\therefore$ $A = K\,dV_r$

Therefore equal areas of annuli correspond to equal steps in velocity therefore the spectrum is flat. Wells points out that the ultrasonic beam width must be wider than the vessel lumen for a flat spectrum to be obtained from a parabolic flow profile.[106]

A flat velocity profile however gives a different frequency/intensity spectrum. Figure 68 (a) shows the type of velocity profile seen in turbulent steady flow. Ten velocity steps were drawn on the

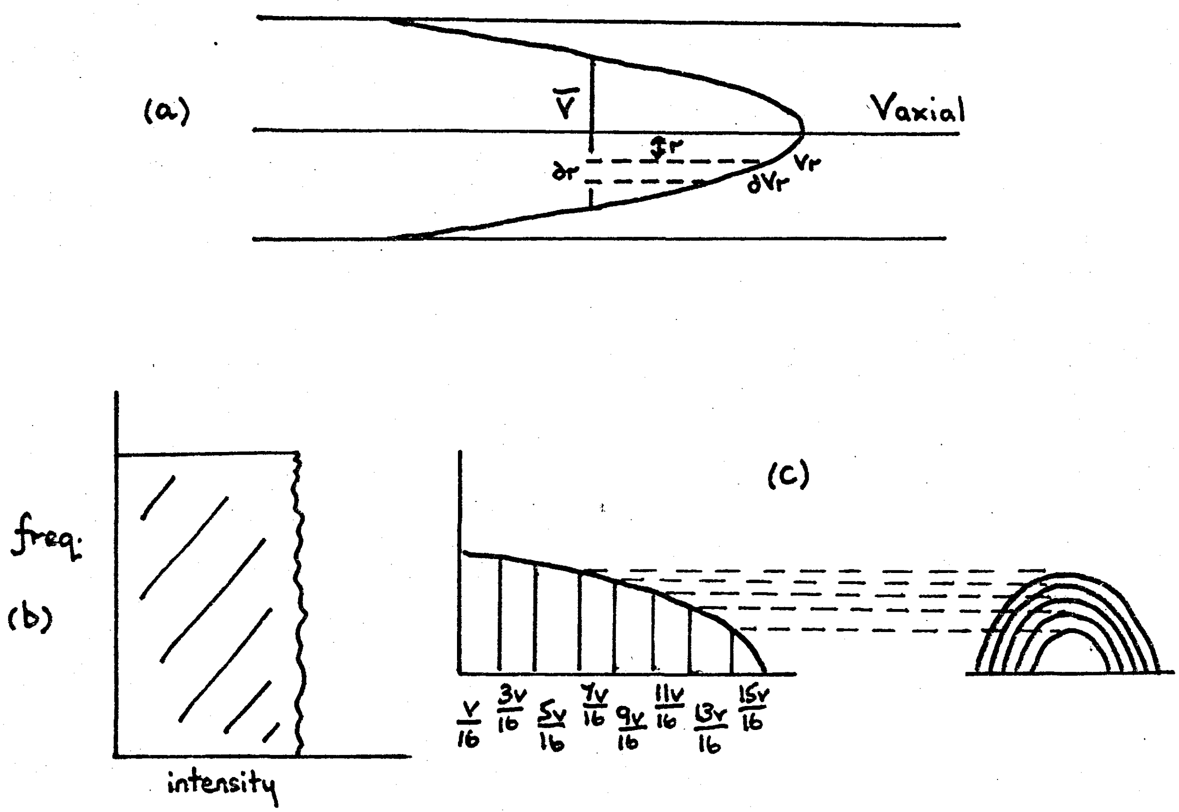

FIGURE 67

The relationship between the velocity profile and the frequency/intensity spectrum. I A parabolic profile.
A parabolic velocity profile (a), divided into equal increments (c) and a flat frequency/intensity ultrasound spectrum (b), (see text).

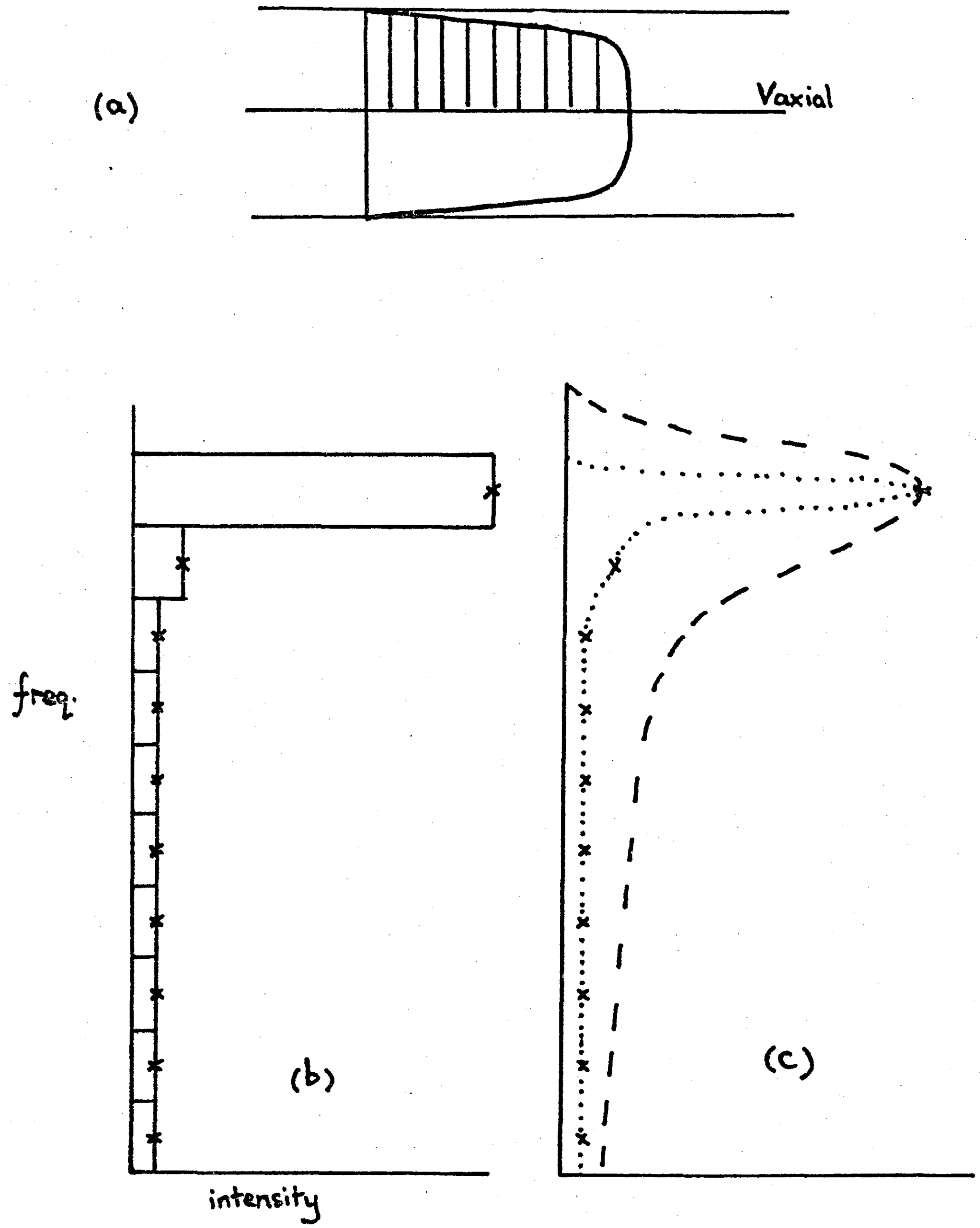

FIGURE 68

The relationship between the velocity profile and the frequency/ intensity spectrum. II. A flat profile.

(a) a flat velocity profile

(b) the frequency/intensity spectrum predicted from theory

(c) an estimate of the effect of turbulence and divergence of the ultrasound beam on the spectrum profile and perpendicular lines drawn from the former to find the radius of each velocity step. In this example they were 0, 10.8, 11.5, 11.8, 12.1, 12.5, 12.9, 13.2, 13.6, 14.0 and 14.3. The area of each annulus was calculated from Equation 5.6:-

$$A = \pi(r_2^{\,2} - r_1^{\,2}) \qquad \text{Equation 5.6}$$

The centre was $\pi(10.8^2 - 0^2)$ and each was normalised with a maximum of 100%. Figure 68 (b) gives the theoretical spectrum predicted from the flat profile in Figure 68 (a) with the estimated effects of turbulence and beam divergence on the spectrum adjacent to it (see Figure 68 [c]).

The analysis of frequency/intensity spectra obtained by Method I, Experiment 5.1 found that under conditions of laminar flow the spectra were flat in agreement with theory and 'waisted' in the case of turbulent spectra. In the latter case the high intensities of the lower frequencies were considered to be due to wall movement. Experiment 3.2 demonstrated that wall movement of Goretex could cause high Doppler shifted frequencies of approximately 2 KHz in the example shown in Figure 38. If the lower frequencies were ignored then the theoretical spectrum was obtained. The definition of turbulence being random motion with time it was shown in Experiment 5.1 that the intensities of turbulent spectra were much more variable with respect to time than laminar ones. The mean frequencies of the turbulent ZZ2 spectra were high and approached the maximum frequency (proportional to V max) again in agreement with theory. Thus from a single #2 display the character of steady flow could be discerned. From the character of #2 displays taken distal to the 2 mm stenosis the implication is that the flow was disturbed only and not truly turbulent. This is borne out by the fact that the "turbulence" was not propagated and laminar flow supervened distal to the stenosis.

The method whereby the intensities of ultrasound spectra of steady turbulent flow were shown to be more variable than those of steady laminar flow could not be readily applied to oscillatory flow owing to the fluctuation in the maximum frequency with time which takes place. Because of this the finding of a greater variation in the intensity of each frequency band in a single #2 display of turbulence compared with one of laminar flow appeared important. (The results of Experiment 5.2 however found this not to be the case).

Sigel et al reported that CW ultrasound could distinguish between laminar and turbulent flow from frequency/intensity spectra using a technique which involved insonation at 2 angles, $\theta = 90^{\circ}$ and $\theta = 25^{\circ}$.[139] They demonstrated an increase in low intensity, high frequency signals in the case of turbulence (which can be demonstrated on Vasoscan or Sonagram #1 displays alone) but the spectra illustrated failed to show the high mean frequency characteristic of turbulence. The results of Experiment 5.1 suggest that their flow was only disturbed.

The finding of irregularities of the maximum frequency envelope (in Experiment 5.1) was expected although it was of interest that they were found on both sides of a stenosis as were vortices whose presence could be recognised from retrograde flow in the spectra.

Turbulence has been demonstrated above Reynolds numbers of 2130 and 3770 in experiments on oscillatory flow in pipes and values higher than these were obtained in Experiments 5.2.1 and 5.2.2.[118,140,141]

Because in steady flow the ratio of the maximum to the mean velocity of flow ie V max : $\bar{V}$ can identify the presence of turbulence, the effect on the maximum velocity of oscillatory flow by altering its stability was investigated. Experiment 5.2.1 found V max to increase with frequency and Experiment 5.2.2 found it to increase with $\bar{V}$. No clear relationship with turbulence was found but it was of interest that in Experiment 5.2.2 when the underlying steady component of flow was below the critical Reynolds number λ was greater than one and when the steady component of flow was greater than the critical Reynolds number λ was less than one. λ is greater than one in the carotid arteries in vivo but most model experiments have a value of less than one. It was not evident whether the low values of λ in Experiment 5.2.2 were merely due to the high value of $\bar{V}$ or whether a high value of λ ie a flow with large amplitude oscillations, is a stabilizing factor.

Neither by an increase in frequency, $\bar{V}$ nor by an increase in the internal diameter of the vessel was any irregularity of the maximum frequency envelope of the Vasoscan displays seen. A spectral window was present which became more evident as frequency, $\bar{V}$ and α increased in Experiments 5.2.2 to 5.2.4. Unfortunately in these experiments it was not possible to visualize turbulence using dye because of the high rates of flow involved. Although the velocity profile has ceased to be parabolic when α is approximately 5 it is not until it is in the range of 7 to 14 that a completely flat velocity profile is attained.[140] The relationship between turbulence and α is important but controversial. Hino et al (from flow studies in a pipe) reported that decreasing α will tend to stabilize the flow but Nerem and Seed (from experimental recordings of aortic blood velocities in humans and other animals) reported the opposite ie decreasing α destabilizes flow.[126,141]

When considering values of α in the common carotid artery a correction factor should be applied which would have the effect of raising α. This is because systole is of much shorter duration than diastole in the cardio-vascular system. Measurements in the carotid arteries from sonagrams obtained from volunteers (in Experiment 1.1) showed that the arterial systolic velocity wave occupied only 15% to 20% of the cardiac cycle. Allowing a similar reverse component as in a sine wave, would give a true period of 30% to 40% of the original. Table 64 shows that the value of α in the common carotid artery is raised considerably if a correction factor is applied.

TABLE 64 Values for α in the Common Carotid Artery

(Calculated Using a Value of $\nu = 3.4 \times 10^{-2}$ stokes)

	Value for α Where Systole Occupies		
Heart Rate (beats/min)	Whole Cardiac Cycle	$^{2}/_{5}$ Cardiac Cycle	$^{1}/_{6}$ Cardiac Cycle
60	2.2	3.4	5.3
72	2.4	3.8	5.8
120	3.1	4.9	7.5
140	3.3	5.2	8.1
213	-	-	10
510	-	10	
1275	10		

Flow disturbances distal to stenoses have been demonstrated in models hence it was not unexpected that the introduction of a stenosis in our model caused a disturbance of flow visualized by dye and also clearly demonstrated using ultrasound with irregularity of the maximum frequency envelope, loss of the spectral window and retrograde flow caused by vortices both proximal and distal to the stenosis.[131,132,135,136,138]

The secondary waves seen in Experiments 5.2.1 to 5.2.4 were considered to be have been caused by the elasticity of the tubing but the introduction of a stenosis affected the time phasing between them. D'Luna et al using PW ultrasound found vortices distal to a stenosis which caused a reduction in luminal diameter of 50% however in Experiment 5.2.4 vortices were detected when there was a less severe stenosis.[138]

The Sonagraph ≠1 displays generally exhibited the same information as those of the Vasoscan although on occasion certain irregularities of the former display were seen. The Sonagraph ≠1 displays were inferior in quality than those of the Vasoscan and these irregularities were considered to be instrumental in origin.

In Experiments 5.2.1 to 5.2.4 and in the carotid arteries of normal patients where a clear window was present the ≠2 displays had the 'waisted' appearance indicative of a flat velocity profile as previously discussed and it was only in diastole in the carotid arteries that the flat spectrum of parabolic laminar flow was seen. In the femoral and subclavian arteries the flat spectrum of a parabolic flow profile was seen at peak systole. Paradoxically at stenoses both in the model and in patients no characteristic #2 spectra were seen. The problem of relating #2 spectra to the velocity profile rather than vice versa is complicated by the fact that flow has to be axisymmetric. Flow is not axisymmetric at the bifurcation of the common carotid artery where the velocity is higher on the medial side of the internal carotid artery, nor is it when there is curvature of the artery.[137,138]

These findings ie where a clear window and 'waisted' #2 spectra are present suggest that a flat velocity profile in systole is the norm with minimal boundary layer effects possibly due to the momentum of the flow wave ie there is not enough time for a fully developed parabolic profile. They also suggest that contrary to the case of steady flow, in oscillatory flow a flat velocity profile occurs in systole in the common carotid artery regardless of the presence of laminar or turbulent flow. Both parabolic and flat velocity profiles, determined using PW instruments, have been reported in systole in the common carotid artery.[127,142]

CW ultrasound can identify that variety of flow disturbance that occurs distal to a stenosis. The shedding of vortices causes large velocity fluctuations but the flow is soon stable downstream and the flow disturbance is not self perpetuating. CW ultrasound however failed to identify turbulence in Experiments 5.2.1 to 5.2.4 and this may be because the velocity fluctuations that occur in the degrees of turbulence described by Hino et al were not large enough and the averaging that takes place in the processing of the signals eliminates them.[141] This might also be the case for the #2 spectra; the fluctuations that occur in the velocity profile of a turbulent flow being too small to be manifested in the frequency/intensity pattern of the #2 spectra.

Other disturbances of flow not investigated in this Chapter but which would probably go undetected using CW ultrasound include a disturbance at an irregular area of the arterial wall and also a disturbance of the central core of the flow with flow undisturbed at the arterial wall.[117] Such disturbances are unlikely to be detected because signals from the rest of the lumen mask those from the disturbances.

G E N E R A L   D I S C U S S I O N

GENERAL DISCUSSION

A thorough knowledge of an instrument in terms of what it can and cannot do is essential for any operator. Furthermore the accuracy and reliability of its performance in relation to its manufacturers claims needs to be investigated hence the experiments described in Chapter 2 were necessary.

In attempting to detect disease at the carotid bifurcation using CW ultrasound it has been shown in Chapter 1 that waveform analysis is only successful in the identification of those stenoses causing a reduction in the lumen of an artery by 50% or more. The result was approximately the same whether the maximum systolic frequency, the degree of spectral broadening or ultrasonic imaging (a combination of the first 2 variables) was used. The poor performance of the resistance parameter is likely to have been due to inaccuracies in the way the instrument measures it.

Neither by eliminating the problem whereby the angle of insonation is unknown and using velocity measurements (described in Chapter 3) nor by calculating an index derived from frequency measurements both proximal and distal to a stenosis (described in Chapter 4) was this result altered.

This implies that mild degrees of carotid stenosis do not affect the maximum velocity or the degree of spectral broadening significantly (even though the patient may be symptomatic) and any simple index based on the maximum frequency envelope is unlikely to be useful despite the claims of certain authors.[71,77,80] This may not apply to the more complicated method of principal component analysis although there is no indication as yet that its use is going to be any more successful.

Atherosclerosis does not always cause a stenosis eg an ulcerated pit, however, the presence of this or a mild degree of stenosis might be detected by a disturbance of flow.

It was shown in Chapter 5 that CW ultrasound could distinguish between laminar and turbulent steady flow, however, flow in the carotid arteries is not steady during systole.

It is widely accepted that an increase in spectral broadening at peak systole indicates turbulence within the artery. However turbulence does not vary in increments in distinction to the degree of spectral broadening which may vary from 0% to 100% (or more). Experiments (5.2.1 to 5.2.3) found that CW ultrasound failed to detect turbulence in a tube but readily detected the disturbance of flow that occurred when a stenosis was introduced. It is likely that at least 2 varieties of disturbances of oscillatory flow occurred in these experiments (there may have been more),

(i) that caused by a stenosis (with high Reynolds numbers over a short distance only) and

(ii) that caused by high Reynolds numbers and high values of α in the whole flow channel (giving rise to a self perpetuating turbulent flow similar to that seen in steady flow under appropriate conditions).

CW can detect the first which is unlikely to be true turbulence (merely a disturbance) but not the second. With regard to the normal carotid artery the occurrence of the second variety of flow disturbance (true turbulence) cannot be excluded because it cannot be detected using CW ultrasound and also high Reynolds numbers and high values of α may be attained depending on the way in which the calculations are performed (see Table 64).

Another paradox in the consideration of spectral broadening is that it was shown in Experiment 5.3 that a flat velocity profile occurs in the normal carotid artery at peak systole (when the degree of spectral broadening is less than 50%). A flat velocity profile occurs in turbulent steady flow. When the degree of spectral broadening increases eg distal to a stenosis, a velocity profile which has a more parabolic configuration would be predicted from theory.

An interesting further experiment would be the effect of a compliant tube, as opposed to an inelastic one, on the stability of oscillatory flow. Attinger et al have looked at oscillatory flow in distensible tubes and reported that turbulence occurs in these tubes at higher

Reynolds numbers than in comparable rigid tubes.[117]

With regard to PW instruments it would be useful to repeat the experiments in Chapter 5 using a Duplex scanner with the construction of the velocity profile across the lumen of the vessel and to investigate the effect on the velocity profile caused by atherosclerotic plaques associated with only a slight narrowing of the carotid artery. The velocity profile has been studied by others both in models and in vivo but its value has not been fully appraised.[83,92,129]

The continued development of Doppler ultrasound (both CW and PW instruments) seems likely to lead to further advances in our understanding of the physiology of the circulation and the detection of carotid artery disease.

R E F E R E N C E S

1 Fry DL. Acute vascular endothelial changes associated with increased blood velocity gradients. Circulation Res 1968; 22:165-197.

2 Texon M, Imparato AM, Helpern M. The role of vascular dynamics in the development of atherosclerosis. JAMA 1965; 194:1226-1230.

3 Carrascal L, Mashiah A, Charlesworth D. Aneurysms of the extracranial carotid arteries. Br J Surg 1978; 65:590-592.

4 Schwartz CJ, Mitchell JRA. Atheroma of the carotid and vertebral arterial systems. Br Med J 1961; ii:1057-1063.

5 Hass WK, Fields WS, North RR, Kricheff II, Chase NE, Bauer RB. Joint study of extracranial arterial occlusion. II. Arteriography, techniques, sites and complications. JAMA 1968; 203:961-968.

6 Singer C, Underwood EA. A short history of medicine. Oxford:Clarendon Press, 1962.

7 Dale WA. The beginnings of vascular surgery. Surgery 1974; 76:849-866.

8 Vesalii A. De humani corporis fabrica. Basileae, 1543. Reprinted, Bruxelles:Culture et civilisation, 1964.

9 Willis T. Pratise of Physick. London:S Pordage, 1664.

10 Gull WW. Thickening and dilatation of the arch of the aorta with occlusion of the innominata and left carotid, and atrophic softening of the brain. Guy's Hospital Reports 1855; Vol 16 (3rd series), 1:12-18.

11 Hunt JR. The role of the carotid arteries in the causation of vascular lesions of the brain with remarks on certain special features of the symptomatology. Am J Med Sciences 1914; 147:704-713.

12 Fisher M. Occlusion of the carotid arteries. Arch Neurol Psych 1954; 72:187-204.

13 Knight S. Jack the Ripper : the final solution. London: Granada, 1977.

14 Hicks SP, Black BK. The relation of cerebrovascular disease to apoplexy. Am Heart J 1949; 38:528-536.

15 Hicks SP, Warren S. Infarction of the brain without thrombosis. Arch Path 1951; 52:403-412.

16 The Registrar General's statistical review of England and Wales. London:HMSO, 1953.

17 The Registrar General's statistical review of England and Wales. London:HMSO, 1963.

18 The Registrar General's statistical review of England and Wales. London:HMSO, 1973.

19 Annual report of the Registrar General for Scotland. Edinburgh:HMSO, 1963.

20 Annual report of the Registrar General for Scotland. Edinburgh:HMSO, 1973.

21 Howe GM. National atlas of disease mortality in the Kingdom. London:Nelson, 1970.

22 Adelman SM. Economic Impact. In:Weinfeld FD, ed. The national survey of stroke. Stroke 1981; 12:Supplement No 1.

23 Toole JF, Janeway R, Choi K, Cordell R, Davis C, Johnston F, Miller HS. Transient ischaemic attacks due to atherosclerosis. Arch Neurol 1975; 32:5-12.

24 Crawford ES, DeBakey ME, Blaidsdell FW, Morris GC, Fields WS. Haemodynamic alterations in patients with cerebral arterial insufficiency before and after operation. Surgery 1960; 48:76-94.

25 May AG, Vande Berg L, DeWeese JA, Rob CG. Critical arterial stenosis. Surgery 1963; 54:250-258.

26 Kety SS. Fundamental aspects of the human cerebral circulation and their implications for cerebrovascular disease. In:Brest AN, Moyer JH ed. Atherosclerotic vascular disease. London:Butterworths, 1967.

27 Knox RA, Breslau PJ, Chikos PM, Strandness DE. The collateral circulation to the brain. In preparation 1986.

28 Russell RWR. Observations on the retinal blood vessels in monocular blindness. Lancet 1961; ii:1422-1428.

29 Crompton MR. Pathology of degenerative arterial disease. In:Russell RWR, ed. Cerebral arterial disease. Edinburgh: Churchill Livingstone, 1976.

30 Meyer JS. Occlusive cerebrovascular disease. Pathogenesis and treatment. Am J Med 1961; 30:577-588.

31 Fields WS, Lemak NA. Joint study of extracranial arterial occlusion. VII. Subclavian steal - a review of 168 cases. JAMA 1972; 222:1139-1143

32 Reivich M, Holling HE, Roberts B, Toole SF. Reversal of blood flow through the vertebral artery and its effect on cerebral circulation. N Engl J Med 1961; 265:878-885.

33 Javid H, Ostermuller WE, Hengesh JW, Dye WS, Hunter JA, Najafi H, Julian OC. Natural history of carotid bifurcation atheroma. Surgery 1970; 67:80-86.

34 Meyer JS, Bauer RB, Rayson GE. Natural history of extracranial insufficiency. In:Brest AN, Moyer JH, ed. Atherosclerotic vascular disease. London:Buttterworths, 1967.

35 Colgan MP, Kingston W, Shanik DG. Asymptomatic carotid stenosis : is prophylactic endarterectomy justifiable? Br J Surg 1985; 72:313.

36 Moore WS, Malone JM, Boren C, Roon AJ, Goldstone J. Asymptomatic ulcerative lesions of the carotid artery - Natural history and effect of surgical therapy combined. Stroke 1979; 10:96.

37 Greenhalgh RM, Ellis M. Waiting for symptoms in patients with asymptomatic carotid bruits. Br J Surg 1983; 70:388.

38 Cooperman M, Martin EW, Evans WE. Significance of asymptomatic carotid bruits. Arch Surg 1978; 113:1339-1340.

39 Marquardsen J. Natural history and prognosis of cerebrovascular disease. In:Russell RWR, ed. Cerebral arterial disease. Edinburgh:Churchill Livingstone, 1976.

40 Marshall J, Kaeser AC. Survival after non haemorrhagic cerebrovascular accidents. Br Med J 1961; ii:73-77.

41 Mundall JM, Quintero P, Von Kaulla KN, Harmon R, Austin J. Transient monocular blindness and increased platelet aggregability treated with aspirin. Neurology 1972; 22: 280-285.

42 Acheson J, Danta G, Hutchinson EC. Controlled trial of dipyrimadole in cerebral vascular disease. Br Med J 1969; i:614-615.

43 Eastcott HHG, Pickering GW, Rob CG. Reconstruction of internal carotid artery in a patient with intermittent attacks of hemiplegia. Lancet 1954; ii:994-996.

44 Fields WS, Maslenikon V, Meyer JS, Hass WK, Remington RD, MacDonald M. Joint study of extracranial arterial occlusion. V. Progress report of prognosis following surgery or non surgical treatment for transient cerebral ischaemia attacks and cervical carotid artery lesions. JAMA 1970; 211:1993-2003.

45 Nunn DB. Carotid endarterectomy : an analysis of 234 operative cases. Ann Surg 1975; 182:733-738.

46 White JS, Sirinek KR, Root HD, Rogers W. Morbidity and mortality of carotid endarterectomy. Arch Surg 1981; 116: 409-412.

47 Thompson JE, Austin DJ, Patman RD. Carotid endarterectomy for cerebrovascular insufficiency : long term results in 592 patients followed up to 13 years. Ann Surg 1970; 172: 663-679.

48 Haynes CD, Dempsey RL. Carotid endarterectomy. Review of 276 cases in a community hospital. Ann surg 1979; 189: 758-762.

49 Riles TS, Lieberman A, Kopelman I, Imparato AM. Symptoms, stenosis and bruit. Interrelationships in carotid artery disease. Arch Surg 1981; 116:218-220.

50 Perry HA, Morros CD. Predicting significant atherosclerosis of the carotid artery. Am Surg 1983; 49:21-25.

51 Murie JA, Sheldon CD, Quin RO. Carotid artery bruit : association with internal carotid artery stenosis and intra-luminal turbulence. Br J Surg 1984; 71:50-52.

52 Thompson JE, Patman RD, Persson AV. Management of asymptomatic carotid bruits. Am Surg 1976; 42:77-80.

53 Krayenbuhl HA, Yasargil HG. Cerebral angiography. London: Butterworths, 1968.

54 Moniz E. Hemiplegies pour trombose de la carotide interne. La Presse Medicale 1937; 52:977.

55 List CF, Burge CH, Hodges FJ. Intracerebral angiography. Radiology 1945; 45:1-14.

56 Hessel SJ, Adams DF, Abrams HL. Complications of angiography. Radiology 1981; 138:273-281.

57 Swanson PD, Calanchini PR, Dyken ML, Gotshall RD, Haever AF, Poskanzer DC. A co-operative study of hospital frequency and character of transient ischaemic attacks. JAMA 1977; 237:2202-2206.

58 Kartchner MM, McRae LP, Crain V, Withaker B. Oculoplethysmography : an adjunct to arteriography in the diagnosis of extracranial carotid occlusive disease. Am J Surg 1976; 132:728-732.

59 Hofferberth B, Gottschaldt M, Dykan S. Comparison of Doppler sonography and plate thermography for detection of carotid artery stenosis. Stroke 1980; 11:27-30.

60 Malone JM, Bean BB, Laguna J, Hamilton R, Labadie E, Moore WS. Diagnosis of carotid artery status. Comparison of oculoplethysmography and Doppler supraorbital examination. Ann Surg 1980; 191:347-354.

61 Kistler JP, Lees RS, Miller A, Cromwell RM, Roberson G. Correlation of spectral phonoangiography and carotid angiography with gross pathology in carotid stenosis. N Engl J Med 1981; 305:417-419.

62 Keagy BA, Pharr WF, Thomas DD, Bowes DE. Oculoplethysmography/carotid phonoangiography. Its value as a screening test in patients with suspected carotid artery stenosis. Arch Surg 1980; 115:1199-1202.

63 Appleberg M, Chambers JL, Lane R. A comparison of non-invasive methods in the assessment of extracranial carotid artery disease. Aust NZ J Surg 1982; 52:258-264.

64 Chapman BLW. Phonoangiography : the clinical significance and origin of sounds in the carotid arteries. PhD Thesis: Univ of Manchester; 1981.

65 O'Leary DH, Persson AV, Clouse ME. Non-invasive testing for carotid artery stenosis. Prospective analysis of 3 methods. A J R 1981; 137:1189-1194.

66 Horrocks M, Roberts VC, Cotton LT. Assessment of carotid artery stenosis using pulse wave transit time. Br J Surg 1979; 66:265-268.

67 Padayachee TS, Lewis RR, Gosling RG. Detection of carotid bifurcation disease : comparison of ultrasound tests with angiography. Br J Surg 1982; 69:218-222.

68 Baskett JJ, Beasley MG, Murphy GJ, Hyams DE, Gosling RG. Screening for carotid junction disease by spectral analysis of Doppler signals. Cardiovasc Res 1977; 11:147-155.

69 Barnes RW, Rittgers SE, Putney WW. Real time Doppler spectrum analysis. Predictive value in defining operable carotid artery disease. Arch Surg 1982; 117:52-57.

70 Zbornikova V, Akesson JA, Lassvik C. Diagnosis of carotid artery disease - comparison between directional Doppler, Duplex scanner and angiography. Acta Neurol Scandinav 1982; 65:335-346.

71 Rutherford RB, Hiatt WR, Kreutzer EW. The use of velocity waveform analysis in the diagnosis of carotid artery occlusive disease. Surgery 1977; 82:695-702.

72 Weaver RG, Howard G, McKinney WM, Ball MR, Jones AM, Toole JF. Comparison of Doppler ultrasonography with arteriography of the carotid artery bifurcation. Stroke 1980; 11:402-404.

73 Johnston KW, deMorais D, Kassam M, Brown PM. Cerebrovascular assessment using a Doppler carotid scanner and real time frequency analysis. J Clin Ultrasound 1981; 9:443-449.

74 Turnipseed WD, Sackett JF, Strother CM, Crummy AB, Mistretta CA. A comparison of standard cerebral arteriography with non-invasive Doppler imaging and intravenous angiography. Arch Surg 1982; 117:419-421.

75 Johnston KW, Brown PM, Kassam M. Problems of carotid Doppler scanning which can be overcome by using frequency analysis. Stroke 1982; 13:660-666.

76 Brown PM, Johnston KW, Douville Y. Detection of occlusive disease of the carotid artery with continuous wave Doppler spectral analysis. Surg Gynaecol Obstet 1982; 155:183-186.

77 Keagy BA, Pharr WF, Thoms D, Bowes DE. Objective criteria for the interpretation of carotid artery spectral analysis patterns. Angiology 1982; 33:213-220.

78 Fell G, Phillips DJ, Chikos PM, Harley JD, Thiele BL, Strandness DE. Ultrasonic Duplex scanning for disease of the carotid artery. Circulation 1981; 64:1191-1195.

79 Breslau PJ, Fell G, Phillips DJ, Thiele BL, Strandness DE. Evaluation of carotid bifurcation disease. The role of common carotid artery velocity patterns. Arch Surg 1982; 117:58-60.

80 Knox RA, Breslau PJ, Strandness DE. A simple parameter for accurate detection of severe carotid disease. Br J Surg 1982; 69:230-233.

81 Thomas M, Otis SM, Rush MM, Zyroff J, Dilley RB, Bernstein EF. The contribution of spectral analysis to the diagnosis of carotid artery disease. J Vasc Surg 1985; 2:270-277.

82 Hennerici M, Freund HJ. Efficiency of CW - Doppler and Duplex system examinations for the evaluation of extra-cranial carotid disease. J Clin Ultrasound 1984; 12:155-161.

83 Hennerici M, Reifschneider G, Trockel U, Aulich A. Detection of early atherosclerotic lesions by Duplex scanning of the carotid artery. J Clin Ultrasound 1984; 12:455-464.

84 Ratcliff DA, Hames TK, Humphries KN, Chant ADB. The detection of carotid disease using Doppler imaging and Duplex scanning. Br J Surg 1984;71:380.

85 Sherriff SB, Barber DC, Martin TRP. Use of principal component factor analysis in the detection of carotid artery disease from Doppler ultrasound. Med Biol Eng Comput 1982; 20:351-356.

86 Wood A. Acoustics. Glasgow:Blackie, 1963.

87 Satomura S. Study of the flow patterns in peripheral arteries by ultrasonics. J Acoust Soc Japan 1959; 15:151-158.

88 Histand MB, Miller CW, McLeod FD. Transcutaneous measurement of blood velocity profiles and flow. Cardiovasc Res 1973; 7:703-712.

89 Allan JS, Terry HJ. The evaluation of an ultrasonic flow detector for the assessment of peripheral vascular disease. Cardiovasc Res 1969; 3:503-509.

90 Reneman RS, Clarke HF, Simmons N, Spencer MP. In vivo comparison of electromagnetic and Doppler flow meters; with special attention to the processing of an analogue Doppler flow signal. Cardiovasc Res 1973; 7:557-566.

91 Johnston KW, Maruzzo BC, Cobbold RSC. Inaccuracies of a zero crossing detector for recording Doppler signals. Surg Forum 1977; 28:201-203.

92 Hoeks APG. On the development of a multi-gate pulsed Doppler system with serial data-processing. Thesis:Univ of Limburg, The Netherlands, 1982.

93 Thiele BL, Hutchinson KJ, Forster FK, Strandness DE. Pulsed Doppler velocity waveform patterns produced by smooth stenosis in the dog thoracic aorta. In:Taylor DEM, Stevens AL, ed. Theory and practices of blood flow measurements. London:Academic Press, 1983.

94 Pourcelot L. Continuous wave Doppler techniques in cerebral vascular disturbances. In:Reneman RS, Hoeks APG, ed. Doppler ultrasound in the diagnosis of cerebrovascular disease. Chichester:Research Studies Press, 1982.

95 Bader H. Dependence of wall stress in the human thoracic aorta on age and pressure. Circulation Res 1967; 20:354-361.

96 Underwood CJ, Charlesworth D. The errors involved in angiographic quantification of vascular stenosis. In preparation. 1986.

97 Thomas M, Rutt DL, Powell SA, Browse NL. Estimation of disease in the atheromatous carotid artery. Br J Surg 1984; 11:899.

98 Bandyk DF, Levine AW, Pohl L, Towne JB. Classification of carotid bifurcation disease using quantitative Doppler spectrum analysis. Arch Surg 1985; 120:306-314.

99 Murie JA, Quin RO, Forrest H, Sheldon CD. Pulsed Doppler imaging and spectrum analysis for detection of carotid artery disease. Angiology 1984; 35:215-221.

100 Rittenhouse EA, Strandness DE. Oscillatory flow patterns in patients with aortic valve disease. Am J Cardiol 1971; 28:568-574.

101 Shepherd JT. Physiology of the circulation in human limbs in health and disease. Philadelphia:Saunders, 1963.

102 Breslau PJ. Ultrasonic Duplex scanning in the evaluation of carotid artery disease. MD Thesis:University of Limburg, The Netherlands, 1982.

103 Spencer MP. Doppler evaluation of the aortocranial circulation using carotid imaging and hand-held probing. In: Reneman RS, Hoeks APG, Doppler ultrasound in the diagnosis of cerebrovascular disease. Chichester:Research Studies Press, 1982.

104 Shung KK, Fei DY, Bronez MA. Effects of atherosclerotic lesions on ultrasonic beam and CW Doppler signals. J Clin Ultrasound 1985; 13:11-18

105 Wells PNT. Ultrasonics in clinical diagnosis. Edinburgh: Churchill Livingstone, 1972, 5.

106 Wells PNT. Biomedial ultrasonics. London:Academic Press, 1977, 361.

107 Woodcock JP. Theory and practice of blood flow measurement. London:Butterworths, 1975.

108 Shoor PM, Fronek AF, Bernstein EF. Quantitative transcutaneous arterial velocity measurements with Doppler flowmeters. Arch Surg 1979; 114:922-928.

109 Reagan TR, Miller CW, Strandness DE. Transcutaneous measurement of femoral artery flow. J Surg Res 1971; 11: 477-482.

110 Fahrbach K. Ein beitrag zur blutgeschwindigkeitsmersung unter anwendungdes Doppler effektes. Elektromedizin 1970; 15:26-36.

111 Duck FA, Hodson CJ. A practical method of eliminating the angular dependence of Doppler flow measurements. Excerpta Medica International Congress Series 1973; 277:15-16.

112 Hansen PL, Cross G, Light LH. In:Woodcock JP, ed. Clinical blood flow measurement. London:Pitman Medical, 1976, page 28.

113 Woodcock JP. Measurement of blood flow using ultrasound. In:Mathie RT ed. Blood flow measurement in man. Kent: Castle House Publications, 1982, 65.

114 Berguer R, Hwang NHC. Critical arterial stenosis : a theoretical and experimental solution. Ann Surg 1974; 180:39-50.

115 Blackshear WM, Phillips DJ, Chikos PM, Harley JD, Thiele BL, Strandness DE. Carotid artery velocity patterns in normal and stenotic vessels. Stroke 1980; 11:67-71.

116 Humphreys WV. The viscosity of blood and its significance in patients with vascular disease. MD Thesis:Univ of Manchester, 1975.

117 Attinger EO, Sugawara H, Navarro A, Anne A. Pulsatile flow patterns in distensible tubes. Circulation Res 1966; 18: 447-456.

118 Yellin EL. Laminar-turbulent transition process in pulsatile flow. Circulation Res 1966; 19:791-804.

119 D'Luna LJ, Newhouse VL. Vortex characterisation and identification by ultrasound Doppler. Ultrasonic Imaging 1981; 3:271-293.

120 Hussain AKMF. Mechanics of pulsatile flows of relevance to the cardiovascular system. In:Hwang NHC, Norman NA, ed. Cardiovascular flow dynamics and measurement in man. Baltimore:Univ Park Press, 1977.

121 Van Dongen MEH, Van Steenhoven AA. Some fluid dynamical aspects of arterial flow. In:Reneman RS, Hoeks APG, ed. Doppler ultrasound in the diagnosis of cerebrovascular disease. Chichester:Research Studies Press, 1982.

122 McDonald DA. Blood flow in arteries. London:Edward Arnold, 1974.

123 Strandness DE, Sumner DS. Hemodynamics for surgeons. New York:Grune and Stratton, 1975.

124 Harris PL. The role of ultrasound in the assessment of peripheral arterial disease. MD Thesis:Univ of Manchester, 1974.

125 Womersley JR. Oscillatory flow in arteries : effect of radial variation in viscosity on rate of flow. J Physiol 1955; 127:38-39.

126 Nerem RM, Seed WA. An in vivo study of aortic flow disturbances. Cardiovasc Res 1976; 6:1-14.

127 Isabey D. Steady and pulsatile flow distribution in a multiple branching network with physiological applications. J Biomech 1982; 15:395-404.

128 Cronestrand R. Blood flow after carotid, subclavian, renal and leg artery reconstruction. In:Roberts C, ed. Blood flow measurement. London:Sector Publishing Ltd, 1972.

129 Bharadvaj BK, Mabon RF, Giddens DP. Steady flow in a model of the human carotid bifurcation. Part I - flow visualisation. J Biomech 1982; 15:349-362.

130 Clark C. The propagation of turbulence produced by a stenosis. J Biomech 1980; 13:591-604.

131 Roach MR, Stockley D. The effects of the geometry of a stenosis on post stenotic flow in models and post stenotic vibration of cannine carotid arteries in vivo. J Biomech 1980; 13:623-634.

132 Kim HB, Corcoran WH. Experimental measurements of turbulence spectra distal to stenoses. J Biomech 1974; 7:335-342.

133 McEvoy NM, Pimmel RL, Nerem RM. A computer analysis of high frequency disturbances in arterial blood flow. Computers and Biomedical Research 1976; 9:75-88.

134 Khalifa AMA, Giddens DP. Analysis of disorder in pulsatile flows with applications to post stenotic blood velocity measurements in dogs. J Biomech 1978; 11:129-141.

135 Cassanova RA, Giddens DP. Disorder distal to modelled stenoses in steady and pulsatile flow. J Biomech 1978; 11: 441-453.

136 Khalifa AMA, Giddens DP. Characterization and evolution of post stenotic flow disturbances. J Biomech 1981; 14: 279-296.

137 Bharadvaj BK, Mabon RF, Giddens DP. Steady flow in a model of the human carotid bifurcation. Part II Laser - Doppler anemometer measurements. J Biomech 1982; 15:363-378.

138 D'Luna LJ, Newhouse VL, Giddens DP. In vitro Doppler detection of axisymmetric stenoses from transverse velocity measurements. J Biomech 1982; 15:647-660.

139 Sigel B, Gibson RJ, Amatneek KV, Felix WR, Edelstein AL, Popky GL. A Doppler ultrasound method for distinguishing laminar from turbulent flow. J Surg Res 1970; 10:221-224.

140 Gerrard JH. An experimental investigation of pulsating turbulent water flow in a tube. J Fluid Mech 1971; 46:43-64.

141 Hino M, Sawamoto M, Takasu S. Experiments on transition to turbulence in oscillatory pipe flow. J Fluid Mech 1976; 75:193-207.

142 Reneman RS, Pourcelot L, Hoeks APG. Prospects and conclusions. In:Reneman RS, Hoeks APG, ed. Doppler ultrasound in the diagnosis of cerebrovascular disease. Chichester: Research Studies Press, 1982.

143 McNeil BJ, Keeler E, Adelstein SJ. Primer on certain elements of medical decision making. N Engl J Med 1975; 293:211-215.

A P P E N D I C E S

APPENDIX 1 The Scale of the Flow Map Display

The scale of the flow map displayed on the screen was determined by "insonating" the intersections on a grid of one cm ruled squares using the 4 MHz probe held in a transverse position in the spatial sensing arm. When the probe was positioned over an intersection extraneous noise was produced causing a dot to appear on the screen. A map of dots was produced (see Figure 69) and the distance between them was measured to be 0.8 cm. This gave a scale for the displayed flow map of 1.25 : 1. It was only at the edges of the screen that this relationship was lost.

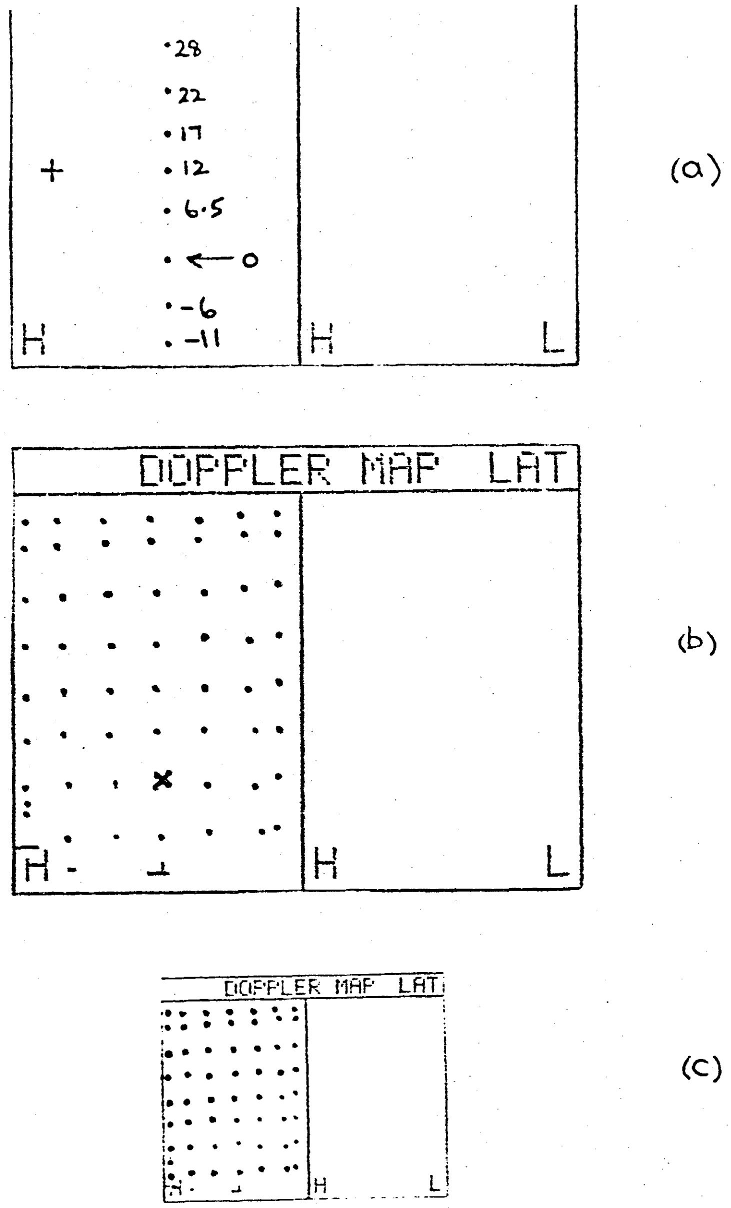

FIGURE 69

The scale of the displays
The scale of the large scale print out [(a) and (b)] was 1.67 : 1 and the scale of the smaller scale print out (c) was 1.33 : 1. This scale was lost at the edges of the screen. In (a) the figures are the distances between the dots in mm.

APPENDIX 2 A Decision Matrix

The method of assessing the accuracy of each variable in Experiment 1.2 was by using decision matrices.[143]

A standard decision matrix is shown in Figure 70. A threshold value is set for the test and a test value greater than or equal to the threshold represents a positive result. The numbers of positive and negative results are compared with the true presence of disease as determined by either arteriograms or surgery. The sensitivity of the test expresses the number of true positive results and the specificity the number of true negative results.

A good diagnostic test will have a high rate of true positive results (sensitivity), a low rate of false positive results; a high rate of true negative results (specificity) and a low rate of false negative results.

Increasing the threshold value increases the specificity of the test but decreases the sensitivity.

DECISION MATRIX

		TEST	
		Abnormal +	Normal −
PRESENCE OF DISEASE	Present +	a	b
	Absent −	c	d

$$\text{Sensitivity} = \frac{a}{a+b}$$

$$\text{Specificity} = \frac{d}{c+d}$$

FIGURE 70

A decision matrix

APPENDIX 3 The Selection of the Ultrasonic Scatterer in the Medium

The ideal ultrasound reflector should be small, evenly distributed in the medium, scatter ultrasound well, stable in the medium, not alter its physical properties and store well. Commercially available Sephadex particles (Dow Corning) are available of size 0.5 μm but are expensive. Several reflectors were used in the experiments in this thesis and problems encountered in their usage were:-

(i) Air bubbles were used in Experiment 3.1.2 but there were difficulties in getting a steady injection rate and even at the lowest setting of the constant infusion pump (0.5 ml /min) the bubbles were still too large.

(ii) Milk was used in several of the experiments and scattered ultrasound well. Furthermore it was inexpensive, readily available, mixed thoroughly in water and did not alter its viscosity. Its major drawback was it quickly deteriorated and added to the offensive smells in the Laboratory! It also left a coating on the surface of the chambers and tubing with which it came into contact and this irregular 'fur' was a source of flow disturbance. Regular cleansing of the apparatus with warm water and a biological detergent was necessary to remove this lining.

(iii) Red blood cells fixed with glutaraldehyde were tried. They were prepared as follows:-

(i) 330 ml of packed red cells (time expired for patient transfusion) were obtained from the hospital blood bank mixed with an equal quantity of 0.9% saline and 1.1 ml of glutaraldehyde and allowed to stand for 5 minutes.

(ii) To obtain a concentrated solution the fixed red cells were washed with 0.9% saline and centrifuged at 2,000 rpm for 12 minutes at 4^{o} C. The washing and spinning was repeated 4 times and the resultant solution stored at 10^{o} C.

In the model the red cells were injected proximal to the test section and were used successfully on some occasions but unfortunately at the low rates of flow necessary to create laminar conditions the stream of red cells drifted slowly to the bottom of the tube and at the high rates of turbulent flow the dispersal of the red cells in the medium was too great to give an adequate backscattered signal.

(iv) An emulsion of Silicone in water eventually proved to be the reflector of choice. The Silicone was immiscible in water and required frequent stirring to ensure dispersal. Its particle size varied, some of the particles were large enough to be visible to the naked eye. The concentration used was not high enough to alter the viscosity of the medium (see Table 55).

APPENDIX 4 A Problem in Flow Characterization Using Dye

An independent technique was necessary to demonstrate the presence of laminar or turbulent flow in the model and this was done by injecting dye 2 m proximal to the test section using a constant infusion pump. Dispersion of the dye in the medium indicated turbulence. It was noticed that the character of the lines of dye in the vessel depended not only on the conditions of flow in the vessel but also on the rate of injection of the dye. This problem was studied because at high rates of flow in the model high rates of injection of dye were necessary to enable its visualisation.

Method

Water was circulated through the model (see Figure 45) under steady conditions of flow and the Reynolds number was steadily increased from 64 to 3449. Dye was injected proximal to the test section and for each value of Reynolds number the rate of injection was varied from 0.5 ml/min to 1.0, 1.5, 2.0, 3.75 and 5.0 ml/min. the character of the dye in the vessel was visually inspected allowing recognition of laminar flow (perfect streamlining of the dye lines), mild disturbances of flow (the lines of dye showed very slight wavering), severe disturbances (the lines of dye widened from the centre stream flow to the periphery and showed marked wavering) and turbulence (irregular mixing of the dye across the lumen). At very high rates of flow the dye was invisible.

Result

Table 65 and Figure 71 give the character of the dye lines at different rates of flow and injection of dye. Increasing the rate of injection of the dye decreased the value of Reynolds number at which disturbances and turbulence were seen in the test section. It was only at the lowest rate of injection ie 0.5 ml/min that the dye was perfectly streamline up to a Reynolds number of 1030.

Discussion

The model contains 2 flow systems, the circuit of tubing and the dye apparatus, and each has its own conditions for the onset of turbulence which together interact. The flow in the test section could be rendered unstable by merely injecting dye to demonstrate its character and therefore caution is necessary in interpreting the results of experiments both in models and in vivo which involve the injection of dye. In the experiments in Chapter 5 an injection rate of 0.5 ml/min only was used.

TABLE 65 The Character of the Flow in the Model at Different Rates of Injection of Dye

	Rate of Injection of Dye (ml/min)					
Reynolds Number	0.5	1.0	1.5	2.0	3.75	5.0
64	PS	PS	PS	MD	VT	VT
128	PS	PS	PS	MD	VT	VT
644	PS	PS	PS	MD	VT	VT
773	PS	PS	PS	MD	VT	VT
1030	PS	MD	MD	SD	SD	SD
1288	MD	MD	MD	SD	SD	SD
1391	MD	MD	MD	SD	SD	SD
1481	SD	SD	SD	SD	SD	SD
1546	SD	SD	SD	SD	SD	SD
1932	NV	SD	SD	SD	SD	SD
2125	NV	NV	NV	VT	VT	VT
2318	NV	NV	NV	NV	NV	NV
3449	NV	NV	NV	NV	NV	NV

PS - perfect streamlines
MD - mild disturbances
SD - severe disturbances
VT - visibly turbulent
NV - dye not visible

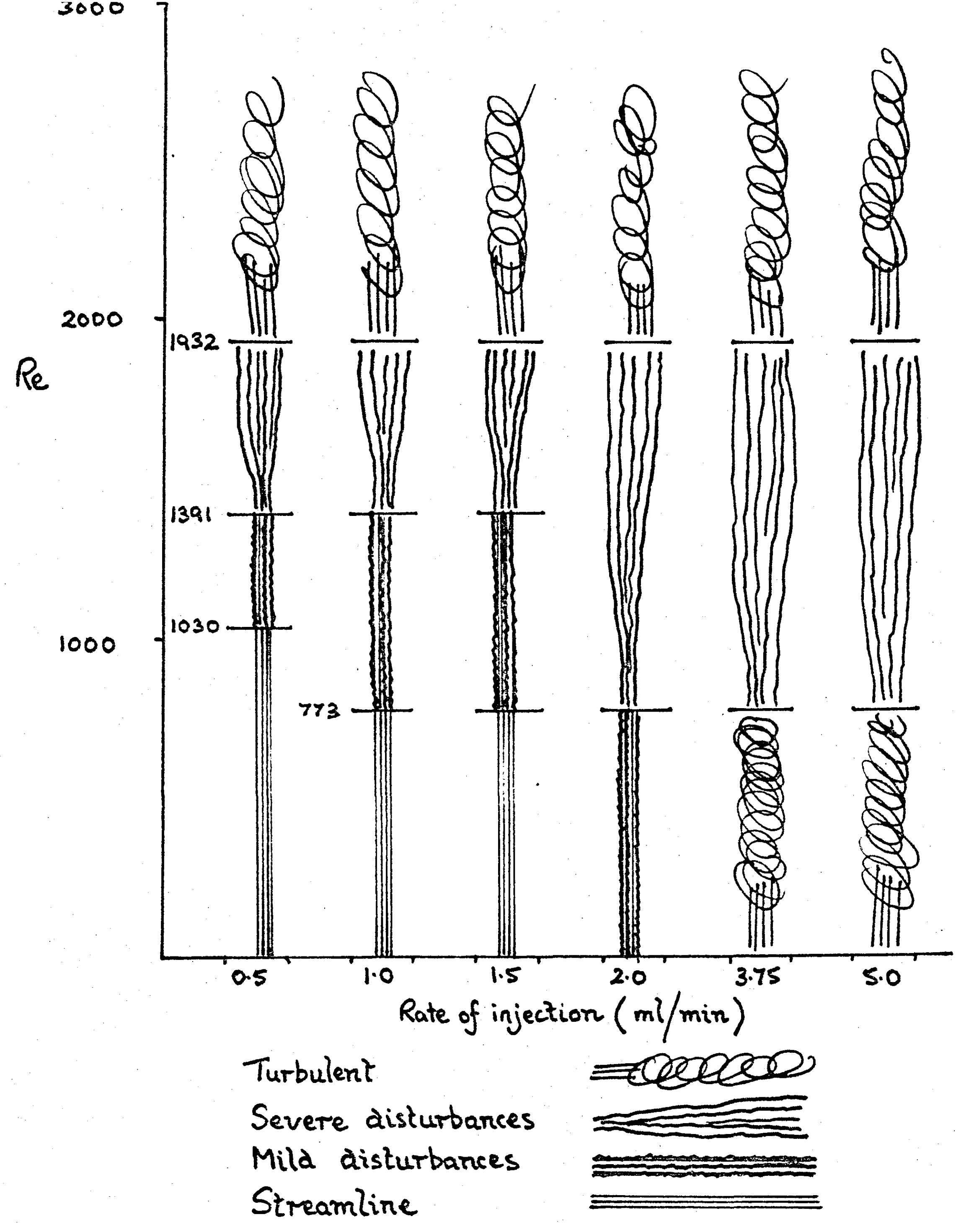

FIGURE 71

Disturbances of flow and the rate of injection of dye

APPENDIX 5 Finding a Critical Reynolds Number in the Model

Method

The rate of flow in the model was increased from 50 ml/min to 2350 ml/min using the roller pump and the constant pressure head to deliver volumes of flow up to 200 ml/min and the gas bomb for higher volumes of flow.

ΔF max was measured in the test section and $\bar{V}$ was calculated from the volume flow. The experiment was repeated twice : the first time using red cells to scatter the ultrasound using an angle of insonation of 60^{o}, the second using milk and an angle of insonation of 45^{o}. Flow was steady at all times.

The correlation coefficient of values (ΔF max, $\bar{V}$) was calculated in each experiment both for conditions of flow considered to be laminar and turbulent.

Results

Table 66 and 67 give the values of $\bar{V}$, Re and ΔF max for each experiment and Figures 72 and 73 values of Re plotted against ΔF max. Table 68 gives the correlation coefficients. A change in the relationship between Re and ΔF max was seen to occur in the first experiment between Reynolds numbers of 1050 and 1700 (Figure 72) and in the second between Reynolds numbers of 1050 and 2500 however the higher value of Re in the second experiment was probably an overestimate (see Figure 73).

TABLE 66 Finding the Critical Reynolds Number

Experiment (i)

$\bar{V}$ (cm/sec)	Re	ΔF max (KHz)
2.4	155	0.4
6.02	388	0.8
6.0	388	1.0
7.6	492	1.0
10.1	653	1.4
16.1	1034	2.1
21.1	1358	2.3
25.9	1668	2.3
40.2	2589	3.4
42.6	2744	3.5
50.2	3233	4.1
57.2	3684	4.2
57.2	3684	4.6
60.2	3684	4.4
68.2	3878	4.6
68.3	4399	5.2
68.3	4399	5.4
80.3	5172	5.8
80.3	5172	6.2
88.4	5692	6.4

TABLE 67 Finding the Critical Reynolds Number

Experiment (ii)

$\bar{V}$ (cm/sec)	Re	ΔF max (KHz)
2.4	142	0.5
2.8	165	0.5
4.6	272	1.0
5.5	325	1.0
6.0	355	1.1
6.8	402	1.1
7.6	449	1.4
8.4	496	1.4
9.6	567	1.6
10	591	1.7
10	591	1.8
12	709	2.0
13.6	804	2.5
14.8	875	2.5
15.6	922	2.5
16	945	2.7
17.5	1034	2.8
20	1182	3.2
22	1300	3.2
23	1359	3.4
24	1418	2.8
42	2482	4.0
45	2659	6.0
45	2659	5.7
51	3014	6.0
53	3132	6.7
60	3545	7.6
69	4077	8.7
72	4255	7.8
72	4255	8.2
81	4786	9.2
117	6914	9.8

TABLE 68 The Relationship Between the Mean Velocity of Flow and ΔF Max for Laminar and Turbulent Steady Flow

$\bar{V} : \Delta F$ max

Experiment	Character of Flow	n	CC	m	c	SE	p
(i)	LAM	6	0.99	7.98	- 0.88	0.6	0.0007
(i)	TURB	13	0.99	14.89	- 9.14	2.19	<0.001
(ii)	LAM	18	0.99	6.34	- 0.85	0.56	<0.001
(ii)	TURB	11	0.88	11.06	- 15.85	10.38	0.0006

The correlation coefficient (CC) of a straight line of gradient (m) in joining values of (ΔF max, $\bar{V}$) cutting the y axis at point c.

SE - standard error of the mean

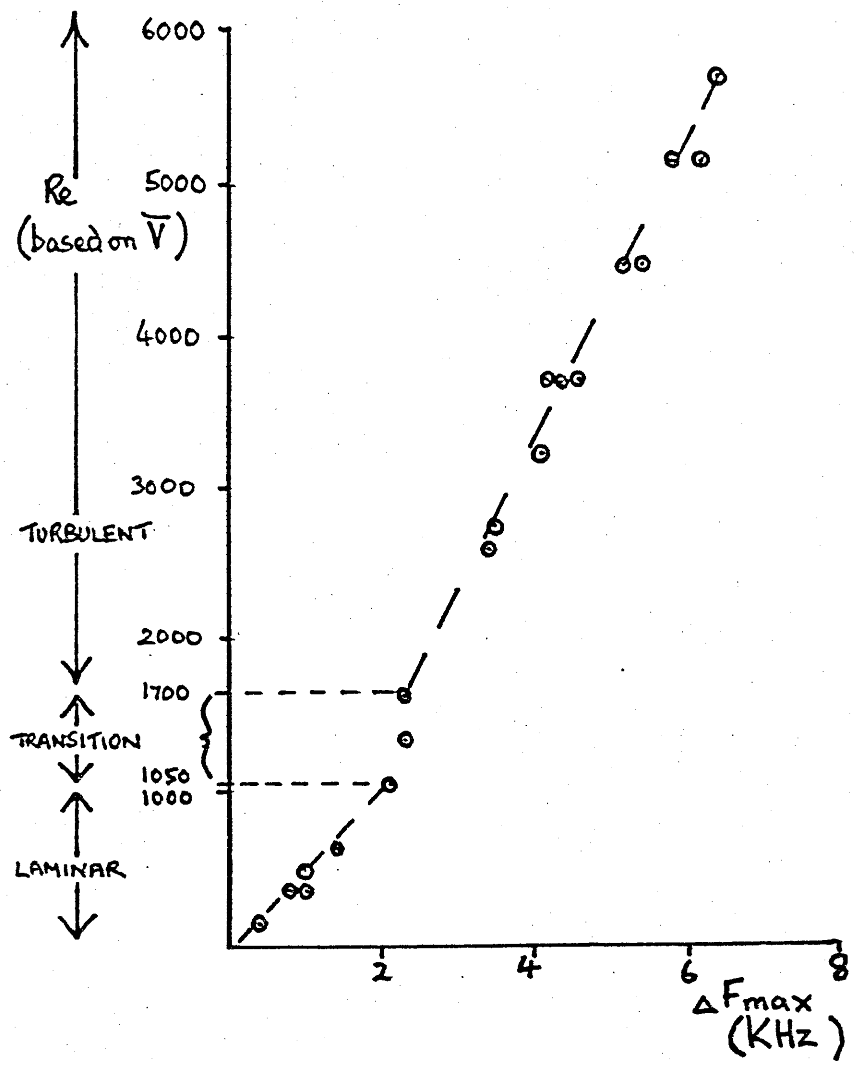

FIGURE 72

Finding the critical Reynolds number, Experiment (i)

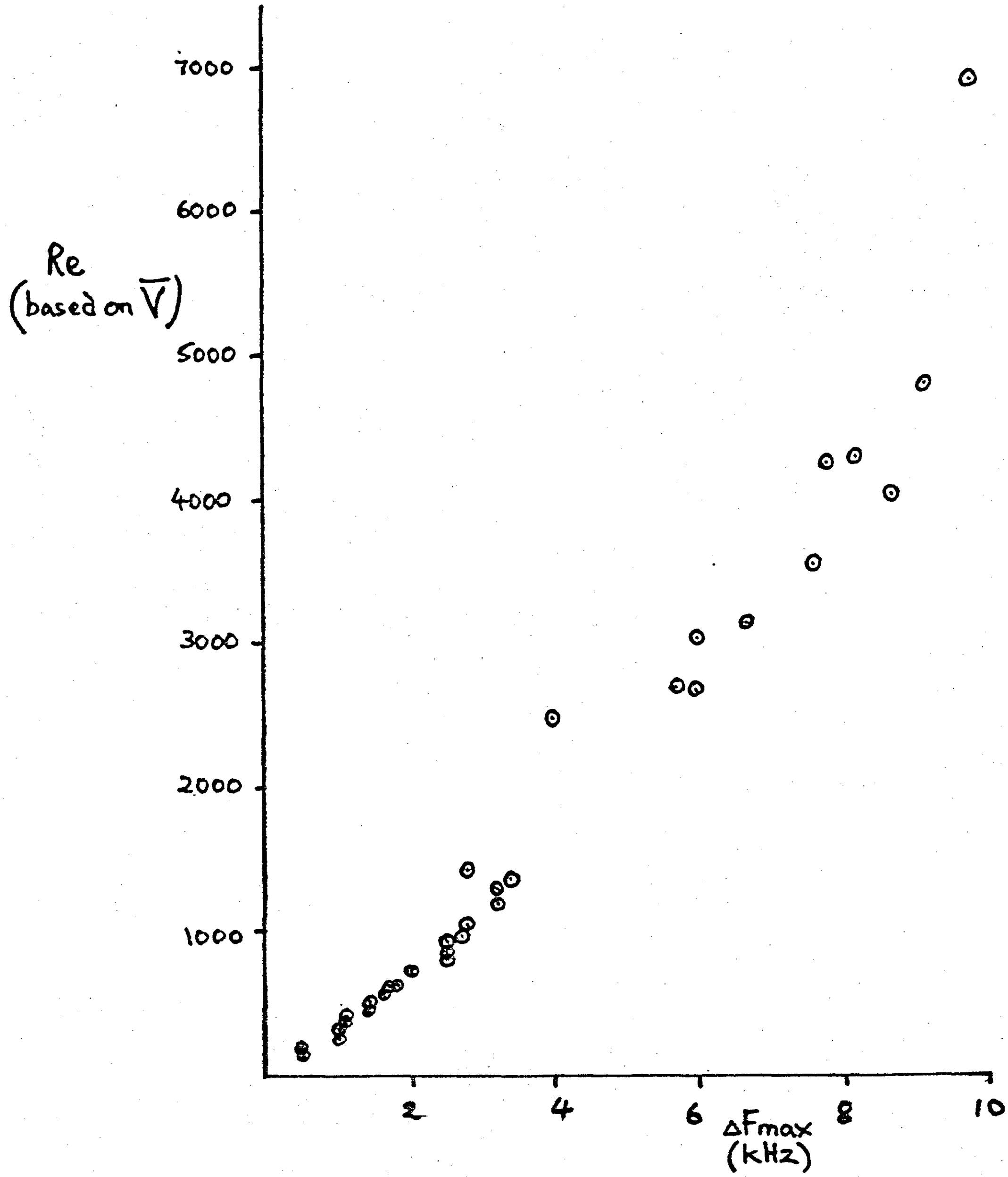

FIGURE 73

Finding the critical Reynolds number, Experiment (ii)

<u>Discussion</u>

The rate of change of $\bar{V}$ compared with ΔF max under laminar conditions of steady flow should in theory be half that of turbulent steady flow due to the change in the nature of the velocity profile that takes place. The ratio of the gradients LAM : TURB was approximately 0·5 in both experiments (see Table 68). The transition period occurred between Reynolds numbers of 1050 and 1700 with a critical Reynolds number of approximately 1700.